

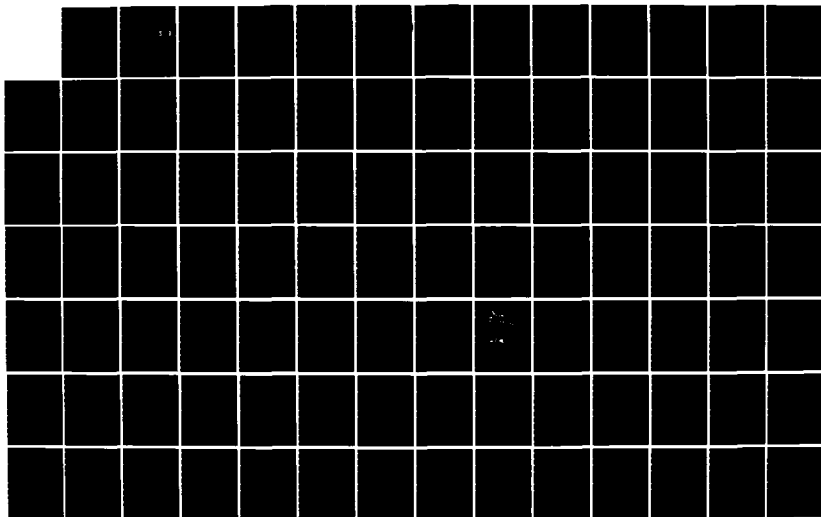
AD-A163 828

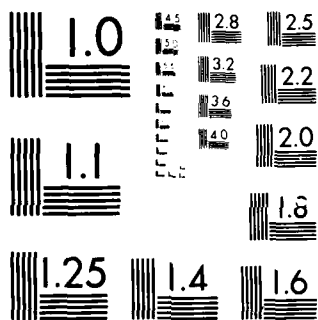
COMPARISON OF ABSORPTION AND RADIATION BOUNDARY
CONDITIONS USING A TIME-D. (U) AIR FORCE INST OF TECH
WRIGHT-PATTERSON AFB OH SCHOOL OF ENGI.. C F WILLIFORD
DEC 85 AFIT/GE/ENG/85D-53 F/G 28/3

1/2

UNCLASSIFIED

NL





MICROCOPY RESOLUTION TEST CHART
 NATIONAL BUREAU OF STANDARDS-1963-A

AD-A163 828



DTIC
ELECTE
FEB 11 1986

S D

COMPARISON OF ABSORPTION AND RADIATION
BOUNDARY CONDITIONS USING A TIME-DOMAIN
THREE-DIMENSIONAL FINITE DIFFERENCE
ELECTROMAGNETIC COMPUTER CODE

THESIS

Clifford F. Williford
Captain, USAF

AFIT/GE/ENG/85D-53

DISTRIBUTION STATEMENT A

Approved for public release
Distribution Unlimited

DEPARTMENT OF THE AIR FORCE
AIR UNIVERSITY

AIR FORCE INSTITUTE OF TECHNOLOGY

Wright-Patterson Air Force Base, Ohio

DTIC FILE COPY

1

DTIC
ELECTE
FEB 11 1986
S D

COMPARISON OF ABSORPTION AND RADIATION
BOUNDARY CONDITIONS USING A TIME-DOMAIN
THREE-DIMENSIONAL FINITE DIFFERENCE
ELECTROMAGNETIC COMPUTER CODE

THESIS

Clifford F. Williford
Captain, USAF

AFIT/GE/ENG/85D-53

Approved for public release; distribution unlimited

COMPARISON OF ABSORPTION AND RADIATION BOUNDARY CONDITIONS
USING A TIME-DOMAIN THREE-DIMENSIONAL FINITE DIFFERENCE
ELECTROMAGNETIC COMPUTER CODE

THESIS

Presented to the Faculty of the School of Engineering
of the Air Force Institute of Technology
Air University
In Partial Fulfillment of the
Requirements for the Degree of
Master of Science in Electrical Engineering

Clifford F. Williford. B.S.E.E
Captain, USAF

December 1985

Accession For	
NTIS CRA&I	<input checked="checked" type="checkbox"/>
DTIC TAB	<input type="checkbox"/>
Unannounced	<input type="checkbox"/>
Justification	
By Distribution	
Availability Codes	
Dist	Availability or Special
A-1	

Approved for public release; distribution unlimited

Acknowledgments

In accomplishing the task outlined in this thesis I have had a great deal of help from many people. I am indebted to 1Lt Jim Hebert for creating the thesis topic and quite adequately filling the job of mentor. I appreciate also my thesis advisor, almost Dr. (1Lt) Randy Jost. His patience, guidance, and support were welcomed. This was especially needed in my case since I completely changed my thesis topic at the end of June. I owe much to my thesis sponsor, AFWAL/FIESL. Hopefully, this does not include the \$35,000 of computer time I used! Last, but most of all, I thank my wife Lori and my sons, Chip and Brandon. My family has put up with many lost family hours, well above and beyond the call of understanding.

Clifford F. Williford

Table of Contents

	Page
Acknowledgments	ii
List of Figures	v
List of Tables	ix
List of Symbols	x
Abstract	xii
1. Introduction	1
Lightning	3
Lightning and Aircraft	3
Electromagnetic Computer Codes	6
Background	7
Problem	11
Scope	11
Assumptions	12
2. Theory	13
Finite Difference Form of Maxwell's Equations	16
Field Locations	20
Three-Dimensional Finite Difference Equations	22
3. Boundary Conditions	31
Absorption Boundary Condition	32
Radiation Boundary Condition	33
4. Modeling the F-16	37
Problem Space	38
Field Locations	41
Cell Size Choices Made for the F-16	42
5. Program Details	50
Basic Code	50
Boundary Conditions	51
Sample Point Locations	51
Source Function	54

	Page
6. Analysis	57
Waveform Appearance	68
Program Considerations	70
Conclusion	71
7. Summary and Recommendations	73
Appendix A: Updated Modified Rymes' Code	76
Appendix B: Rymes' Code with Radiation Boundary Conditions	95
Appendix C: Sensor Plots	121
Bibliography	162
VITA	170

List of Figures

Figure	Page
1. Three-dimensional Field Representation	15
2. Differencing Points	19
3. Decentralizing Mesh in One-dimension	21
4. Location of Difference Fields	23
5. Finite Conductivity at Boundary Edges	32
6. Basic Grid Block	39
7. Field Locations with the Decentralizing Grid System	41
8. F-16 Fighting Falcon	43
9. Gridding of the F-16, Side View	44
10. Gridding of the F-16, Front View	45
11. Gridding of the F-16, Top View	46
12. Three-dimensional Drawing of F-16 as Blocks	47
13. Photograph of F-16 Block Model	49
14. Sensor Locations on a Block F-16 Model	53
15. Expanded Plot of Source (First 250 nanoseconds)	55
16. Normalized Double Exponential Source Function	56
17. Sensor One, H-field, Right Wing	58
18. Sensor Two, H-field, Nose	59
19. Sensor Three, H-field, Engine Burner Can	60
20. Sensor Four, H-field, Forward Fuselage Bottom	61
21. Sensor Five, H-field, Rear Fuselage Bottom	62
22. Sensor Six, H-field, Vertical Stabilizer	63
23. Sensor Seven, H-field, Left Wing	64

Figure	Page
24. Sensor Eight, E-field, Right Wing	65
25. Sensor Nine, E-field, Middle Fuselage Top	66
26. Sensor Ten, E-field, Left Wing	67
27. Sensor One, H-field, Right Wing, $H_x(18,10,6)$	122
28. Sensor One, H-field, Right Wing, $H_x(18,10,6)$	123
29. Sensor One, H-field, Right Wing, $H_x(18,10,6)$	124
30. Sensor One, H-field, Right Wing, $H_x(18,10,6)$	125
31. Sensor Two, H-field, Nose, $H_z(4,10,13)$	126
32. Sensor Two, H-field, Nose, $H_z(4,10,13)$	127
33. Sensor Two, H-field, Nose, $H_z(4,10,13)$	128
34. Sensor Two, H-field, Nose, $H_z(4,10,13)$	129
35. Sensor Three, H-field, Engine Burner Can, $H_z(24,11,13)$	130
36. Sensor Three, H-field, Engine Burner Can, $H_z(24,11,13)$	131
37. Sensor Three, H-field, Engine Burner Can, $H_z(24,11,13)$	132
38. Sensor Three, H-field, Engine Burner Can, $H_z(24,11,13)$	133
39. Sensor Four, H-field, Forward Fuselage Bottom, $H_z(10,4,14)$	134
40. Sensor Four, H-field, Forward Fuselage Bottom, $H_z(10,4,14)$	135
41. Sensor Four, H-field, Forward Fuselage Bottom, $H_z(10,4,14)$	136
42. Sensor Four, H-field, Forward Fuselage Bottom, $H_z(10,4,14)$	137
43. Sensor Five, H-field, Rear Fuselage Bottom, $H_z(19,4,14)$	138

Figure	Page
44. Sensor Five, H-field, Rear Fuselage Bottom, H _z (19,4,14)	139
45. Sensor Five, H-field, Rear Fuselage Bottom, H _z (19,4,14)	140
46. Sensor Five, H-field, Rear Fuselage Bottom, H _z (19,4,14)	141
47. Sensor Six, H-field, Vertical Stabilizer, H _x (22,18,14)	142
48. Sensor Six, H-field, Vertical Stabilizer, H _x (22,18,14)	143
49. Sensor Six, H-field, Vertical Stabilizer, H _x (22,18,14)	144
50. Sensor Six, H-field, Vertical Stabilizer, H _x (22,18,14)	145
51. Sensor Seven, H-field, Left Wing, H _x (18,10,23) . .	146
52. Sensor Seven, H-field, Left Wing, H _x (18,10,23) . .	147
53. Sensor Seven, H-field, Left Wing, H _x (18,10,23) . .	148
54. Sensor Seven, H-field, Left Wing, H _x (18,10,23) . .	149
55. Sensor Eight, E-field, Right Wing, E _y (17,11,10) .	150
56. Sensor Eight, E-field, Right Wing, E _y (17,11,10) .	151
57. Sensor Eight, E-field, Right Wing, E _y (17,11,10) .	152
58. Sensor Eight, E-field, Right Wing, E _y (17,11,10) .	153
59. Sensor Nine, E-field, Middle Fuselage Top, E _y (15,13,14)	154
60. Sensor Nine, E-field, Middle Fuselage Top, E _y (15,13,14)	155
61. Sensor Nine, E-field, Middle Fuselage Top, E _y (15,13,14)	156
62. Sensor Nine, E-field, Middle Fuselage Top, E _y (15,13,14)	157
63. Sensor Ten, E-field, Left Wing, E _y (17,11,18) . . .	158

Figure	Page
64. Sensor Ten, E-field, Left Wing, $E_y(17,11,18)$. . .	159
65. Sensor Ten, E-field, Left Wing, $E_y(17,11,18)$. . .	160
66. Sensor Ten, E-field, Left Wing, $E_y(17,11,18)$. . .	161

List of Tables

Table	Page
1. Ten Sampled Points	52
2. CDC Cyber 845 Computer Run Data	71

List of Symbols

- A generic quantity, 'A' = a vector, otherwise a magnitude in the subscripted direction (could be E-field or H-field).
- ABC Absorption Boundary Condition.
- c speed of light (3×10^8 meters/second).
- det determinant of the matrix which follows.
- E-field (E) electric field (volts/meter), underbar indicates a vector quantity, subscript indicates magnitude in subscripted direction.
- f(a) ... 'f' is a function of 'a'.
- f{i,j,k} 'f' value evaluated at the point i,j,k.
- x,y,z .. magnitude in a particular direction as defined by the Cartesian coordinate system.
- $\hat{x}, \hat{y}, \hat{z}$.. unit vector in direction as defined by Cartesian coordinate system.
- h small distance (or increment) as used in the definition of a derivative.
- H-field (H) magnetic field (ampere/meter), underbar indicates a vector quantity, subscript indicates magnitude in subscripted direction.
- I current (ampere).
- i,j,k .. number designating a location in a three-dimensional grid space in a Cartesian coordinate system relative to x,y,z.
- J current density (ampere/meter²).
- N integer number of number of cells in problem space.
- r radius (meter).
- RBC Radiation Boundary Condition.
- t time (seconds).
- < left side less than right side.

3DFD ... three-dimensional finite-difference computer code
 by Rymes'.

$\nabla \times$ curl operator.

$\nabla \cdot$ divergence operator.

ϵ (epsilon) permittivity (farad/meter).

μ (mu) permeability (henry/meter).

ρ (rho) electric charge density (coulomb/meter³).

σ (sigma) conductivity (mho/meter)

Δ (delta) small increment as in a derivative.

(#) general reference to entire reference # found in
 the bibliography.

(###) . reference from page ## of bibliography reference #.

(##) . general reference from reference # and ##.

(###;a) reference #, page ## and general reference 'a'.

{ } ... standing alone defines a point in the problem space
 (e.g., {i,j,k}).

∂ partial derivative

π (pi) = 3.14

Abstract

The Three-Dimensional Finite Difference (3DFD) computer code is compared using Absorption Boundary Conditions (ABS) versus Radiation Boundary Conditions (RBC). This comparison is made when the 3DFD code is used to study the interaction of lightning with an aircraft. The 3DFD computer code is a modified version of Rymes' 3DFD. The aircraft modeled for the paper is an F-16 'Fighting Falcon'. The ABC used simulates an infinite free-space by setting the conductivity of the boundary space to that of distilled water, to "absorb" the outgoing electromagnetic waves. The RBC simulates free-space by assigning the boundary fields to a previously calculated value. The value is calculated with a parabolic interpolation of three previous field values, which are offset in space. Therefore, the calculated value is also extrapolated to account for the time delay and position change. The results of incorporating RBC were dramatic. The ten locations sampled for the test showed marked improvement in the waveforms when using RBC's. Depending on the purpose of the analysis, this improved waveform output may be overshadowed by the 25% increase in CPU time that is needed for the more sophisticated RBC.

1. Introduction

This thesis compares Radiation Boundary Conditions (RBC) with Absorption Boundary Conditions (ABC) in a time-domain three-dimensional finite difference computer code (3DFD). In this application, the 3DFD computer code is used to analyze lightning's electromagnetic interaction with an F-16 aircraft. The major tasks accomplished during this thesis effort include:

- a. The F-16 'Fighting Falcon' aircraft was electromagnetically modeled, and implemented in a modified version of the Rymes' 3DFD code (16).
- b. The 3DFD code with its original absorption boundary conditions was updated, corrected and run for a typical nose-to-tail lightning strike (Appendix 1) (48). The fields calculated were recorded at 10 monitor locations on the F-16 aircraft (Appendix 3).
- c. The 3DFD code was then modified to implement the radiation boundary conditions (Appendix 2) (59).
- d. The 3DFD code with the new radiation boundary conditions was run for the same nose-to-tail lightning strike on the F-16

geometric model. The fields calculated were sampled and recorded at the same 10 locations during both runs (Appendix 3).

e. The results of the two computer runs for the first two microseconds were compared (Chapter 6). The comparisons were based on one complete run with the absorption boundary conditions and one run with the radiation boundary conditions. The comparisons were made for the same 10 sample points on the F-16 (Appendix 3).

The F-16 was geometrically modeled and implemented into computer code in a manner suitable for analysis by a modified version of the Rymes' 3DFD computer code (48; 16). The Rymes' 3DFD code was modified and used by 1Lt Hebert at the Air Force Wright Aeronautical Laboratories Atmospheric Electricity Hazards Group (AFWAL/FIESL), Wright-Patterson AFB, Ohio (16). Hebert implemented the code with absorption boundary conditions, and modeled a CV-580 aircraft for his study (16). During this thesis effort radiation boundary conditions similar to those discussed in a paper by Kunz and Lee were developed, encoded, and written into the modified 3DFD code (27). The computer codes were run for a direct lightning strike, nose-to-tail, on an F-16 aircraft. The results are compared and presented in this thesis.

Lightning

Lightning brings to mind a flash of light in the sky, a loud clapping sound and rumbling thunder. This flash of light and the associated sounds are the discharging and neutralization of the atmosphere's large charge centers from one cloud to another, or from clouds to the earth (61:1). Lightning in this text is to be thought of as a high current electric discharge which has a path length measured in kilometers (61:1). Aircraft in the presence of these highly charged areas can become part of the high current channel (35:90-1). In fact, Mazur believes the aircraft itself triggers lightning (35:90-2). Shaeffer agrees with this, except with the qualification that a highly charged air mass, one which is conducive to a lightning discharge, must already exist before the aircraft can trigger the lightning discharge (50:67).

Lightning and Aircraft

Lightning poses a possible catastrophic threat to any aircraft (11:i). Lightning strikes account for more than one-half of the total USAF weather-related aircraft mishaps (36:vi). Since little can be done to prevent an aircraft from being struck by lightning, aircraft protection for the critical components is of utmost importance (45). Critical

components, such as flight control computers, fuel systems, and structurally critical airframe/propulsion units, are vulnerable to electrical disruption and/or mechanical failure (45). As electronic complexity has increased, the size and weight have decreased. However, the probability of lightning strikes has remained relatively constant (40:8). It is interesting to note that Pierce concludes, using basically the same logic, that the lightning hazard to aircraft operation is increasing (42:17). Therefore, the importance of characterizing lightning and its effects is of growing importance, as indicated by the number of articles written on the subject (8; 23; 31; 35; 36; 40; 42; 43; 46; 47; 49; 50). An aircraft, such as the F-16, with a "fly-by-wire" flight control system, were it unprotected, could be rendered inoperable by a lightning strike (1:1).

The starting point in characterizing lightning's effects with a computer program is to model the aircraft's outer skin. Studying the propagation of the electromagnetic energy from the entry to the exit point, as it redistributes on the surface of the aircraft's fuselage, is the first goal (34:2,16). Determining this redistribution can lead to coupling the surface currents to the interior components. The final goal is understanding lightning's effect on the sensitive electronic components, and then protecting sensitive components from these effects. An accurate computer code could be a valuable tool in designing

protection against lightning's effects. It would allow protection to be designed and tested before the production stage of new aircraft development.

All-metal aircraft are shielded from many of lightning's effects, as the all-metal skin presents a Faraday cage type enclosure for the electronics bay (19; 45; 52; 58). Recent efforts to use the new, lighter, advanced composite and thermoplastic materials in aircraft reduces this shielding protection (10:1). As early as 1952, Burkley was looking at plywood, plastics, laminated fiberglass, and other non-conductive materials to be used as aircraft structural components (5). Burkley was studying the effects of, and the necessary protection needed from, the high current surges associated with lightning strikes on these non-conductive materials (5). Examples and techniques of various protection schemes can be found in numerous sources. Sommer of Boeing Company, Weinstock of McDonnell Aircraft Company, and Fisher of General Electric are just three of the many authors publishing in this area of aircraft lightning protection (51; 63; 14).

Electromagnetic Computer Codes

Electromagnetic computer codes allow the engineer to characterize and study the electromagnetic interaction with aircraft. The engineer can then design protection against those effects which cause electronic upset or damage. As previously stated, the use of advanced composite materials and sensitive microelectronics in more modern aircraft makes them more susceptible to the effects of lightning strikes. This increased susceptibility demands more accurate electromagnetic modeling (46:220). This modeling is to be used in the development of lightning protection. Accurate models, when used in design for lightning protection, allow the use of optimal lightning protection. This protection is optimal in that excessive lightning protection would add weight that is not in proportion to the risk reduction gained (63:34-1).

While accurate, these models must also be flexible enough to handle new lightning channel models. A recent inflight lightning characterization program has shown that intracloud lightning attachment is even more severe than previously estimated, with faster risetimes and higher charge transfers (19:1). This demonstrates the need for flexible analysis systems which can be easily modified to incorporate new findings without completely reworking each study.

Many electromagnetic computer codes are available to approximate a solution to Maxwell's equations (2; 13; 28; 34; 60). One type of code solves Maxwell's equations in the integral form based upon Harrington's Method of Moments, such as Auckland's study of an F-14 (15; 4). Another type of code solves Maxwell's equations in their differential form using the Finite Difference Method of approximation, such as Holland's "THREDE" (20; 21; 22). The time-domain finite difference electromagnetic code approximation of Maxwell's equations was used during this thesis effort. In a study by Longmire of Mission Research Corporation, it is stated that the finite difference method is the fastest way of solving Maxwell's equations (33:2341). And, in a recent article, Mei states that he believes the finite difference method is the most adaptable to the virtual memory systems of minicomputers which are in growing use in industry (37:1145).

Background

In the study of lightning's interaction with aircraft, it is often necessary to have a computer model for analytical comparisons. Hebert has successfully modified a finite difference electromagnetic code written by M.D. Rymes of Electromagnetic Applications, Inc., to analyze a CV-580 lightning strike aircraft test-bed (48; 16). Other

modifications to Rymes 3DFD code and an expanded user's guide are detailed in Hebert's report (16). This modified 3DFD code presently uses absorption boundary conditions (Appendix 1), which cause the boundaries to artificially reflect unabsorbed electromagnetic energy. This gives less than desired accuracy, as the reflected waves return to the aircraft's surface at later time steps (55:626).

3DFD is a finite difference formulation of the time-domain electromagnetic-field problem. This code's major advantage is that it does not require the memory or the time needed to invert the matrices encountered in the MOM codes (33:2340). As Mur states it, though, the finite difference method has as its major problem the limited size of the problem space (41:377). It must be remembered that it is the problem space size that is the problem, not the size of the object inside. For example, an aircraft as large as a B-52 has been studied using 3DFD (21). A Cartesian finite difference method uses a rectangular problem space, totally enclosing the object to be studied (e.g., aircraft). The object to be studied is defined in the problem space by assigning values of permittivity and conductivity to each component of the total electric field (E-field), which describes the geometry of the object. This geometry has the restriction of being described by a limited number of predetermined rectangular shapes, which make up the problem space in the Cartesian coordinate system.

The computer code solves Maxwell's time dependent curl equations, which in turn solve the boundary conditions for the object in a "natural way" (62:397). The code progresses through the problem space in time steps using an algorithm originally developed by Yee (64). Since an infinite problem space cannot be defined on the computer, difficulties arise when the propagating wave reaches the problem space boundary. These boundaries cause reflections unless they are modified to account for the ideal analytical situation of free space. Thus, additional algorithms are needed to account for the radiation conditions. Taylor was the first to implement Yee's algorithm. He used absorption boundary conditions to account for the previously-mentioned reflections at the problem space boundaries (59:585).

Yee originally started with "hard" lattice truncation (another way of expressing the boundary condition) (64). Hard lattice truncation is defined as forcing the outside boundary of the problem space to be a perfect conductor. This is done by assigning the tangential E-field the value of zero at the boundary (55:626). This is also known as "tin can" boundary conditions, as the problem space is totally enclosed by perfectly conducting metal boundaries (16:22).

The two methods that are examined in this thesis are both referred to as either "soft" lattice truncation methods, or "soft" boundary conditions. These are the

absorption boundary condition and the radiation boundary condition. The absorption boundary condition is accomplished by assigning increasing values of conductivity to the cells of the problem space near the boundaries, thereby effectively chipping away at the E-field, a small amount at a time (55:626). The other method, the radiation boundary condition, reduces the magnitude of the E-field by a factor of $1/r$, which is the radiation condition characteristic of an electromagnetic wave propagating in free-space (39:41). Here 'r' is the radial distance from the origin of a centrally located coordinate system.

The finite difference codes have been found to agree, within 1 dB and 1 lattice cell, with known analytical and experimental quantities (54:202). Due to the accuracy and efficiency of Yee's basic algorithm, Taflove, Kunz, Umashankar, Merewether, Fisher, Mei, and others have published many papers on combined methods, hybrids, curved surfaces, and other modifications, making this a very competitive method for a numerical solution of Maxwell's equations (14; 26; 37; 38; 56; 62).

Problem

First, an electromagnetic model of an F-16 aircraft had to be implemented on the computer for a new study using the present modified code. During the computer runs using the absorption boundary conditions (ABC), sample data from several points was stored for further study. This required the correct geometrical modeling of the aircraft into the three-dimensional finite difference problem space. Next, the code was modified to incorporate the radiation boundary conditions (which were believed to limit previous reflections). Then the code was run with the same F-16 model, sampling the same points as before. The final task was to compare the results of both computer runs and analyze the findings.

Scope

This study was limited to developing a geometrically correct electromagnetic model of the F-16 using the subroutine AIRPLN from an AFWAL/FIESL technical report by 1Lt Hebert (16). The subroutine AIRPLN, modeling an F-16, was run with the present modified computer code for a nose-to-tail lightning strike. Samples were recorded at 10 locations (7 H-fields and 3 E-fields) for predetermined orientations. The code was then changed to incorporate the

radiation boundary conditions (RBC). The modified version of the code with radiation boundary conditions was run with the same subroutine AIRPLN . The same 10 sample points were recorded and the results were analyzed.

Assumptions

The assumptions were that the AFWAL/FIESL technical report, and previous studies which determined that RBC would be more accurate than ABC, were correct (16). An isotropic, linear, and homogeneous medium was considered. The region of interest was considered source-free except for the injected lightning strike.

2. Theory

The three-dimensional finite difference code uses the time-domain differential form of Maxwell's equations (64:302). The E-field and H-field magnitudes in each of the three vector directions that define the Cartesian coordinate system are calculated using these equations (64). The calculations are made while stepping through the grid problem space (NxNxN) at a particular time. It is necessary to increment the time step after each complete pass through the grid space calculating the E-field or H-field. All units are in the MKS system unless otherwise specified. The form of Maxwell's equations for isotropic material used here is (24:361)

$$\mu \frac{\partial \underline{H}}{\partial t} = - \nabla \times \underline{E} \quad (2.1)$$

$$\epsilon \frac{\partial \underline{E}}{\partial t} = \nabla \times \underline{H} - \sigma \underline{E} \quad (2.2)$$

$$\nabla \cdot (\epsilon \underline{E}) = \rho \quad (2.3)$$

$$\nabla \cdot (\mu \underline{H}) = 0 \quad (2.4)$$

where

H = magnetic field (amps/meter)
 E = electric field (volts/meter)
 t = time (seconds)
 μ = (mu) permeability (henry/meter)
 ϵ = (epsilon) permittivity (farad/meter)
 ρ = (rho) electric charge density (coulomb/meter³)
 σ = (sigma) conductivity (mho/meter)
 $\nabla \times$ = curl operator
 $\nabla \cdot$ = divergence operator

These are point relationships ($J = \sigma E$). In the finite difference code, the term 'decentralizing mesh' is often used to refer to the gridding of the problem space. This is not to be confused with the mesh relationship of the integral form of Maxwell's equations.

A necessary process in understanding the finite difference code is to develop the three-dimensional finite difference form of Maxwell's equations. This development will be using a central differencing estimation for a derivative (32:163). The first operation in the process is to put Maxwell's equations in a finite difference form. Then one must both understand where the fields are located in the problem space, and comprehend the makeup of the problem space itself. In particular, the single point reference system references fields located on three sides of the rectangular box. A point in the three-dimensional grid, and the associated fields are shown in Figure 1. Finally, one must put all of this together and express the three-dimensional finite difference equations in a form useful to algorithm development. A source-free region is considered for the development of the algorithm.

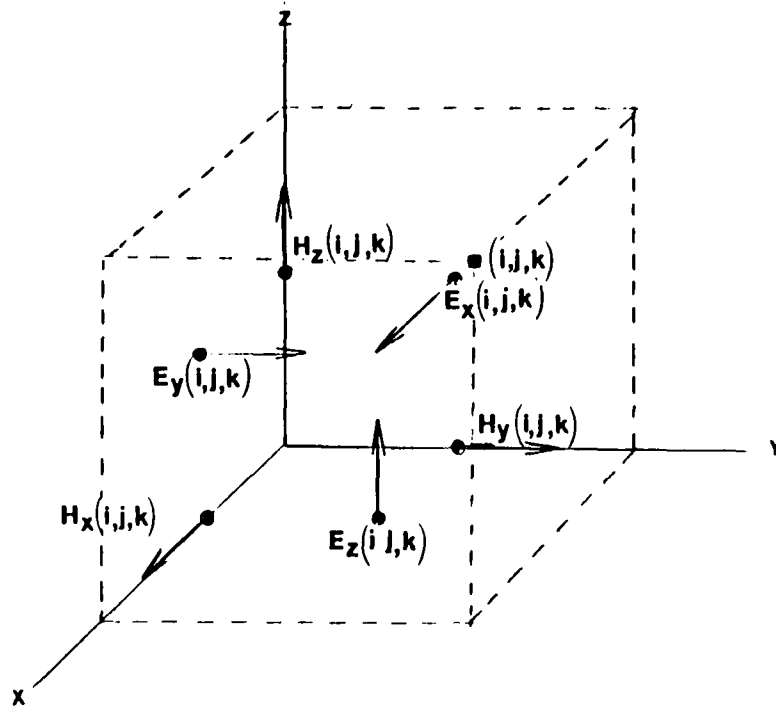


Figure 1. Three-dimensional Field Representation

Since the computer memory available is a limited quantity, some boundary must be placed on the problem space in order to arrive at a meaningful solution. Each author has his own style of implementing boundary conditions. The two compared in this thesis are often referred to as "soft" boundary conditions, or "soft" lattice truncation conditions. The first to be used is the absorption boundary condition which Rymes implemented in 3DFD (48). The second boundary condition is the radiation boundary condition used by Kunz (29).

Finite Difference Form of Maxwell's Equations

The finite difference form of Maxwell's equations uses Eq (2.1) thru Eq (2.4), manipulated in the Cartesian coordinate system, to arrive at a convenient algorithmic form for programming.

In the Cartesian coordinate system, the electric and magnetic field vectors are as found in Thiele's notation (53:11):

$$\underline{A} = A_x \hat{a}_x + A_y \hat{a}_y + A_z \hat{a}_z \quad (2.5)$$

where 'A' is equal to the magnitude of the E-field or H-field component and 'a' is the unit vector in the x, y, or z direction.

The curl of A in the Cartesian coordinate system is expressed as follows (24:178):

$$\text{curl } \underline{A} = \nabla \times \underline{A} = \det \begin{vmatrix} \hat{a}_x & \hat{a}_y & \hat{a}_z \\ \frac{\partial}{\partial x} & \frac{\partial}{\partial y} & \frac{\partial}{\partial z} \\ A_x & A_y & A_z \end{vmatrix} \quad (2.6)$$

When the determinant (det) of Eq (2.6) is found, it is

expressed as (59:556):

$$\text{curl } \underline{A} = \left(\frac{\partial A_z}{\partial y} - \frac{\partial A_y}{\partial z} \right) \hat{a}_x + \left(\frac{\partial A_x}{\partial z} - \frac{\partial A_z}{\partial x} \right) \hat{a}_y + \left(\frac{\partial A_y}{\partial x} - \frac{\partial A_x}{\partial y} \right) \hat{a}_z \quad (2.7)$$

In general, 'A' may also be a function of time.

Substituting E or H for A into Eq (2.7), replacing the curls in Eq (2.1) and Eq (2.2) with the results from Eq (2.7), and lastly separating the vector components yields:

$$\mu \frac{\partial H_x}{\partial t} = - \frac{\partial E_z}{\partial y} + \frac{\partial E_y}{\partial z} \quad (2.8a)$$

$$\mu \frac{\partial H_y}{\partial t} = - \frac{\partial E_x}{\partial z} + \frac{\partial E_z}{\partial x} \quad (2.8b)$$

$$\mu \frac{\partial H_z}{\partial t} = - \frac{\partial E_y}{\partial x} + \frac{\partial E_x}{\partial y} \quad (2.8c)$$

$$\epsilon \frac{\partial E_x}{\partial t} + \sigma E_x = \frac{\partial H_z}{\partial y} - \frac{\partial H_y}{\partial z} \quad (2.9a)$$

$$\epsilon \frac{\partial E_y}{\partial t} + \sigma E_y = \frac{\partial H_x}{\partial z} - \frac{\partial H_z}{\partial x} \quad (2.9b)$$

$$\epsilon \frac{\partial E_z}{\partial t} + \sigma E_z = \frac{\partial H_y}{\partial x} - \frac{\partial H_x}{\partial y} \quad (2.9c)$$

These equations are now in a form convenient for use in the algorithm of the finite difference computer code.

The derivatives in Eq (2.8) and Eq (2.9) are replaced by a finite difference approximation. The exact definition of a derivative using forward differencing is (25:289; 7:297):

$$f'(x) = \frac{df(x)}{dx} = \lim_{h \rightarrow 0} \frac{f(x+h) - f(x)}{h} \approx \frac{f(x+h) - f(x)}{h} \quad (2.10)$$

The finite differencing approximation used in this work is the central differencing approximation defined by (7:298):

$$\frac{df(x)}{dx} \approx \frac{f(x+h/2) - f(x-h/2)}{h} \quad (2.11)$$

and is illustrated graphically in Figure 2.

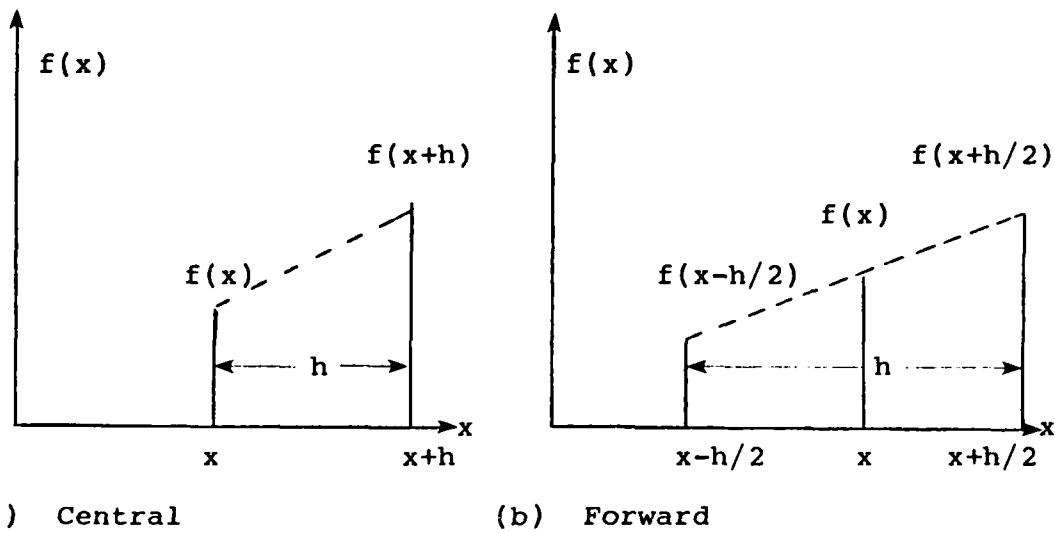


Figure 2. Differencing Points

By using a Taylor series approximation of Eq (2.11) and Eq (2.12), the errors can be compared (32; 16). The result is that the central differencing approximation is a second order approximation as opposed to forward differencing, which is a first order approximation (32:297, 298). Both of the codes (Appendix A and Appendix B) were run using the central differencing approximations for each derivative.

Field Locations

The points (i,j,k) which describe the location of the fields in each cell space are reference points on a decentralizing mesh scheme. This decentralizing mesh scheme is best described by first considering the one-dimensional decentralizing mesh (Figure 3). Note that the E-fields and H-fields are not co-located. This displacement keeps one from knowing the E-field and H-field components at the same point in space. The fields are only known at $1/2$ the differential distance $(\Delta x/2, \Delta y/2, \Delta z/2)$ in any particular coordinate system direction. Also note that the E-field and H-field are not known at the same time, but that they are separated by $1/2$ the time step $(\Delta t/2)$.

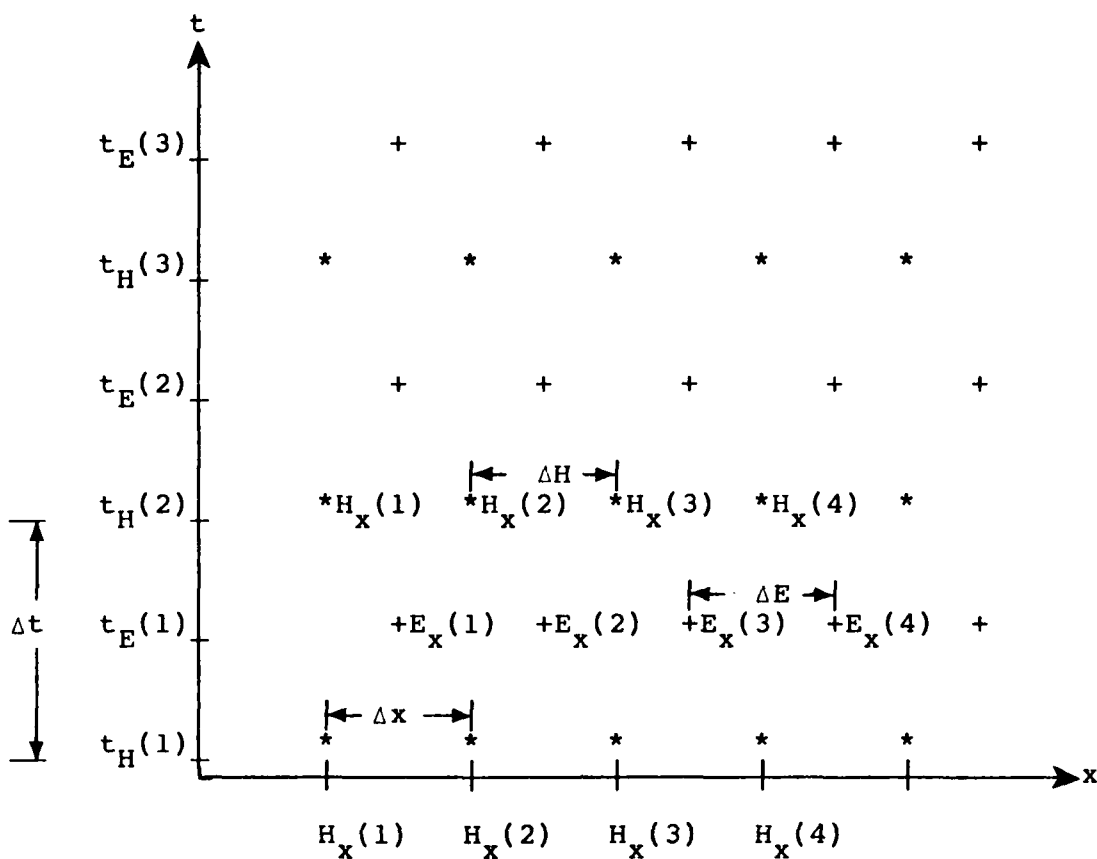


Figure 3. Decentralizing Mesh in One-dimension

To form the derivatives required in Eq (2.8) and Eq (2.9), the dH/dt and dE/dt are needed. As demonstrated graphically in Figure 3, these values are available using this decentralizing mesh concept.

Three-Dimensional Finite Difference Equations

The Three-Dimensional Finite Difference Equations can be derived by combining the differential form of Maxwell's equations, the definition of curl in the Cartesian coordinate system, and the central differencing approximation to a derivative.

Magnetic-Field Algorithm Development. An example in terms of H_x would combine Eq (2.8a) and Eq (2.11) at a point specified as:

$$\{(i-1/2)\Delta x, j\Delta y, k\Delta z, (n-1/2)\Delta t\}$$

and yield:

$$\begin{aligned} & \frac{H_x\{(i-1/2)\Delta x, j\Delta y, k\Delta z, n\Delta t\} - H_x\{(i-1/2)\Delta x, j\Delta y, k\Delta z, (n-1)\Delta t\}}{\Delta t} \\ &= \frac{E_y\{(i-1/2)\Delta x, j\Delta y, (k+1/2)\Delta z, (n-1/2)\Delta t\}}{\mu\Delta z} \\ &- \frac{E_y\{(i-1/2)\Delta x, j\Delta y, (k-1/2)\Delta z, (n-1/2)\Delta t\}}{\mu\Delta z} \\ &- \frac{E_z\{(i-1/2)\Delta x, (j+1/2)\Delta y, k\Delta z, (n-1/2)\Delta t\}}{\mu\Delta y} \\ &+ \frac{E_z\{(i-1/2)\Delta x, (j-1/2)\Delta y, k\Delta z, (n-1/2)\Delta t\}}{\mu\Delta y} \end{aligned} \quad (2.12)$$

In using this equation, an approximation for H_x can be obtained by knowing E_y and E_z at $1/2$ a space increment on

either side of H_x , at $\Delta t/2$ earlier and H_x one Δt earlier. Figure 4 illustrates these relationships. Taflove and Umashankar have shown that this approximation is within the accuracy of computer calculations (54; 62).

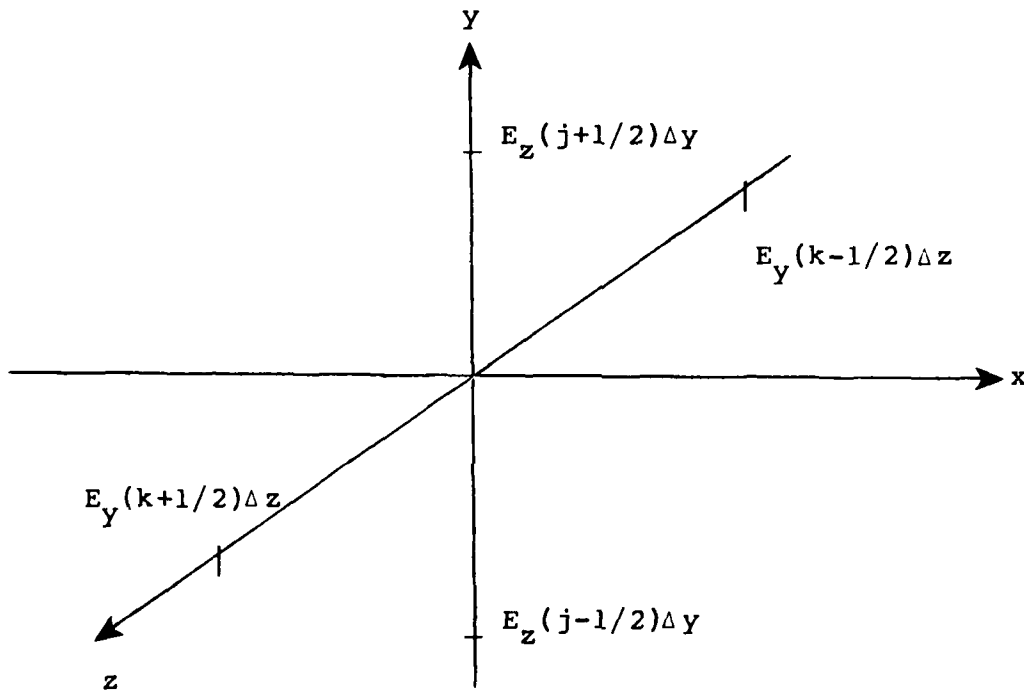


Figure 4. Location of Difference Fields
 Note: The origin is centered at $\{(i-1/2)\Delta x, j\Delta y, k\Delta z\}$, at the time $n\Delta t$.

Next, the E-field can be determined in a similar manner $\Delta t/2$ later at $1/2$ a space increment in the x direction. The program steps through the decentralizing mesh in half-space increments and half-time increments until the entire grid space is covered ($N_x N_y N_z$).

Similar modifications transform Eq (2.8b) and Eq (2.8c) into

$$\begin{aligned}
 & \frac{H_y\{i\Delta x, (j-1/2)\Delta y, k\Delta z, n\Delta t\} - H_y\{i\Delta x, (j-1/2)\Delta y, k\Delta z, (n-1)\Delta t\}}{\Delta t} \\
 &= \frac{E_z\{(i+1/2)\Delta x, (j-1/2)\Delta y, k\Delta z, (n-1/2)\Delta t\}}{\mu\Delta x} \\
 &- \frac{E_z\{(i-1/2)\Delta x, (j-1/2)\Delta y, k\Delta z, (n-1/2)\Delta t\}}{\mu\Delta x} \\
 &- \frac{E_x\{i\Delta x, (j-1/2)\Delta y, (k+1/2)\Delta z, (n-1/2)\Delta t\}}{\mu\Delta z} \\
 &+ \frac{E_x\{i\Delta x, (j-1/2)\Delta y, (k-1/2)\Delta z, (n-1/2)\Delta t\}}{\mu\Delta z}
 \end{aligned} \tag{2.13}$$

at point location $\{i\Delta x, (j-1/2)\Delta y, k\Delta z, (n-1/2)\Delta t\}$ and

$$\begin{aligned}
 & \frac{H_z\{i\Delta x, j\Delta y, (k-1/2)\Delta z, n\Delta t\} - H_z\{i\Delta x, j\Delta y, (k-1/2)\Delta z, (n-1)\Delta t\}}{\Delta t} \\
 &= \frac{E_x\{i\Delta x, (j+1/2)\Delta y, (k-1/2)\Delta z, (n-1/2)\Delta t\}}{\mu\Delta y} \\
 &- \frac{E_x\{i\Delta x, (j-1/2)\Delta y, (k-1/2)\Delta z, (n-1/2)\Delta t\}}{\mu\Delta y} \\
 &- \frac{E_y\{(i+1/2)\Delta x, j\Delta y, (k-1/2)\Delta z, (n-1/2)\Delta t\}}{\mu\Delta x} \\
 &+ \frac{E_y\{(i-1/2)\Delta x, j\Delta y, (k-1/2)\Delta z, (n-1/2)\Delta t\}}{\mu\Delta x}
 \end{aligned} \tag{2.14}$$

at point location $\{i\Delta x, j\Delta y, (k-1/2)\Delta z, (n-1/2)\Delta t\}$.

Electric Field Algorithm Development. Operating on the E-field in Eq (2.9a) at grid point

$$\{(i-1)\Delta x, (j-1/2)\Delta y, (k-1/2)\Delta z, n\Delta t\}$$

E_x is first needed at $t = (n+1/2)\Delta t$. Using the average of E_x at $\Delta t/2$, before and after t ,

$$E_x(n\Delta t) = \frac{E_x\{(n+1/2)\Delta t\} + E_x\{(n-1/2)\Delta t\}}{2} \quad (2.15)$$

substituting in the space coordinates, one finds

$$\begin{aligned} E_x\{(i-1)\Delta x, (j-1/2)\Delta y, (k-1/2)\Delta z, n\Delta t\} \\ = \frac{E_x\{(i-1)\Delta x, (j-1/2)\Delta y, (k-1/2)\Delta z, (n+1/2)\Delta t\}}{2} \\ + \frac{E_x\{(i-1)\Delta x, (j-1/2)\Delta y, (k-1/2)\Delta z, (n-1/2)\Delta t\}}{2} \end{aligned} \quad (2.16)$$

and substituting into Eq (2.9a), then expanding the right side as was done in Eq (2.8), the result is

$$\begin{aligned}
& (\epsilon/\Delta t + \sigma/2)(E_x\{(i-1)\Delta x, (j-1/2)\Delta y, (k-1/2)\Delta z, (n+1/2)\Delta t\}) \\
& - (\epsilon/\Delta t - \sigma/2)(E_x\{(i-1)\Delta x, (j-1/2)\Delta y, (k-1/2)\Delta z, (n-1/2)\Delta t\}) \\
& = \frac{H_z\{(i-1)\Delta x, j\Delta y, (k-1/2)\Delta z, n\Delta t\}}{\Delta y} \\
& - \frac{H_z\{(i-1)\Delta x, (j-1)\Delta y, (k-1/2)\Delta z, n\Delta t\}}{\Delta y} \\
& - \frac{H_y\{(i-1)\Delta x, (j-1/2)\Delta y, k\Delta z, n\Delta t\}}{\Delta z} \\
& + \frac{H_y\{(i-1)\Delta x, (j-1/2)\Delta y, (k-1)\Delta z, n\Delta t\}}{\Delta z}
\end{aligned} \tag{2.17}$$

Now sigma, the conductivity, is in the equation. This is the area, that if one were dealing with something other than a perfect conductor, changes in the conductivity could be made. In the data base, one can express the conductivity at each grid point. In the program it is averaged in this manner:

$$\begin{aligned}
\sigma_x &= \sigma \{(i-1)\Delta x, (j-1/2)\Delta y, (k-1/2)\Delta z\} \\
&= \frac{\sigma\{(i-1/2)\Delta x, (j-1/2)\Delta y, (k-1/2)\Delta z\}}{2} \\
&+ \frac{\sigma\{(i-3/2)\Delta x, (j-3/2)\Delta y, (k-1/2)\Delta z\}}{2}
\end{aligned} \tag{2.18}$$

And epsilon, the permittivity is

$$\epsilon_x = \epsilon\{(i-1)\Delta x, (j-1/2)\Delta y, (k-1/2)\Delta z\} \quad (2.19)$$

Similar operations for E_y at

$$\{(i-1/2)\Delta x, (j-1)\Delta y, (k-1/2)\Delta z, n\Delta t\}$$

yields

$$\begin{aligned} & (\epsilon/\Delta t + \sigma/2)(E_y\{(i-1/2)\Delta x, (j-1)\Delta y, (k-1/2)\Delta z, (n+1/2)\Delta t\}) \\ & - (\epsilon/\Delta t - \sigma/2)(E_y\{(i-1/2)\Delta x, (j-1)\Delta y, (k-1/2)\Delta z, (n-1/2)\Delta t\}) \\ & = \frac{H_x\{(i-1/2)\Delta x, (j-1)\Delta y, k\Delta z, n\Delta t\}}{\Delta z} \\ & - \frac{H_x\{(i-1/2)\Delta x, (j-1)\Delta y, (k-1)\Delta z, n\Delta t\}}{\Delta z} \\ & - \frac{H_z\{i\Delta x, (j-1)\Delta y, (k-1/2)\Delta z, n\Delta t\}}{\Delta x} \\ & + \frac{H_z\{(i-1)\Delta x, (j-1)\Delta y, (k-1/2)\Delta z, n\Delta t\}}{\Delta x} \end{aligned} \quad (2.20)$$

and for E_z at $\{(i-1/2)\Delta x, (j-1/2)\Delta y, (k-1)\Delta z, n\Delta t\}$

$$\begin{aligned}
& (\epsilon/\Delta t + \sigma/2)(E_z\{(i-1/2)\Delta x, (j-1/2)\Delta y, (k-1)\Delta z, (n+1/2)\Delta t\}) \\
& - (\epsilon/\Delta t - \sigma/2)(E_z\{(i-1/2)\Delta x, (j-1/2)\Delta y, (k-1)\Delta z, (n-1/2)\Delta t\}) \\
& = \frac{H_y\{i\Delta x, (j-1/2)\Delta y, (k-1)\Delta z, n\Delta t\}}{\Delta x} \\
& - \frac{H_y\{(i-1)\Delta x, (j-1/2)\Delta y, (k-1)\Delta z, n\Delta t\}}{\Delta x} \\
& - \frac{H_x\{(i-1/2)\Delta x, j\Delta y, (k-1)\Delta z, n\Delta t\}}{\Delta y} \\
& + \frac{H_x\{(i-1/2)\Delta x, (j-1)\Delta y, (k-1)\Delta z, n\Delta t\}}{\Delta y}
\end{aligned} \tag{2.21}$$

Finally, in rearranging the electric field equation and the magnetic field equation, one arrives at a form which is useful in understanding the relationship between various fields and the code. For example:

$$\begin{aligned}
H_x\{i, j, k, n\Delta t\} &= H_x\{i, j, k, (n-1)\Delta t\} \\
&+ \left(\frac{\Delta t}{\mu}\right) \left(\frac{E_y\{i, j, (k+1/2), (n-1/2)\Delta t\}}{\Delta z} \right. \\
&- \frac{E_y\{i, j, (k-1/2), (n-1/2)\Delta t\}}{\Delta z} \\
&- \frac{E_z\{i, (j+1/2), k, (n-1/2)\Delta t\}}{\Delta y} \\
&+ \left. \frac{E_z\{i, (j-1/2), k, (n-1/2)\Delta t\}}{\Delta y} \right)
\end{aligned} \tag{2.22}$$

and

$$\begin{aligned}
 E_x\{i,j,k,(n+1/2)\Delta t\} = & E_x\{i,j,k,(n-1/2)\Delta t\} \left(\frac{\epsilon/\Delta t - \sigma/2}{\epsilon/\Delta t + \sigma/2} \right) \\
 & + \left(\frac{1}{(\epsilon/\Delta t + \sigma/2)} \right) \left(\frac{H_z\{i,(j+1/2),k,n\Delta t\}}{\Delta y} \right. \\
 & - \frac{H_z\{i,(j-1/2),k,n\Delta t\}}{\Delta y} \\
 & - \frac{H_y\{i,j,(k+1/2),n\Delta t\}}{\Delta z} \\
 & \left. + \frac{H_y\{i,j,(k-1/2),n\Delta t\}}{\Delta z} \right)
 \end{aligned} \tag{2.23}$$

In this manner, the E_x can be calculated knowing the H-field $\Delta t/2$ earlier at the four adjacent points in the orthogonal plane, $\Delta y/2$ and $\Delta z/2$ away, and the E_x $\Delta t/2$ earlier at the same point. A similar statement can be made about H_x , Eq (2.23).

Thus, at every time step ($\Delta t/2$), a complete set of either E or H fields is calculated for the entire problem space. This process is continued in time until a steady state response is reached.

For computational stability, Δt must satisfy the Courant stability condition (27:329; 64:303),

$$\Delta t < \frac{1}{V_{\max} (\Delta x^{-2} + \Delta y^{-2} + \Delta z^{-2})^{1/2}} \quad (2.24)$$

where V_{\max} is the maximum velocity of propagation in the medium. Eq.(2.24) means that the increment of the time steps must be smaller than the time it takes the wave to travel. This keeps the magnitude of the field finite differences small, so that the solution is stable. In other words, the finite differences are small because the passage of time was small enough to allow only small changes in magnitudes.

3. Boundary Conditions

Boundary conditions are necessary because space in general is infinite, but the computer has to have a finite number of values to make its calculations. An infinite space is simulated by truncating the problem space with carefully chosen boundary conditions. Examining Eq (2.22) and (2.23), it can be shown (as in Hebert's development of the propagation in one direction) that some type of boundary condition is absolutely necessary for the finite difference code (16). Without boundary conditions, the fields at the problem space boundary would be undefined and would not allow the calculation of the next field when stepping through the space. The end result is a decreasing data base of past fields from which to calculate the subsequent solutions.

There are numerous boundary conditions imposed by different authors in the algorithms of the finite difference codes. The first author that developed the finite difference algorithm, Yee, simply forced the outer problem space boundary to be a perfect conductor (64). This causes 'noise' in the solution, due to the reflections off the boundary (55:626). Others use a combination of Yee's, "hard" boundary conditions and "soft" ones, which reduce the reflection problem (55:626). The two "soft" boundary conditions considered are the absorption and the radiation boundary conditions.

Absorption Boundary Condition

The conductivity of the problem space is set to zero in the center, but at the outer edges it is set to some small value, such as that of distilled water (Figure 5). This has the effect of "absorbing" the fields to the point that the reflected waves from the outermost boundary will not perturb the solution of the fields in the center of the problem space.

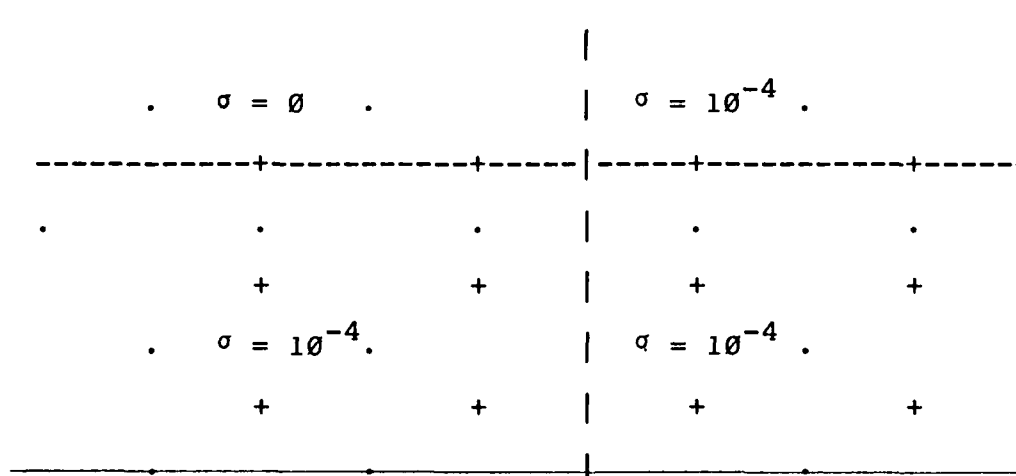


Figure 5. Finite Conductivity at Boundary Edges

This absorption boundary condition requires approximately one wavelength's distance to the boundary to simulate a low reflectivity surface (55:626). This additional size added onto the problem space greatly increases the computer memory

and time for calculations (55:626). This particular boundary condition was used in Rymes' code (48).

Radiation Boundary Condition

The radiation boundary condition uses a far-field approximation and the radiation condition to emulate an ideal infinite problem space. The general form of the radiation condition was originally introduced by Merewether (38:41). Bayless and Turkel have shown that the radiation boundary condition is a very valid mathematical technique (4). The form of the radiation boundary condition is: some function of time $f(t-r/c)$ divided by radial distance, r , from the center of the problem space (38:41).

$$E = \frac{f(t-r/c)}{r} \quad (3.1)$$

where

f = causal vector function

t = time

c = speed of light

r = large distance from the center of the test object

The function, ' f ', used by Merewether will be the one incorporated into the modified Rymes' code (38:42). The fields at the boundary are found by parabolic interpolation

in time, of the fields that are one cell in from the outer boundary, at $n\Delta t$, $(n-1)\Delta t$ and $(n+1)\Delta t$. This is expressed as E_z at the outer boundary point (i,j,k) , maximum j -plane boundary, in the y -direction as:

$$E_z^{n+1}(i,j,k) = \frac{R_z(i,j-1,k)}{2R_z(i,j,k)} f\{\theta, E(t)\} \quad (3.2)$$

where

$$\begin{aligned} f\{\theta, E(t)\} = & \theta_{zy}(\theta_{zy} - 1)E_z^{n-1}(i,j-1,k) \\ & + 2(1 - \theta_{zy}^2)E_z^n(i,j-1,k) \\ & + \theta_{zy}(\theta_{zy} + 1)E_z^{n+1}(i,j-1,k) \end{aligned}$$

$$R_z(i,j,k) = \{x(i)^2 + y(j)^2 + z(k)^2\}^{1/2}$$

$$\theta_{zy} = 1 - \frac{R_z(i,j,k) - R_z(i,j-1,k)}{c\Delta t}$$

and the x,y,z position coordinates for the outer boundaries are such that the coordinate system's origin is in the center of the problem space. The ' c ' here is taken to be the speed of light in free space, and Δt is the time elapsed since last grid position. Similarly, E_x can be expressed for this boundary. Two components, for each of the remaining five sides of the problem space, are also expressed in the same way. Eq (3.2) works for a constant

cell size problem space. More elaborate expressions are required for an expanding cell size grid (20:2419).

Implementing Eq.(3.2) into code turned out to be a major task. In fact, half the time spent on this thesis was devoted to simply understanding this radiation boundary condition. Researching the radiation boundary condition's origin, and then implementing it into the 3DFD computer code, was a much larger task than originally estimated. References were not found which specifically covered a non-uniform problem space. A non-uniform problem space in this text is one with three different size sides to each element's rectangular box. A major clue was found in a report by Merewether and Fisher (39:74). Looking at Eq.(3.2), the expression for θ contains a '1' and a $c\Delta t$. The expression directly coded into FORTRAN gave disastrous results.

This direct programing caused the calculated field magnitudes to blow up. In looking into the problem, it became obvious that $c\Delta t$ had to be different for each direction considered. This was taken care of by realizing that $c\Delta t$ was the distance traveled in the increment of time in a particular direction. This could simply be replaced by the space increment dimension over which the derivative was being considered. Note that the '1' now needs to represent an integer one higher than the quantity being subtracted away in the expression for θ (7:120). If this last

precaution is not taken, the sign of θ varies and the parabolic interpolation is incorrect. Detailed expressions can be found in Appendix B.

A smoother waveform is the expected result when using the radiation boundary conditions instead of the absorption boundary conditions. The reflected waves which are caused by the discontinuities at the changes in problem space conductivity, are expected to be reduced. Because of this, the interaction of the reflected waves should be greatly reduced or eliminated. In general, the reflective waves can be thought of as destructive and constructive interference of the output/resulting waveform. This interference is believed to be the cause of the abnormal magnitude variations. Therefore, reducing this destructive and constructive interference caused by the reflected waves should result in a smoother-appearing output waveform.

4. Modeling the F-16

The F-16 'Fighting Falcon' was chosen as the aircraft to be modeled in this thesis. The F-16 was chosen because of the current lightning susceptibility testing being conducted. The thesis sponsor, AFWAL/FIESL, was performing lightning strike tests on the new LANTIRN navigation pod installed on a F-16 (9). Another reason for the choice of the F-16 was due to its being the first operational fighter with a "fly-by-wire" flight control system. The high interest in the survivability of the "fly-by-wire" system after a lightning strike caused many studies to be performed, supplemented with many on-going efforts to protect this system (6). A large data base was therefore available for follow-on comparisons and studies. First, the problem space will be described in general. Then the choices which were made to model the F-16 in the time-domain finite difference problem space, will be explained. The last area to be covered will be the location of the ten sample points.

Problem Space

The problem space is made up of a rectangular area subdivided into 19,683 rectangular cells. The positions within this problem space are defined in terms of the Cartesian coordinate system. This particular choice of coordinate systems is well-suited to the finite difference formulation previously mentioned. The space is divided into rectangular grids referenced by integers such as $(i,j,k)=(1,1,1)$. The particular length of each grid is chosen to enhance the description of the geometry of the subject object. Each of the three directions is divided into the same number of grids, although this is not required. The best way to describe this is by an example. The program used for this thesis incorporates a $27 \times 27 \times 27$ ($=19,683$) grid space. In meters, the x-direction increment is 0.69 meters, y-direction is 0.22 meters, and the z-direction is 0.45 meters (Figure 6). Since the grids remain a uniform size in a given direction, this makes the overall physical size of the grid space 18.63, 5.94, and 12.15 meters respectively, in the x,y,z directions.

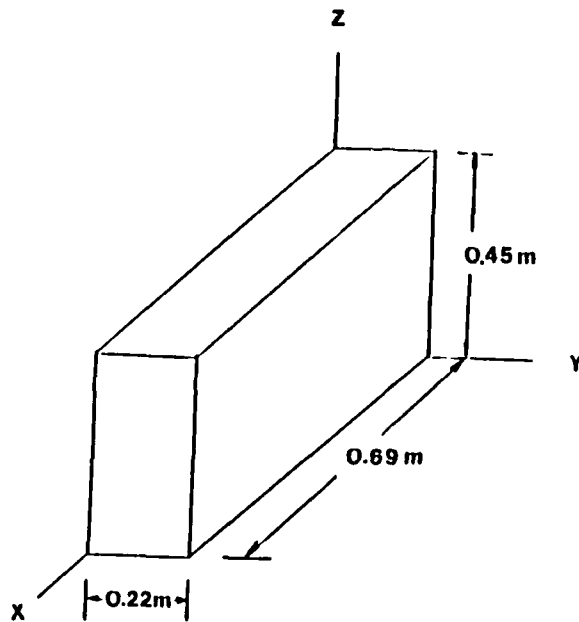


Figure 6. Basic Grid Block

The constraint of memory size and processing time are the main limiting factors for the number of grid divisions used (e.g., 27X27X27). Each of the 19,683 grid points has six fields associated with it. After one complete run of the program through the problem space, 118,098 fields have been calculated. This run through the problem space occurs at every time increment ($\Delta t/2$). The time step in this thesis was 0.366667 nanoseconds. A valid run may include up to two microseconds of data. More time results in large numerical errors (13:50). Two microseconds corresponds to 5455 complete cycles through the problem space. Clearly, this is already amounting to large amounts of memory and

central processor (CPU) time. When the amount of calculations per cycle is considered, the problem becomes evident.

The finest detail needed to be represented on the model determines the increment size in each direction. Complete descriptions can be found on the problem space in most finite difference users' manuals (18; 20; 29; 48; 60). These same users' manuals will contain information on implementing the most efficient dimensions for the problem space and element blocks. The 27 cubed problem space was used in comparing both the radiation and absorption boundary conditions. The aircraft was allowed to take up a large portion of the problem space.

The remainder of the problem space left a minimal number of rectangular blocks beyond the aircraft dimensions. The blocks outside the aircraft's dimensions are used for the boundary conditions. Using a minimum number of blocks is not a good practice in general, but was intentionally done to exercise the boundary conditions under a worst case scenario. In particular, only three blocks were used to implement the boundary conditions. The aircraft's maximum dimensions were extended into an aircraft grid space 21X21X21, centered in the 27X27X27 problem space. This leaves the 6 blocks (3 on each face of the box) in each direction for use in implementing the boundary conditions.

Field Locations

Each corner of a rectangular box in the problem space defines a set of fields (Figure 7). The 6 fields described are the 3 electric fields and the 3 magnetic fields in each vector direction. The fields are only defined by these points; they are not actually located there. The E-fields defined by point (i,j,k) are perpendicular and centered on the three sides of the rectangular box, not touching the defining point. The H-fields lie on the edges of these same sides most distant from the defining point. The directional nature of these 6 fields is as established by the coordinate system used (Figure 7).

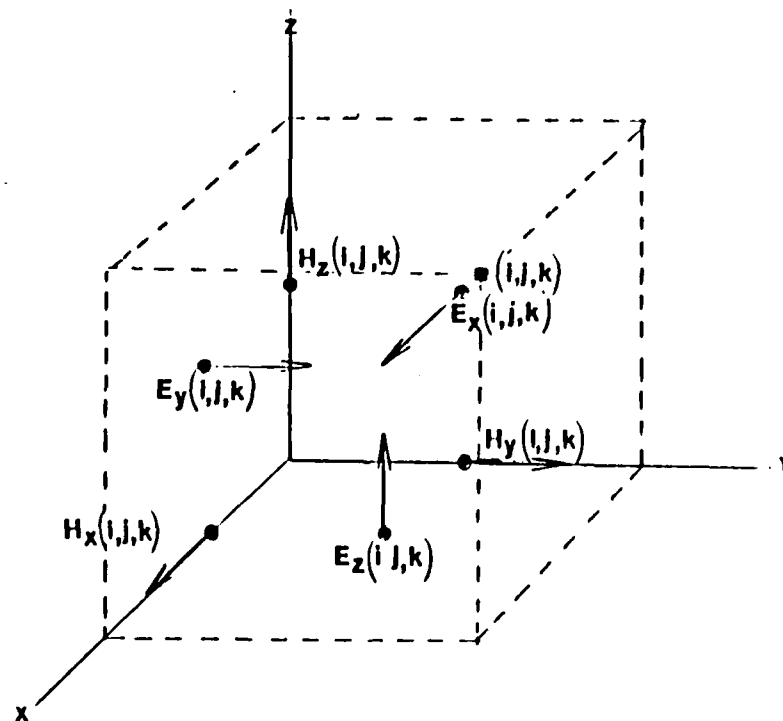


Figure 7. Field Locations with the Decentralizing Grid System

Cell Size Choices Made for the F-16

The F-16 is a very smooth, aerodynamically designed aircraft. This aerodynamic design consists of many curved surfaces (Figure 8). These curved surfaces presented a challenge to model with the rectangular blocks of the Cartesian coordinate system in the problem space. The F-16 has an overall length of 15.09 meters, width of 9.45 meters, and a height of 4.6 meters (Figure 8) (9:FO-3). The x coordinate is associated with the length of the aircraft (Figure 9). The x direction increment of 0.69 meters was chosen as a compromise to better model the geometrical structure of the wings in the xz plane (Figure 9). The y coordinate is associated with the height of the aircraft (Figure 10). The y direction increment of 0.22 meters was selected primarily to model the wing root area of the F-16 (Figure 10). The z coordinate is associated with the width of the aircraft (Figure 11). The z direction increment of 0.45 meters was chosen to model the detail of the speed brake and the base of the vertical stabilizer. The result of these choices was a good geometrical model which matches the F-16's predominant details (Figure 12).

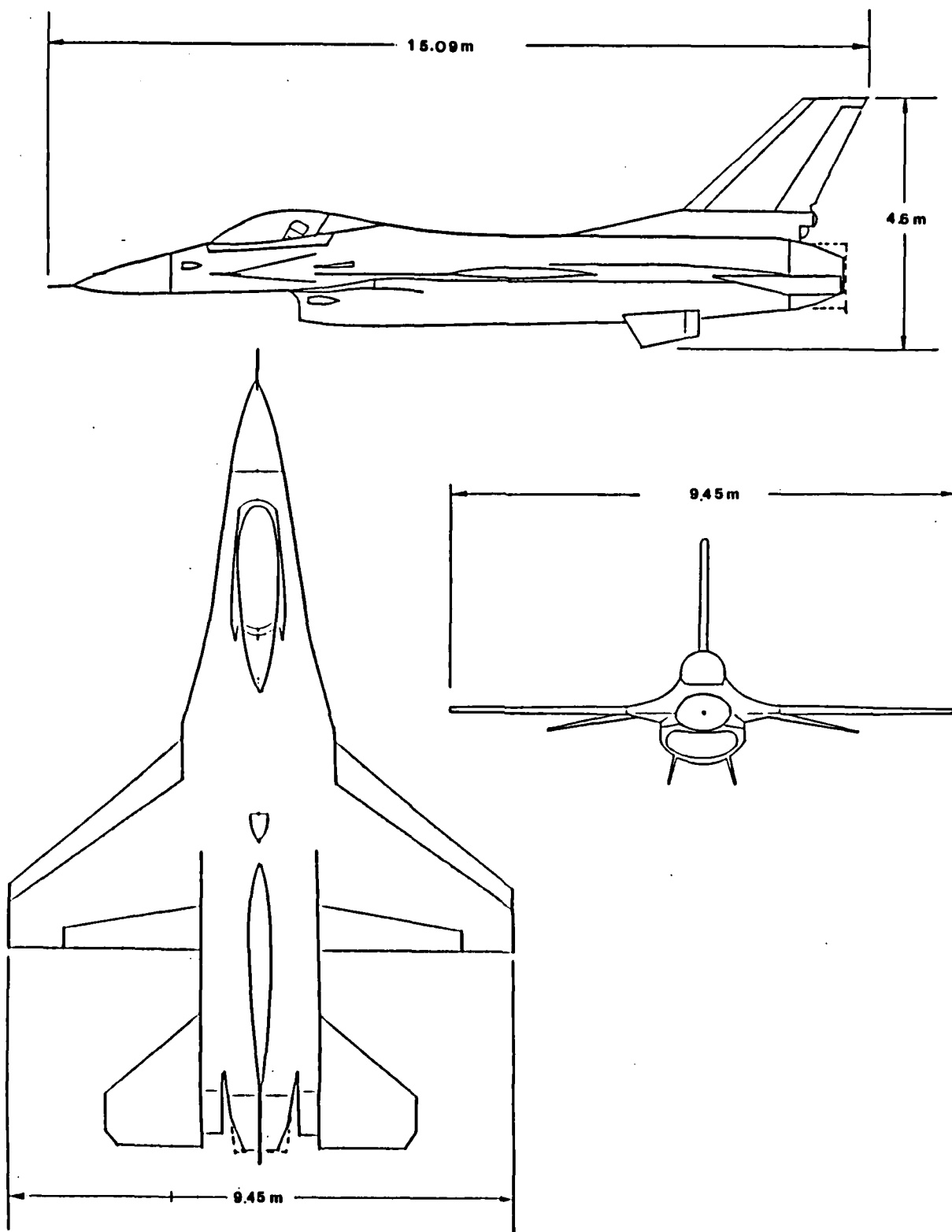


Figure 8. F-16 Fighting Falcon

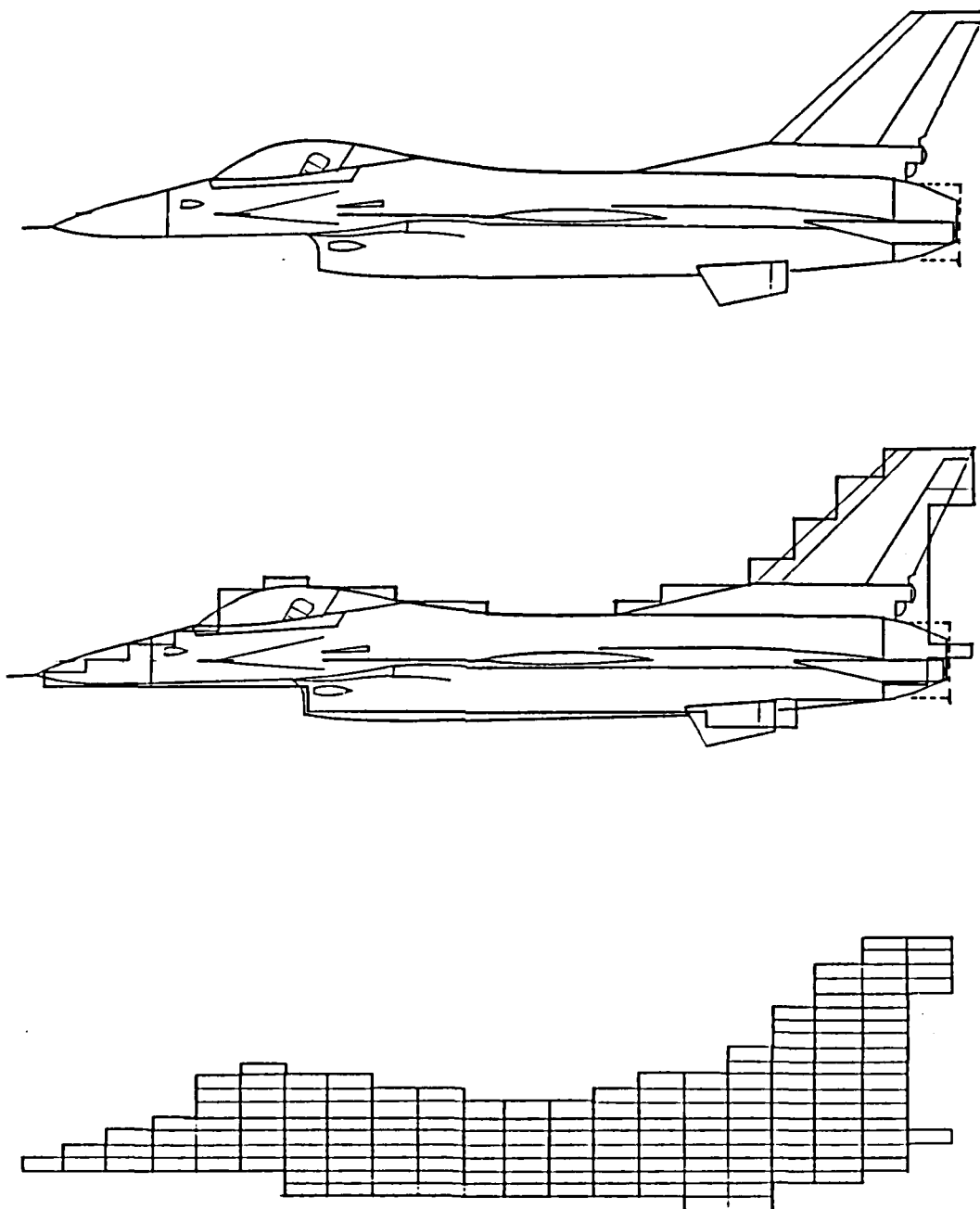


Figure 9. Gridding of the F-16, Side View

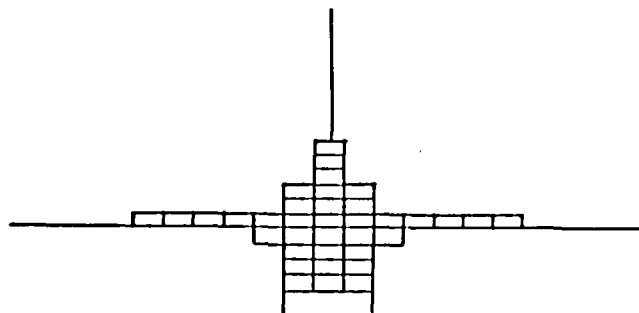
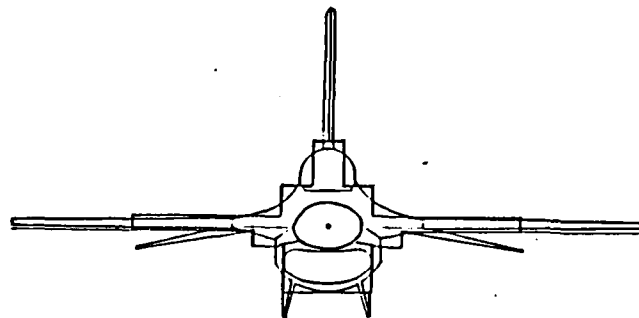
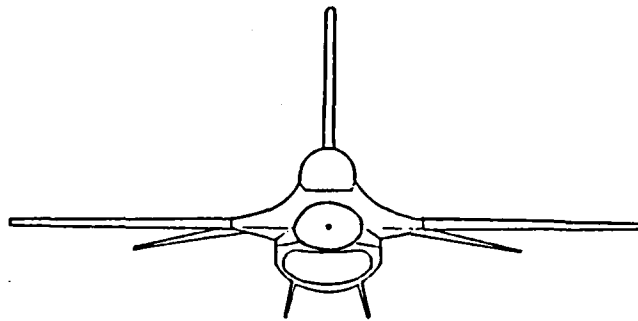


Figure 10. Gridding of the F-16, Front View

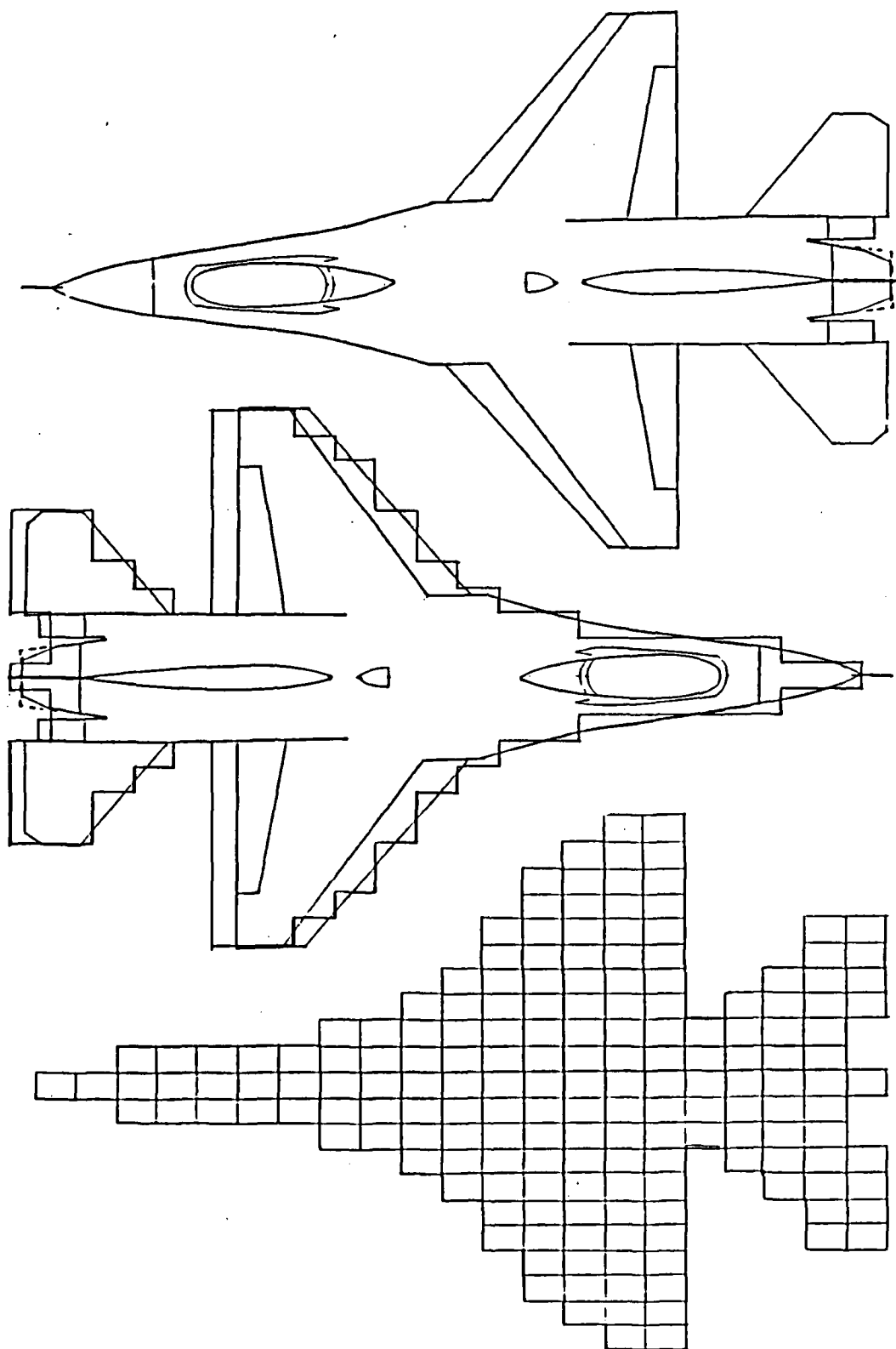


Figure 11. Gridding of the F-16, Top View

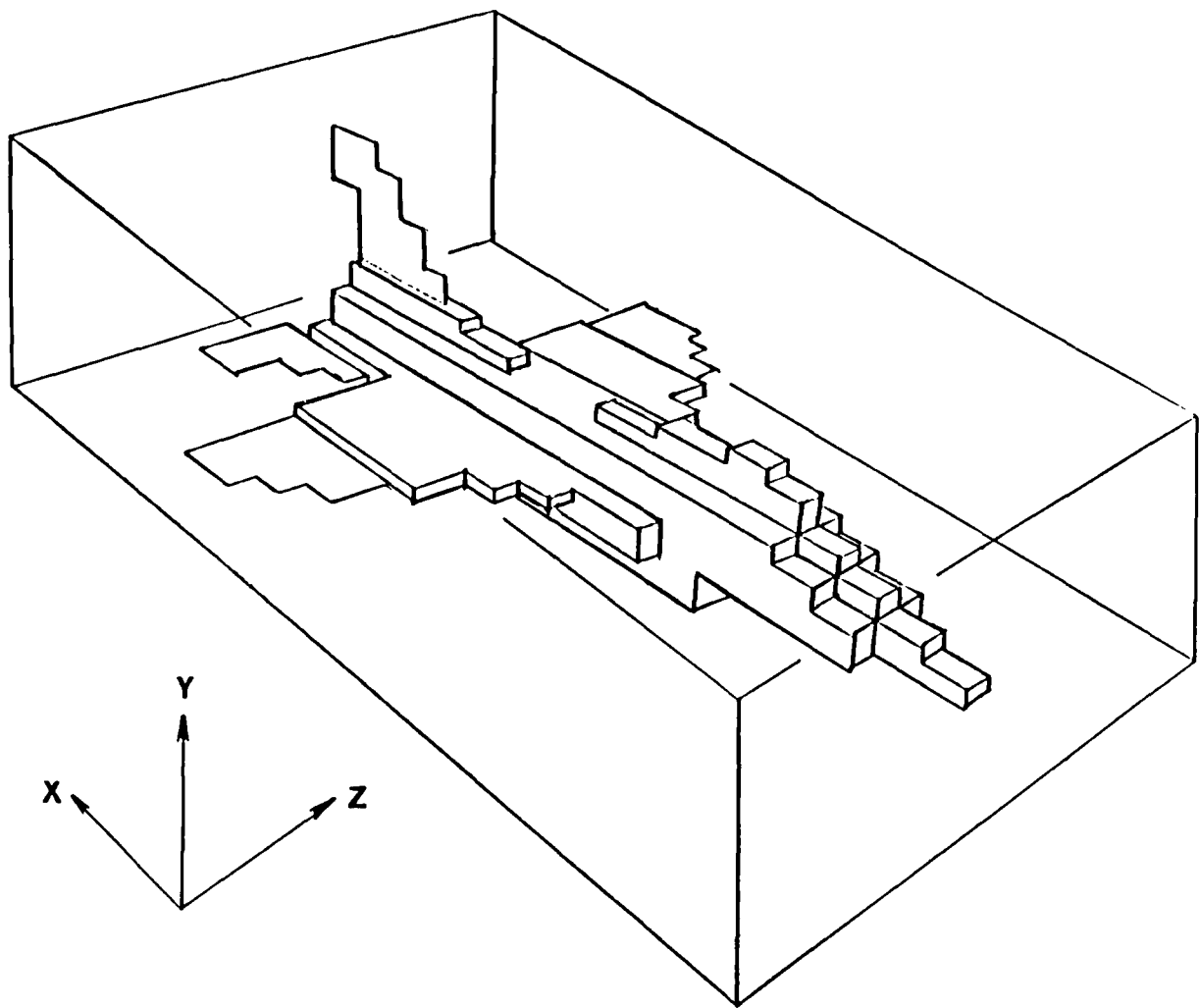
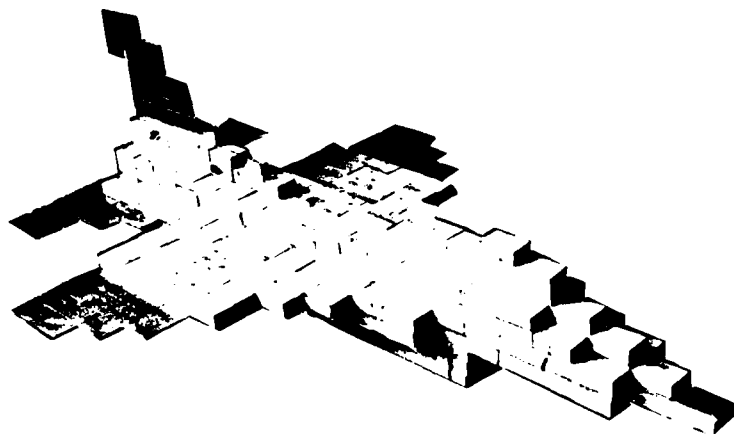


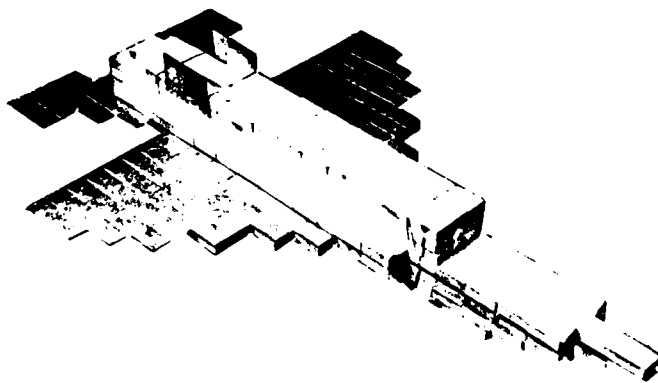
Figure 12. Three-dimensional Drawing of F-16 as Blocks

The aircraft is described to the computer in subroutine 'AIRPLN' (Appendix A). The description of the geometry of the aircraft is accomplished by defining the tangential E-

fields of the surfaces. The building of the model (Figure 13) was an extremely important step in defining the location of the tangential surface fields. Each field must be assigned by grid space location and magnitude. The tangential surface E-fields, surface normal H-fields and all interior fields are set equal to zero in the case of a perfectly conducting surface. Refer to Appendixes A and B for listings of all of the computer codes used, including the subroutine AIRPLN. A useful device for detailing the field locations was a clear plexiglas cube, with the field locations accordingly marked such as Figure 1. Another technique used in modeling the F-16 was to take the wood and metal model and position the xz-planes, or layers, of the mock-up on a scaled grid plane. This enabled actually seeing where the fields were physically located. The coding of the subroutine AIRPLN and understanding the field locations was greatly simplified with this technique.



(a) Top View



(b) Bottom View

Figure 13. Photograph of F-16 Block Model

5. Program Details

The modified Rymes' code was reviewed in great detail. Some changes were made to the modified code before running the F-16 with the absorption boundary conditions. The code was then modified to include the radiation boundary conditions. The sensor locations were selected and encoded in subroutines 'EADV' and 'HADV'. Lastly, the source was updated to reflect parameters recently measured in flight (8; 17; 47; 49).

Basic Code

The assumptions made about the modified Rymes' 3DFD code were basically sound. In reviewing the modified code, only a few minor omissions and corrections were made. The results after complete computer runs on the F-16 model were as expected. The changes made to the modified code with the absorption boundary conditions enhanced the results (Appendix C). A completely updated and corrected copy of the code is in Appendix A.

Boundary Conditions

After running the code with the absorption boundary condition, the radiation boundary condition was implemented. The specific listing can be found in Appendix B, subroutine 'RADBC' and 'HADV'. A significant amount of time was spent in transforming the rather simple-appearing parabolic interpolation of (Eq 3.2) into Fortran 77 code. The basic problem was caused by a lack of details in the literature. The missing details were definitions of time increments in relation to the three different dimensions of the basic problem space block (Figure 6). In particular, the calculation of ' θ ' is very sensitive to the definition of $c\Delta t$ (Eq 3.2).

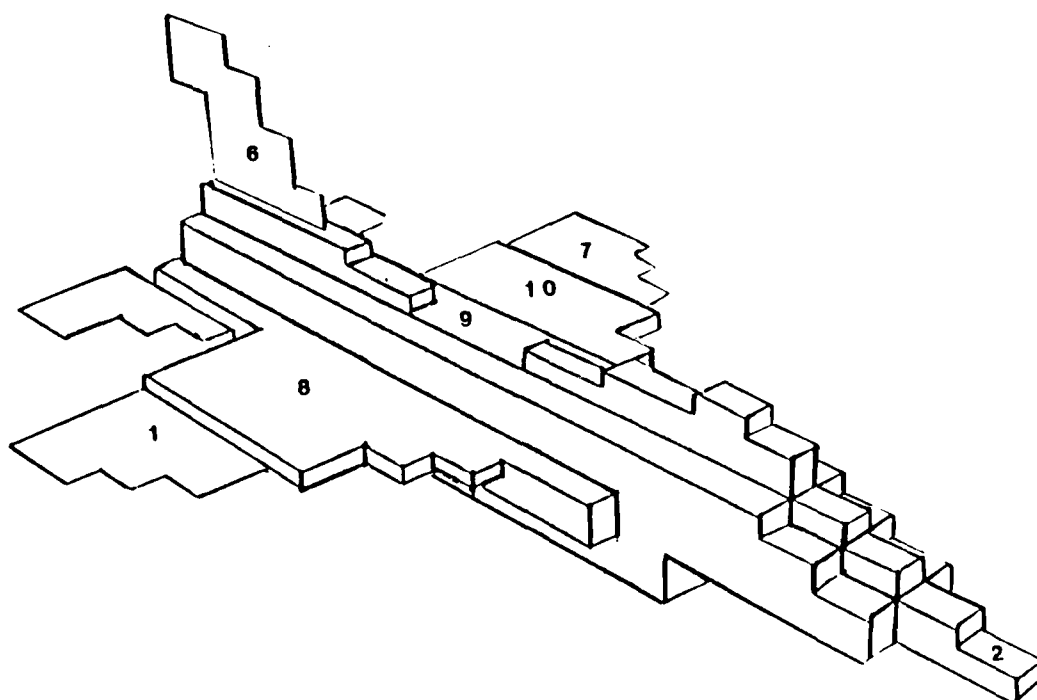
Sample Point Locations

Ten locations were selected as typical for field sensor layouts on the aircraft. Similar locations were used in a CV-580 flight test conducted by AFWAL (16). Any of the three orientations of either the E-field or the H-field could have been selected at any point in the problem space for monitoring. The selections made are detailed in Table 1.

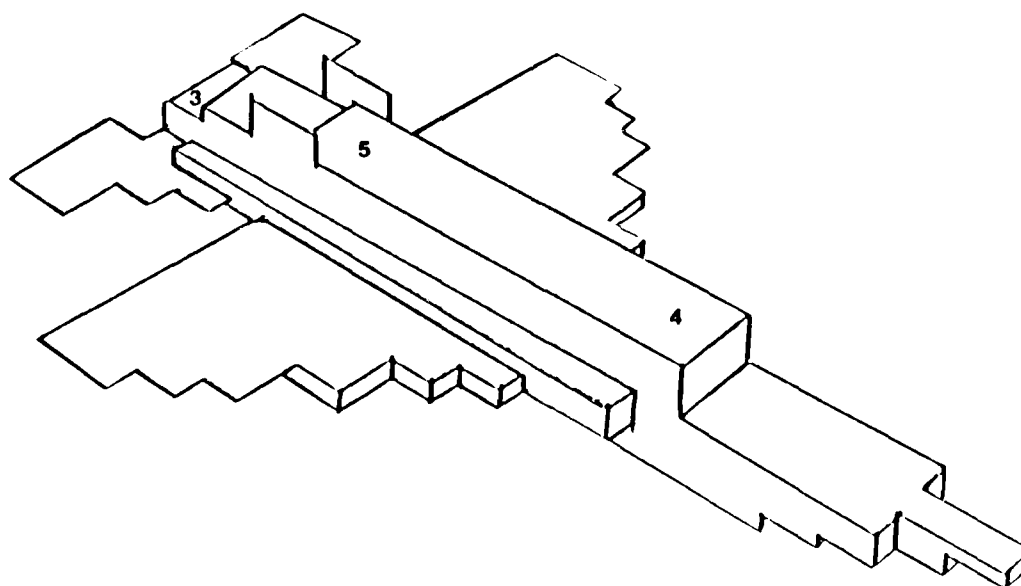
TABLE 1. Ten Sampled Points

Sensor #	Type H or E	Location Description	Direction Component	Coordinates (i,j,k)
1	H-field	right wing	x	(18,10,6)
2	H-field	nose	z	(4,10,13)
3	H-field	engine feathers	z	(24,11,13)
4	H-field	bottom fuselage	z	(10,4,14)
5	H-field	bottom fuselage	z	(19,4,14)
6	H-field	vertical stab	x	(22,18,14)
7	H-field	left wing	x	(18,10,23)
8	E-field	right wing	y	(17,11,10)
9	E-field	top fuselage	y	(15,13,14)
10	E-field	left wing	y	(17,11,18)

The sensor locations are shown in Figure 14. Appendix A, subroutine 'EADV' and 'HADV' show the code used to sample these points at each time step. This sampling will be found under 'sample points of interest' at the end of both subroutines.



(a) Top View



(b) Bottom View

Figure 14. Sensor Locations on a Block F-16 Model

Source Function

A couple of the changes made to the code were in the source function. The "transparent" source function utilized in the modified Rymes' code caused some unnatural growth in the response (19). The so-called "transparent" source added the scattered fields to the source fields, resulting in an ever-increasing source function. Modifications made in the code appearing in Appendix A corrected this growth and gave much better results. The risetime (10% to 90% of the maximum amplitude) was changed to 100 nanoseconds (Figure 15). This was found, by AFWAL measurements, to be more characteristic of cloud-to-cloud lightning strikes (8:128). The normalized source function is plotted in Figure 16 out to the 50% falloff point, which occurs at 20.4 microseconds.

Numerous programs, or researchers, use this double exponential as the source function, which is sometimes called the 'Bruce-Golde' model (8:36). This source function emulates a lightning strike's characteristic waveform (19). The source is attached to the aircraft with a surface current injection technique, as described by Kunz (30:1423). This surface current injection technique is basically accomplished by inserting an H-field into the grid space boundary conditions. The insertion of the H-field takes place around the point that the lightning attachment is being simulated. The H-field is approximated from the

relationship, $H = I/(2 r)$; where 'I' is the time-varying, analytical current model for the lightning channel desired, and 'r' is the radial distance from the point of desired injection to the nearest H-fields surrounding that point (24:165).

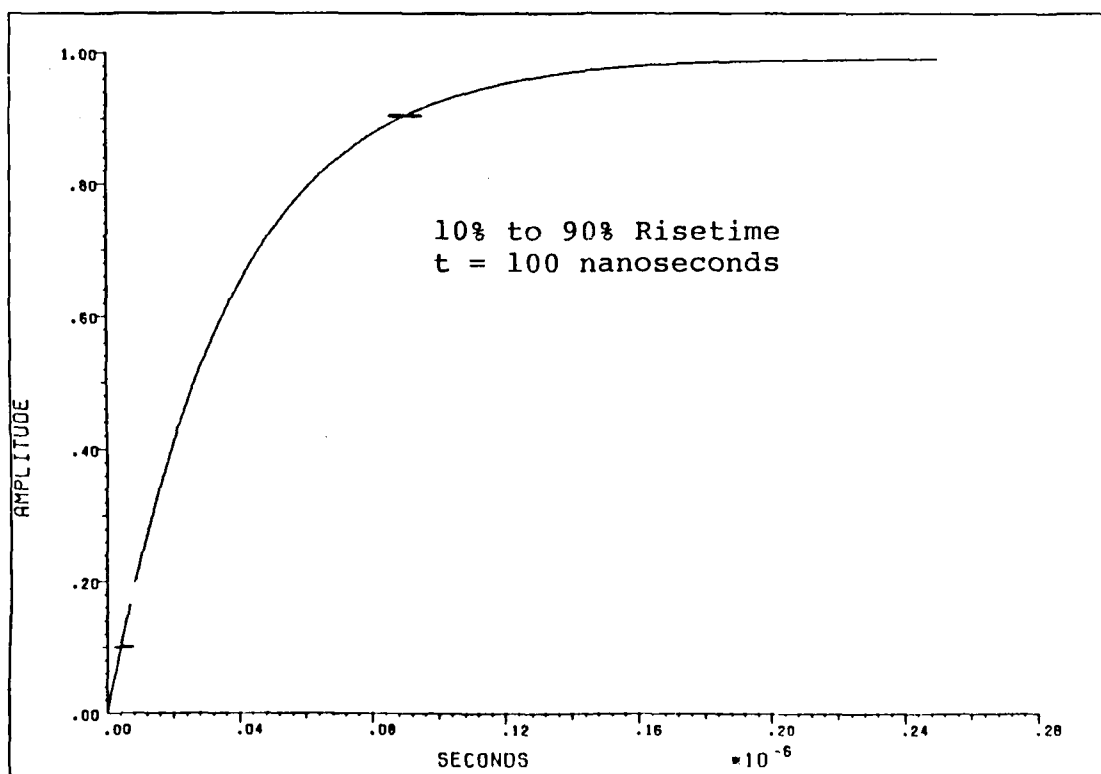


Figure 15. Expanded Plot of Source (First 250 nanoseconds)

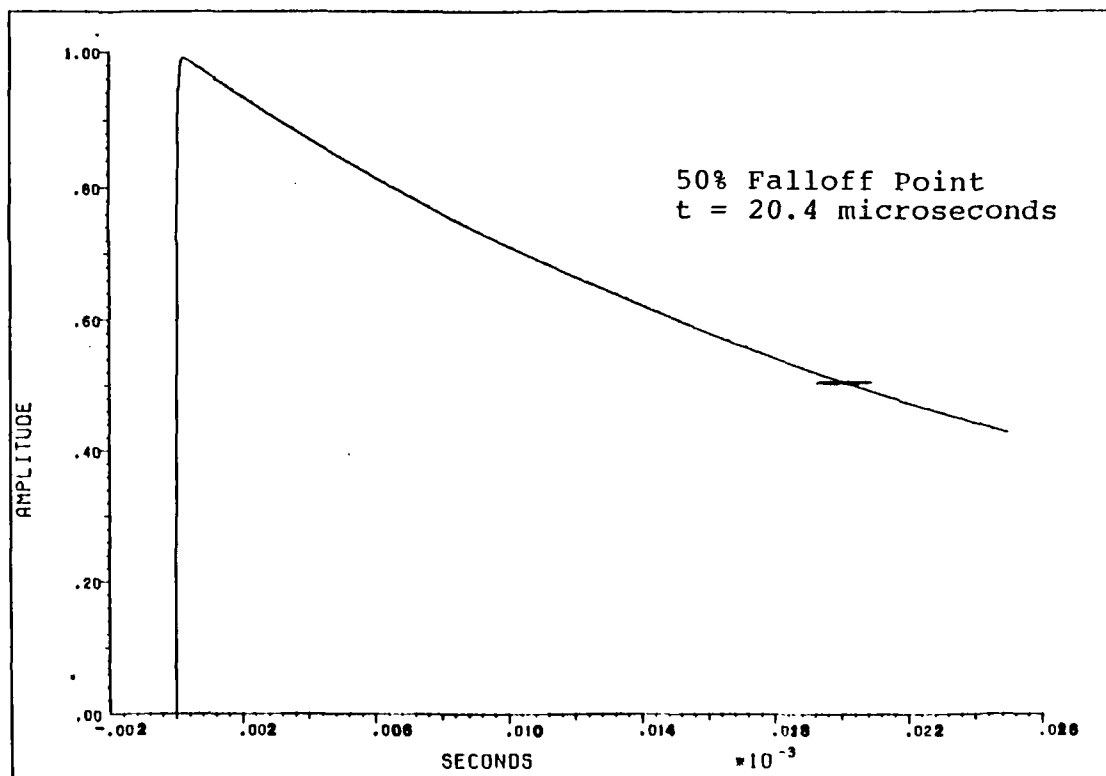


Figure 16. Normalized Double Exponential Source Function

6. Analysis

The result of implementing the radiation boundary conditions appears to be an improvement over the absorption boundary conditions results. The absorption boundary condition results contain many fluctuations in amplitude that can be attributed to the boundary conditions (19; 55). When the waves travel and hit the discontinuity at the element rectangular cells which have increased conductivity, they reflect back with a discrete magnitude. These reflected waves cause the additional amplitude fluctuations not found with the radiation boundary condition. All ten sensors showed the same results: a general smoothing of the amplitude of the response on the aircraft's skin (Appendix C). All the field plots (Appendix C) had the same basic shape before and after the boundary conditions were changed. The first 300 nanoseconds of each field's response are plotted in this chapter (Figure 17 thru Figure 26). Each sensor's response is plotted on the same graph for both absorption boundary conditions and radiation boundary conditions. The absorption boundary condition plots are annotated with an '*'. The smoother response of the radiation boundary condition resembles the MIE solutions as calculated by Holland (20:206). Note that the disparity in the polarity of the E-field response (sensor 8 & 10) was possibly caused by a resonance effect in the wing region.

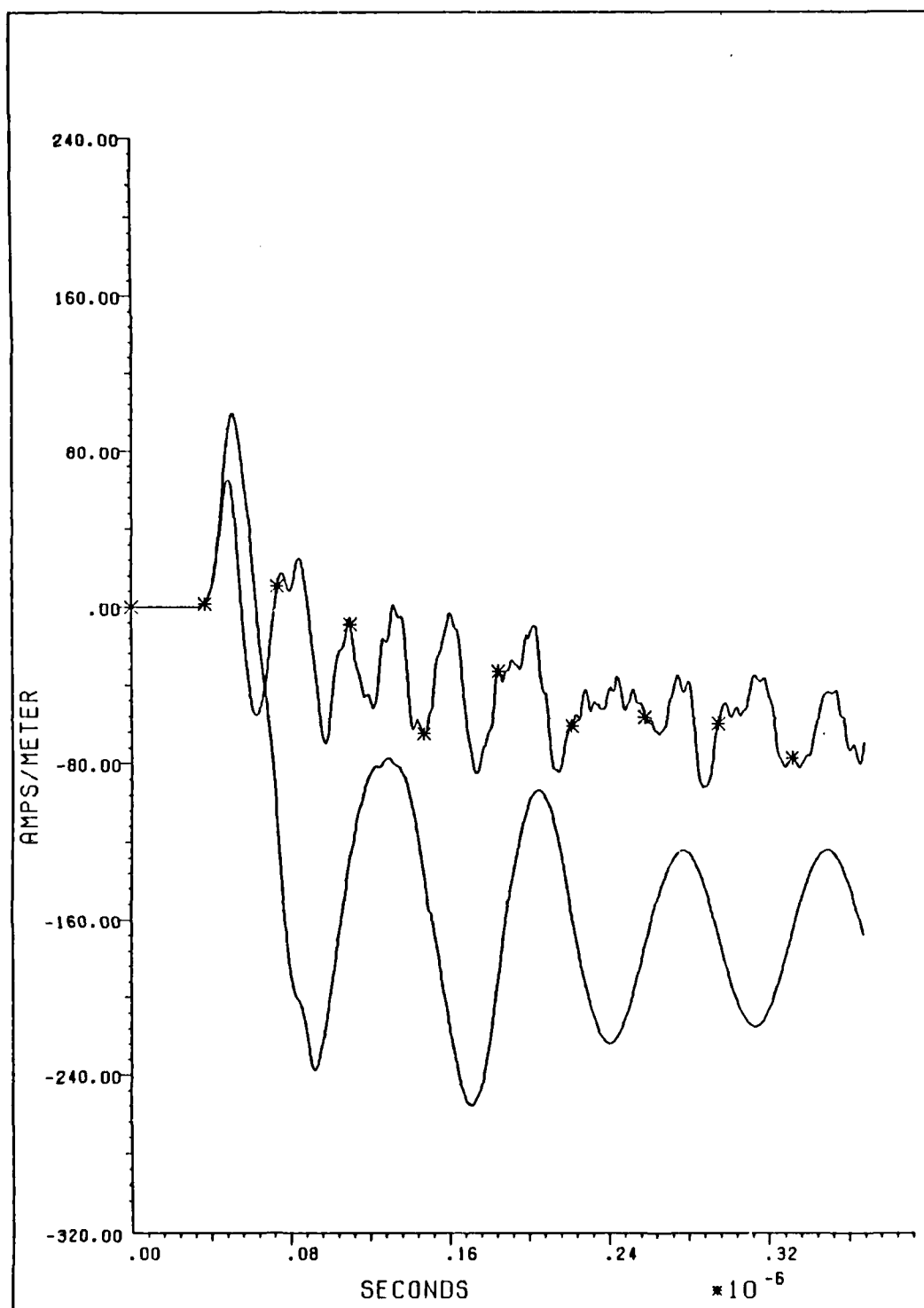


Figure 17. Sensor One, H-field, Right Wing

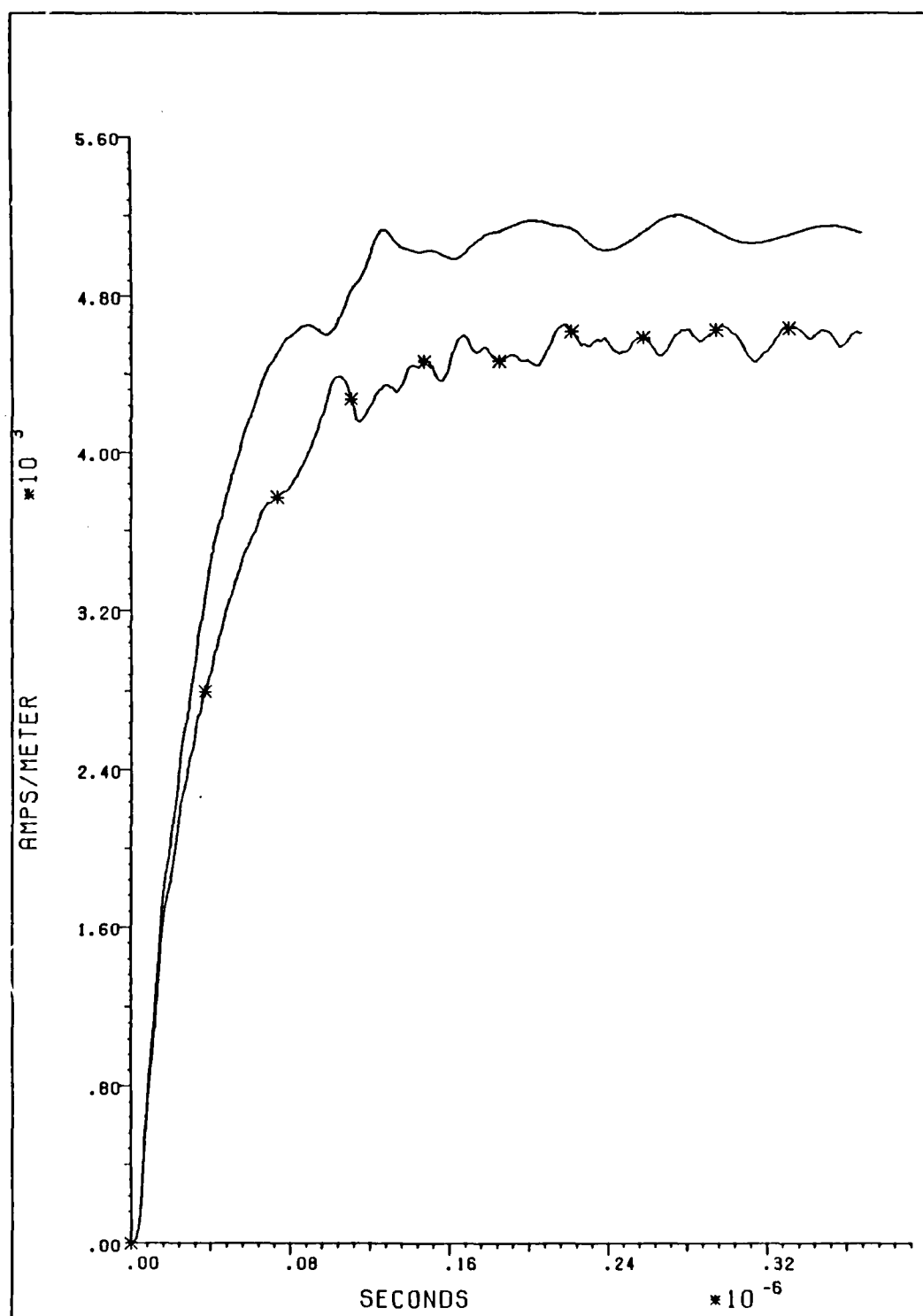


Figure 18. Sensor Two, H-field, Nose

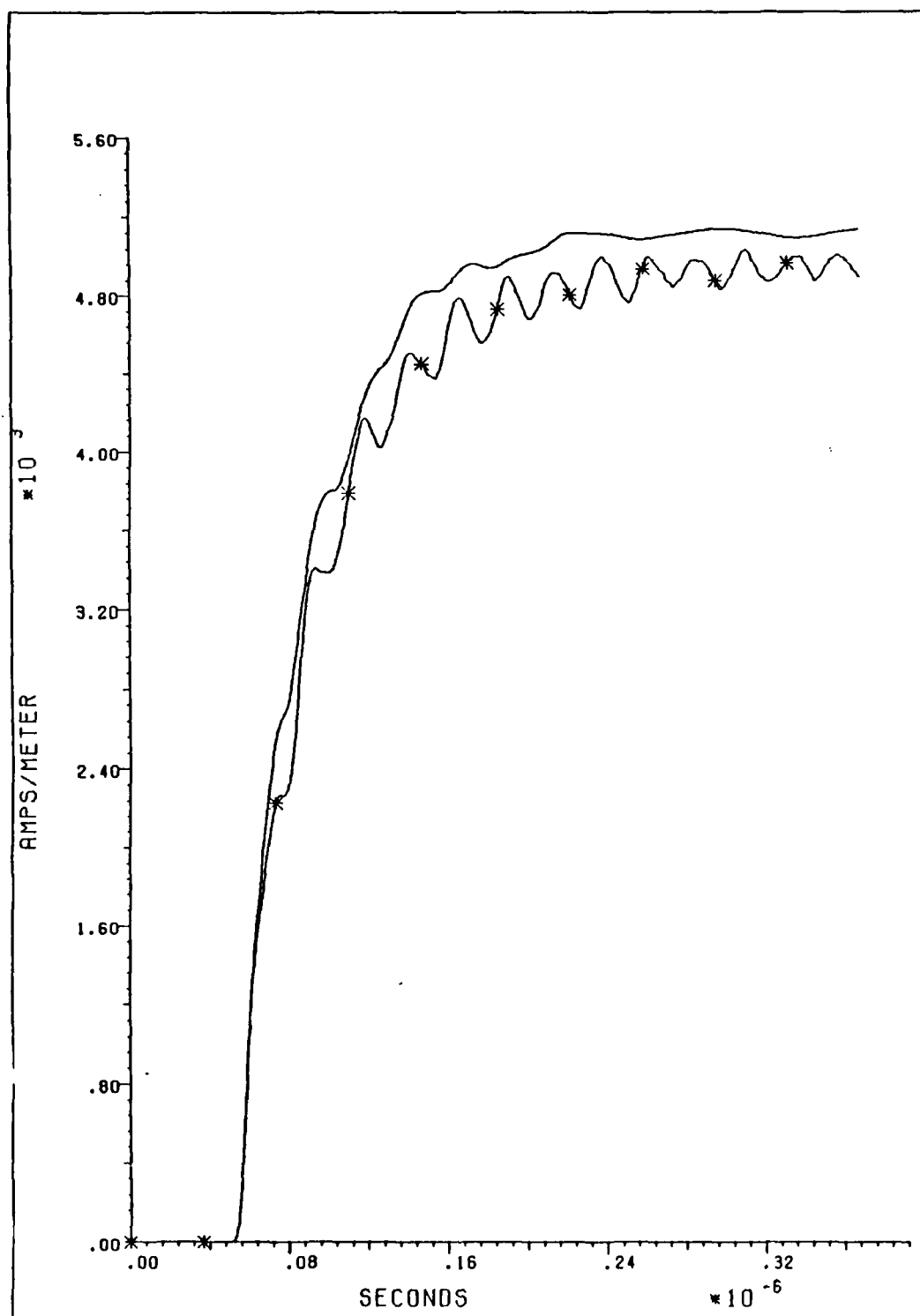


Figure 19. Sensor Three, H-field, Engine Burner Can

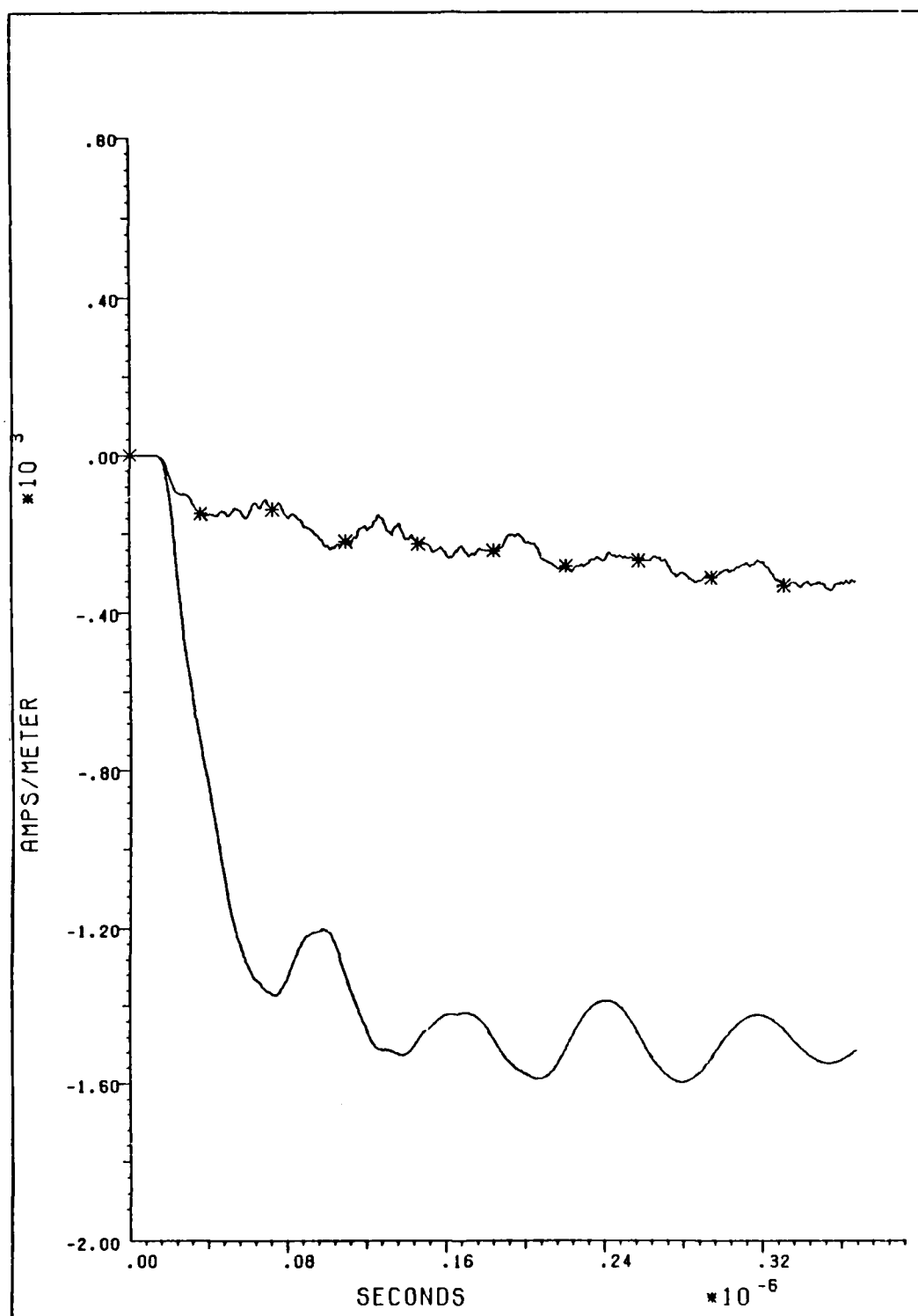


Figure 20. Sensor Four, H-field, Forward Fuselage Bottom

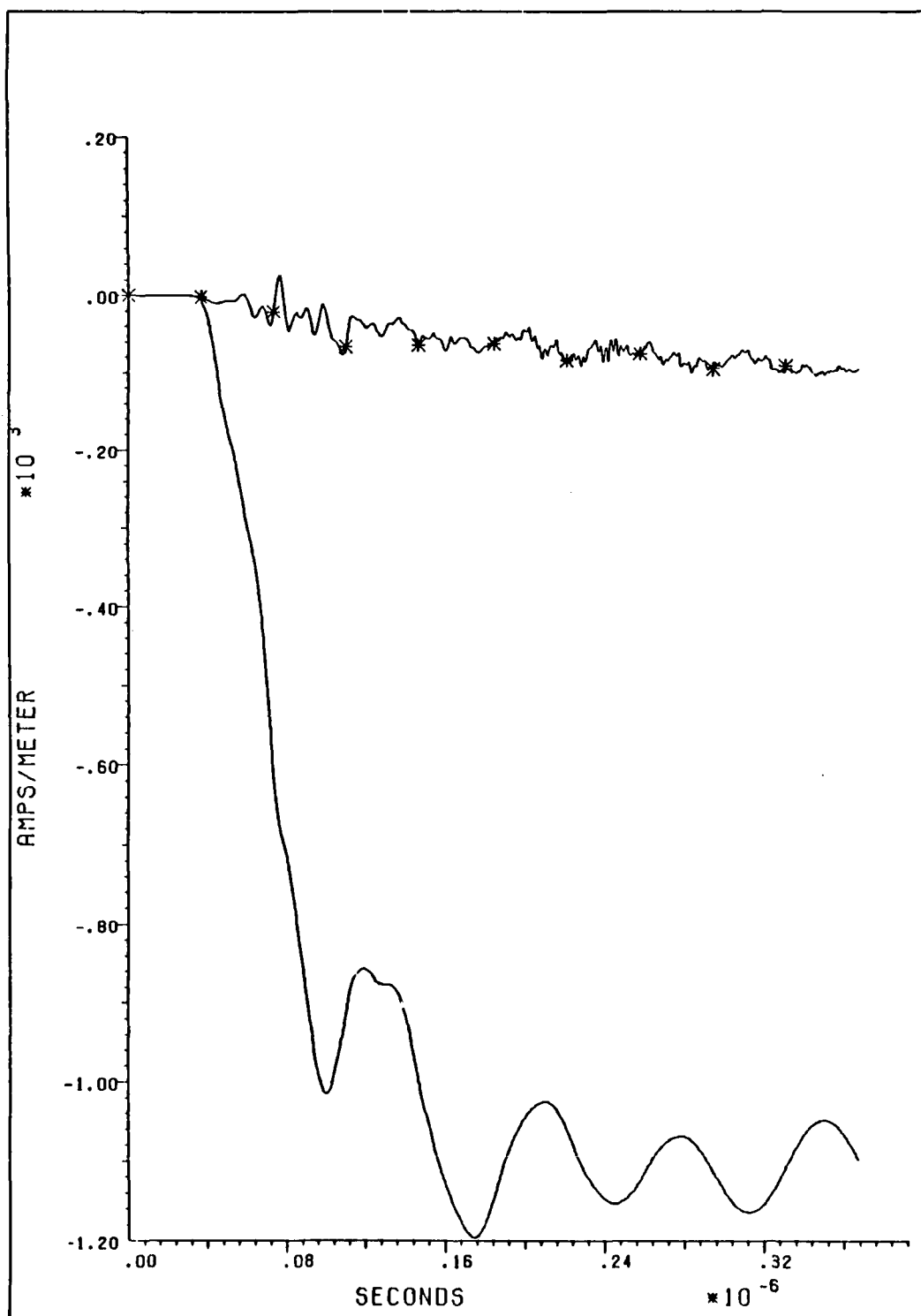


Figure 21. Sensor Five, H-field, Rear Fuselage Bottom

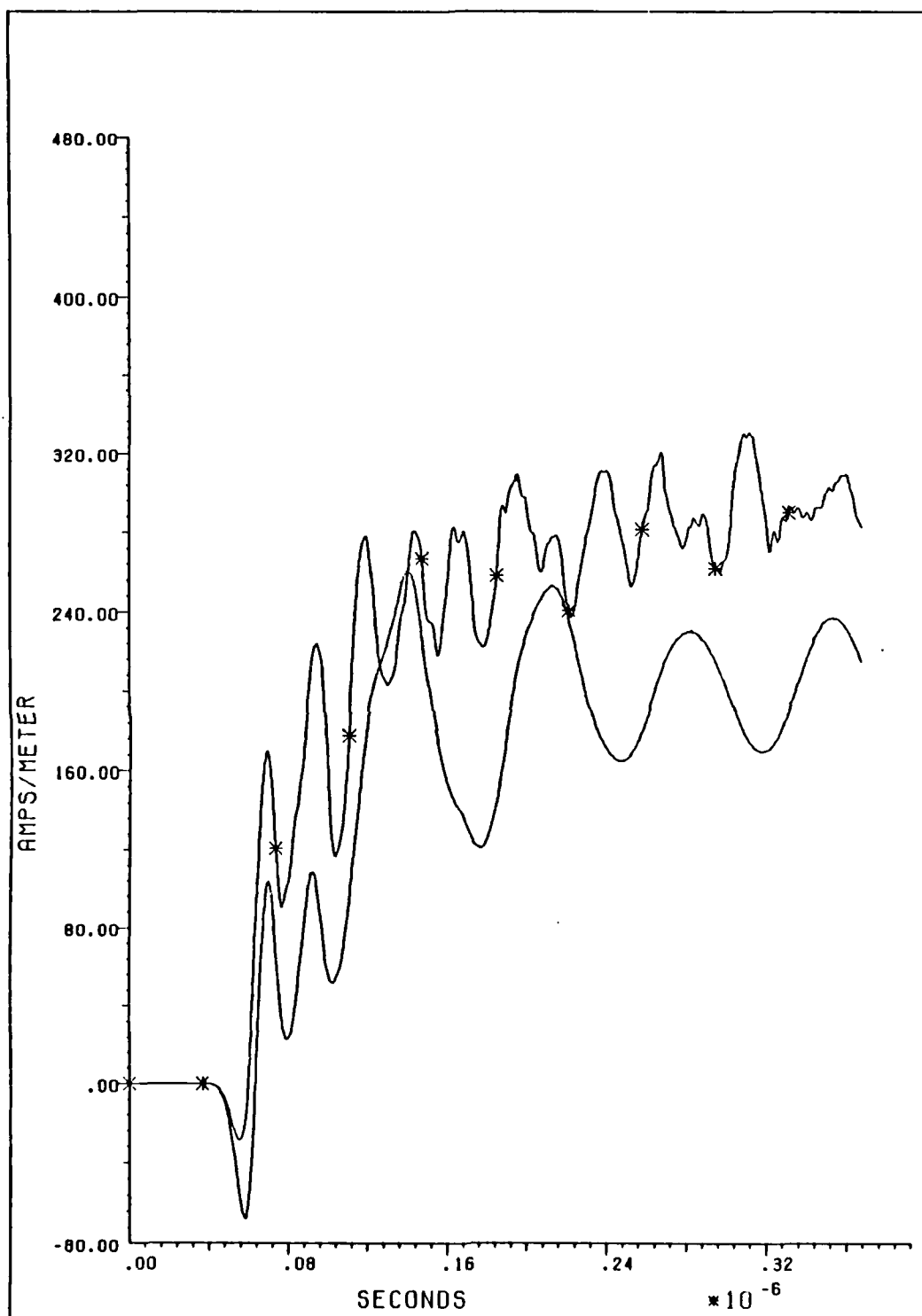


Figure 22. Sensor Six, H-field, Vertical Stabilizer

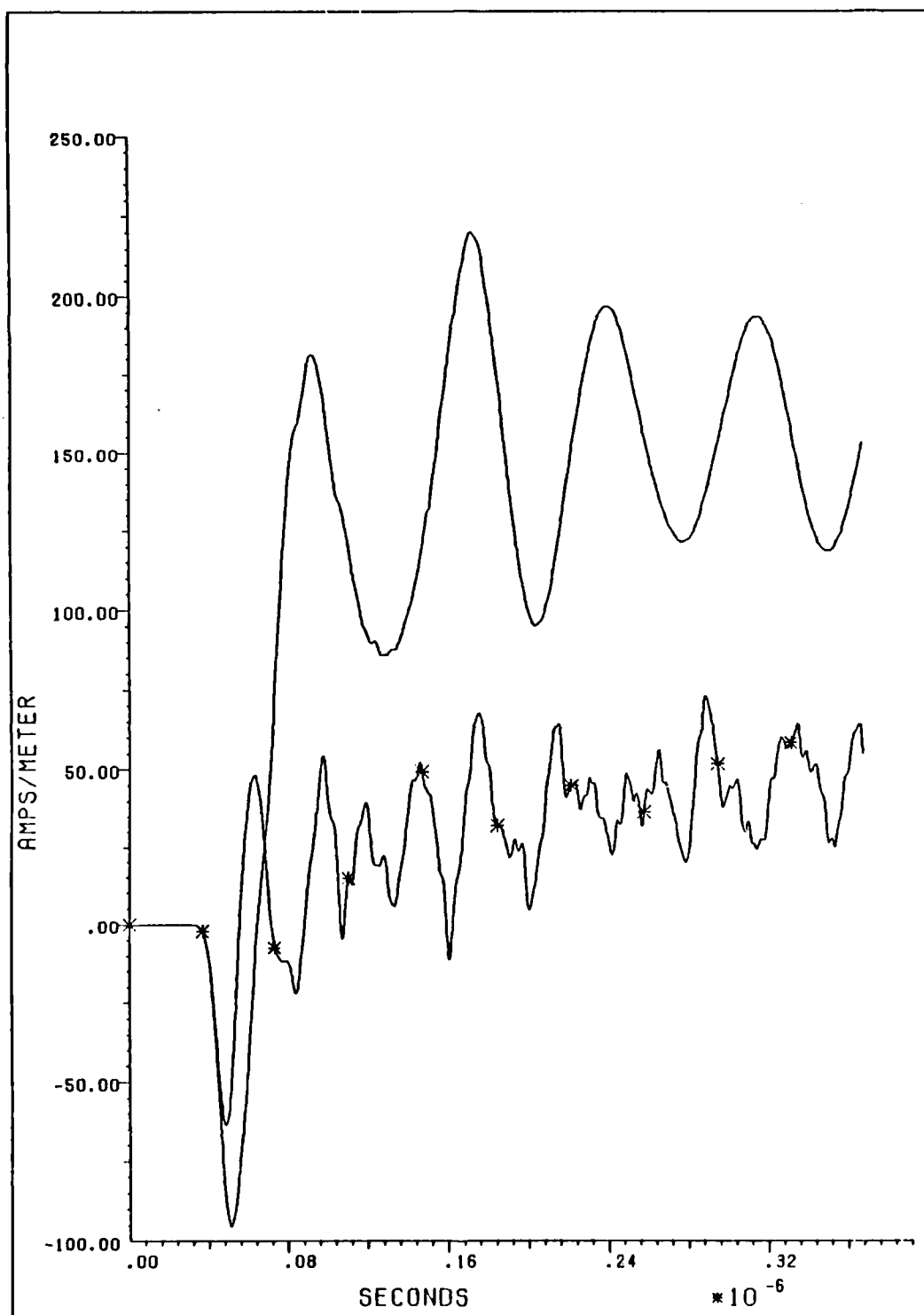


Figure 23. Sensor Seven, H-field, Left Wing

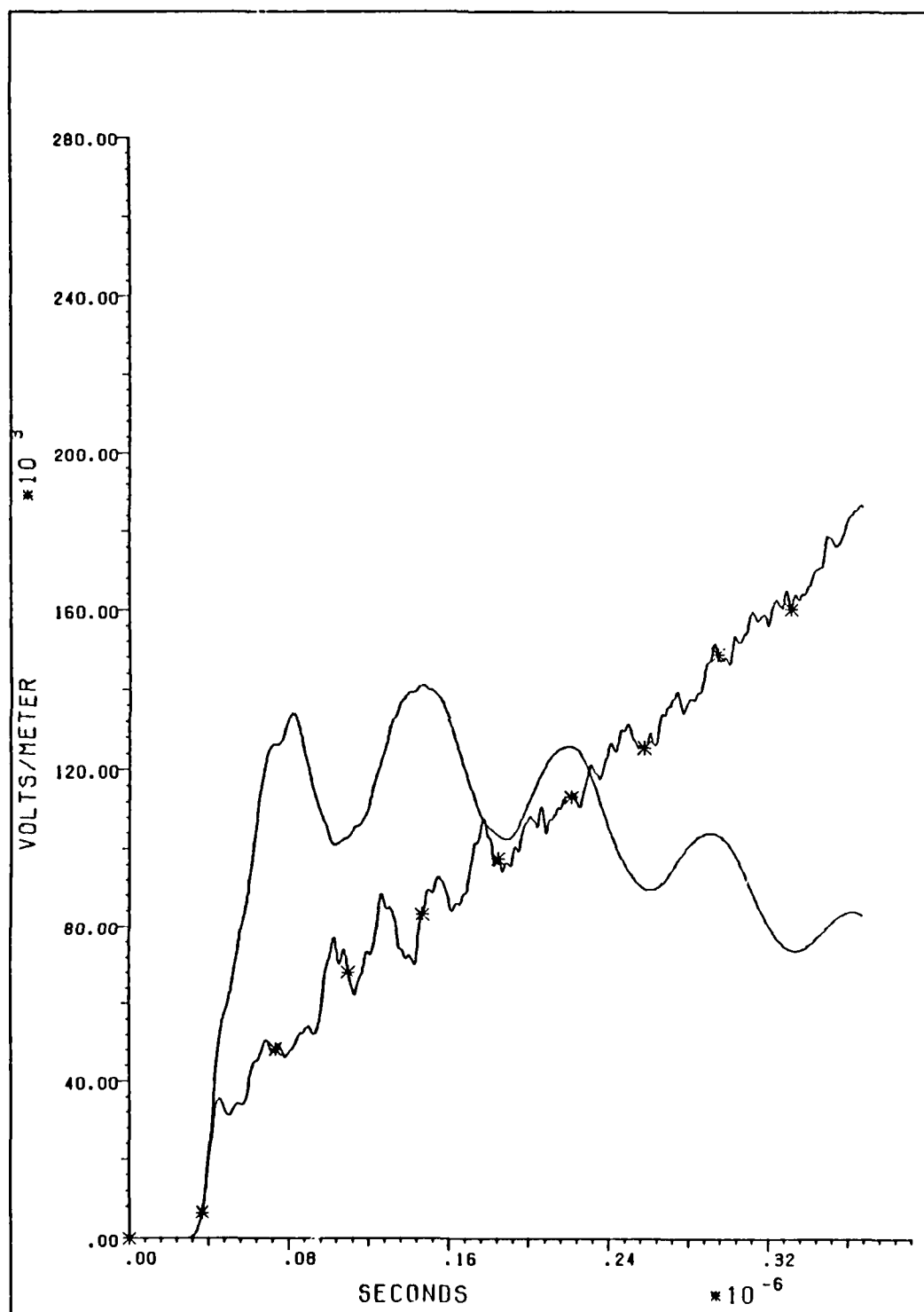


Figure 24. Sensor Eight, E-field, Right Wing

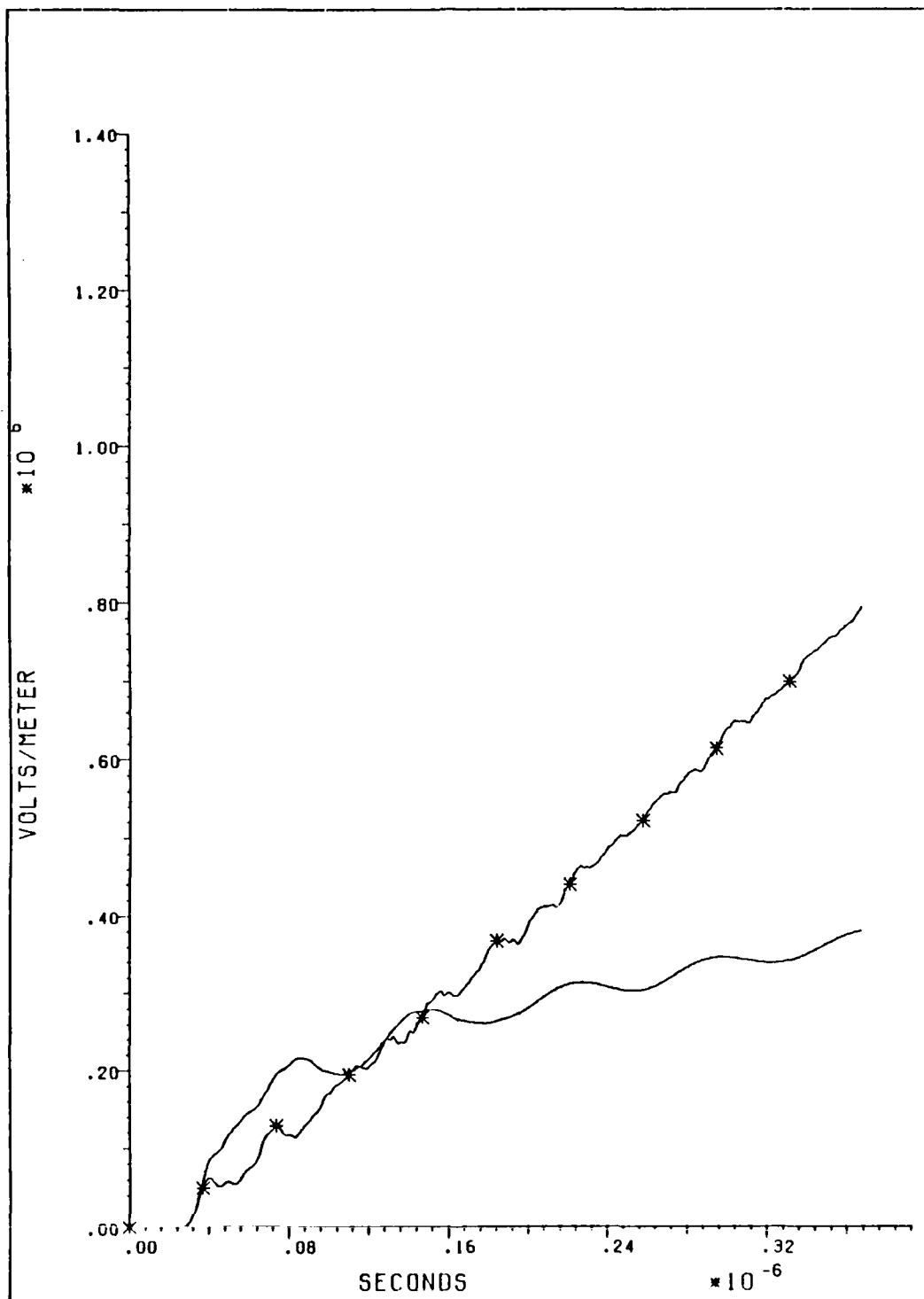


Figure 25. Sensor Nine, E-field, Middle Fuselage Top

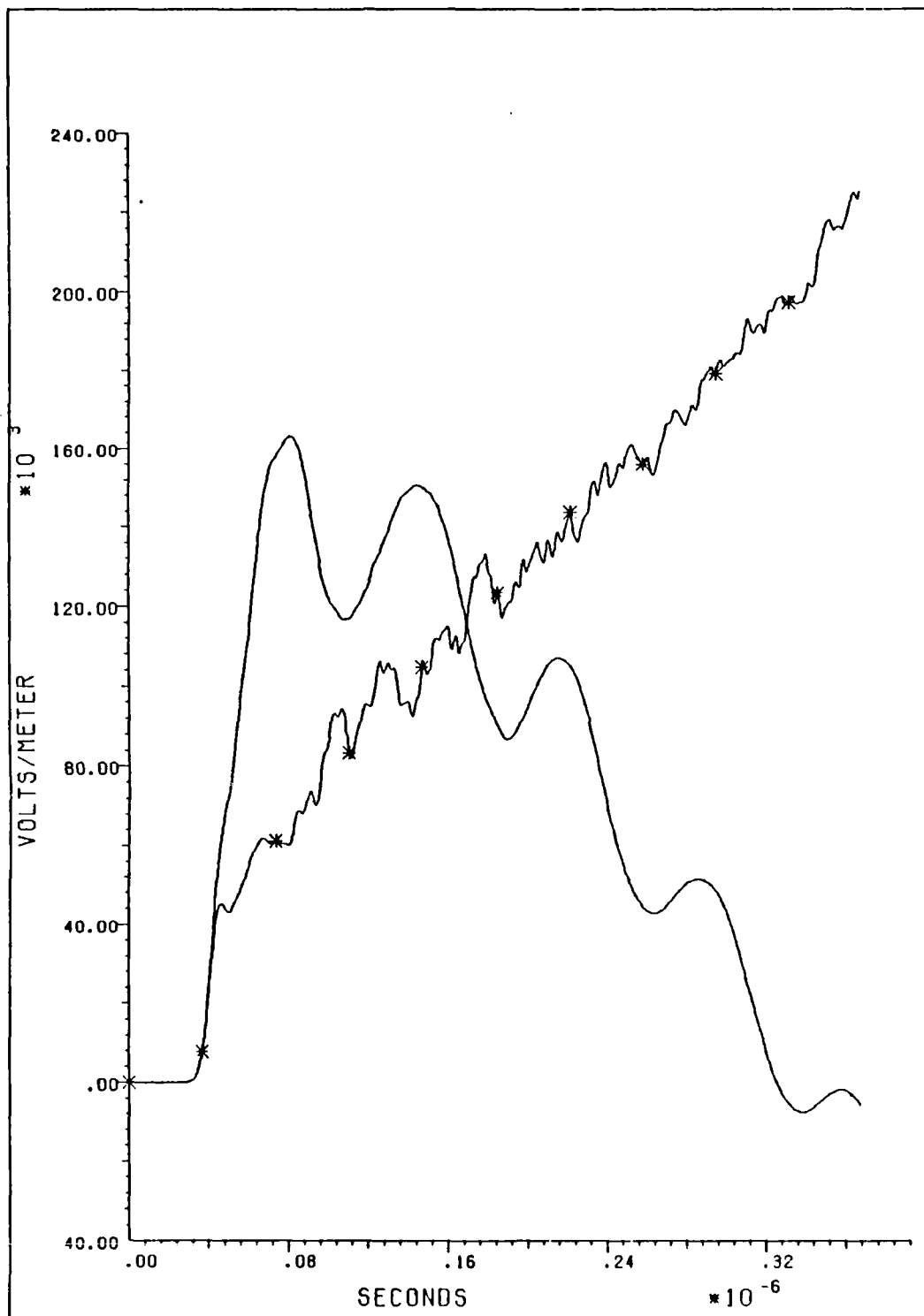


Figure 26. Sensor Ten, E-field, Left Wing

Waveform Appearance

The general appearance of the responses from the different boundary conditions was dramatic. The amplitude oscillation frequency of the radiation boundary condition response was less distinct than that of the absorption boundary condition. As Figure 17 thru Figure 26 display, the radiation condition gave a much smoother response. The overall response for the entire two microseconds of each of the computer runs was consistent. In each and every graph of the response, the radiation boundary condition curve was smoother and settled to a steady state response much quicker than that of the absorption boundary condition.

Note also that the amplitude, in general, of the radiation boundary curves are higher than those of the absorption boundary condition. This lower absorption amplitude was due in part to the source itself being absorbed. That is, the source actually goes through a couple of element blocks which have a finite conductivity. However, a small portion of the amplitude differences could be due to constructive and destructive interference of the reflected and surface waves.

The absorption boundary condition's H-field response of Figure 17 has an average period of 3.6 nanoseconds, which corresponds to a wavelength of 1.08 meters. The radiation boundary condition's H-field response for the same time span is different (Figure 17). It has a average period of 7.2 nanoseconds, which corresponds to a wavelength of 2.16 meters. Using the aircraft's length as the predominant resonance structure, the wavelength of the response calculated for radiation boundary conditions was a quarter wavelength multiple of the aircraft's length. The absorption boundary condition did not have this same relationship, as its multiple was in thirds of the aircraft's length. This is only a general conclusion. Time did not permit taking the major surface dimensions of each sensor's local area, and correlating the calculated field response's frequency to the major local surface dimensions. But, the result is as expected; that is, the major geometrical object's characteristic wavelength will dominate. More time would have permitted looking at the problem space's dominant cavity frequency, and its contribution to the response curve's shape.

Program Considerations

Implementing the radiation boundary conditions has many effects. One positive effect was just discussed, that of smoothing the response waveform. Other effects, such as increased storage and run time, are not desirable. The amount of storage for running the program of Appendix A with its absorption boundary condition is doubled when the radiation boundary condition is implemented. An additional 363 lines of code were added to the program, to implement the radiation boundary condition. The worst effect was the CPU time per 100 nanoseconds of program time increased by 25% for the radiation boundary condition over the absorption boundary condition. Table 2 contains some details from the CDC Cyber 845 after the first 100 nanoseconds of data was calculated. No claim is made that any code optimization for run time, speed or memory utilization was attempted. However these times are comparable to those given in Eriksen's report (13:50). This is a first attempt at a comparison on the same code with only the boundary condition changed. The similarity of the plots at each sensor alone, support the validity of the program as modified with radiation boundary conditions.

TABLE 2. CDC Cyber 845 Computer Run Data

	Absorption Boundary Condition	Radiation Boundary Condition	Percent Increase
Time elapsed within program	100 ns	100 ns	-
SRU's CDC 845	8388.6	11534.3	37.5
CPU seconds execution time	3471.4	4341.2	25.1
Number cycles through program	272	272	-
CPU cost @ \$320/hour	\$308.57	\$385.88	25.1
Cost per cycle (0.1833 ns)	\$1.13	\$1.42	25.1

Conclusion

The smoother response curves of the radiation boundary condition are quite clear. Assuming this smoothing is due to ridding the solution of unwanted resonances by changing the boundary conditions, a more accurate result has been accomplished. But, as with all things, more study needs to be done before real confidence can be placed in this computer solution. Checks were run on both of the computer programs to verify them. Techniques, such as running the codes without sources, or without an object in the problem space, were performed. The results of the checks of the

program proved that it worked properly in those aspects. But more experimentation needs to be performed. On the surface, the radiation boundary conditions give response curves of the same general shape as found in lightning strike characterization papers. This comparison is made, in general, with other calculation methods of response curve generation. A lot of questions yet to be answered have to do with whether or not the increased cost of this program is justified. Can the analysis be accomplished, with the results of the absorption boundary conditions, to the desired accuracy? Which degree of accuracy is needed? What is the decision point for using one boundary condition over the other?

In comparing the response curves side-by-side, it is noted that the general wave patterns for each sensor are the same. Therefore, implementing the radiation boundary condition did not alter the basic wave pattern. And the radiation boundary condition did smooth the waveforms. This tends to back up the premise that the spurious reflections caused by the absorption boundary condition's changes in conductivity, are seemingly removed by the radiation boundary condition. The objective of ridding the output of spurious reflections seems to have been accomplished.

7. Summary and Recommendations

The major objectives of this study have been successfully completed. The code for modeling an F-16 into the Rymes' 3DFD computer code was written and implemented successfully. The 3DFD computer code was run with absorption boundary conditions for two microseconds of response time. The 3DFD code was then rewritten to incorporate the radiation boundary conditions, and run with the radiation boundary conditions for two microseconds of response time. During each complete run, ten points on the surface of the simulated aircraft were sampled. These samples are in the form of magnetic field responses and electric field responses.

The responses for each sample point were compared for the different boundary conditions. The radiation boundary condition produced a much smoother response, apparently accomplishing the task set forth by the sponsor, AFWAL/FIESL. That is, the radiation boundary conditions removed many of the unwanted variations in the amplitude. The major drawbacks of implementing the radiation boundary conditions over the absorption boundary conditions were discussed. The 25% increase in the cost of running the radiation boundary condition program was a major disadvantage. However, the overall results verified that

the radiation boundary conditions do remove unwanted problem space reflections. The sponsor (AFWAL/FIESL) was very pleased with the results.

Future projects to parallel this effort could be numerous. Comparisons should be made of 3DFD output data with measured, actual inflight lightning strikes. Another possibility, would be exploring in greater detail the result of this study for more subtle effects of the different boundary conditions that were not readily apparent. Or researchers could take on the very challenging task of optimizing the code for minimum run time and maximum efficiency in storage use. A detailed examination should be made to explain why the E-fields of sensors 8 and 10, seem to have opposite polarities for the different boundary conditions. An interesting technique would be to use the aircraft symmetry in such a manner that only half the problem need be solved, which, in theory, would reduce the expense by half. Researching combinations of boundary conditions would also be of great interest. One possibility would be to allow a small amount of absorption in the outermost cell, in combination with the radiation condition. Another possibility would be to create variations in the cell dimensions in a given direction, as opposed to adding extra grid cells (which cause cost increases or loss of details in the modeling of the object being studied).

Many studies have been performed in the area of Finite Difference Codes, as attested to by the many listings in the bibliography. However, few real comparisons of the varied techniques are available in any detail. Much can be accomplished with this code. The 3DFD is very flexible and allows cell-by-cell assignment of material properties. This flexibility makes this code an issue of possibly great interest in the study of composite aircraft materials in many electromagnetic pulse environments.

Future implementation on specialized parallel processing computers, and/or the CRAY super computer, would greatly reduce the major disadvantage of the 3DFD code, which is the CPU runtime. Of course, the increased cost of the use of these newer computers must be weighed against the benefits. The last suggestion that will be made in this thesis is that an interactive modeling system be developed for electromagnetic codes in general. Modeling an aircraft is a very time-consuming task. Cooperation with the aeronautical engineers and their detailed drawing capabilities would open new frontiers for the electromagnetic community. The ability to take the aeronautical engineer's detailed structural drawing and converting them into electromagnetic models by software, would be a great stride forward for any electromagnetic computer code utilization.

Appendix A

Updated Modified Rymes' Code

This appendix contains the Modified Rymes' Code, with absorption boundary conditions, written by Hebert (16). The code listing is complete as implemented and runs on a CDC Cyber 845. Improvements are included which correct minor errors in the code mechanics, and an improved source is also implemented. The code compiles on the Cyber 845 using FTN5, and runs with no problem when suppressing ANSI errors. The compile time is approximately 2.603 CPU seconds. The run time is 3,472 CPU seconds for 100 nanoseconds of sample time elapsed. The aircraft modeled in this code is an F-16 'Fighting Falcon'. This code will run as listed only for the first 150 nanoseconds. For continued runs, modifications must be made as annotated in the program. Additionally 'TAPE1' must be saved from the previous run.

```

C      PROGRAM ABC (OUTF15,TAPE4=OUTF15,TAPE2)
C
C      THE MODIFIED RYMES 3-D CODE F16
C
C      COMMON /SET1/ NMAX,EPST,SIGD,C,TMUO,DELT
C      COMMON /SET2/ ICAN,ICM1,ICP1,JCAN,JCM1,JCP1,KCAN,KCM1,KCP1
C      COMMON /SET3/ DELX,DELY,DELZ
C      COMMON /TIME/ TEN,THN
C      COMMON /ARRAYS/ A1(27,27),B1(39),A2(27,27),B2(39),A3(27,27),
+      B3(39),A4(27,27),B4(39),A5(27,27),B5(39),A6(27,27),B6(39),
+      A7(27,27),B7(39),A8(27,27),B8(39),A9(27,27),B9(39),
+      A10(27,27),B10(39),A11(27,27),B11(39)
C      DIMENSION INDEX(190)
C      CALL OPENMS(2,INDEX,190,0)
C
C      READ INPUT DATA
C
C      CALL SETUP
C
C      ZERO THE FIELDS INITIALLY.
C      PROGRAM USES A MASTER STORAGE FILE TO STORE FIELDS AND CONDUCTIVITY
C      OF EACH LATTICE POINT. INDEX K GOES FROM 1 TO 27.
C      EX   K
C      EY   K+27
C      EZ   K+54(27*2)
C      HX   K+81(27*3)
C      HY   K+108(27*4)
C      HZ   K+135(27*5)
C      SIG  K+162(27*6)
C
C      *****
C      *****DELETE FROM HERE TO STOP DELETE*****
C      TO REMOVE THE ZEROING OF TAPE1
C      FOR CONTINUED RUNS BEYOND THE
C      INITIAL TMAX STOPPING TIME
C      DO 100 I=1,27
C      DO 100 J=1,27
100  A1(I,J)=0.0
C      DO 200 K=1,189
200  CALL WRITMS(2,A1(1,1),768,K,0)
C
C      *****STOP DELETE GO THE THN/TEN*****
C      *****
C      PRESET THE CONDUCTIVITY ARRAY
C
C      CALL SIGSET
C
C      TIME STEP LOOP
C
C      DO 1000 N=1,NMAX
C      CALL APERT
C

```

```

C      COMPUTE TIME CONSTANTS
C
C*****
C*****FOR CONTINUED RUNS BEYOND TMAX*****
C      ADD THE STOPPING TIME FROM PREVIOUS
C      RUNS TO THN AND TEN PLUS 1/2 OF DELTA T
C
C
C      EXAMPLE
C
C      AFTER FIRST RUN
C
C      THN=DELTA*(FLOAT(N)-1.0)+1.50183E-7
C      TEN=DELTA*(FLOAT(N)-.5)+1.50183E-7
C*****
C      THN=DELTA*(FLOAT(N)-1.0)
C      TEN=DELTA*(FLOAT(N)-.5)
C
C      ADVANCE THE H-FIELDS BY Z-PLANES
C
C      CALL HADV
C
C      ADVANCE THE E-FIELDS BY Z-PLANES
C
C      CALL EADV
1000  CONTINUE
C
C      END OF TIME LOOP
C
C      CALL CLOSMS(2)
C      STOP
C      END
C      SUBROUTINE SETUP
C
C      CODE USES A UNIFORM GRID.
C
C      COMMON /SET1/ NMAX,EPST,SIGD,C,TMUD,DELTA
C      COMMON /SET2/ ICAN,ICM1,ICP1,JCAN,JCM1,JCP1,KCAN,KCM1,KCP1
C      COMMON /SET3/DELX,DELY,DELZ
C
C      INPUT DATA PROVIDED BY USER.
C
C      DATA C,EPST,EPST,XMUD,SIGD/3.0E8,8.8542E-12,1.0,1.2566E-6,1.E-4/
C      DATA ICP1,JCP1,KCP1/27,27,27/
C      DATA DELX,DELY,DELZ/.69,.22,.45/
C      DATA TMAX/1.5E-7/
C
C      ICAN=ICP1-1
C      ICM1=ICAN-1
C      JCAN=JCP1-1
C      JCM1=JCAN-1
C      KCAN=KCP1-1

```

```

      KCM1=KCAN-1
C
C
C
      IF (ICAN.EQ.2*(ICAN/2).AND.JCAN.EQ.2*(JCAN/2).AND.
+KCAN.EQ.2*(KCAN/2))GO TO 1
      PRINT *, ' THE NUMBER OF GRID POINTS MUST BE ODD '
      STOP
1
      CONTINUE
C
C
C
      DELT IS THE TIME INCREMENT (IT SATISFIES COURANT CONDITION).
      NMAX IS THE TOTAL NUMBER OF TIME INCREMENTS FIELDS WOULD BE ADVANCED.
C
      DELT=AMINI(DELX,DELY,DELZ)/(2.*C)
      NMAX=TMAX/DELT
      EPST=EPSO*EPSR/DELT
      TMUD=DELT/XMUD
      RETURN
      END
      SUBROUTINE SIGSET
C
C
C
      SIG(I,J) AT K1=K+162 IS THE CONDUCTIVITY AT THE POINT (X(I),Y(J),Z(K)).
      X(I)=(I-.5)*DELX, Y(J)=(J-.5)*DELY, Z(K)=(K-.5)*DELZ
C
      COMMON /ARRAYS/ SIG(27,27),BI(39)
      COMMON /SET1/ NMAX,EPCT,SIG0,C,TMUD,DELT
      COMMON /SET2/ ICAN,ICM1,ICP1,JCAN,JCM1,JCP1,KCAN,KCM1,KCP1
C
C
C
      PRESET THE CONDUCTIVITY TO 1E-4 EVERYWHERE IN SPACE.
C
      DO 10 I=1,ICAN
      DO 10 J=1,JCAN
10
      SIG(I,J)=SIG0
C
C
      NOW WRITE THE SIG ARRAY TO MASS STORAGE
C
      DO 20 K=1,KCAN
      K1=K+162
20
      CALL WRITMS(2,SIG(1,1),768,K1,1)
C
C
      THEN ESTABLISH FREE SPACE CONDITIONS
C
      ICM2=ICAN-2
      JCM2=JCAN-2
      KCM2=KCAN-2
      DO 30 I=3,ICM2
      DO 30 J=3,JCM2
30
      SIG(I,J)=0.0
C
C
      NOW OVERWRITE THIS PORTION OF THE SIG ARRAY
C
      DO 40 K=3,KCM2

```

```

      K1=K+162
40  CALL WRITMS(2,SIG(1,1),768,K1,1)
      RETURN
      END
      SUBROUTINE EADV
C
C  THIS SUBROUTINE ADVANCES THE E-FIELDS TWO Z-PLANES AT A TIME.
C  RECORDS OF H-FIELDS FOR TWO SUCCESSION Z-PLANES MUST BE KEPT IN
C  ORDER TO TAKE DERIVATIVES IN THE Z-DIRECTION.
C  RECORDS OF SIG FOR TWO SUCCESSION Z-PLANES MUST BE KEPT IN ORDER TO TAKE
C  AVERAGES IN THE Z-DIRECTION.
C
      COMMON /SET1/ NMAX, EPST, SIG0, C, TMUD, DELT
      COMMON /SET2/ ICAN, ICM1, JCP1, JCAN, JCM1, JCP1, KCAN, KCM1, KCP1
      COMMON /SET3/ DELX, DELY, DELZ
      COMMON /TIME/ TEN, THN
      COMMON /ARRAYS/ EX(27,27), B1(39), EY(27,27), B2(39), EZ(27,27),
+ B#(39), HXA(27,27), B4(39), HXB(27,27), B5(39), HYA(27,27), B6(39),
+ HYB(27,27), B7(39), HZA(27,27), B8(39), HZB(27,27), B9(39),
+ SIGA(27,27), B10(39), SIGB(27,27), B11(39)
C
C  ADVANCE E-FIELDS BY Z-PLANES
C  READ IN FIRST H-PLANES
C
      CALL READMS(2,HXA(1,1),768,82)
      CALL READMS(2,HYA(1,1),768,109)
C
C  DO FOR ALL Z-PLANES
C
      MN8=8
      MN9=9
      MN10=10
      DO 1000 KLOOP=1,KCAN,2
      K=KLOOP
      KP1=K+1
      K2=K+27
      K3=K+54
      K4=K+82
      K5=K+109
      K6=K+135
      K7=K+162
C
C  READ IN SECOND H-PLANES AND OLD E-FIELDS
C
      CALL READMS(2,EX(1,1),768,K)
      CALL READMS(2,EY(1,1),768,K2)
      CALL READMS(2,EZ(1,1),768,K3)
      CALL READMS(2,HXB(1,1),768,K4)
      CALL READMS(2,HYB(1,1),768,K5)
      CALL READMS(2,HZA(1,1),768,K6)
      CALL READMS(2,SIGA(1,1),768,K7)
C

```



```

DO 200 J=1, JCAN
JP1=J+1
DO 200 I=2, ICAN
C
C   SIG(X0,Y,Z)=.5*(SIG(X-DELX,Y,Z)+SIG(X,Y,Z))
C   SIG(X,Y0,Z)=.5*(SIG(X,Y-DELY,Z)+SIG(X,Y,Z))
C   SIG(X,Y,Z0)=.5*(SIG(X,Y,Z-DELZ)+SIG(X,Y,Z))
C
C   SIG2=.25*(SIGA(I,J)+SIGA(I-1,J))
C   A=EPST-SIG2
C   B=1./(EPST+SIG2)
C   EX(I,J)=(A*EX(I,J)+(HZA(I,JP1)-HZA(I,J))/DELY -
+ (HYB(I,J)-HYA(I,J))/DELZ)*B
200 CONTINUE
DO 300 I=1, ICAN
IP1=I+1
DO 300 J=2, JCAN
SIG2=.25*(SIGA(I,J-1)+SIGA(I,J))
A=EPST-SIG2
B=1./(EPST+SIG2)
EY(I,J)=(A*EY(I,J)+(HXB(I,J)-HXA(I,J))/DELZ -
+ (HZA(IP1,J)-HZA(I,J))/DELX)*B
300 CONTINUE
C
C   WRITE NEW EX,EY PLANES TO MASS STORAGE
C
C   CALL WRITMS(2,EX(1,1),768,K,1)
C   CALL WRITMS(2,EY(1,1),768,K2,1)
C   IF (K.EQ.1)GO TO 450
C   DO 400 I=1, ICAN
C   IP1=I+1
C   DO 400 J=1, JCAN
C   JP1=J+1
C   SIG2=.25*(SIGA(I,J)+SIGB(I,J))
C   A=EPST-SIG2
C   B=1./(EPST+SIG2)
C   EZ(I,J)=(A*EZ(I,J)+(HYA(IP1,J)-HYA(I,J))/DELX-
+ (HXA(I,JP1)-HXA(I,J))/DELY)*B
400 CONTINUE
C
C   WRITE NEW EZ PLANE TO MASS STORAGE
C
C   CALL WRITMS(2,EZ(1,1),768,K3,1)
C
C   SAMPLE POINTS OF INTEREST(ODD K PLANES)
C
111   FORMAT (I4,2(IX,1PIE11.4))
112   FORMAT (I4,2(IX,1PIE11.4),2(/))
C
C
450 CONTINUE
K=KP1

```

```

      KP1=K+1
      K2=K2+1
      K3=K3+1
      K4=K4+1
      K5=K5+1
      K6=K6+1
      K7=K7+1

C
C   READ IN SECOND OLD E-PLANES AND NEXT H-PLANES OFER A PLANE
C
      CALL READMS(2,EX(1,1),768,K)
      CALL READMS(2,EY(1,1),768,K2)
      CALL READMS(2,EZ(1,1),768,K3)
      CALL READMS(2,HXA(1,1),768,K4)
      CALL READMS(2,HYA(1,1),768,K5)
      CALL READMS(2,HZB(1,1),768,K6)
      CALL READMS(2,SIGB(1,1),768,K7)
      DO 600 J=1,JCAN
        JP1=J+1
        DO 600 I=2,ICAN
          SIG2=.25*(SIGB(I,J)+SIGB(I-1,J))
          A=EPST-SIG2
          B=1./(EPST+SIG2)
          EX(I,J)=(A*EX(I,J)+(HJB(I,JP1)-HZB(I,J))/DELZ -
+ (HYA(I,J)-HYB(I,J))/DELZ)*B
600    CONTINUE
        DO 700 I=1,ICAN
          IP1=I+1
          DO 700 J=2,JCAN
            SIG2=.25*(SIGB(I,J-1)+SIGB(I,J))
            A=EPST-SIG2
            B=1./(EPST+SIG2)
            EY(I,J)=(A*EY(I,J)+(HXA(I,J)-HXB(I,J))/DELZ -
+ (HZB(IP1,J)-HZB(I,J))/DELX)*B
700    CONTINUE
        DO 800 I=1,ICAN
          IP1=I+1
          DO 800 J=1,JCAN
            JP1=J+1
            SIG2=.25*(SIGB(I,J)+SIGA(I,J))
            A=EPST-SIG2
            B=1./(EPST+SIG2)
            EZ(I,J)=(A*EZ(I,J)+(HYB(IP1,J)-HYB(I,J))/DELX -
+ (HXB(I,JP1)-HXB(I,J))/DELY)*B
800    CONTINUE
C
C   WRITE NEW EX,EY,EZ PLANES TO MASS STORAGE
C
      CALL WRITMS(2,EX(1,1),768,K,1)
      CALL WRITMS(2,EY(1,1),768,K2,1)
      CALL WRITMS(2,EZ(1,1),768,K3,1)
C

```

AD-A163 828

COMPARISON OF ABSORPTION AND RADIATION BOUNDARY
CONDITIONS USING A TIME-D. (U) AIR FORCE INST OF TECH
WRIGHT-PATTERSON AFB OH SCHOOL OF ENGI.. C F WILLIFORD
DEC 85 AFIT/GE/ENG/85D-53 F/G 28/3

2/2

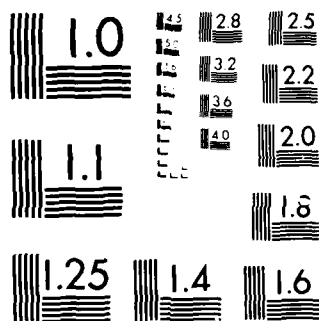
UNCLASSIFIED

NL

END

FILED

UIC



MICROCOPY RESOLUTION TEST CHART
NATIONAL BUREAU OF STANDARDS-1963-A

```

C   SAMPLE POINTS OF INTEREST (EVEN K PLANES)
C
      IF (K.EQ.10) WRITE (4,111) MN8,TEN,EY(17,11)
      IF (K.EQ.18) WRITE (4,112) MN10,TEN,EY(17,11)
C
      IF (K.EQ.14) THEN
        WRITE (4,111) MN9,TEN,EY(15,13)
      ELSE
        END IF
C
1000 CONTINUE
C
C   ZERO THE ELECTRIC FIELD WITHIN THE METAL COMPONENTS OF AIRCRAFT.
C
      CALL AIRPLN
      RETURN
      END
      SUBROUTINE HADV
C
C   THIS SUBROUTINE ADVANCES THE H-FIELDS TWO Z-PLANES AT A TIME.
C   RECORDS OF E-FIELDS FOR TWO SUCCESSIVE PLANES MUST BE KEPT IN ORDER TO TAKE
C   DERIVATIVES IN THE Z-DIRECTION.
C
      COMMON /SET1/ NMAX,EPST,SIG0,C,TMU0,DELT
      COMMON /SET2/ ICAN,ICM1,ICP1,JCAN,JCM1,JCP1,KCAN,KCM1,KCP1
      COMMON /SET3/ DELX,DELY,DELZ
      COMMON /TIME/ TEN,THN
      COMMON /ARRAYS/ EXA(27,27),B1(39),EXB(27,27),B2(39),
      +EYA(27,27),B3(39),EYB(27,27),B4(39),EZA(27,27),B5(39),
      +EZB(27,27),B6(39),HXA(27,27),B7(39),HYA(27,27),B8(39),
      +HZ(27,27),B9(39)
C
C   DO FOR ALL Z-PLANES
      MN1=1
      MN2=2
      MN3=3
      MN4=4
      MN5=5
      MN6=6
      MN7=7
C
      DO 900 KLOOP=1,KCAN,2
      K=KLOOP
      KM1=K-1
      K2=K+27
      K3=K+54
      K4=K+81
      K5=K+108
      K6=K+135
      CALL READMS(2,EXB(1,1),768,K)
      CALL READMS(2,EYB(1,1),768,K2)
      CALL READMS(2,HZ(1,1),768,K6)

```

```

IF (K.EQ.1) GO TO 350
CALL READMS(2,EZB(1,1),768,K3)
CALL READMS(2,HX(1,1),768,K4)
CALL READMS(2,HY(1,1),768,K5)
DO 200 J=2,JCAN
DO 200 I=1,ICAN
HX(I,J)=HX(I,J)+TMUD*((EYB(I,J)-EYA(I,J))/DELZ -
+ (EZB(I,J)-EZB(I,J-1))/DELY)
200 CONTINUE
DO 300 I=1,ICM1
IP1=I+1
DO 300 J=1,JCAN
HY(IP1,J)=HY(IP1,J)+TMUD*((EZB(IP1,J)-EZB(I,J))/DELX -
+ (EXB(IP1,J)-EXA(IP1,J))/DELZ)
300 CONTINUE
C
C APPROXIMATES H FIELDS IN PLANE PERPENDICULAR TO WIRE
C BY  $H=I/2*\pi*R$ .
C SOURCE FUNCTION, ODD K REFERENCE PLANES, HY
C CURRENT PULSE MOVING IN X DIRECTION ATTACHES TO THE NOSE OF THE AIRPLANE
C AT (X,Y,Z)=(0,10,14), EXITS BY THE TAIL AT (X,Y,Z)=(22,10,14).
C AT TIME T=0.0 PULSE IS LOCATED AT X0(0).
C
IF (K.NE.15) GO TO 1
DO 10 I=2,3
TPULSE=THN-.69*(FLOAT(I)-3.)/C
IF (TPULSE.LE.0.0) GO TO 10
C
X=EXP(-3.5E04*TPULSE)-EXP(-2.625E7*TPULSE)
C
HYS=7.07E3*X
HY(I,9)=-HYS
10 CONTINUE
DO 30 I=25,26
TPULSE=THN-.69*(FLOAT(I)-3.0)/C
IF (TPULSE.LE.0.0) GO TO 30
X=EXP(-3.5E4*TPULSE)-EXP(-2.625E7*TPULSE)
HYS=7.07E3*X
HY(I,10)=-HYS
30 CONTINUE
1 CONTINUE
C
C WRITE NEW HX, HY PLANES TO MASS STORAGE
C
CALL WRITMS(2,HX(1,1),768,K4,1)
CALL WRITMS(2,HY(1,1),768,K5,1)
350 CONTINUE
DO 400 I=1,ICM1
IP1=I+1
DO 400 J=1,JCM1
JP1=J+1
HZ(IP1,JP1)=HZ(IP1,JP1)+TMUD*((EXB(IP1,JP1)-EXB(IP1,J))/DELY -

```

```

+ (EYB(IP1,JP1)-EYB(I,JP1))/DELX)
400 CONTINUE
C
C WRITE NEW HZ PLANE TO MASS STORAGE
C
CALL WRITMS(2,HZ(1,1),768,K6,1)
C
C SAMPLE POINTS OF INTEREST (ODD K PLANES)
C
IF (K.EQ.13) WRITE (4,111) MN2,THN,HZ(4,10)
IF (K.EQ.13) WRITE (4,111) MN3,THN,HZ(24,11)
IF (K.EQ.23) WRITE (4,111) MN7,THN,HX(18,10)
C
112 FORMAT (I4,2(1X,1PIE11.4),2(/))
111 FORMAT (I4,2(1X,1PIE11.4))
C
K=K+1
KM1=K-1
K2=K2+1
K3=K3+1
K4=K4+1
K5=K5+1
K6=K6+1
C
C READ IN NEXT PLANES OF E AND H
C
CALL READMS(2,EXA(1,1),768,K)
CALL READMS(2,EYA(1,1),768,K2)
CALL READMS(2,EZA(1,1),768,K3)
CALL READMS(2,HX(1,1),768,K4)
CALL READMS(2,HY(1,1),768,K5)
CALL READMS(2,HZ(1,1),768,K6)
DO 600 J=1, JCM1
JP1=J+1
DO 600 I=1, ICAN
HX(I,JP1)=HX(I,JP1)+TMUD*((EYA(I,JP1)-EYB(I,JP1))/DELZ -
+ (EZA(I,JP1)-EZA(I,J))/DELY)
600 CONTINUE
DO 700 I=1, ICN1
IP1=I+1
DO 700 J=1, JCAN
HY(IP1,J)=HY(IP1,J)+TMUD*((EZA(IP1,J)-EZA(I,J))/DELX -
+ (EXA(IP1,J)-EXB(IP1,J))/DELZ)
700 CONTINUE
C
C SOURCE FUNCTION, EVEN K REFERENCE PLANES, HY
C
IF (K.NE.14) GO TO 2
DO 20 I=2,3
TPULSE=THN-.69*(FLOAT(I)-3.)/C
IF (TPULSE.LE.0.0) GO TO 20
X=EXP(-3.5E4*TPULSE)-EXP(-2.625E7*TPULSE)

```

```

      HYS=7.07E3*X
      HY(1,9)=+HYS
20    CONTINUE
      DO 40 I=25,26
      TPULSE=THN-.69*(FLOAT(I)-3.)/C
      IF (TPULSE.LE.0.0)GO TO 40
      X=EXP(-3.5E4*TPULSE)-EXP(-2.625E7*TPULSE)
      HYS=7.07E3*X
      HY(1,10)=+HYS
40    CONTINUE
2    CONTINUE
      DO 800 I=1,ICM1
      IP1=I+1
      DO 800 J=1,JCM1
      JP1=J+1
      HZ(IP1,JP1)=HZ(IP1,JP1)+TMUD*((EXA(IP1,JP1)-EXA(IP1,J))/DELY -
+ (EYA(IP1,JP1)-EYA(I,JP1))/DELX)
800   CONTINUE
C
C
C    SOURCE FUNCTION, EVEN K REFERENCE PLANE, HZ
      IF (K.NE.14)GO TO 4
      DO 60 I=2,3
      TPULSE=THN-.69*(FLOAT(I)-3.)/C
      IF (TPULSE.LE.0.0)GO TO 60
      X=(EXP(-3.5E4*TPULSE)-EXP(-2.625E7*TPULSE))
      HZS=1.447E4*X
      HZ(1,9)=-HZS
      HZ(1,10)=+HZS
60    CONTINUE
      DO 80 I=25,26
      TPULSE=THN-.69*(FLOAT(I)-3.)/C
      IF (TPULSE.LE.0.0)GO TO 80
      X=(EXP(-3.5E4*TPULSE)-EXP(-2.625E7*TPULSE))
      HZS=1.447E4*X
      HZ(1,10)=-HZS
      HZ(1,11)=HZS
80    CONTINUE
4    CONTINUE
      CALL WRITMS(2,HX(1,1),768,K4,1)
      CALL WRITMS(2,HY(1,1),768,K5,1)
      CALL WRITMS(2,HZ(1,1),768,K6,1)
C
C
C    SAMPLE POINTS OF INTEREST (EVEN K PLANES)
      IF (K.EQ.14) THEN
      WRITE (4,111) MN4,THN,HZ(10,4)
      WRITE (4,111) MN5,THN,HZ(19,4)
      WRITE (4,111) MN6,THN,HX(22,18)
      ELSE
      END IF
C

```



```

      IF (K.EQ.6) WRITE (4,111) MNI,TIN,HX(18,18)
C
900  CONTINUE
      RETURN
      END
      SUBROUTINE APERT
      RETURN
      END
      SUBROUTINE AIRPLN
C
C ZEROES THE ELECTRIC FIELDS WITHIN THE F16 AIRCRAFT AND
C TANGENTIAL ELECTRIC FIELD COMPONENTS AT THE SURFACE
C
      COMMON /ARRAYS/ FLD (27,27),B1 (39)
C
C      EX ZEROED
C
      DO 1000 K=3,25
      CALL READMS (2,FLD(1,1),768,K)
C      WING
      IF (K.NE.3) GO TO 40
      FLD(18,9)=0.0
      FLD(19,9)=0.0
40    IF (K.NE.4) GO TO 50
      DO 41 I=17,19
41    FLD(I,9)=0.0
50    IF (K.LT.5.OR.K.GT.6) GO TO 70
      DO 51 I=16,19
51    FLD(I,9)=0.0
70    IF (K.LT.7.OR.K.GT.8) GO TO 90
      DO 71 I=15,19
      DO 71 J=9,10
71    FLD(I,J)=0.0
      FLD(23,9)=0.0
      FLD(24,9)=0.0
90    IF (K.NE.9) GO TO 100
      DO 91 I=14,19
      DO 91 J=9,10
91    FLD(I,J)=0.0
      DO 92 I=22,24
92    FLD(I,9)=0.0
100   IF (K.NE.10) GO TO 110
      DO 101 I=13,19
      DO 101 J=9,10
101   FLD(I,J)=0.0
      DO 102 I=21,24
102   FLD(I,9)=0.0
110   IF (K.NE.11) GO TO 120
      DO 111 I=11,23
      DO 111 J=9,10
111   FLD(I,J)=0.0
      DO 112 I=11,22

```

```

112   FLD(I,8)=0.0
C     MAIN FUSELAGE
120   IF (K.LT.12.OR.K.GT.15) GO TO 126
      DO 121 I=10,19
      DO 121 J=5,12
121   FLD(I,J)=0.0
C
C     FORWARD FUSELAGE
C
      DO 122 I=6,9
      DO 122 J=8,10
122   FLD(I,J)=0.0
      DO 123 I=8,9
      DO 123 J=11,12
123   FLD(I,J)=0.0
      FLD(7,11)=0.0
C     REAR FUSELAGE
      DO 124 I=20,22
124   FLD(I,6)=0.0
      DO 125 I=20,23
      DO 125 J=7,12
125   FLD(I,J)=0.0
126   IF (K.NE.12.OR.K.NE.15) GO TO 130
      DO 127 I=19,20
      DO 127 J=3,4
127   FLD(I,J)=0.0
      FLD(20,5)=0.0
130   IF (K.LT.13.OR.K.GT.14) GO TO 135
      FLD(24,9)=0.0
      FLD(24,10)=0.0
C     NOSE AND COCKPIT
      DO 131 I=4,5
      DO 131 J=8,9
131   FLD(I,J)=0.0
      FLD(5,10)=0.0
      FLD(6,11)=0.0
      FLD(7,12)=0.0
      DO 132 I=8,11
      DO 132 J=13,14
132   FLD(I,J)=0.0
      FLD(12,13)=0.0
      FLD(13,13)=0.0
      FLD(9,15)=0.0
C
C     RIGHT VERTICAL STABILIZER
C
135   IF (K.NE.13) GO TO 140
      DO 136 I=19,23
      DO 136 J=13,14
136   FLD(I,J)=0.0
      FLD(17,13)=0.0
      FLD(18,13)=0.0

```

```

140 IF (K.NE.14) GO TO 160
    DO 141 I=18,23
    DO 141 J=13,14
141 FLD(I,J)=0.0
    FLD(17,23)=0.0
    DO 142 I=20,23
    DO 142 J=15,19
142 FLD(I,J)=0.0
    FLD(20,15)=0.0
    FLD(20,16)=0.0
    DO 143 I=22,23
    DO 143 J=20,22
143 FLD(I,J)=0.0
    FLD(24,21)=0.0
    FLD(24,22)=0.0
    DO 144 I=23,24
    DO 144 J=23,24
144 FLD(I,J)=0.0
160 IF (K.NE.16) GO TO 170
    DO 161 I=11,22
    DO 161 J=8,10
161 FLD(I,J)=0.0
    FLD(23,9)=0.0
    FLD(23,10)=0.0
170 IF (K.NE.17) GO TO 180
C WING
    DO 171 I=13,19
    DO 171 J=9,10
171 FLD(I,J)=0.0
C
C RIGHT HORIZONTAL STABILIZER
C
    DO 172 I=21,24
172 FLD(I,9)=0.0
180 IF (K.NE.18) GO TO 190
    DO 181 I=14,19
    DO 181 J=9,10
181 FLD(I,J)=0.0
    DO 182 I=22,24
182 FLD(I,9)=0.0
190 IF (K.LT.19.OR.K.GT.20) GO TO 210
    DO 191 I=15,19
    DO 191 J=9,10
191 FLD(I,J)=0.0
    FLD(23,9)=0.0
    FLD(24,9)=0.0
210 IF (K.LT.21.OR.K.GT.22) GO TO 230
    DO 211 I=16,19
211 FLD(I,9)=0.0
230 IF (K.NE.23) GO TO 240
    DO 231 I=17,19
231 FLD(I,9)=0.0

```

```

240  IF (K.NE.24) GO TO 1000
      FLD(18,9)=0.0
      FLD(19,9)=0.0
C     STORE EX FIELDS BACK IN TO MASS STORAGE
1000  CALL WRITMS(2,FLD(1,1),768,K,1)
C     ZERO EY
      DO 2000 K=3,24
      L=K+27
      CALL READMS (2,FLD(1,1),768,L)
      IF (K.LT.7.OR.K.GT.10) GO TO 1110
      DO 1081 I=14,19
1081   FLD(I,10)=0.0
      IF (K.NE.9) GO TO 1100
      FLD(13,10)=0.0
1100   IF (K.NE.10) GO TO 1110
      FLD(12,10)=0.0
      FLD(13,10)=0.0
1110   IF (K.NE.11) GO TO 1120
      DO 1111 I=10,22
      DO 1111 J=9,10
1111   FLD(I,J)=0.0
      FLD(23,10)=0.0
C     MAIN FUSELAGE
1120   IF (K.LT.1*.OR.K.GT.15) GO TO 1130
      DO 1121 I=9,19
      DO 1121 J=6,12
1121   FLD(I,J)=0.0
C     FWD FUSELAGE
      DO 1122 I=5,8
      DO 1122 J=9,10
1122   FLD(I,J)=0.0
      DO 1123 I=7,8
      DO 1123 J=11,12
1123   FLD(I,J)=0.0
      FLD(6,11)=0.0
C     REAR FUSELAGE
      DO 1124 I=20,22
      DO 1124 J=7,12
1124   FLD(I,J)=0.0
      DO 1125 J=8,12
1125   FLD(23,J)=0.0
1130   IF (K.LT.13.OR.K.GT.14) GO TO 1126
      FLD(24,10)=0.0
1126   IF (K.NE.12.OR.K.NE.15) GO TO 1131
      DO 1127 I=10,20
      DO 1127 J=4,5
1127   FLD(I,J)=0.0
      FLD(20,6)=0.0
1131   IF (K.LT.13.OR.K.GT.14) GO TO 1135
      FLD(3,9)=0.0
      FLD(4,9)=0.0
      FLD(4,10)=0.0

```

```

      FLD(5,11)=0.0
      FLD(6,12)=0.0
      DO 1132 I=7,13
1132      FLD(1,13)=0.0
      DO 1133 I=7,11
1133      FLD(1,14)=0.0
      FLD(8,15)=0.0
      FLD(9,15)=0.0
1135      IF (K.NE.13) GO TO 1140
      DO 1136 I=16,23
1136      FLD(1,13)=0.0
      DO 1137 I=18,23
1137      FLD(1,14)=0.0
1140      IF (K.NE.14) GO TO 1160
      DO 1141 I=22,23
      DO 1141 J=13,24
1141      FLD(1,J)=0.0
      DO 1142 J=21,24
1142      FLD(24,J)=0.0
      DO 1143 J=20,22
1143      FLD(21,J)=0.0
      DO 1144 J=17,19
      DO 1144 I=20,21
1144      FLD(1,J)=0.0
      DO 1145 I=19,21
      DO 1145 J=15,16
1145      FLD(1,J)=0.0
      DO 1146 I=17,21
1146      FLD(1,14)=0.0
      DO 1147 I=16,21
1147      FLD(1,13)=0.0
1160      IF (K.NE.16) GO TO 1170
      DO 1161 I=10,22
      DO 1161 J=9,10
1161      FLD(1,J)=0.0
      FLD(23,10)=0.0
C      WING
1170      IF (K.NE.17) GO TO 1180
      DO 1171 I=12,19
1171      FLD(1,10)=0.0
1180      IF (K.NE.18) GO TO 1190
      DO 1181 I=13,19
1181      FLD(1,10)=0.0
1190      IF (K.LT.19.OR.K.GT.20) GO TO 2000
      DO 1191 I=14,19
1191      FLD(1,10)=0.0
C      STORE EY BACK TO MASS STORAGE
2000      CALL WRITMS(2,FLD(1,1),768,L,1)
C      EZ ZEROED
      DO 3000 K=3,24
      L=K+54
      CALL READMS(2,FLD(1,1),768,L)

```

```

C      WING TIP
      IF (K.NE.4) GO TO 2050
      DO 2041      I=17,19
2041      FLD(I,9)=0.0
2050      IF (K.NE.5) GO TO 2060
      DO 2051 I=16,19
2051      FLD(I,9)=0.0
C      PLANE
2060      IF (K.LT.6.OR.K.GT.7) GO TO 2080
      DO 2061 I=15,19
2061      FLD(I,9)=0.0
C      WING
2080      IF (K.NE.8) GO TO 2090
      DO 2081 J=9,10
      DO 2081 I=14,19
2081      FLD(I,J)=0.0
C
C      RIGHT HAND STABILIZER
C
      DO 2082 I=22,24
2082      FLD(I,9)=0.0
2090      IF (K.NE.9) GO TO 2100
      DO 2091 I=14,19
      DO 2091 J=9,10
2091      FLD(I,J)=0.0
      DO 2092 I=22,24
2092      FLD(I,9)=0.0
2100      IF (K.NE.10) GO TO 2110
      DO 2101 I=13,19
      DO 2101 J=9,10
2101      FLD(I,J)=0.0
      DO 2102 I=21,24
2102      FLD(I,9)=0.0
2110      IF (K.NE.11) GO TO 2120
      DO 2111 I=12,24
2111      FLD(I,9)=0.0
      DO 2112 I=12,19
2112      FLD(I,10)=0.0
2120      IF (K.NE.12) GO TO 2130
      DO 2121 I=10,22
      DO 2121 J=8,10
2121      FLD(I,J)=0.0
      FLD(23,9)=0.0
      FLD(23,10)=0.0
2130      IF (K.LT.13.OR.K.GT.15) GO TO 2140
      DO 2131 I=9,19
      DO 2131 J=5,12
2131      FLD(I,J)=0.0
      DO 2132 I=5,8
      DO 2132 J=8,10
2132      FLD(I,J)=0.0
      DO 2133 I=7,8

```

```

DO 2133 J=11,12
2133   FLD(I,J)=0.0
      FLD(6,11)=0.0
DO 2134 I=20,22
DO 2134 J=6,12
2134   FLD(I,J)=0.0
DO 2135 J=7,12
2135   FLD(23,J)=0.0
2140   IF (K.NE.14) GO TO 2160
      FLD(24,9)=0.0
      FLD(24,10)=0.0
DO 2141 I=3,4
DO 2141 J=8,9
2141   FLD(I,J)=0.0
      FLD(4,10)=0.0
      FLD(5,11)=0.0
      FLD(6,12)=0.0
DO 2142 I=7,11
DO 2142 J=13,14
2142   FLD(I,J)=0.0
      FLD(12,13)=0.0
      FLD(13,13)=0.0
      FLD(18,15)=0.0
      FLD(19,15)=0.0
DO 2143 I=16,23
2143   FLD(I,13)=0.0
DO 2144 I=18,23
2144   FLD(I,14)=0.0
2160   IF (K.NE.16) GO TO 2170
DO 2161 I=10,22
DO 2161 J=8,10
2161   FLD(I,J)=0.0
      FLD(23,9)=0.0
      FLD(23,10)=0.0
2170   IF (K.NE.17) GO TO 2180
DO 2171 I=12,24
2171   FLD(I,9)=0.0
DO 2172 I=12,19
2172   FLD(I,10)=0.0
2180   IF (K.NE.18) GO TO 2190
DO 2181 I=13,19
DO 2181 J=9,10
2181   FLD(I,J)=0.0
DO 2182 I=21,24
2182   FLD(I,9)=0.0
2190   IF (K.LT.19.OR.K.GT.20) GO TO 2210
DO 2191 I=14,19
DO 2191 J=9,10
2191   FLD(I,J)=0.0
DO 2192 I=22,24
2192   FLD(I,9)=0.0
2210   IF (K.LT.21.OR.K.GT.22) GO TO 2230

```

```

DO 2211 I=15,19
2211     FLD(I,9)=0.0
2230     IF (K.NE.23) GO TO 2240
DO 2231 I=16,19
2231     FLD(I,9)=0.0
2240     IF (K.NE.24) GO TO 3000
DO 2241 I=17,19
2241     FLD(I,9)=0.0
C
C     STORE EZ BACK TO MASS STORAGE
C
3000     CALL WRITMS (2,FLD(1,1),768,L,1)
RETURN
END

```


Appendix B

Rymes' Code with Radiation Boundary Conditions

This appendix contains a complete listing of the modified Rymes' code with the radiation boundary conditions implemented. The compile time is 3.722 CPU seconds. The run time for the first 100 nanoseconds was 4342 CPU seconds. The F-16 is modeled in subroutine AIRPLN, as it is in the previous appendix. The major changes include expansion of the memory required and a complete rewrite of subroutine SIGSET, now renamed RADBC. The code listing is complete as implemented, and runs on a CDC Cyber 845. Improvements are included which correct minor errors in code mechanics, and also an improved source is implemented. The code compiles on the Cyber 845 using FTN5, and runs with no problem when suppressing ANSI errors. Continued runs require the changes annotated in the code in addition to saving 'TAPE1' from the previous run.

```

PROGRAM RBC (OUTF16,TAPE6=OUTF16,TAPE 1)

C
C   THE MODIFIED RYMES 3-D CODE F16
C*****
C   TO INCLUDE RADIATION BOUNDARY CONDITIONS DEVELOPED
C   DEVELOPED BY MEREWETHER AND INCORPORATED INTO THIS
C   CODE BY WILLIFORD AND HEBERT
C*****
C
COMMON /SET1/ NMAX,EPST,SIGD,C,TMUO,DELT
COMMON /SET2/ ICAN,ICM1,ICP1,JCAN,JCM1,JCP1,KCAN,KCM1,KCP1
COMMON /SET3/ DELX,DELY,DELZ
COMMON /TIME/ TEN,THN
COMMON /ARRAYS/ A1(27,27),B1(39),A2(27,27),B2(39),A3(27,27),
+ B3(39),A4(27,27),B4(39),A5(27,27),B5(39),A6(27,27),B6(39),
+ A7(27,27),B7(39),A8(27,27),B8(39),A9(27,27),B9(39),
+ A10(27,27),B10(39),A11(27,27),B11(39),A12(27,27),B12(39),
C*****
+ A13(27,27),B13(39),A14(27,27),B14(39),A15(27,27),B15(39),
+ A16(27,27),B16(39),A17(27,27),B17(39),A18(27,27),B18(39),
+ A19(27,27),B19(39),A*0(27,27),B20(39)
C
C   DIMENSION INDEX(352)
C   CALL OPENMS(1,INDEX,352,0)
C*****
C
C   READ INPUT DATA
C
C   CALL SETUP
C
C   ZERO THE FIELDS INITIALLY.
C   PROGRAM USES A MASTER STORAGE FILE TO STORE FIELDS AND CONDUCTIVITY
C   OF EACH LATTICE POINT. INDEX K GOES FROM 1 TO 27.
C   EX   K
C   EY   K+27
C   EZ   K+54(27*2)
C   HX   K+81(27*3)
C   HY   K+108(27*4)
C   HZ   K+135(27*5)
C   SIG  K+162(27*6)
C*****
C   HXTM2 K+189(27*7)
C   HYTM2 K+216(27*8)
C   HZTM2 K+243(27*9)
C   C1    K+270(27*10)
C   C2    K+297(27*11)
C   C3    K+324(27*12)
C*****
C*****DELETE FROM HERE TO STOP DELETE*****
C   TO REMOVE THE ZEROING OF TAPE1
C   FOR CONTINUED RUNS BEYOND THE
C   INITIAL TMAX STOPING TIME

```

```

C*****
DO 100 I=1,27
DO 100 J=1,27
100 A1(I,J)=0.0
C*****
DO 200 K=1,351
C*****
200 CALL WRITMS(1,A1(1,1),768,K,0)
C
C*****STOP DELETE HERE GO TO THN= *****
C
C
C PRESET THE CONDUCTIVITY ARRAY
C
C CALL RADBC
C
C TIME STEP LOOP
C
DO 1000 N=1,NMAX
CALL APERT
C
C COMPUTE TIME CONSTANTS
C
C*****FOR CONTINUED RUNS BEYOND TMAX*****
C ADD THE STOPPING TIME FROM PREVIOUS
C RUNS TO THN AND TEN PLUS 1/2 OF DELTA T
C
C EXAMPLE
C
C AFTER FIRST RUN
C
C THN=DELTA*(FLOAT(N)-1.0)+1.00183E-7
C TEN=DELTA*(FLOAT(N)-.5)+1.00183E-7
C*****
C THN=DELTA*(FLOAT(N)-1.0)
C TEN=DELTA*(FLOAT(N)-.5)
C
C ADVANCE THE H-FIELDS BY Z-PLANES
C
C CALL HADV
C
C ADVANCE THE E-FIELDS BY Z-PLANES
C
C CALL EADV
1000 CONTINUE
C
C END OF TIME LOOP
C
C CALL CLOSNS(1)
C STOP
C END
C SUBROUTINE SETUP

```

```

C   CODE USES A UNIFORM GRID.
C
COMMON /SET1/ NMAX,EPST,SIGD,C,TMUJ,DELT
COMMON /SET2/ ICAN,ICM1,ICP1,JCAN,JCM1,JCP1,KCAN,KCM1,KCP1
COMMON /SET3/DETX,DELY,DELZ

C*****
C
C
C
C*****
C   INPUT DATA PROVIDED BY USER.
C
C*****
C   SET SIGD=0.0 TO STOP ABSORPTION BC
DATA C,EPST,EPJR,XTMU,SIGD/3.0E8,8.8542E-12,1.0,1.2566E-6,0.0/
C*****
DATA ICP1,JCP1,KCP1/27,27,27/
DATA DETX,DELY,DELZ/.69,.22,.45/
DATA TMAX/1.E-7/

C
ICAN=ICP1-1
ICM1=ICAN-1
JCAN=JCP1-1
JCM1=JCAN-1
KCAN=KCP1-1
KCM1=KCAN-1

C
C   VERIFY THAT ICP1,JCP1,KCP1 ARE ODD.
C
IF(ICAN.EQ.2*(ICAN/2).AND.JCAN.EQ.2*(JCAN/2).AND.
+KCAN.EQ.2*(KCAN/2))GO TO 1
PRINT *, ' THE NUMBER OF GRID POINTS MUST BE ODD '
STOP
1
CONTINUE

C
C   DELT IS THE TIME INCREMENT (IT SATISFIES COURANT CONDITION).
C   NMAX IS THE TOTAL NUMBER OF TIME INCREMENTS FIELDS WOULD BE ADVANCED.
C
DELT=AMIN1(DETX,DELY,DELZ)/(2.*C)
NMAX=TMAX/DELT
EPST=EPST*EPJR/DELT
TMUJ=DELT/XTMU
RETURN
END
SUBROUTINE RADBC

C
C   SIG(I,J) AT K1=K+162 IS THE CONDUCTIVITY AT THE POINT (X(I),Y(J),Z(K)).
C   X(I)=(I-.5)*DETX, Y(J)=(J-.5)*DELY, Z(K)=(K-.5)*DELZ
C
C*****
REAL RN(27,27),RNP(27,27),THETA,RCON
COMMON /ARRAYS/ SIG(27,27),B1(39)

```

```

+ A13(27,27), B13(39), A14(27,27), B14(39), C1(27,27), B15(39),
+ C2(27,27), B16(39), C3(27,27), B17(39), A18(27,27), B18(39),
+ A19(27,27), B19(39), A20(27,27), B20(39)
COMMON /SET3/ DELX, DELY, DELZ

C
C
C*****
COMMON /SET1/ NMAX, EPST, SIGO, C, THUD, DELT
COMMON /SET2/ ICAN, ICM1, ICPI, JCAN, JCM1, JCP1, KCAN, KCM1, KCP1

C
C
C PRESET THE CONDUCTIVITY HERE IF NEEDED
C*****
C
C CALCULATE GEOMETRIC CONSTANTS FOR RADBC
C
C FINDING CENTER OF SHIFTED COORDINATE SYSTEM
IX0=ICAN/2+1
IY0=JCAN/2+1
IZ0=KCAN/2+1

C
DO 50 K=1, KCAN
K11=K+270
K12=K+297
K13=K+324

C
CALL READMS (1, C1(1,1), 768, K11)
CALL READMS (1, C2(1,1), 768, K12)
CALL READMC (1, C3(1,1), 768, K13)
IF (K.EQ.2.OR.K.EQ.KCAN) THEN

C
C FACE
KN=IABS(K-IZ0)
KNP=KN+1
DO 60 I=1, ICAN
DO 70 J=1, JCAN

C
IN=IABS(I-IX0)
JN=IABS(J-IY0)

C
RN(I,J)=SQRT((FLOAT(IN)*DELX)**2.0+(FLOAT(JN)*DELY)**2.0
+(FLOAT(KN)*DELZ)**2.0)
RNP(I,J)=SQRT((FLOAT(IN)*DELX)**2.0+(FLOAT(JN)*DELY)**2.0
+(FLOAT(KNP)*DELZ)**2.0)
THETA=(IFIX((RNP(I,J)-RN(I,J))/(DELZ)+0.5))-
((RNP(I,J)-RN(I,J))/(DELZ))

C
RCOM=RN(I,J)/(2.0+RNP(I,J))

C
C1(I,J)=RCOM*(THETA*(THETA-1.0))
C2(I,J)=RCOM*2.0*(1.0-(THETA**2.0))
C3(I,J)=RCOM*THETA*(THETA+1.0)

```

```

70 CONTINUE
60 CONTINUE
C
ELSE
C SIDES OF K-PLANES
KN=IABS(K-120)
C
ICM2=ICAN-2
JCM2=JCAN-2
C SIDES OF I=2 & ICAN
DO 80 I=2, ICAN, ICM2
DO 90 J=1, JCAN
C
IN=IABS(I-120)
INP=IN+1
JN=IABS(J-120)
C
RN(I,J)=SQRT((FLOAT(IN)*DELX)**2.0+(FLOAT(JN)*DELY)**2.0
$+(FLOAT(KN)*DELZ)**2.0)
RNP(I,J)=SQRT((FLOAT(INP)*DELX)**2.0+(FLOAT(JN)*DELY)**2.0
$+(FLOAT(KN)*DELZ)**2.0)
C
THETA=(IFIX((RNP(I,J)-RN(I,J))/(DELX)+0.5))-
$((RNP(I,J)-RN(I,J))/(DELX))
RCOM=RN(I,J)/(2.0*RNP(I,J))
C
C1(I,J)=RCOM*(THETA*(THETA-1.0))
C2(I,J)=RCOM*2.0*(1.0-(THETA**2.0))
C3(I,J)=RCOM*(THETA*(THETA+1.0))
C
90 CONTINUE
80 CONTINUE
C SIDES AT J=2 & JCAN
DO 100 J=2, JCAN, JCM2
DO 110 I=1, ICAN
C
IN=IABS(I-120)
JN=IABS(J-120)
JNP=JN+1
C
RN(I,J)=SQRT((FLOAT(IN)*DELX)**2.0+(FLOAT(JN)*DELY)**2.0
$+(FLOAT(KN)*DELZ)**2.0)
RNP(I,J)=SQRT((FLOAT(IN)*DELX)**2.0+(FLOAT(JNP)*DELY)**2.0
$+(FLOAT(KN)*DELZ)**2.0)
C
THETA=(IFIX((RNP(I,J)-RN(I,J))/(DELY)+0.5))-
$((RNP(I,J)-RN(I,J))/(DELY))
RCOM=RN(I,J)/(2.0*RNP(I,J))
C
C1(I,J)=RCOM*(THETA*(THETA-1.0))
C2(I,J)=RCOM*2.0*(1.0-(THETA**2.0))
C3(I,J)=RCOM*(THETA*(THETA+1.0))

```

```

110 CONTINUE
100 CONTINUE
C
END IF
C
CALL WRITMS (1,C1(1,1),768,K11,1)
CALL WRITMS (1,C2(1,1),768,K12,1)
CALL WRITMS (1,C3(1,1),768,K13,1)
C
50 CONTINUE
C
C
C*****
C
RETURN
END
SUBROUTINE EADV
C
C THIS SUBROUTINE ADVANCES THE E-FIELDS TWO Z-PLANES AT A TIME.
C RECORDS OF H-FIELDS FOR TWO SUCCESSION Z-PLANES MUST BE KEPT IN
C ORDER TO TAKE DERIVATIVES IN THE Z-DIRECTION.
C RECORDS OF SIB FOR TWO SUCCESSION Z-PLANES MUST BE KEPT IN ORDER TO TAKE
C AVERAGES IN THE Z-DIRECTION.
C
COMMON /SET1/NMAX,EPST,SIG0,C,TMU0,DELT
COMMON /SET2/ ICAN,ICM1,ICP1,JCAN,JCM1,JCP1,KCAN,KCM1,KCP1
COMMON /SET3/ DELX,DELY,DELZ
COMMON /TIME/ TEN,THN
COMMON /ARRAYS/ EX(27,27),B1(39),EY(27,27),B2(39),EZ(27,27),
+ B3(39),HXA(27,27),B4(39),HXB(27,27),B5(39),HYA(27,27),B6(39),
+ HYB(27,27),B7(39),HZA(27,27),B8(39),HXB(27,27),B9(39),
+ SIGA(27,27),B10(39),SIGB(27,27),B11(39)
C
ADVANCE E-FIELDS BY Z-PLANES
READ IN FIRST H-PLANES
C
CALL READMS(1,HXA(1,1),768,82)
CALL READMS(1,HYA(1,1),768,109)
C
DO FOR ALL Z-PLANES
C
MN0=8
MN9=9
MN10=10
DO 1000 KLOOP=1,KCAN,2
K=KLOOP
KP1=K+1
K2=K+27
K3=K+54
K4=K+82
K5=K+109
K6=K+135

```

```

      K7=K+162
C
C      READ IN SECOND H-PLANES AND OLD E-FIELDS
C
      CALL READMS(1,EX(1,1),768,K)
      CALL READMS(1,EY(1,1),768,K2)
      CALL READMS(1,EZ(1,1),768,K3)
      CALL READMS(1,HXB(1,1),768,K4)
      CALL READMS(1,HYB(1,1),768,K5)
      CALL READMS(1,HZA(1,1),768,K6)
      CALL READMS(1,SIGA(1,1),768,K7)
C
      DO 200 J=1,JCAN
      JP1=J+1
      DO 200 I=2,ICAN
C
C      SIG(X0,Y,Z)=.5*(SIG(X-DELX,Y,Z)+SIG(X,Y,Z))
C      SIG(X,IY0,Z)=.5*(SIG(X,Y-DELY,Z)+SIG(X,Y,Z))
C      SIG(X,Y,IZ0)=.5*(SIG(X,Y,Z-DELZ)+SIG(X,Y,Z))
C
      SIG2=.25*(SIGA(I,J)+SIGA(I-1,J))
      A=EPST-SIG2
      B=1./(EPST+SIG2)
      EX(I,J)=(A*EX(I,J)+(HZA(I,JP1)-HZA(I,J))/DELY -
+ (HYB(I,J)-HYA(I,J))/DELZ)*B
200  CONTINUE
      DO 300 I=1,ICAN
      IP1=I+1
      DO 300 J=2,JCAN
      SIG2=.25*(SIGA(I,J-1)+SIGA(I,J))
      A=EPST-SIG2
      B=1./(EPST+SIG2)
      EY(I,J)=(A*EY(I,J)+(HXB(I,J)-HXA(I,J))/DELZ -
+ (HZA(IP1,J)-HZA(I,J))/DELX)*B
300  CONTINUE
C
C      WRITE NEW EX,EY PLANES TO MASS STORAGE
C
      CALL WRITMS(1,EX(1,1),768,K,1)
      CALL WRITMS(1,EY(1,1),768,K2,1)
      IF (K.EQ.1)GO TO 450
      DO 400 I=1,ICAN
      IP1=I+1
      DO 400 J=1,JCAN
      JP1=J+1
      SIG2=.25*(SIGA(I,J)+SIGB(I,J))
      A=EPST-SIG2
      B=1./(EPST+SIG2)
      EZ(I,J)=(A*EZ(I,J)+(HYA(IP1,J)-HYA(I,J))/DELX -
+ (HXA(I,JP1)-HXA(I,J))/DELY)*B
400  CONTINUE
C

```



```

C   WRITE NEW EZ PLANE TO MASS STORAGE
C
C   CALL WRITMS(1,EZ(1,1),768,K3,1)
C
C   SAMPLE POINTS OF INTEREST(ODD K PLANES)
C
111   FORMAT (I4,2(1X,1PIE11.4))
112   FORMAT (I4,2(1X,1PIE11.4),2(/))
C
C
450  CONTINUE
      K=KP1
      KP1=K+1
      K2=K2+1
      K3=K3+1
      K4=K4+1
      K5=K5+1
      K6=K6+1
      K7=K7+1
C
C   READ IN SECOND OLD E-PLANES AND NEXT H-PLANES OVER A PLANE
C
      CALL READMS(1,EX(1,1),768,K)
      CALL READMS(1,EY(1,1),768,K2)
      CALL READMS(1,EZ(1,1),768,K3)
      CALL READMS(1,HXA(1,1),768,K4)
      CALL READMS(1,HYA(1,1),768,K5)
      CALL READMS(1,HZB(1,1),768,K6)
      CALL READMS(1,SIGB(1,1),768,K7)
      DO 600 J=1,JCAN
        JP1=J+1
        DO 600 I=2,ICAN
          SIG2=.25*(SIGB(I,J)+SIGB(I-1,J))
          A=EPST-SIG2
          B=1./(EPST+SIG2)
          EX(I,J)=(A*EX(I,J)+(HZB(I,JP1)-HZB(I,J))/DELZ -
+ (HYA(I,J)-HYB(I,J))/DELZ)*B
600    CONTINUE
        DO 700 I=1,ICAN
          IP1=I+1
          DO 700 J=2,JCAN
            SIG2=.25*(SIGB(I,J-1)+SIGB(I,J))
            A=EPST-SIG2
            B=1./(EPST+SIG2)
            EY(I,J)=(A*EY(I,J)+(HXA(I,J)-HXB(I,J))/DELZ -
+ (HZB(IP1,J)-HZB(I,J))/DELX)*B
700    CONTINUE
        DO 800 I=1,ICAN
          IP1=I+1
          DO 800 J=1,JCAN
            JP1=J+1
            SIG2=.25*(SIGB(I,J)+SIGB(I,J))

```

```

A=EPST-SIG2
B=1./(EPST+SIG2)
EZ(I,J)=(A+EZ(I,J)+(HYB(IP1,J)-HYB(I,J))/DELX -
+(HXB(I,JP1)-HXB(I,J))/DELY)*B
800 CONTINUE
C
C WRITE NEW EX,EY,EZ PLANES TO MASS STORAGE
C
CALL WRITMS(1,EX(1,1),768,K,1)
CALL WRITMS(1,EY(1,1),768,K2,1)
CALL WRITMS(1,EZ(1,1),768,K3,1)
C
C SAMPLE POINTS OF INTEREST (EVEN K PLANES)
C
IF (K.EQ.10) WRITE (6,111) MN8,TEN,EY(17,11)
IF (K.EQ.18) WRITE (6,112) MN10,TEN,EY(17,11)
C
IF (K.EQ.14) THEN
WRITE (6,111) MN9,TEN,EI(15,13)
ELSE
END IF
C
1000 CONTINUE
C
C ZERO THE ELECTRIC FIELD WITHIN THE METAL COMPONENTS OF AIRCRAFT.
C
CALL AIRPLN
RETURN
END
SUBROUTINE HADV
C
C THIS SUBROUTINE ADVANCES THE H-FIELDS TWO Z-PLANES AT A TIME.
C RECORDS OF E-FIELDS FOR TWO SUCCESSIVE PLANES MUST BE KEPT IN ORDER TO TAKE
C DERIVATIVES IN THE Z-DIRECTION.
C*****
C ALSO MOST MODIFICATIONS FOR THE RADIATION
C BOUNDARY CONDITIONS WERE PLACED HERE
C*****
C
COMMON /SET1/ NMAX,EPST,SIG0,C,TMUD,DELT
COMMON /SET2/ ICAN,ICM1,ICP1,JCAN,JCM1,JCP1,KCAN,KCM1,KCP1
COMMON /SET3/ DELX,DELY,DELZ
COMMON /TIME/ TEN,TIN
COMMON /ARRAYS/ EXA(27,27),B1(39),EXB(27,27),B2(39),
+EYA(27,27),B3(39),EYB(27,27),B4(39),EZA(27,27),B5(39),
+EZB(27,27),B6(39),HXA(27,27),B7(39),HYA(27,27),B8(39),
+HZ(27,27),B9(39),
C*****
+A10(27,27),B10(39),A11(27,27),B11(39),HXTM2(27,27),B12(39),
+HYTM2(27,27),B13(39),HZTM2(27,27),B14(39),C1(27,27),B15(39),
+C2(27,27),B16(39),C3(27,27),B17(39),HXKM1(27,27),B18(39),
+HYKM1(27,27),B19(39),HZKM1(27,27),B20(39)

```

```

      REAL HXTM1(27,27),HYTM1(27,27),HZTM1(27,27)
C
C*****
C
C
C      DO FOR ALL Z-PLANES
          MN1=1
          MN2=2
          MN3=3
          MN4=4
          MN5=5
          MN6=6
          MN7=7
C
      DO 900 KLOOP=1,KCAN,2
      K=KLOOP
      KM1=K-1
      K2=K+27
      K3=K+54
      K4=K+81
      K5=K+108
      K6=K+135
C*****
      K10=K+243
      K11=K+270
      K12=K+297
      K13=K+324
      CALL READMS(1,HZTM2(1,1),768,K10)
      CALL READMS(1,C1(1,1),768,K11)
      CALL READMS(1,C2(1,1),768,K12)
      CALL READMS(1,C3(1,1),768,K13)
C*****
      CALL READMS(1,EXB(1,1),768,K)
      CALL READMS(1,EYB(1,1),768,K2)
      CALL READMS(1,HZ(1,1),768,K6)
      IF (K.EQ.1)GO TO 350
C*****
      K8=K+189
      K9=K+216
      CALL READMS(1,HXTM2(1,1),768,K8)
      CALL READMS(1,HYTM2(1,1),768,K9)
C*****
      CALL READMS(1,EZB(1,1),768,K3)
      CALL READMS(1,HX(1,1),768,K4)
      CALL READMS(1,HY(1,1),768,K5)
      DO 200 J=2,JCAN
      DO 200 I=1,ICAN
C*****
      HXTM1(I,J)=HX(I,J)
C*****
      HX(I,J)=HX(I,J)+TMUO*((EYB(I,J)-EYA(I,J))/DELZ -
      +(EZB(I,J)-EZB(I,J-1))/DELY)

```

```

200  CONTINUE
    DO 300 I=1, ICM1
      IP1=I+1
      DO 300 J=1, JCAN
C*****
        HYTM1(IP1,J)=HY(IP1,J)
C*****
        HY(IP1,J)=HY(IP1,J)+TMUD*((EZB(IP1,J)-EZB(I,J))/DELX -
          +(EXB(IP1,J)-EXA(IP1,J))/DELZ)
300  CONTINUE
C
C    APPROXIMATES H FIELDS IN PLANE PERPENDICULAR TO WIRE
C    BY  $H=I/2\pi R$ .
C    SOURCE FUNCTION, ODD K REFERENCE PLANES, HY
C    CURRENT PULSE MOVING IN X DIRECTION ATTACHES TO THE NOSE OF THE AIRPLANE
C    AT (X,Y,Z)=(3,9,15), EXITS BY THE TAIL AT (X,Y,Z)=(25,10,15).
C    AT TIME T=0.0 PULSE IS LOCATED AT X(3).
C
      IF(K.NE.15)GO TO 1
      DO 10 I=2,3,1
        TPULSE=TIM-.69*(FLOAT(I)-3.)/C
        IF (TPULSE.LE.0.0)GO TO 10
C
        X=EXP(-3.5E04*TPULSE)-EXP(-2.625E7*TPULSE)
C
        HYS=7.07E3*X
        HY(I,9)=-HYS
10    CONTINUE
        DO 30 I=25,26,1
          TPULSE=TIM-.69*(FLOAT(I)-3.0)/C
          IF (TPULSE.LE.0.0)GO TO 30
          X=EXP(-3.5E4*TPULSE)-EXP(-2.625E7*TPULSE)
          HYS=7.07E3*X
          HY(I,10)=-HYS
30    CONTINUE
1    CONTINUE
C*****
C    SIDES WHEN I=1 & ICP1
      ICM2=ICAN-2
      DO 310 I=2, ICAN, ICM2
        DO 320 J=1, JCAN
          IF (I.EQ.2) THEN
            IB=1
          ELSE
            IB=ICAN+1
          END IF
          HY(IB,J)=C1(I,J)*HYTM2(I,J)+C2(I,J)*HYTM1(I,J)+C3(I,J)*HY(I,J)
          HYTM2(I,J)=HYTM1(I,J)
          IF (J.GE.2) THEN
            HZ(IB,J)=C1(I,J)*HZTM2(I,J)+C2(I,J)*HZTM1(I,J)+C3(I,J)*HZ(I,J)
            HZTM2(I,J)=HZTM1(I,J)
          ELSE

```

```

      END IF
320  CONTINUE
310  CONTINUE
C    SIDES WHEN J=1 & JCP1
      JCM2=JCAN-2
      DO 330 J=2, JCAN, JCM2
      DO 340 I=1, ICAN
        IF (J.EQ.2) THEN
          JB=1
        ELSE
          JB=JCAN+1
        END IF
      HX(I,JB)=C1(I,J)*HXTM2(I,J)+C2(I,J)*HXTM1(I,J)+C3(I,J)*HX(I,J)
      HXTM2(I,J)=HXTM1(I,J)
      IF (I.GE.2) THEN
      HZ(I,JB)=C1(I,J)*HZTM2(I,J)+C2(I,J)*HZTM1(I,J)+C3(I,J)*HZ(I,J)
      HZTM2(I,J)=HZTM1(I,J)
      ELSE
      END IF
340  CONTINUE
330  CONTINUE
      HZ(1,1)=HZ(2,1)
      HZ(1,27)=HZ(2,27)
      HZ(27,1)=HZ(27,2)
      HZ(27,"7")=HZ(27,26)
C*****
C
C    WRITE NEW HX, HY PLANES TO MASS STORAGE
C
      CALL WRITMS(1,HX(1,1),768,K4,1)
      CALL WRITMS(1,HY(1,1),768,K5,1)
C*****
      CALL WRITMS(1,HZ(1,1),768,K6,1)
      CALL WRITMS(1,HXTM2(1,1),768,K8,1)
      CALL WRITMS(1,HXTM2(1,1),768,K9,1)
      CALL WRITMS(1,HZTM2(1,1),768,K10,1)
C*****
350  CONTINUE
      DO 400 I=1, ICM1
      JP1=I+1
      DO 400 J=1, JCM1
      JP1=J+1
C*****
      HZTM1(IP1,JP1)=HZ(IP1,JP1)
C*****
      HZ(IP1,JP1)=HZ(IP1,JP1)+TMID*((EXB(IP1,JP1)-EXB(IP1,J))/DELY -
      +(EYB(IP1,JP1)-EYB(I,JP1))/DELX)
400  CONTINUE
C*****
C    SIDES I=1 & ICP1
      ICM2=ICAN-2
      DO 610 I=2, ICAN, ICM2

```

```

DO 620 J=2, JCAN
  IF (I.EQ.2) THEN
    IB=1
  ELSE
    IB=ICAN+1
  END IF
C
  HZ(IB,J)=C1(I,J)*HZTM2(I,J)+C2(I,J)*HZTM1(I,J)+C3(I,J)*HZ(I,J)
  HZTM2(I,J)=HZTM1(I,J)
620 CONTINUE
610 CONTINUE
  JCM2=JCAN-2
C
  SIDES J=1 & JCP1
  DO 630 J=2, JCAN, JCM2
    DO 640 I=2, ICAN
      IF (J.EQ.2) THEN
        JB=1
      ELSE
        JB=JCAN+1
      END IF
      HZ(I,JB)=C1(I,J)*HZTM2(I,J)+C2(I,J)*HZTM1(I,J)+C3(I,J)*HZ(I,J)
      HJTM2(I,J)=HZTM1(I,J)
640 CONTINUE
630 CONTINUE
      HZ(1,1)=HZ(2,1)
      HZ(1,27)=HZ(2,27)
      HZ(27,1)=HZ(27,2)
      HZ(27,27)=HZ(27,26)
C
      WRITE NEW HZ PLANE TO MASS STORAGE
C
      CALL WRITMS(1,HZ(1,1),768,K6,1)
      CALL WRITMS(1,HZTM2(1,1),768,K10,1)
C*****
C
C   SAMPLE POINTS OF INTEREST (ODD K PLANES)
C
      IF (K.EA.13) WRITE(6,111) MN2, THN, HZ(4,10)
      IF (K.EQ.13) WRITE(6,111) MN3, THN, HZ(24,11)
      IF (K.EQ.23) WRITE(6,111) MN7, THN, HX(18,10)
C
111   FORMAT (14,2(1X,1PIE11.4))
C
      K=K+1
      KM1=K-1
      K2=K2+1
      K3=K3+1
      K4=K4+1
      K5=K5+1
      K6=K6+1
C*****
      K8=K+189
      K9=K+216

```

```

K10=K+243
K11=K+270
K12=K+297
K13=K+324
CALL READMS(1,HXTM2(1,1),768,K8)
CALL READMS(1,HYTM2(1,1),768,K9)
CALL READMS(1,HZTM2(1,1),768,K1 )
CALL READMS(1,C1(1,1),768,K11)
CALL READMS(1,C2(1,1),768,K12)
CALL READMS(1,C3(1,1),768,K13)
C   FACE
      IF (K.EQ.2.OR.K.EQ.KCAN) THEN
        IF (K.EQ.2) THEN
          KM1X=K+80
          KM1Y=K+107
          KM1Z=K+134
        CALL READMS (1,HXKM1(1,1),768,KM1X)
        CALL READMS (1,HYKM1(1,1),768,KM1Y)
        CALL READMS (1,HZKM1(1,1),768,KM1Z)
        ELSE
          KM1X=K+82
          KM1Y=K+109
          KM1Z=K+136
        CALL READMS (1,HXKM1(1,1),768,KM1X)
        CALL READMS (1,HYKM1(1,1),768,KM1Y)
        CALL READMS (1,HZKM1(1,1),768,KM1Z)
        END IF
      ELSE
        END IF
C*****
C
C   BEAD IN NEXT PLANES OF E AND H
C
      CALL READMS(1,EXA(1,1),768,K1)
      CALL READMS(1,EYA(1,1),768,K2)
      CALL READMS(1,EZA(1,1),768,K3)
      CALL READMS(1,HX(1,1),768,K4)
      CALL READMS(1,HY(1,1),768,K5)
      CALL READMS(1,HZ(1,1),768,K6)
      DO 600 J=1,JCM1
        JP1=J+1
      DO 600 I=1,ICAN
C*****
        HXTM1(I,JP1)=HX(I,JP1)
C*****
        HX(I,JP1)=HX(I,JP1)+TMUD*((EYA(I,JP1)-EYB(I,JP1))/DELZ -
+ (EZA(I,JP1)-EZA(I,J1))/DELY)
      600 CONTINUE
      DO 700 I=1,ICM1
        IP1=I+1
      DO 700 J=1,JCAN
C*****

```

```

      HYTM1(IP1,J)=HY(IP1,J)
C*****
      HY(IP1,J)=HY(IP1,J)+TMUD*((EZA(IP1,J)-EZA(I,J))/DELX -
+ (EXA(IP1,J)-EXB(IP1,J))/DELZ)
700  CONTINUE
C
C      SOURCE FUNCTION, EVEN K REFERENCE PLANES, HY
C
      IF (K.NE.14)GO TO 2
      DO 20 I=2,3,1
      TPULSE=THN-.69*(FLOAT(I)-3.)/C
      IF (TPULSE.LE.0.0)GO TO 20
      X=EXP(-3.5E4*TPULSE)-EXP(-2.625E7*TPULSE)
      HYS=7.07E3*X
      HY(I,9)=+HYS
20    CONTINUE
      DO 40 I=25,26,1
      TPULSE=THN-.69*(FLOAT(I)-3.)/C
      IF (TPULSE.LE.0.0)GO TO 40
      X=EXP(-3.5E4*TPULSE)-EXP(-2.625E7*TPULSE)
      HYS=7.07E3*X
      HY(I,10)=HYS
40    CONTINUE
2      CONTINUE
      DO 800 I=1,ICM1
      IP1=I+1
      DO 800 J=1,JCM1
      JP1=J+1
C*****
      HZTM1(IP1,JP1)=HZ(IP1,JP1)
C*****
      HZ(IP1,JP1)=HZ(IP1,JP1)+TMUD*((EXA(IP1,JP1)-EXA(IP1,J))/DELY -
+ (EYA(IP1,JP1)-EYA(I,JP1))/DELX)
800  CONTINUE
C
C
C      SOURCE FUNCTION, EVEN K REFERENCE PLANE, HZ
      IF(K.NE.14)GO TO 4
      DO 60 I=2,3,1
      TPULSE=THN-.69*(FLOAT(I)-3.)/C
      IF (TPULSE.LE.0.0)GO TO 60
      X=(EXP(-3.5E4*TPULSE)-EXP(-2.625E7*TPULSE))
      HZS=1.447E4*X
      HZ(I,9)=-HZS
      HZ(I,10)=HZS
60    CONTINUE
      DO 80 I=25,26,1
      TPULSE=THN-.69*(FLOAT(I)-3.)/C
      IF (TPULSE.LE.0.0)GO TO 80
      X=(EXP(-3.5E4*TPULSE)-EXP(-2.625E7*TPULSE))
      HZS=1.447E4*X
      HZ(I,10)=-HZS

```



```

      HZ(I,11)=HZS
80      CONTINUE
4       CONTINUE
C*****
C      FACE
      IF (K.EQ.2.OR.K.EQ.KCAN) THEN
          DO 210 I=2, ICAN
              DO 220 J=2, JCAN
                  HXKM1(I,J)=C1(I,J)*HXTM2(I,J)+C2(I,J)*HXTM1(I,J)+C3(I,J)*HX(I,J)
                  HXTM2(I,J)=HXTM1(I,J)
                  HYKM1(I,J)=C1(I,J)*HYTM2(I,J)+C2(I,J)*HYTM1(I,J)+C3(I,J)*HY(I,J)
                  HYTM2(I,J)=HYTM1(I,J)
                  HZKM1(I,J)=C1(I,J)*HZTM2(I,J)+C2(I,J)*HZTM1(I,J)+C3(I,J)*HZ(I,J)
                  HZTM2(I,J)=HZTM1(I,J)
220      CONTINUE
210      CONTINUE
C      EDGES OF FACES
      ICM2=ICAN-2
      DO 410 I=2, ICAN, ICM2
          DO 420 J=2, JCAN
              IF (I.EQ.2) THEN
                  IB=1
              ELSE
                  IB=ICAN+1
              END IF
              HXKM1(IB,J)=HXKM1(I,J)
420      CONTINUE
410      CONTINUE
      JCM2=JCAN-2
      DO 430 J=2, JCAN, JCM2
          DO 440 I=2, ICAN
              IF (J.EQ.2) THEN
                  JB=1
              ELSE
                  JB=JCAN+1
              END IF
              HYKM1(I,JB)=HYKM1(I,J)
440      CONTINUE
430      CONTINUE
      CALL WRITMS(1,HXKM1(1,1),768,KM1X,1)
      CALL WRITMS(1,HYKM1(1,1),768,KM1Y,1)
      CALL WRITMS(1,HZKM1(1,1),768,KM1Z,1)
      ELSE
          END IF
      ICM2=ICAN-2
C      SIDED I= 1 & ICP1
      DO 230 I=2, ICAN, ICM2
          DO 240 J=1, JCAN
              IF (I.EQ.2) THEN
                  IB=1
              ELSE
                  IB=ICAN+1

```

```

      END IF
      HY(18,J)=C1(I,J)*HYTM2(I,J)+C2(I,J)*HYTM1(I,J)+C3(I,J)*HY(I,J)
      HYTM2(I,J)=HYTM1(I,J)
      IF (J.GE.2) THEN
      HZ(18,J)=C1(I,J)*HZTM2(I,J)+C2(I,J)*HZTM1(I,J)+C3(I,J)*HZ(I,J)
      HZTM2(I,J)=HZTM1(I,J)
      ELSE
      END IF
240  CONTINUE
230  CONTINUE
      JCM2=JCAN-2
      DO 250 J=2, JCAN, JCM2
      DO 260 I=1, ICAN
        IF (J.EQ.2) THEN
          JB=1
        ELSE
          JB=JCAN+1
        END IF
      HX(1,JB)=C1(I,J)*HXTM2(I,J)+C2(I,J)*HXTM1(I,J)+C3(I,J)*HX(I,J)
      HXTM2(I,J)=HXTM1(I,J)
      IF (I.GE.2) THEN
      HZ(1,JB)=C1(I,J)*HZTM2(I,J)+C2(I,J)*HZTM1(I,J)+C3(I,J)*HZ(I,J)
      HZTM2(I,J)=HZTM1(I,J)
      ELSE
      END IF
260  CONTINUE
250  CONTINUE
      HZ(1,1)=HZ(2,1)
      HZ(1,27)=HZ(2,27)
      HZ(27,1)=HZ(27,2)
      HZ(27,27)=HZ(27,26)
      CALL WRITMS (1,HXTM2(1,1),768,K8,1)
      CALL WRITMS (1,HYTM2(1,1),768,K9,1)
      CALL WRITMS (1,HZTM2(1,1),768,K10,1)
C*****
      CALL WRITMS(1,HX(1,1),768,K4,1)
      CALL WRITMS(1,HY(1,1),768,K5,1)
      CALL WRITMS(1,HZ(1,1),768,K6,1)
C
C  SAMPLE POINTS OF INTEREST (EVEN K PLANES)
C
      IF (K.EQ.14) THEN
        WRITE (6,111) MN4,TIN,HZ(10,4)
        WRITE (6,111) MN5,TIN,HZ(19,4)
        WRITE (6,111) MN6,TIN,HX(22,18)
      ELSE
      END IF
C
      IF (K.EQ.6) WRITE(6,111) MN1,TIN,HX(18,18)
C
900  CONTINUE
      RETURN

```

```

END
SUBROUTINE APERT
RETURN
END
SUBROUTINE AIRPLN

C
C ZEROES THE ELECTRIC FIELDS WITHIN THE F16 AIRCRAFT AND
C TANGENTIAL ELECTRIC FIELD COMPONENTS AT THE SURFACE
C
COMMON /ARRAYS/ FLD (27,27),B1 (39)
C
C EX ZEROED
C
DO 1000 K=3,25
CALL READMS (1,FLD(1,1),768,K)
C WING
IF (K.NE.3) GO TO 40
FLD(18,9)=0.0
FLD(19,9)=0.0
40 IF (K.NE.4) GO TO 50
DO 41 I=17,19
41 FLD(I,9)=0.0
50 IF (K.LT.5.OR.K.GT.6) GO TO 70
DO 51 I=16,19
51 FLD(I,9)=0.0
70 IF (K.LT.7.OR.K.GT.8) GO TO 90
DO 71 I=15,19
DO 71 J=9,10
71 FLD(I,J)=0.0
FLD(23,9)=0.0
FLD(24,9)=0.0
90 IF (K.NE.9) GO TO 100
DO 91 I=14,19
DO 91 J=9,10
91 FLD(I,J)=0.0
DO 92 I=22,24
92 FLD(I,9)=0.0
100 IF (K.NE.10) GO TO 110
DO 101 I=10,19
DO 101 J=9,10
101 FLD(I,J)=0.0
DO 102 I=21,24
102 FLD(I,9)=0.0
110 IF (K.NE.11) GO TO 120
DO 111 I=11,23
DO 111 J=9,10
111 FLD(I,J)=0.0
DO 112 I=11,22
112 FLD(I,8)=0.0
C MAIN FUSELAGE
120 IF (K.LT.12.OR.K.GT.15) GO TO 126
DO 121 I=10,19

```

```

      DO 121 J=5,12
121  FLD(I,J)=0.0
C
C  FORWARD FUSELAGE
C
      DO 122 I=6,9
      DO 122 J=8,10
122  FLD(I,J)=0.0
      DO 123 I=8,9
      DO 123 J=11,12
123  FLD(I,J)=0.0
      FLD(7,11)=0.0
C  REAR FUSELAGE
      DO 124 I=20,22
124  FLD(I,6)=0.0
      DO 125 I=20,23
      DO 125 J=7,12
125  FLD(I,J)=0.0
126  IF (K.NE.12.OR.K.NE.15) GO TO 130
      DO 127 I=19,20
      DO 127 J=3,4
127  FLD(I,J)=0.0
      FLD(20,5)=0.0
130  IF (K.LT.13.OR.K.GT.14) GO TO 135
      FLD(24,9)=0.0
      FLD(24,10)=0.0
C  NOSE AND COCKPIT
      DO 131 I=4,5
      DO 131 J=8,9
131  FLD(I,J)=0.0
      FLD(5,10)=0.0
      FLD(6,11)=0.0
      FLD(7,12)=0.0
      DO 132 I=8,11
      DO 132 J=13,14
132  FLD(I,J)=0.0
      FLD(12,13)=0.0
      FLD(13,13)=0.0
      FLD(9,15)=0.0
C
C  RIGHT VERTICAL STABILIZER
C
135  IF (K.NE.13) GO TO 140
      DO 136 I=19,23
      DO 136 J=13,14
136  FLD(I,J)=0.0
      FLD(17,13)=0.0
      FLD(18,13)=0.0
140  IF (K.NE.14) GO TO 160
      DO 141 I=18,23
      DO 141 J=13,14
141  FLD(I,J)=0.0

```

```

      FLD(17,23)=0.0
      DO 142 I=20,23
      DO 142 J=15,19
142   FLD(I,J)=0.0
      FLD(20,15)=0.0
      FLD(20,16)=0.0
      DO 143 I=22,23
      DO 143 J=20,22
143   FLD(I,J)=0.0
      FLD(24,21)=0.0
      FLD(24,22)=0.0
      DO 144 I=23,24
      DO 144 J=23,24
144   FLD(I,J)=0.0
160   IF (K.NE.16) GO TO 170
      DO 161 I=11,22
      DO 161 J=8,10
161   FLD(I,J)=0.0
      FLD(23,9)=0.0
      FLD(23,10)=0.0
170   IF (K.NE.17) GO TO 180
C     WING
      DO 171 I=13,19
      DO 171 J=9,10
171   FLD(I,J)=0.0
C
C     RIGHT HORIZONTAL STABILIZER
C
      DO 172 I=21,24
172   FLD(I,9)=0.0
180   IF (K.NE.18) GO TO 190
      DO 181 I=14,19
      DO 181 J=9,10
181   FLD(I,J)=0.0
      DO 182 I=22,24
182   FLD(I,9)=0.0
190   IF (K.LT.19.OR.K.GT.20) GO TO 210
      DO 191 I=15,19
      DO 191 J=9,10
191   FLD(I,J)=0.0
      FLD(23,9)=0.0
      FLD(24,9)=0.0
210   IF (K.LT.21.OR.K.GT.22) GO TO 230
      DO 211 I=16,19
211   FLD(I,9)=0.0
230   IF (K.NE.23) GO TO 240
      DO 231 I=17,19
231   FLD(I,9)=0.0
240   IF (K.NE.24) GO TO 1000
      FLD(18,9)=0.0
      FLD(19,9)=0.0
C     STORE EX FIELDS BACK IN TO MASS STORAGE

```

```

1000 CALL WRITMS(1,FLD(1,1),'68,K,1)
C      ZERO EY
      DO 2000 K=3,24
      L=K+27
      CALL READMS (1,FLD(1,1),768,L)
      IF (K.LT.7.OR.K.GT.10) GO TO 1110
      DO 1001 I=14,19
1001      FLD(I,10)=0.0
      IF (K.NE.9) GO TO 1100
      FLD(13,10)=0.0
1100      IF (K.NE.10) GO TO 1110
      FLD(12,10)=0.0
      FLD(13,10)=0.0
1110      IF (K.NE.11) GO TO 1120
      DO 1111 I=10,22
      DO 1111 J=9,10
1111      FLD(I,J)=0.0
      FLD(23,10)=0.0
C      MAIN FUSELAGE
1120      IF (K.LT.12.OR.K.GT.15) GO TO 1130
      DO 1121 I=9,19
      DO 1121 J=6,12
1121      FLD(I,J)=0.0
C      FWD FUSELAGE
      DO 1122 I=5,8
      DO 1122 J=9,10
1122      FLD(I,J)=0.0
      DO 1123 I=7,8
      DO 1123 J=11,12
1123      FLD(I,J)=0.0
      FLD(6,11)=0.0
C      REAR FUSELAGE
      DO 1124 I=20,22
      DO 1124 J=7,12
1124      FLD(I,J)=0.0
      DO 1125 J=8,12
1125      FLD(23,J)=0.0
1130      IF (K.LT.13.OR.K.GT.14) GO TO 1126
      FLD(24,10)=0.0
1126      IF (K.NE.12.OR.K.NE.15) GO TO 1131
      DO 1127 I=18,20
      DO 1127 J=4,5
1127      FLD (I,J)=0.0
      FLD(20,6)=0.0
1131      IF (K.LT.13.OR.K.GT.14) GO TO 1135
      FLD(3,9)=0.0
      FLD(4,9)=0.0
      FLD(4,10)=0.0
      FLD(5,11)=0.0
      FLD(6,12)=0.0
      DO 1132 I=7,13
1132      FLD(I,13)=0.0

```

```

1133      FLD(I,14)=0.0
          FLD(8,15)=0.0
          FLD(9,15)=0.0
1135      IF (K.NE.13) GO TO 1140
          DO 1136 I=16,23
1136      FLD(I,13)=0.0
          DO 1137 I=18,23
1137      FLD(I,14)=0.0
1140      IF (K.NE.14) GO TO 1160
          DO 1141 I=22,23
          DO 1141 J=13,24
1141      FLD(I,J)=0.0
          DO 1142 J=21,24
1142      FLD(24,J)=0.0
          DO 1143 J=20,22
1143      FLD(21,J)=0.0
          DO 1144 J=17,19
          DO 1144 I=20,21
1144      FLD(I,J)=0.0
          DO 1145 I=19,21
          DO 1145 J=15,16
1145      FLD(I,J)=0.0
          DO 1146 I=17,21
1146      FLD(I,14)=0.0
          DO 1147 I=16,21
1147      FLD(I,13)=0.0
1160      IF (K.NE.16) GO TO 1170
          DO 1161 I=18,22
          DO 1161 J=9,10
1161      FLD(I,J)=0.0
          FLD(23,10)=0.0
C        WING
117      IF (K.NE.17) GO TO 1180
          DO 1171 I=12,19
1171      FLD(I,10)=0.0
1180      IF (K.NE.18) GO TO 1190
          DO 1181 I=13,19
1181      FLD(I,10)=0.0
119      IF (K.LT.19.OR.K.GT.20) GO TO 2000
          DO 1191 I=14,19
1191      FLD(I,10)=0.0
C        STORE EY BACK TO MASS STORAGE
2000      CALL WRITMS(1,FLD(1,1),768,L,1)
C        EZ ZEROED
          DO 3000 K=3,24
              L=K+54
          CALL READMS(1,FLD(1,1),768,L)
C        WING TIP
          IF (K.NE.4) GO TO 2050
          DO 2041 I=17,19
2041      FLD(I,9)=0.0
2050      IF (K.NE.5) GO TO 2060

```

```

DO 2051 I=16,19
2051   FLD(I,9)=0.0
C     PLANE
2060   IF (K.LT.6.OR.K.GT.7) GO TO 2080
DO 2061 I=15,19
2061   FLD(I,9)=0.0
C     WING
2080   IF (K.NE.8) GO TO 2090
DO 2081 J=9,10
DO 2081 I=14,19
2081   FLD(I,J)=0.0
C
C     RIGHT HAND STABILIZER
C
DO 2082 I=22,24
2082   FLD(I,9)=0.0
2090   IF (K.NE.9) GO TO 2100
DO 2091 I=14,19
DO 2091 J=9,10
2091   FLD(I,J)=0.0
DO 2092 I=22,24
2092   FLD(I,9)=0.0
2100   IF (K.NE.10) GO TO 2110
DO 2101 I=13,19
DO 2101 J=9,10
2101   FLD(I,J)=0.0
DO 2102 I=21,24
2102   FLD(I,9)=0.0
2110   IF (K.NE.11) GO TO 2120
DO 2111 I=12,24
2111   FLD(I,9)=0.0
DO 2112 I=12,19
2112   FLD(I,10)=0.0
2120   IF (K.NE.12) GO TO 2130
DO 2121 I=10,22
DO 2121 J=8,10
2121   FLD(I,J)=0.0
FLD(23,9)=0.0
FLD(23,10)=0.0
2130   IF (K.LT.13.OR.K.GT.15) GO TO 2140
DO 2131 I=9,19
DO 2131 J=5,12
2131   FLD(I,J)=0.0
DO 2132 I=5,8
DO 2132 J=8,10
2132   FLD(I,J)=0.0
DO 2133 I=7,8
DO 2133 J=11,12
2133   FLD(I,J)=0.0
FLD(6,11)=0.0
DO 2134 I=20,22
DO 2134 J=6,12

```



```

2134      FLD(I,J)=0.0
          DO 2135 J=7,12
2135      FLD(23,J)=0.0
2140      IF (K.NE.14) GO TO 2160
          FLD(24,9)=0.0
          FLD(24,10)=0.0
          DO 2141 I=3,4
          DO 2141 J=8,9
2141      FLD(I,J)=0.0
          FLD(4,10)=0.0
          FLD(5,11)=0.0
          FLD(6,12)=0.0
          DO 2142 I=7,11
          DO 2142 J=13,14
2142      FLD(I,J)=0.0
          FLD(12,13)=0.0
          FLD(13,13)=0.0
          FLD(8,15)=0.0
          FLD(9,15)=0.0
          DO 2143 I=16,23
2143      FLD(I,13)=0.0
          DO 2144 I=18,23
2144      FLD(I,14)=0.0
2160      IF (K.NE.16) GO TO 2170
          DO 2161 I=10,22
          DO 2161 J=8,10
2161      FLD(I,J)=0.0
          FLD(23,9)=0.0
          FLD(23,10)=0.0
2170      IF (K.NE.17) GO TO 2180
          DO 2171 I=12,24
2171      FLD(I,9)=0.0
          DO 2172 I=12,19
2172      FLD(I,10)=0.0
2180      IF (K.NE.18) GO TO 2190
          DO 2181 I=13,19
          DO 2181 J=9,10
2181      FLD(I,J)=0.0
          DO 2182 I=21,24
2182      FLD(I,9)=0.0
2190      IF (K.LT.19.OR.K.GT.20) GO TO 2210
          DO 2191 I=14,19
          DO 2191 J=9,10
2191      FLD(I,J)=0.0
          DO 2192 I=22,24
2192      FLD(I,9)=0.0
2210      IF (K.LT.21.OR.K.GT.22) GO TO 2230
          DO 2211 I=15,19
2211      FLD(I,9)=0.0
2230      IF (K.NE.23) GO TO 2240
          DO 2231 I=16,19
2231      FLD(I,9)=0.0

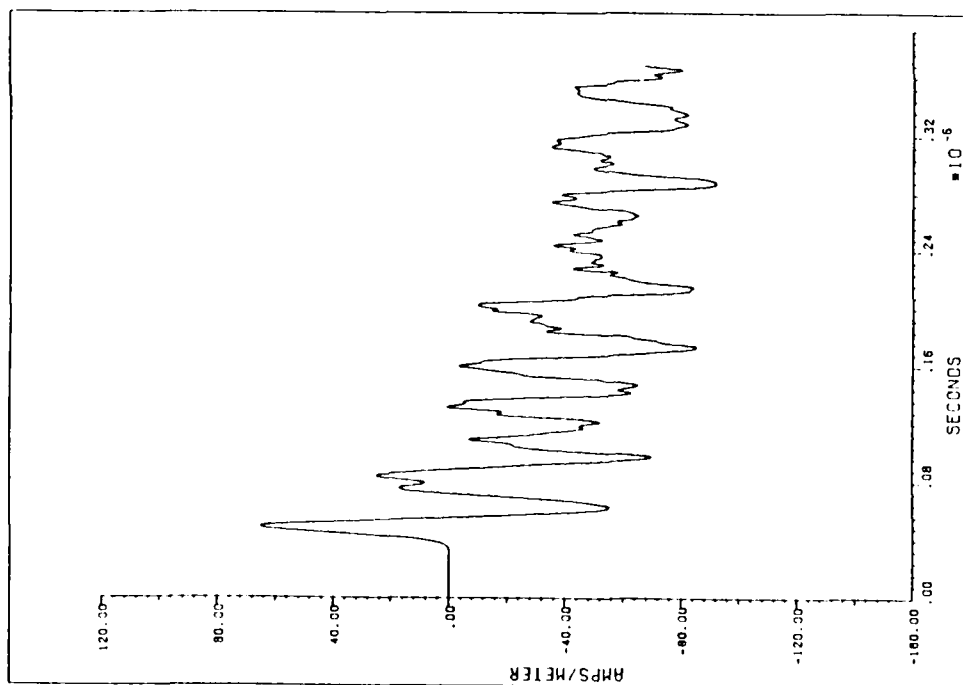
```

2240 IF (K.NE.24) GO TO 3000
DO 2241 I=17,19
2241 FLD(I,9)=0.0
C
C STORE EZ BACK TO MASS STORAGE
C
3000 CALL WRITMS (1,FLD(1,1),768,L,1)
RETURN
END
END OF FILE

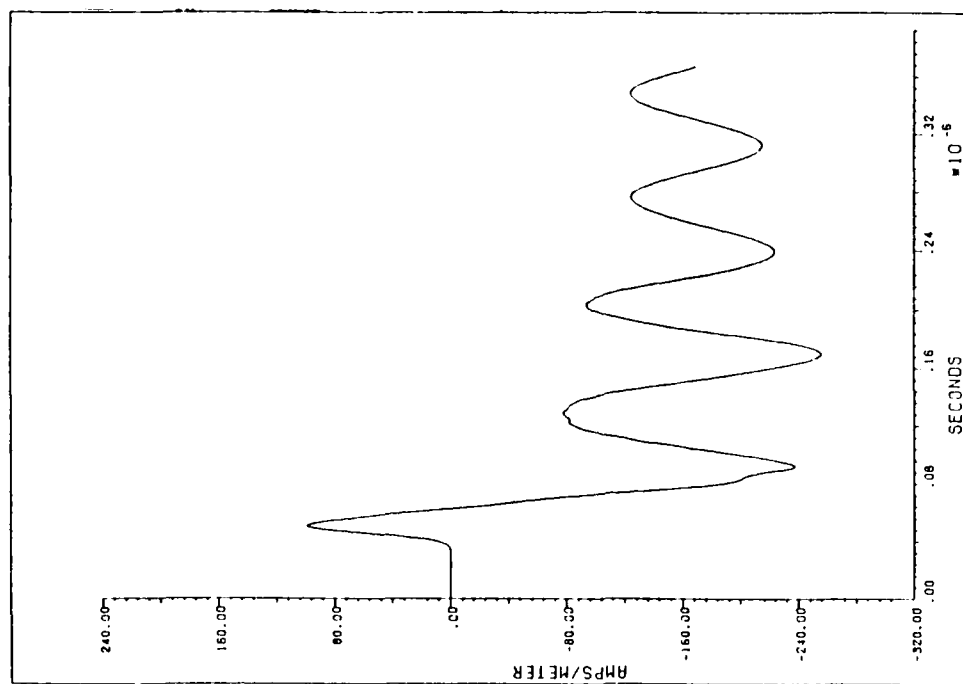
Appendix C

Sensor Plots

This appendix contains graphs of the ten sensors for both the radiation and absorption boundary conditions. Each page contains one graph for the absorption boundary conditions and one graph for the radiation boundary condition. Each graph is made up of 1000 data points calculated from the corresponding programs in Appendix A or B. The points were connected with a natural cubic spline. The only differences in the two codes are the boundary conditions as annotated in the program. Both plots on the same page are for identical time periods so that side-by-side comparisons could be made. The programs were run for results out to 2.5 microseconds. The graphs in this appendix only reflect the first 1.0 microseconds. The graphs beyond 1.0 microseconds were only continuations of the same trends as previous graphs, so they were deleted for brevity. Also, Absorption and Radiation Boundary Conditions are abbreviated ABC and RBC respectively on the plots.

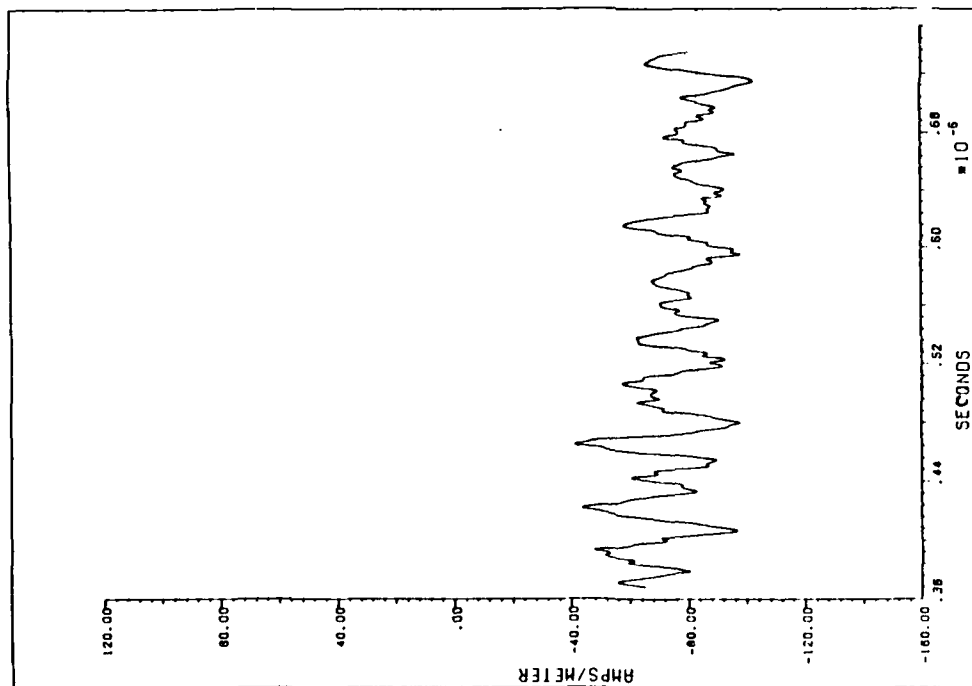


(a) ABC

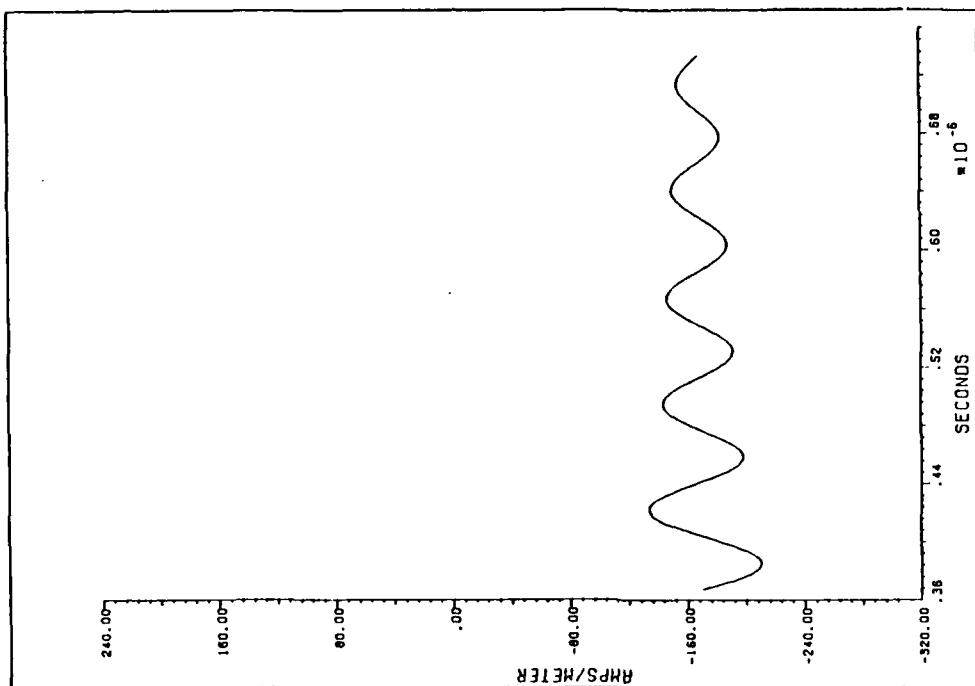


(b) RBC

Figure 27. Sensor One, H-field, Right Wing, $H_x(18,10,6)$

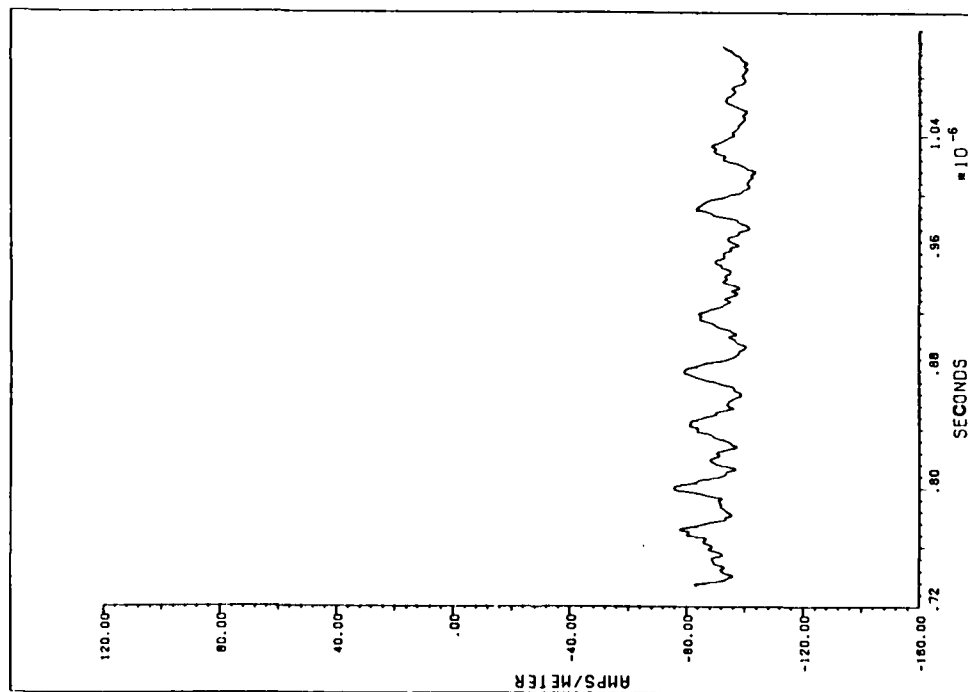


(a) ABC

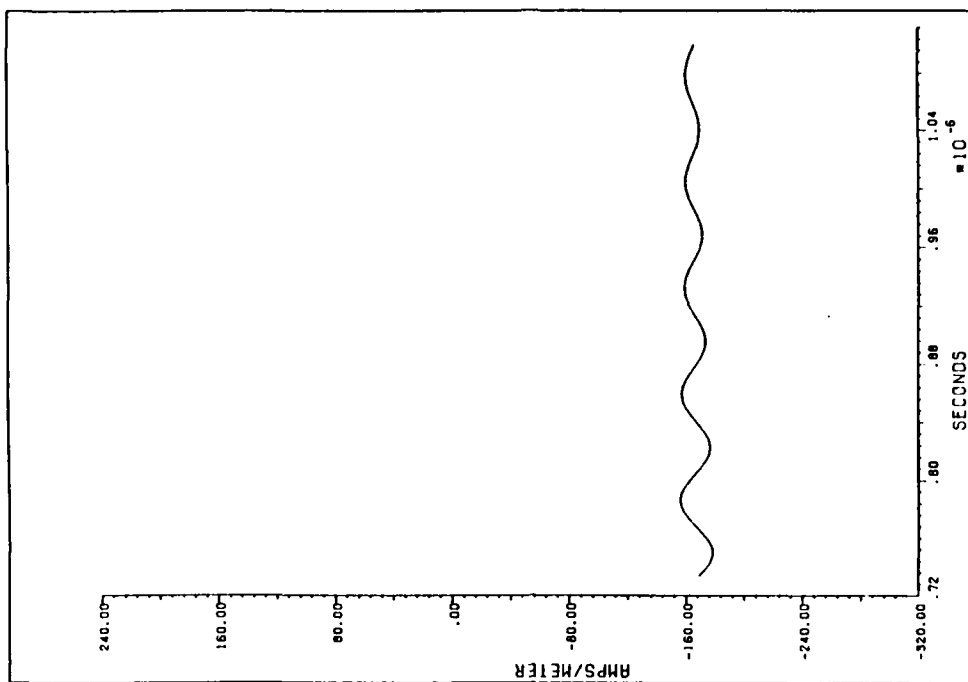


(b) RBC

Figure 28. Sensor One, H-field, Right Wing, $H_x(18,10,6)$

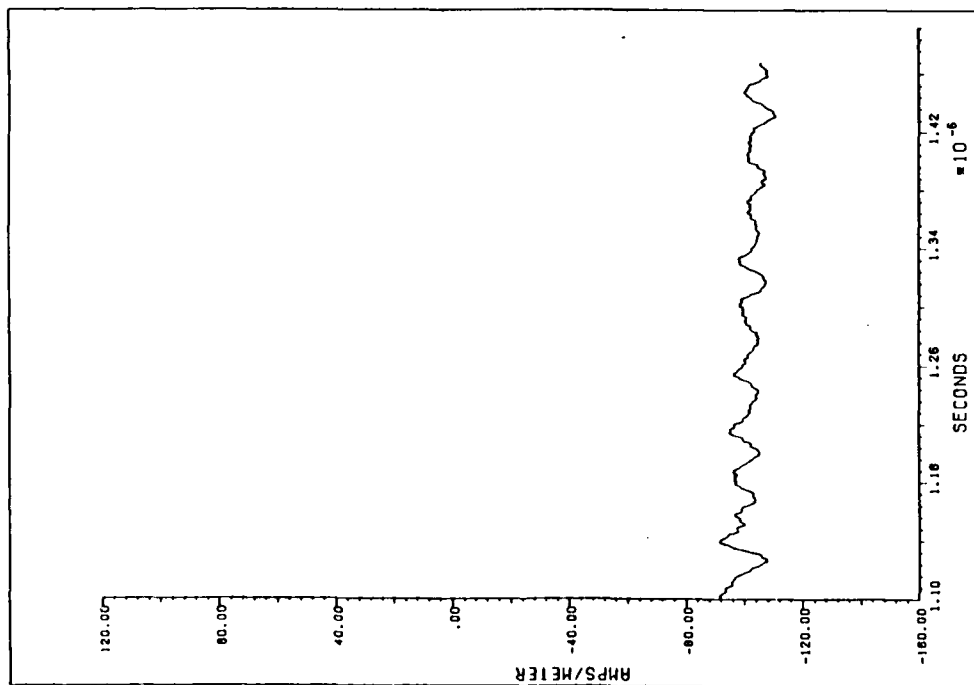


(a) ABC

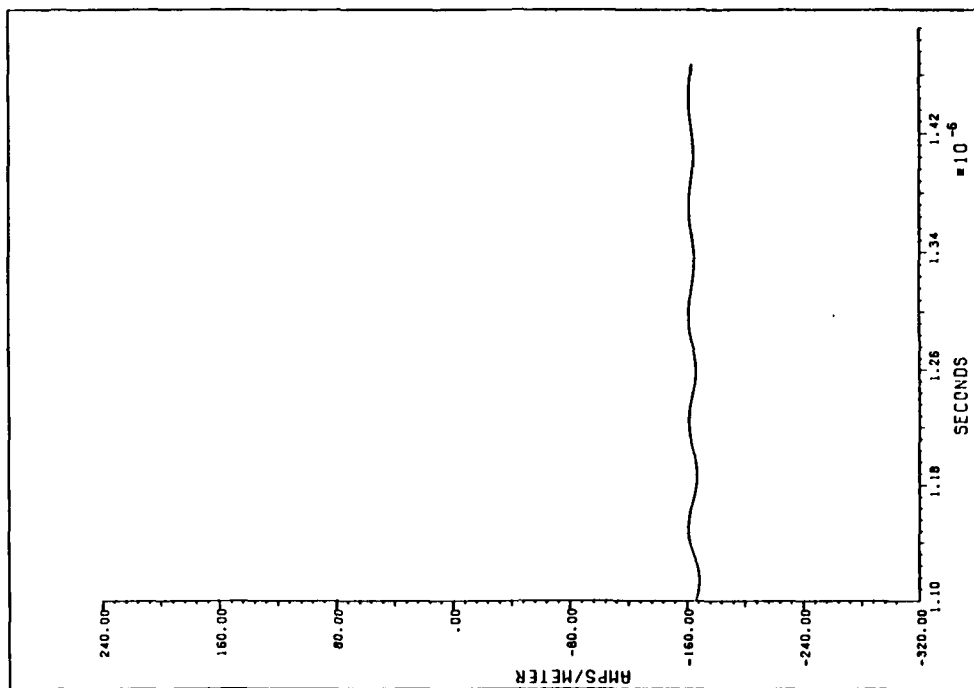


(b) RBC

Figure 29. Sensor One, H-field, Right Wing, $H_x(18,10,6)$

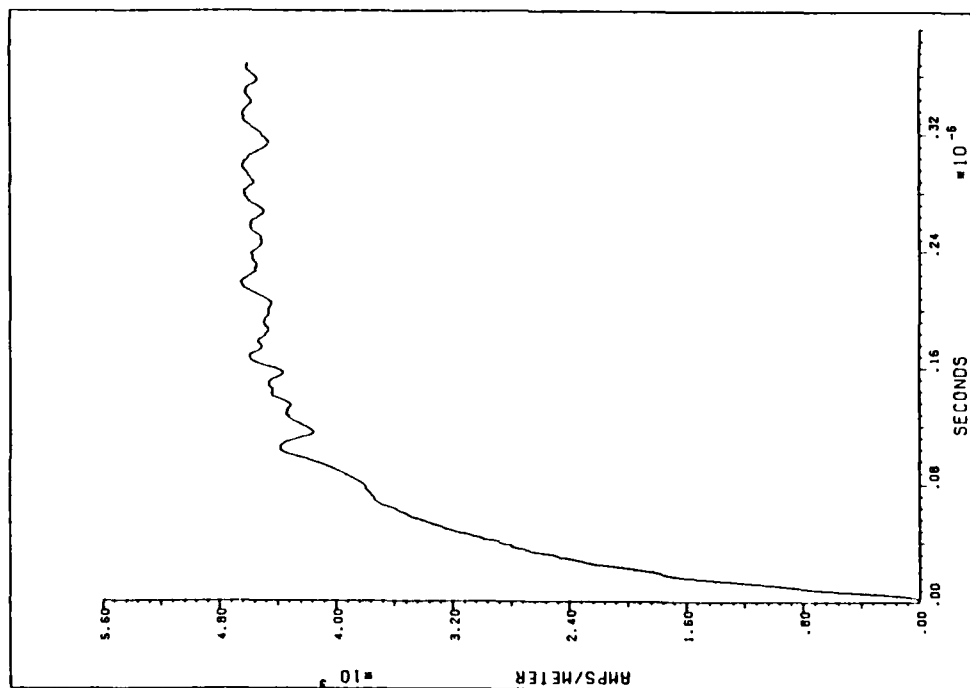


(a) ABC

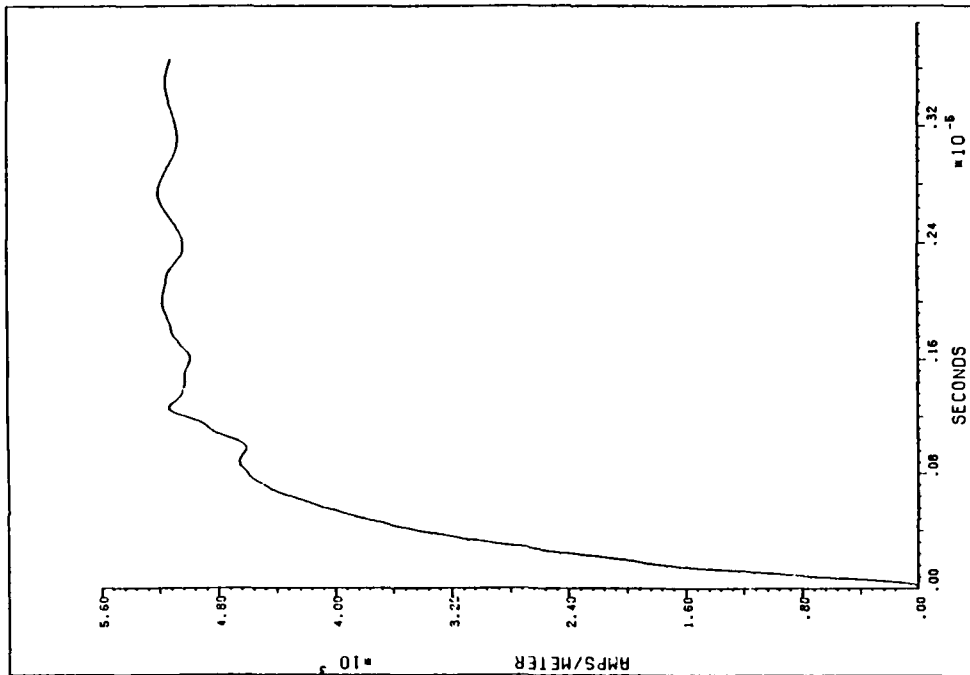


(b) RBC

Figure 30. Sensor One, H-field, Right Wing, $H_x(18,10,6)$

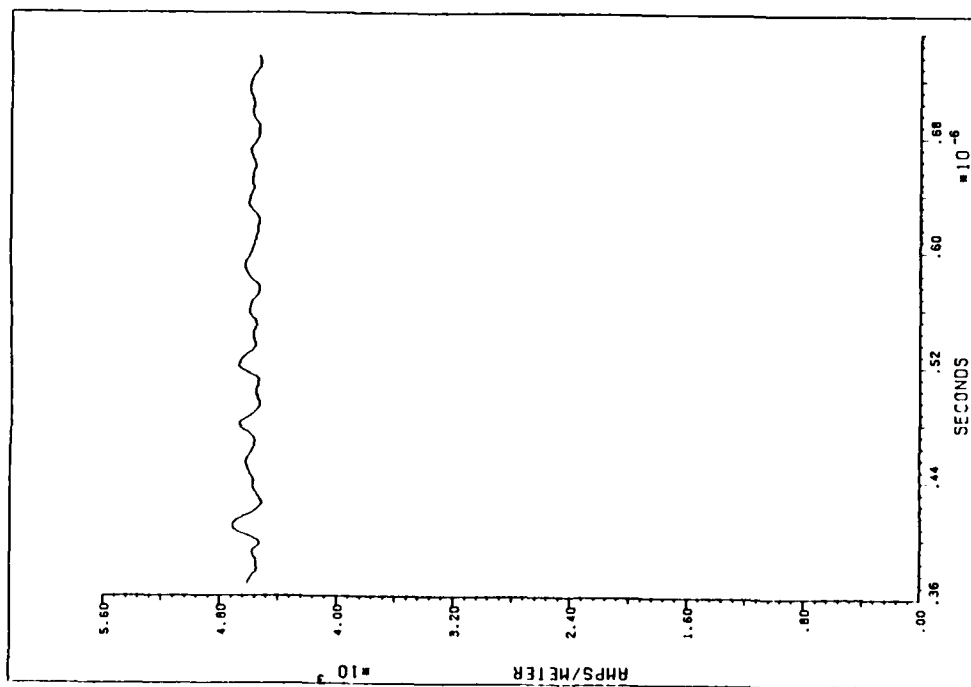


(a) ABC

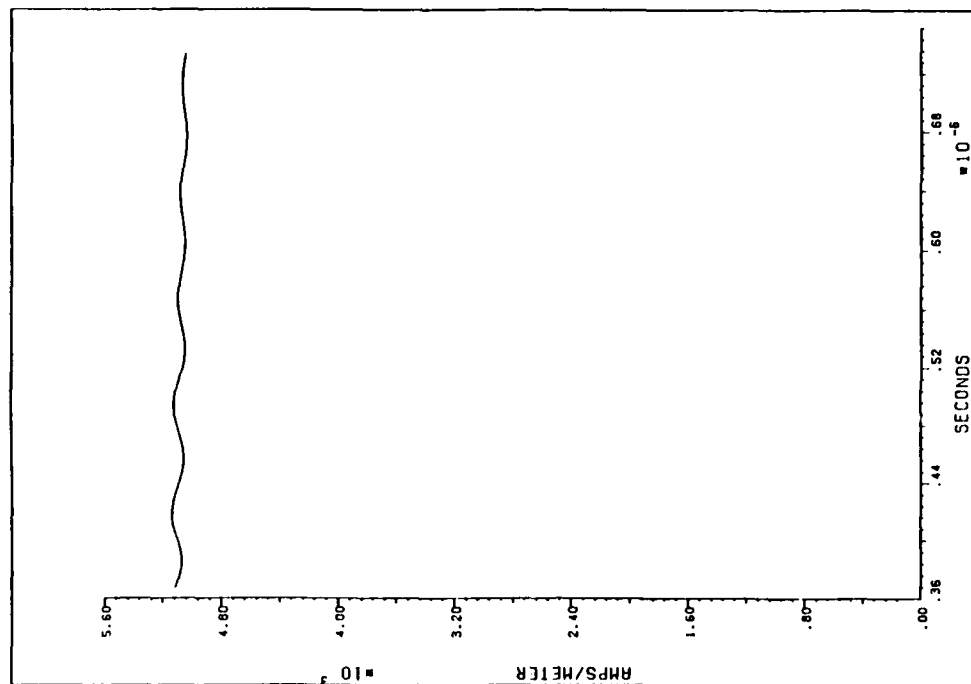


(b) RBC

Figure 31. Sensor Two, H-field, Nose, $H_z(4,10,13)$

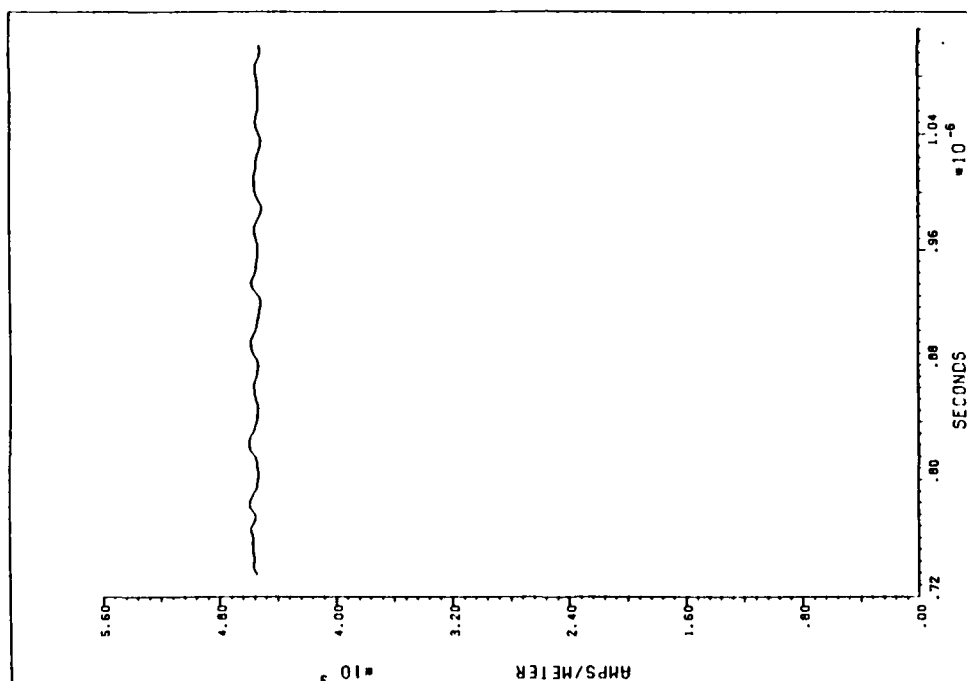


(a) ABC

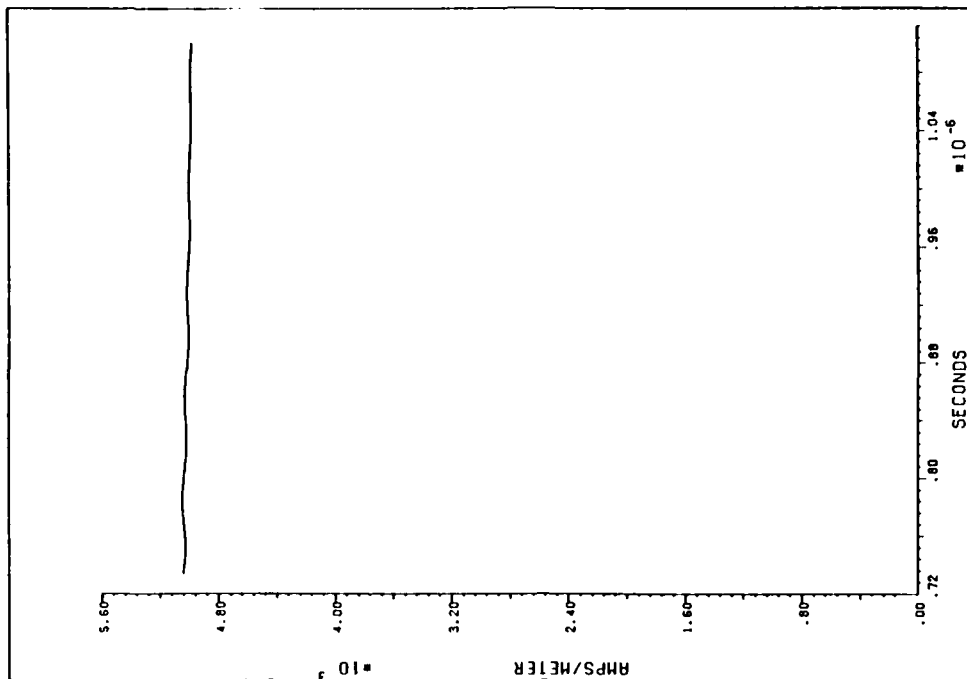


(b) RBC

Figure 32. Sensor Two, H-field, Nose, $H_z(4,10,13)$

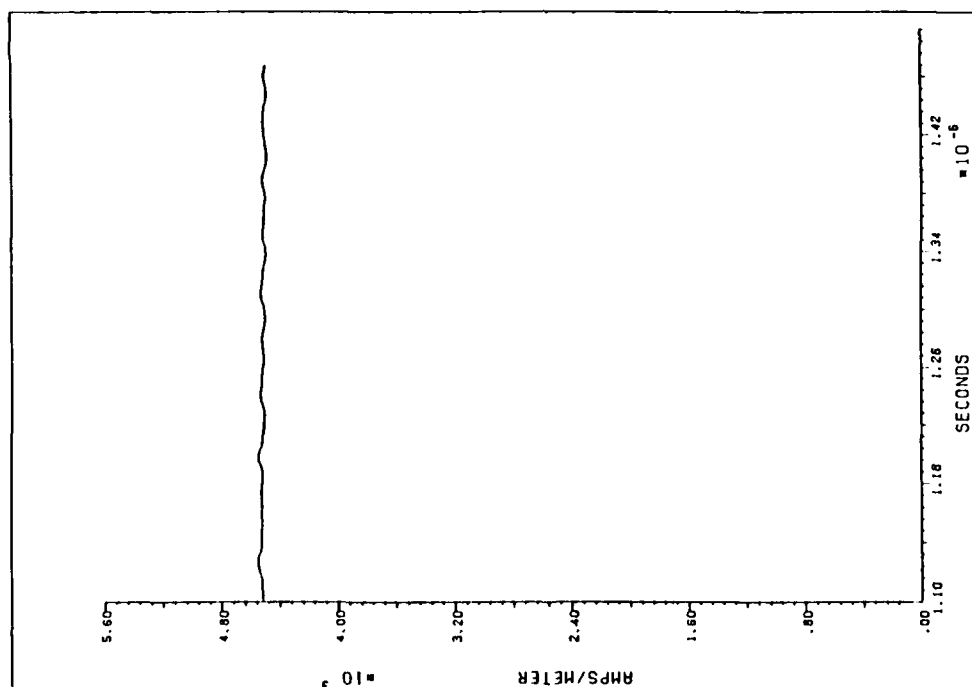


(a) ABC

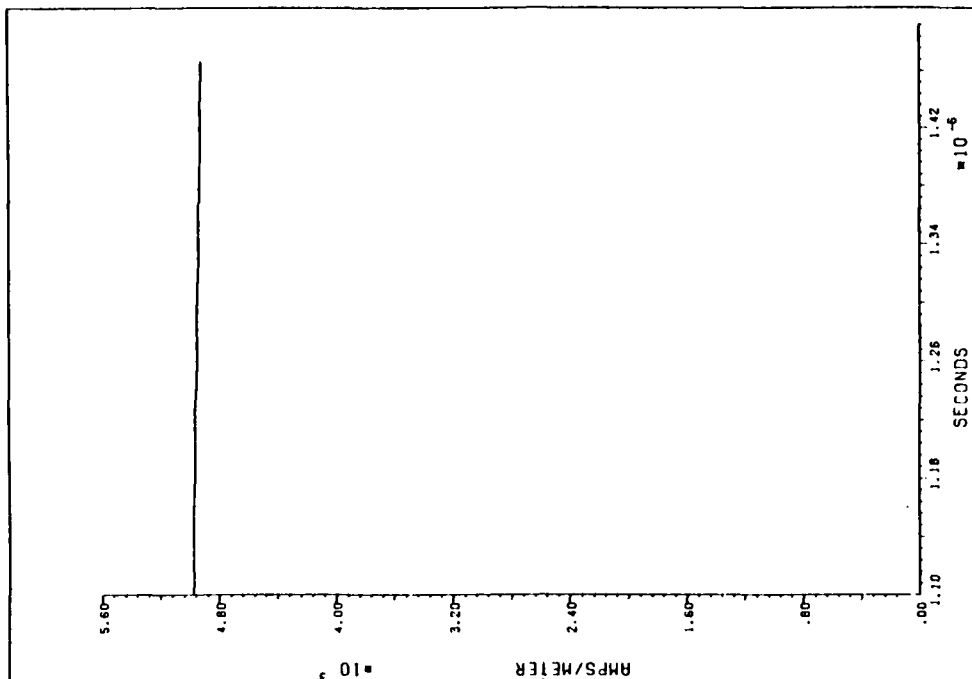


(b) RBC

Figure 33. Sensor Two, H-field, Nose, $H_z(4,10,13)$



(a) ABC



(b) RBC

Figure 34. Sensor Two, H-field, Nose, $H_z(4,10,13)$

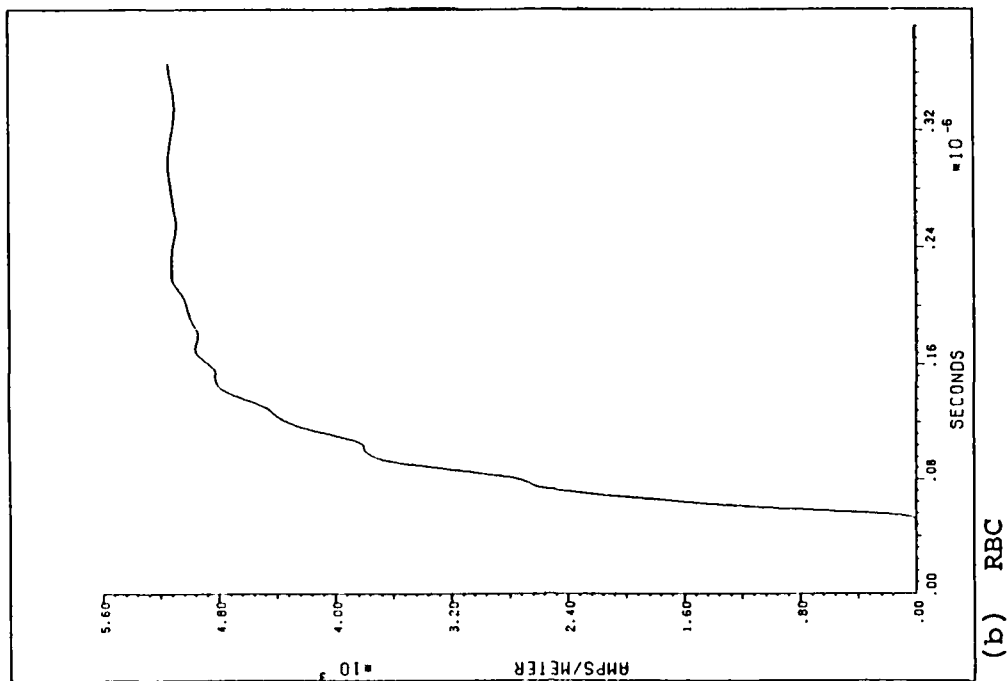
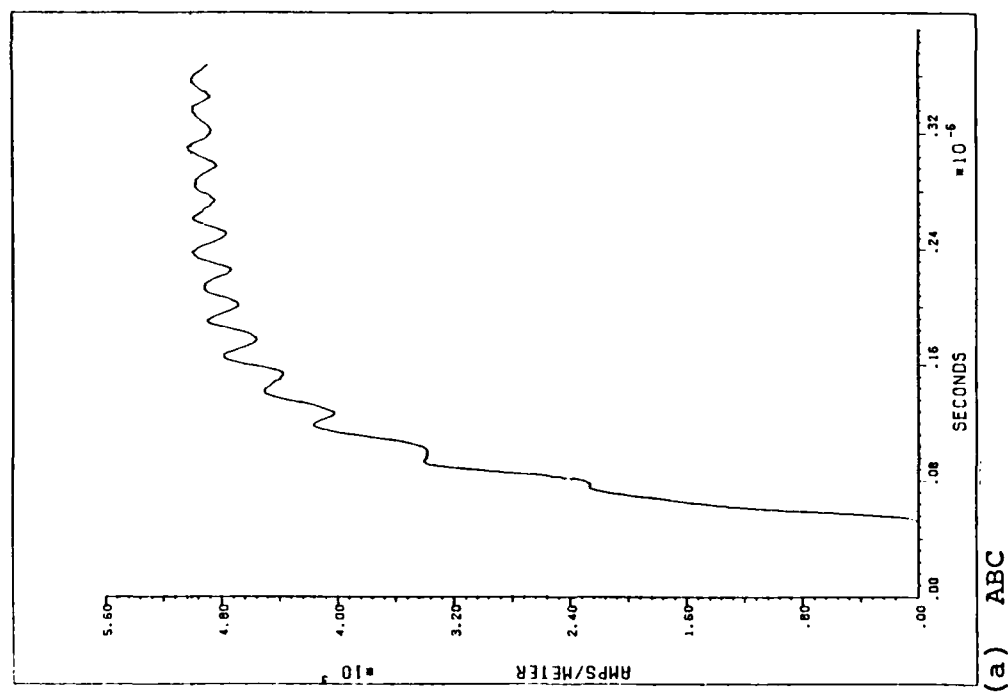
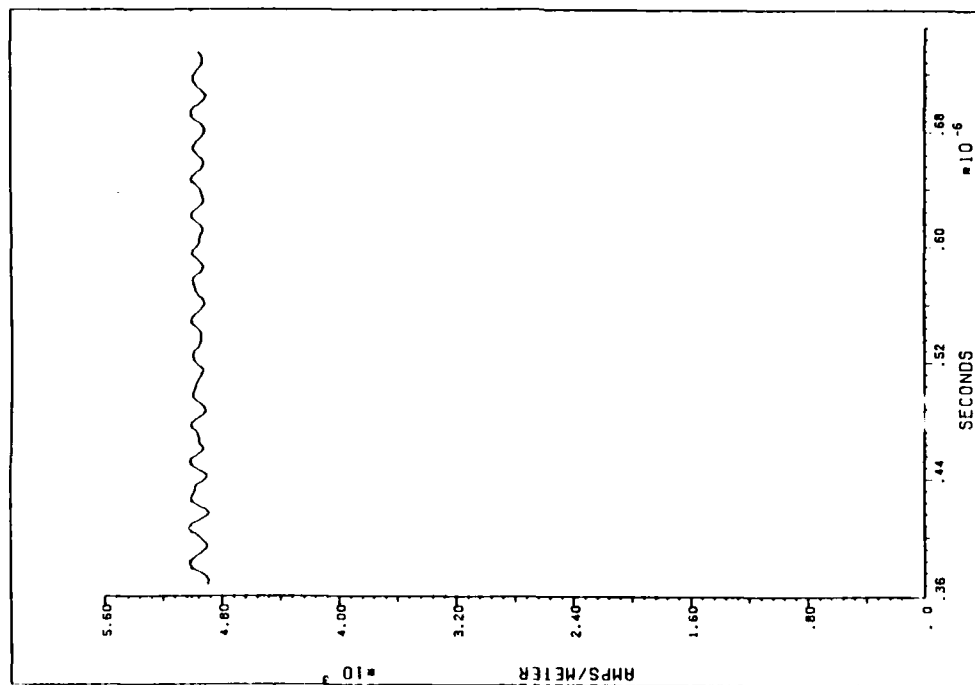
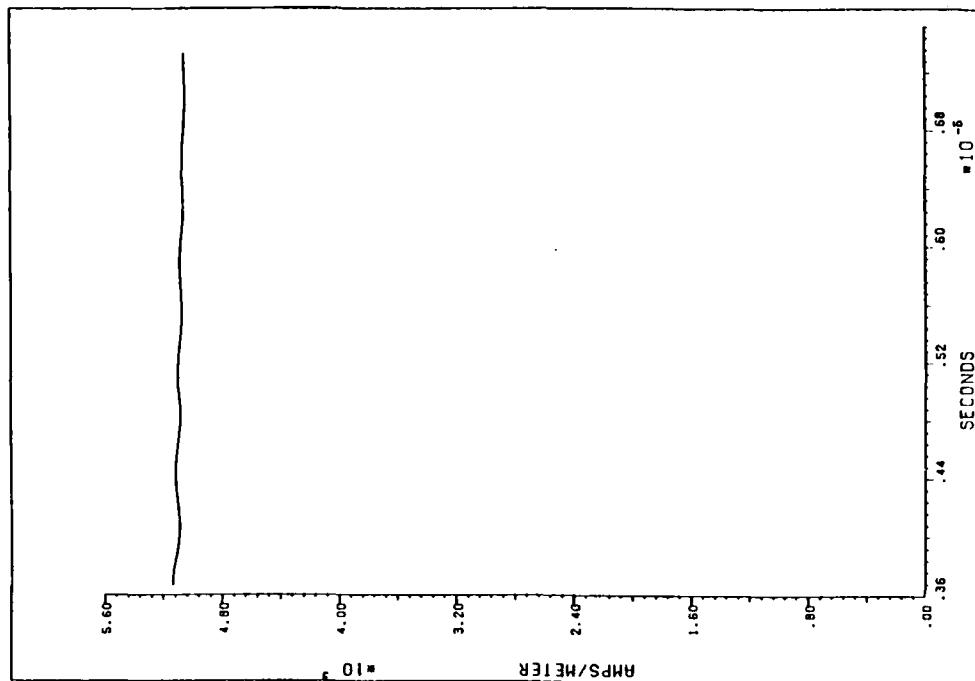


Figure 35. Sensor Three, H-field, Engine Burner Can, $H_z(24,11,13)$

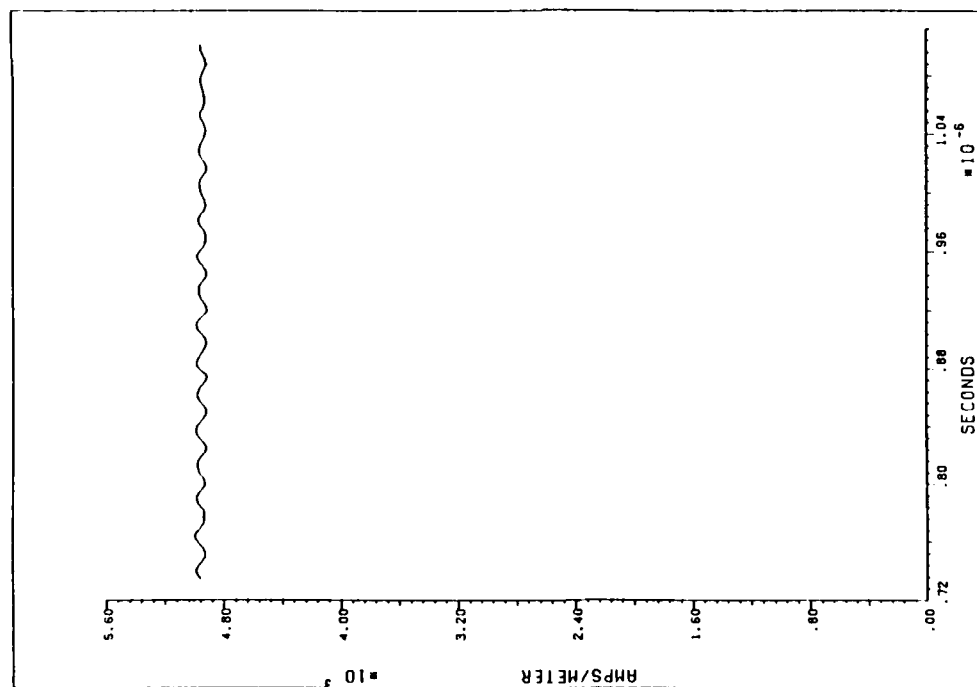


(a) ABC

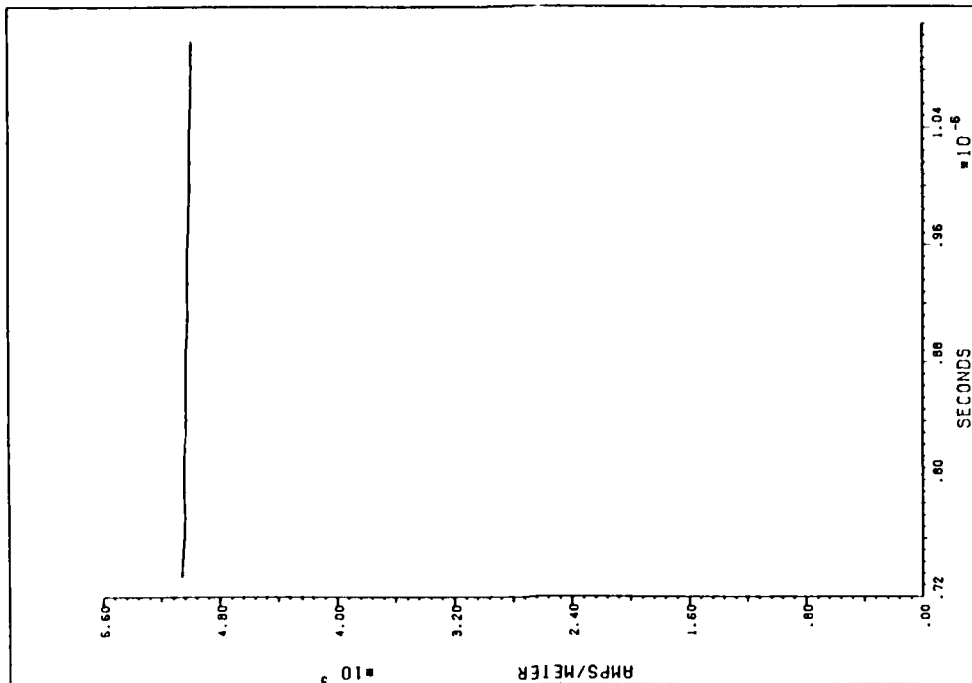


(b) RBC

Figure 36. Sensor Three, H-field, Engine Burner Can, H_z (24,11,13)

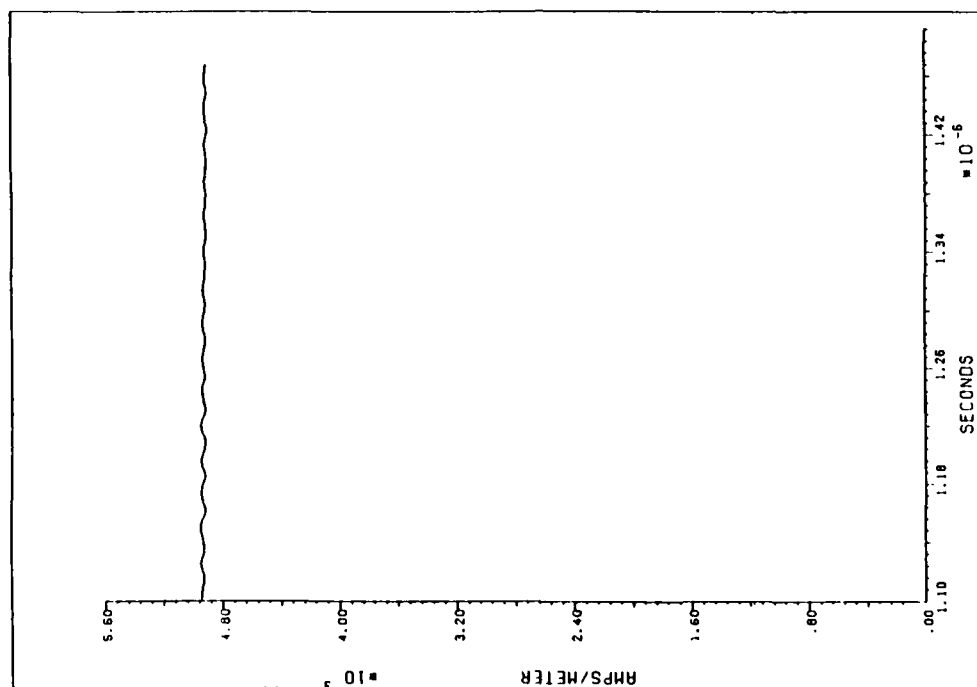


(a) ABC

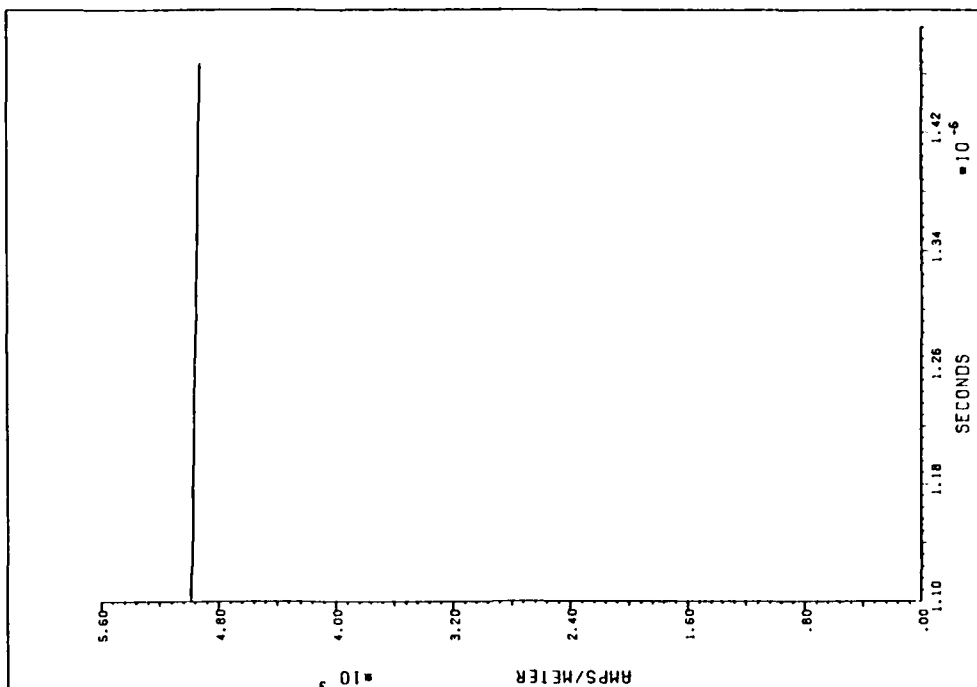


(b) RBC

Figure 37. Sensor Three, H-field, Engine Burner Can, H_z(24,11,13)

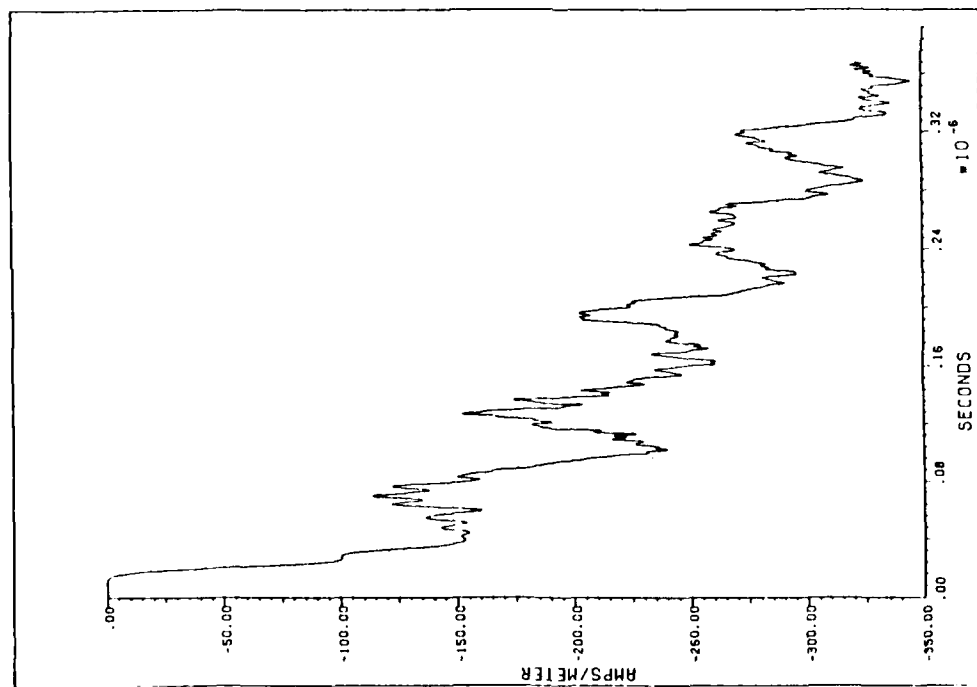


(a) ABC

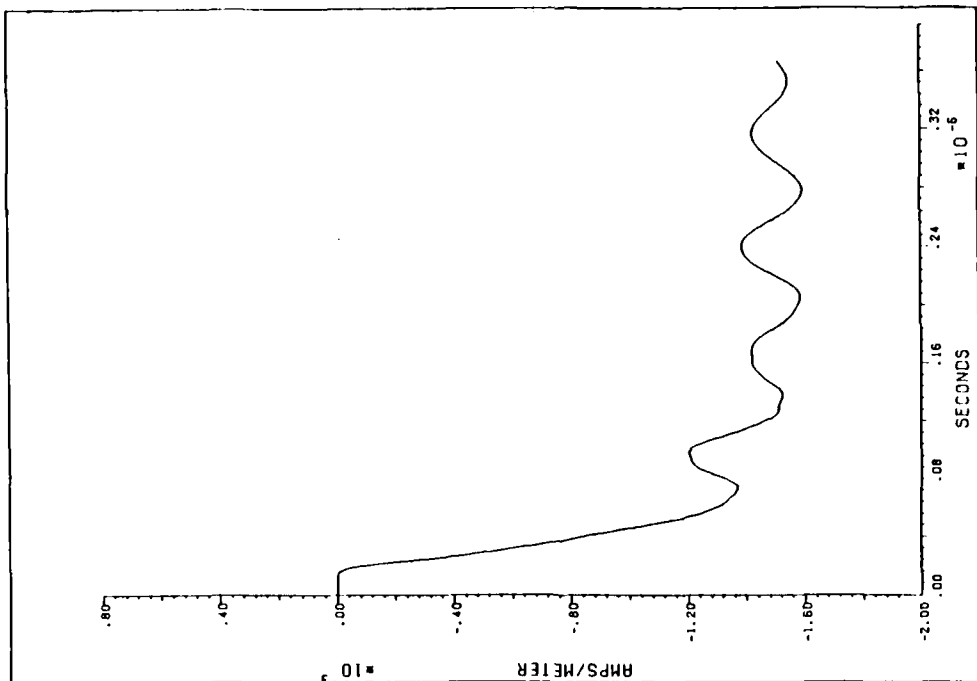


(b) RBC

Figure 38. Sensor Three, H-field, Engine Burner Can, H_z(24,11,13)

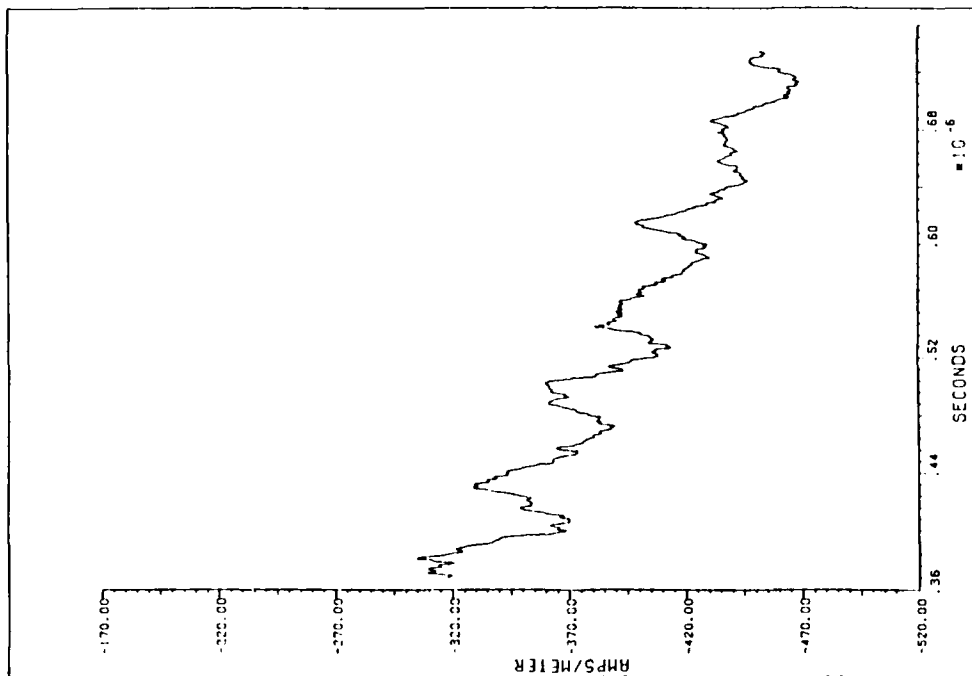


(a) ABC

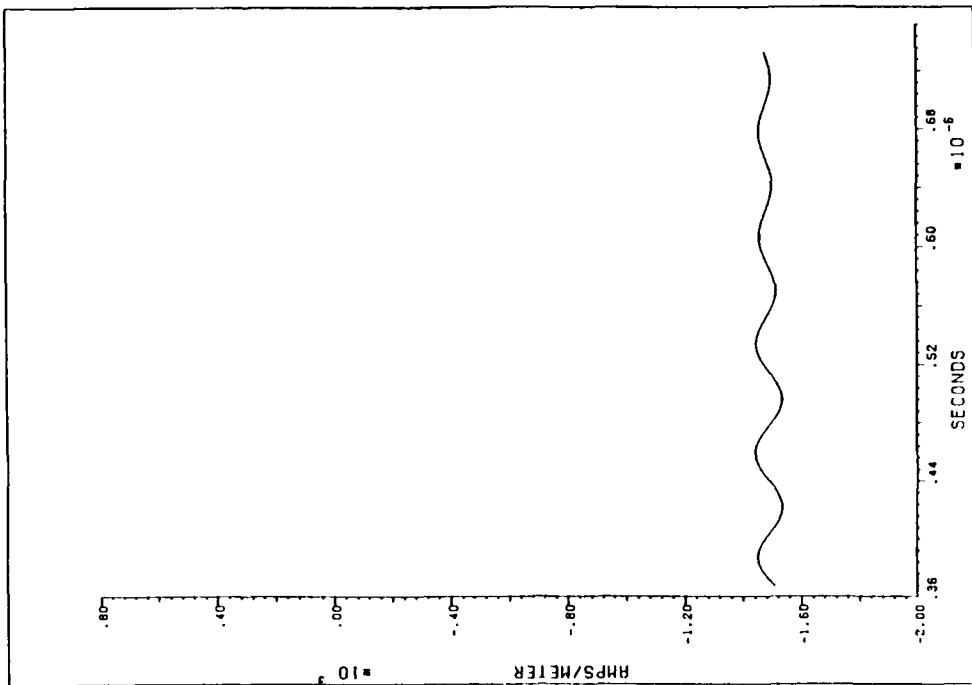


(b) RBC

Figure 39. Sensor Four, H-field, Forward Fuselage Bottom, $H_z(10,4,14)$

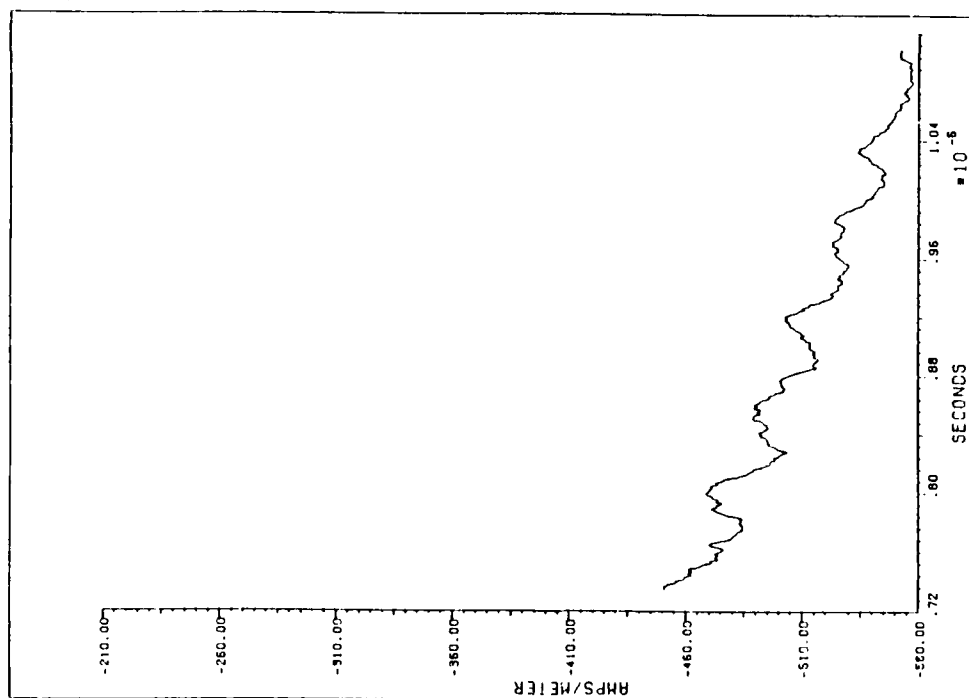


(a) ABC

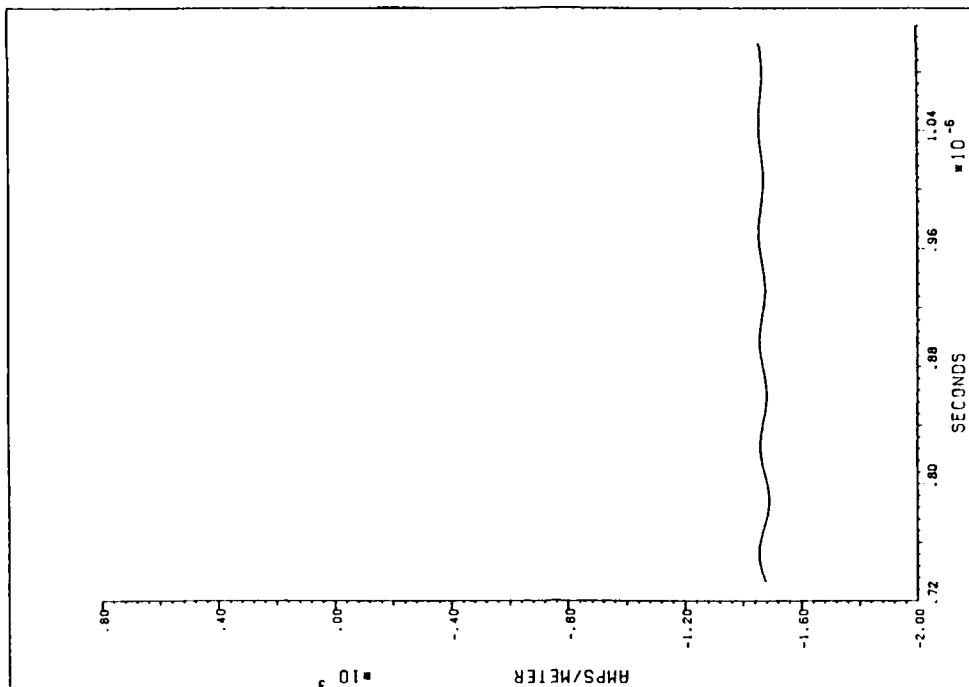


(b) RBC

Figure 40. Sensor Four, H-field, Forward Fuselage Bottom, $H_z(10,4,14)$

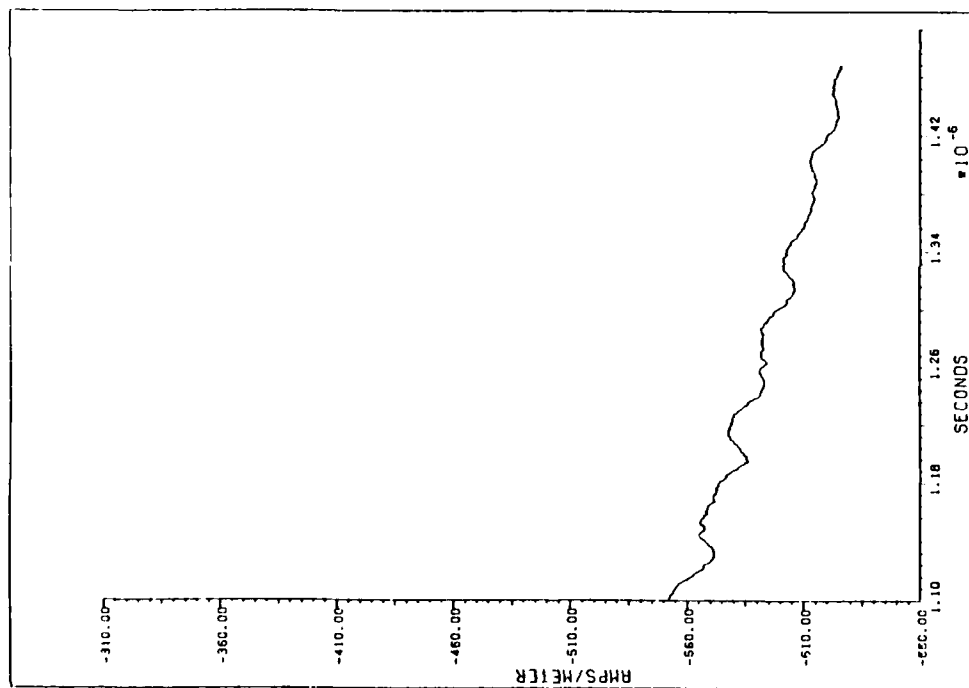


(a) ABC

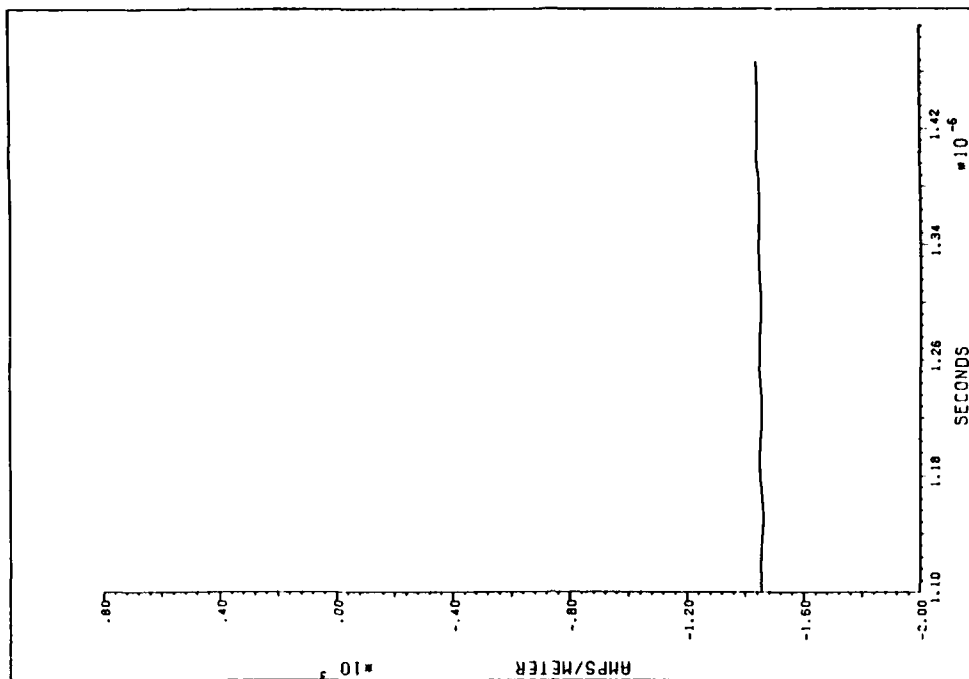


(b) RBC

Figure 41. Sensor Four, H-field, Forward Fuselage Bottom, $H_z(10,4,14)$

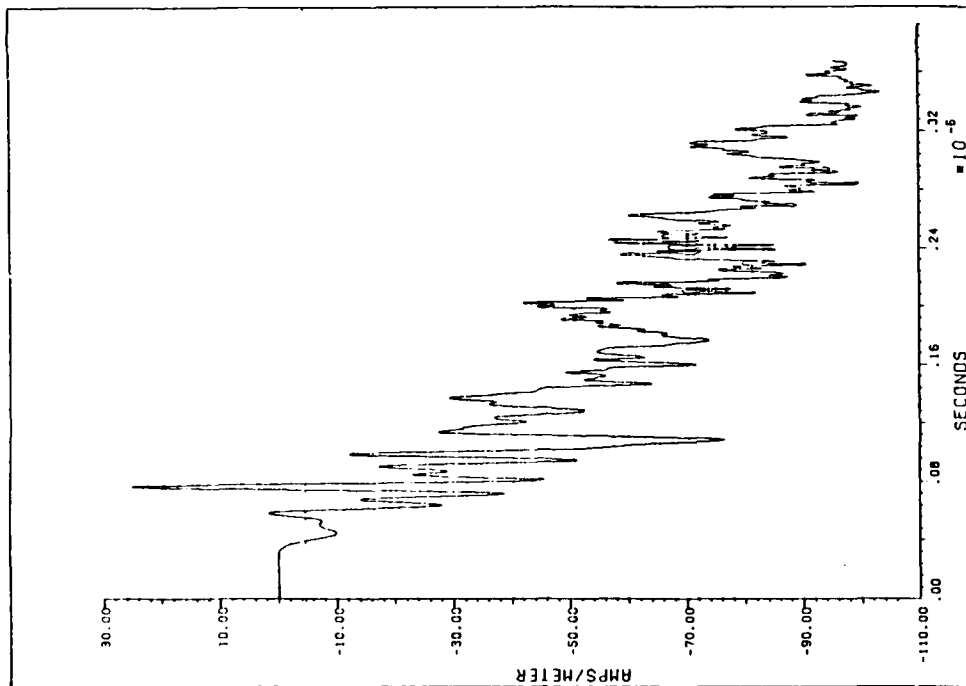


(a) ABC

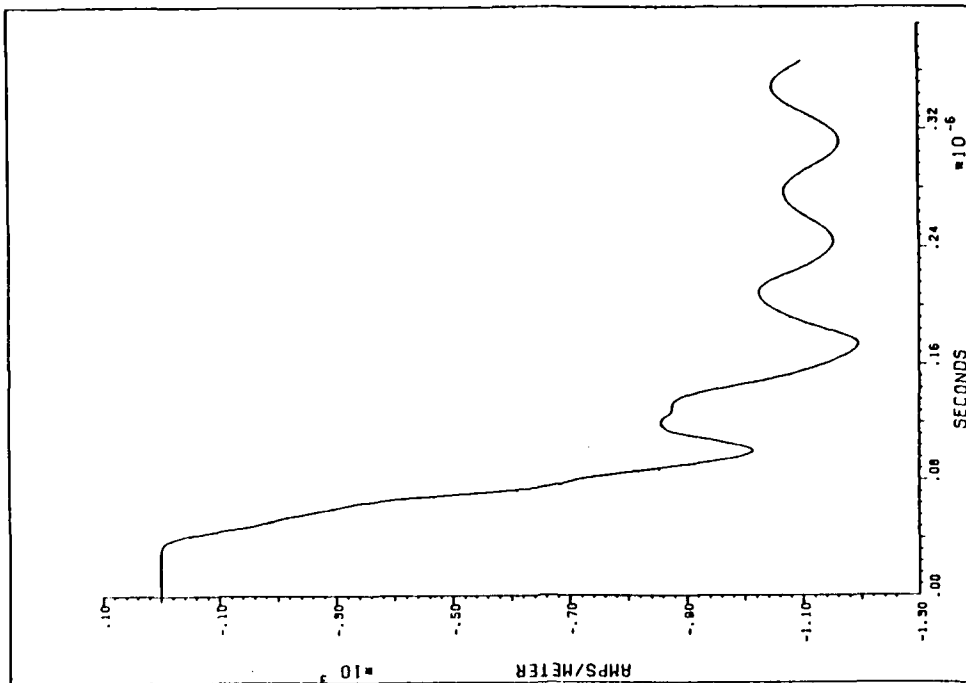


(b) RBC

Figure 42. Sensor Four, H-field, Forward Fuselage Bottom, $H_z(10,4,14)$

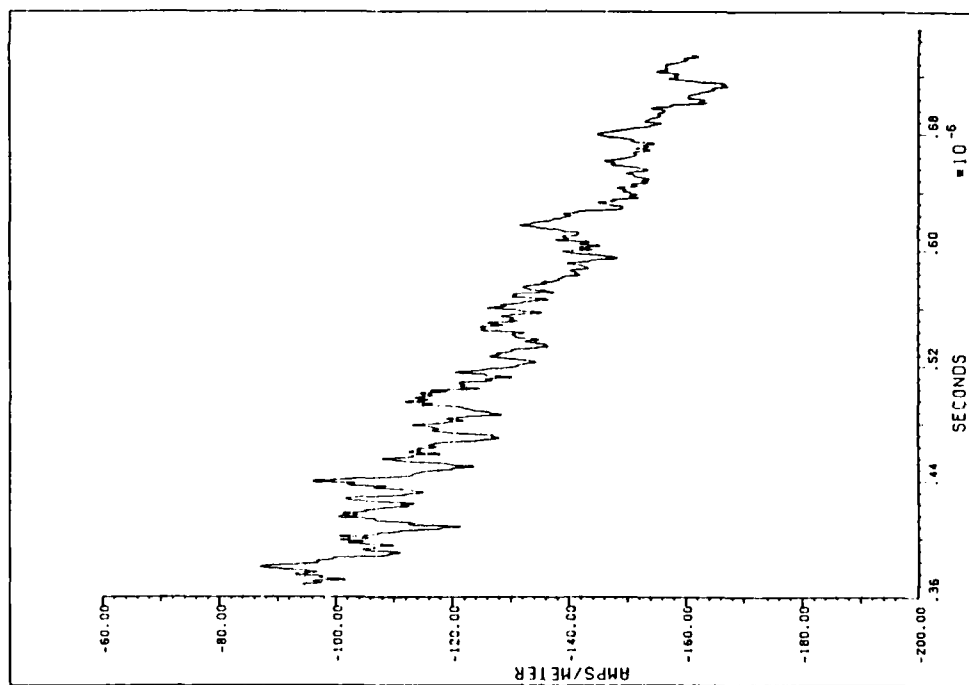


(a) ABC

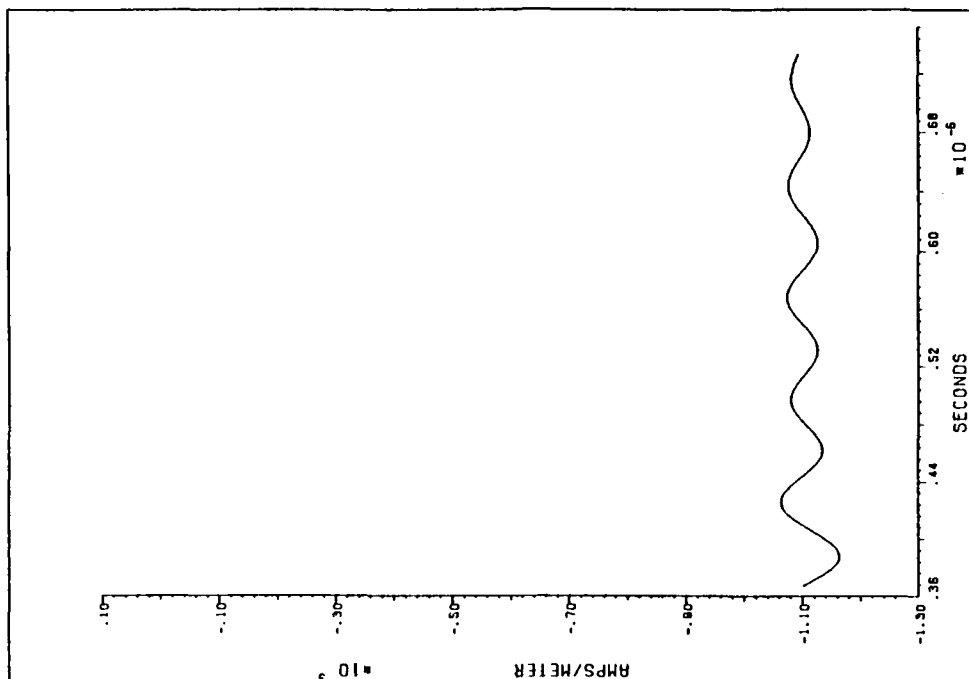


(b) RBC

Figure 43. Sensor Five, H-field, Rear Fuselage Bottom, $H_z(19,4,14)$

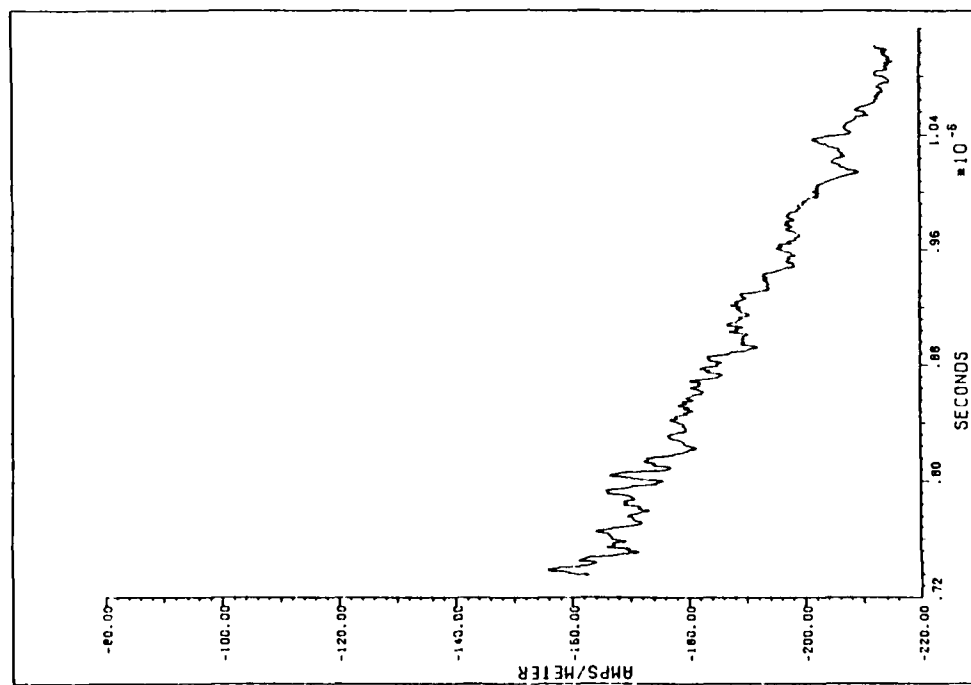


(a) ABC

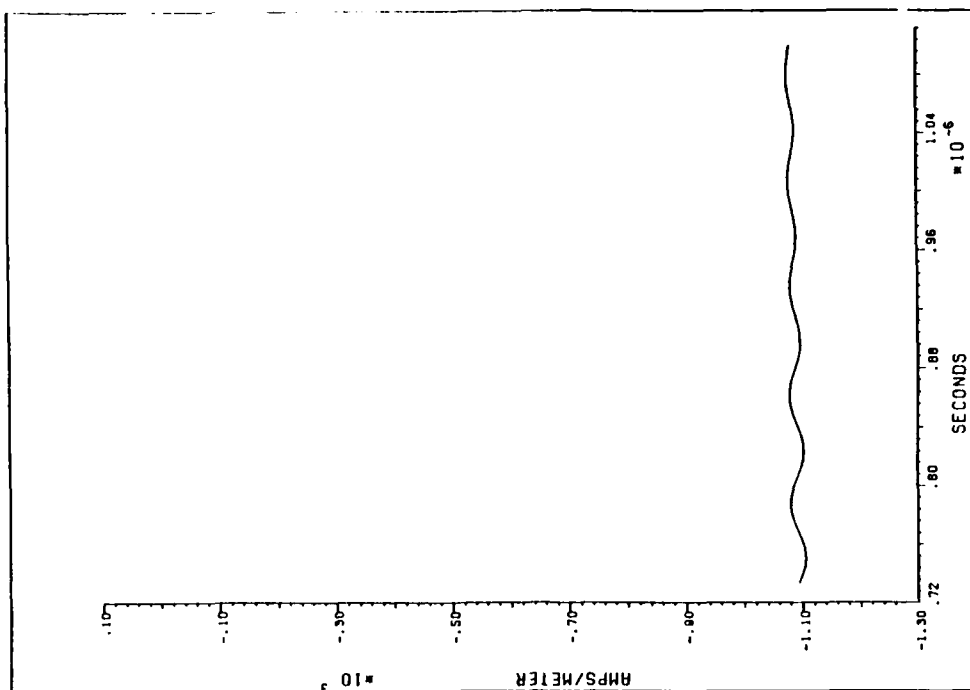


(b) RBC

Figure 44. Sensor Five, H-field, Rear Fuselage Bottom, $H_z(19,4,14)$

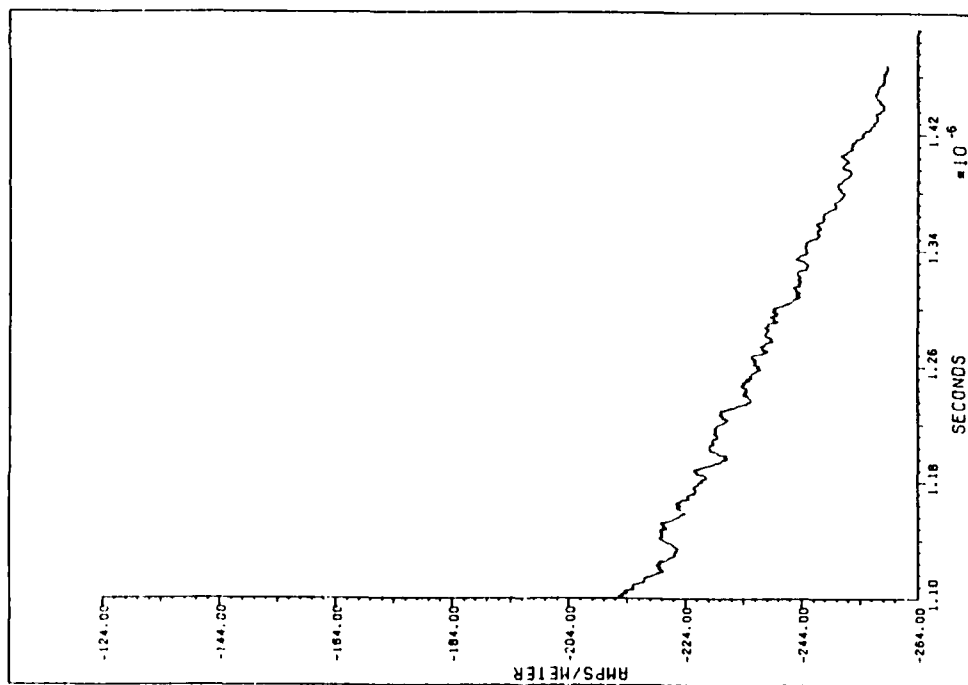


(a) ABC

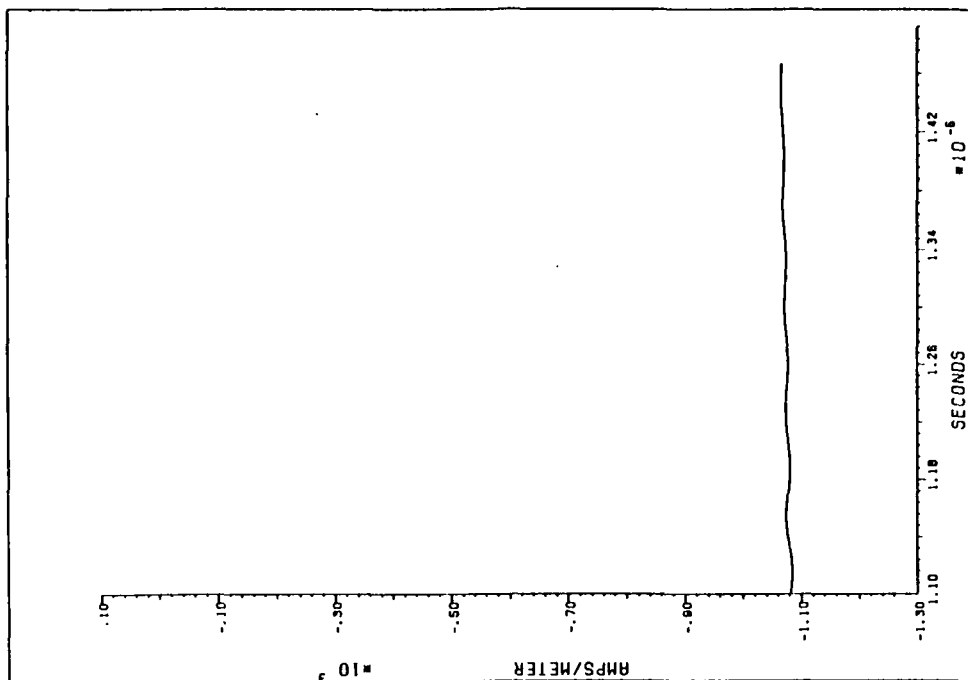


(b) RBC

Figure 45. Sensor Five, H-field, Rear Fuselage Bottom, $H_z(19,4,14)$

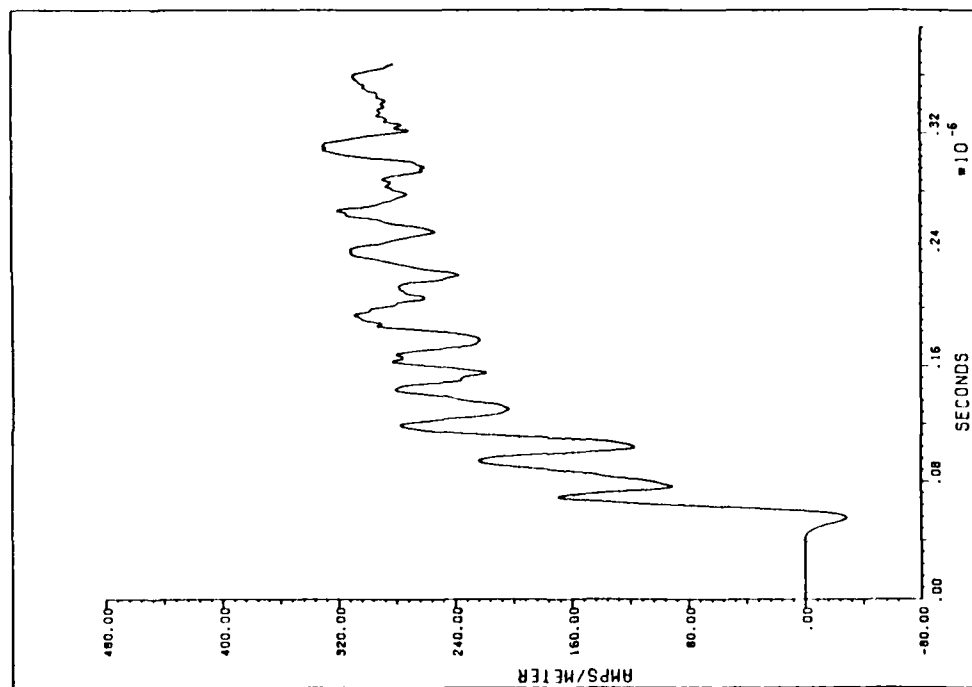


(a) ABC

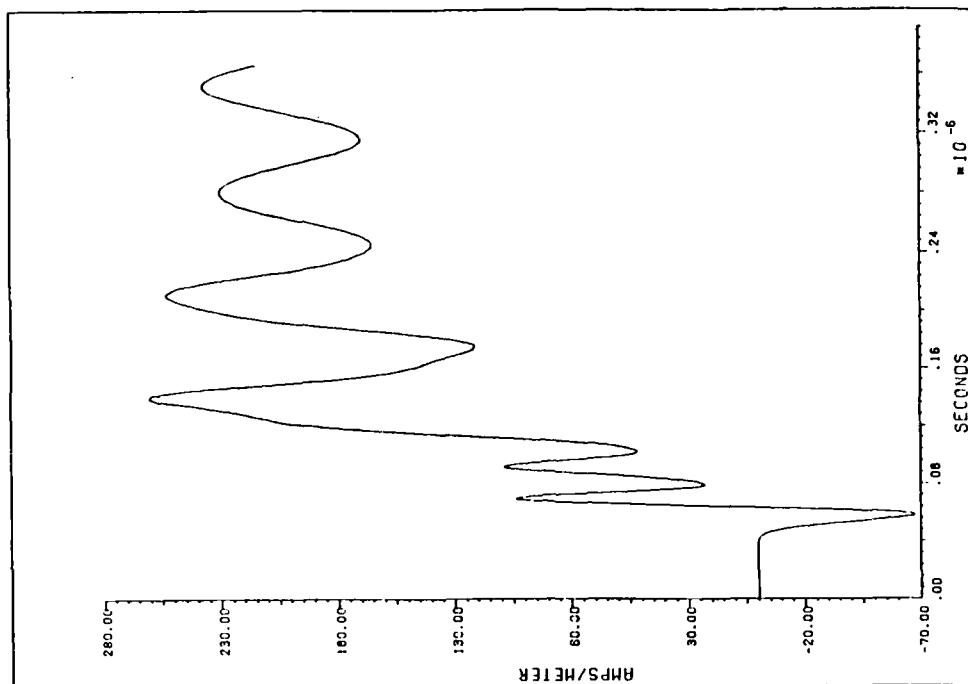


(b) RBC

Figure 46. Sensor Five, H-field, Rear Fuselage Bottom, $H_z(19,4,14)$

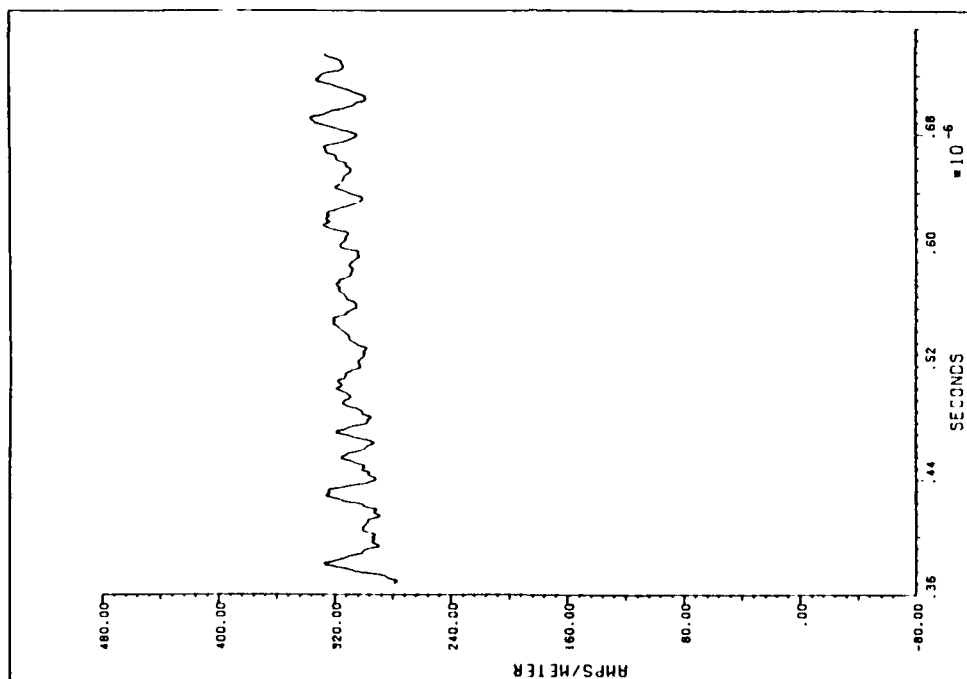


(a) ABC

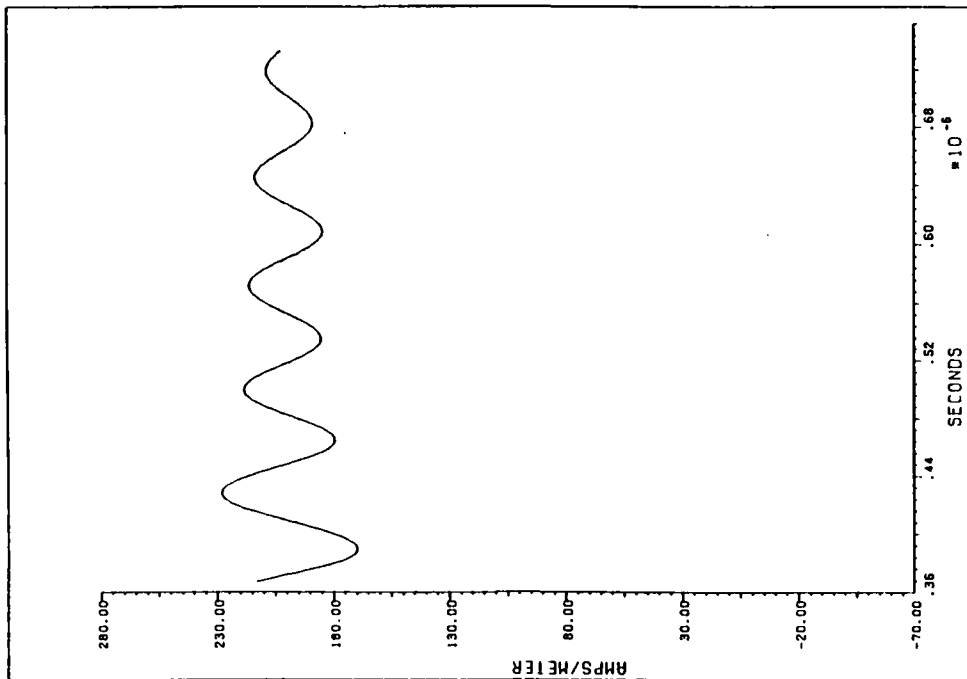


(b) RBC

Figure 47. Sensor Six, H-field, Vertical Stabilizer, $H_x(22,18,14)$

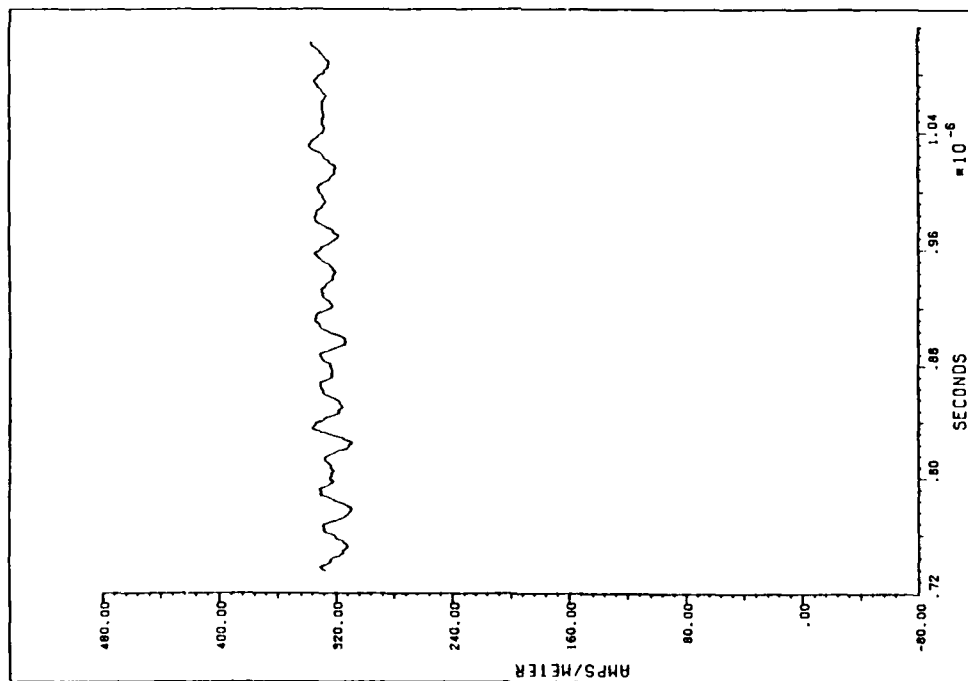


(a) ABC

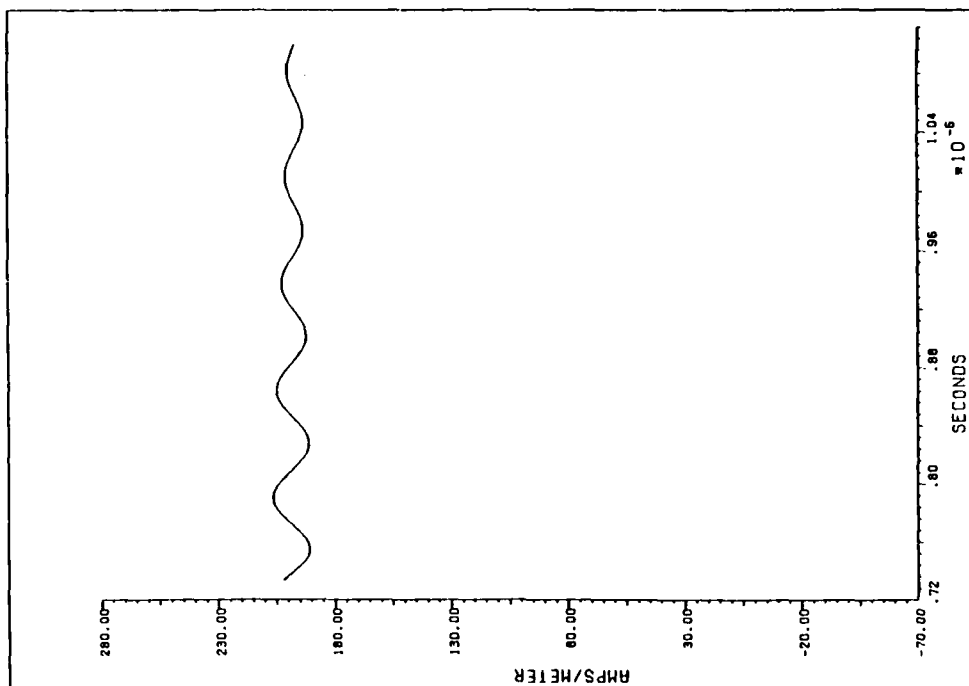


(b) RBC

Figure 48. Sensor Six, H-field, Vertical Stabilizer, $H_x(22,18,14)$

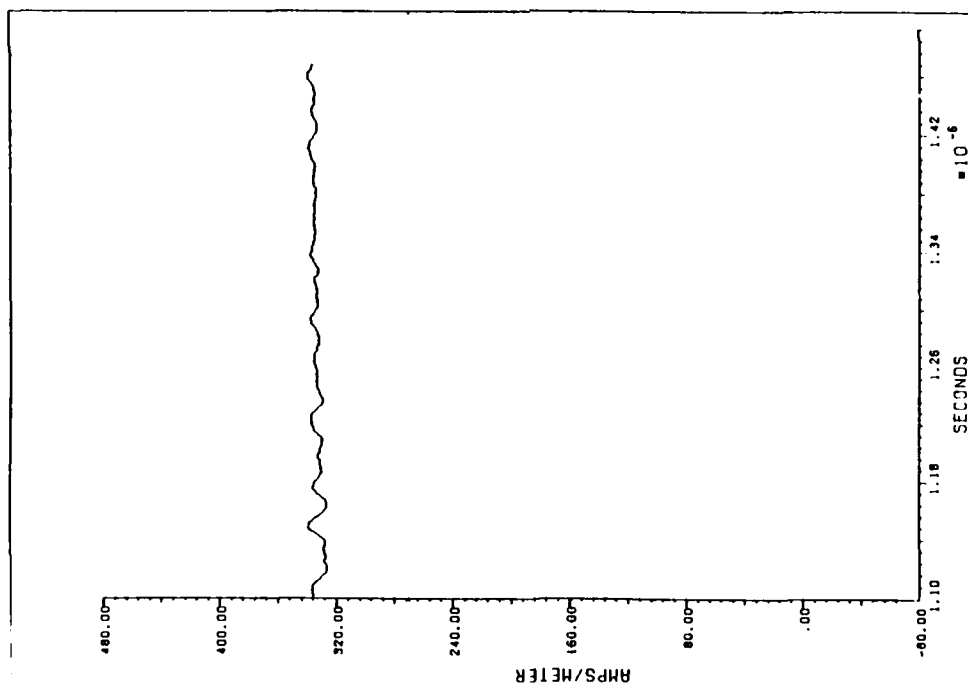


(a) ABC

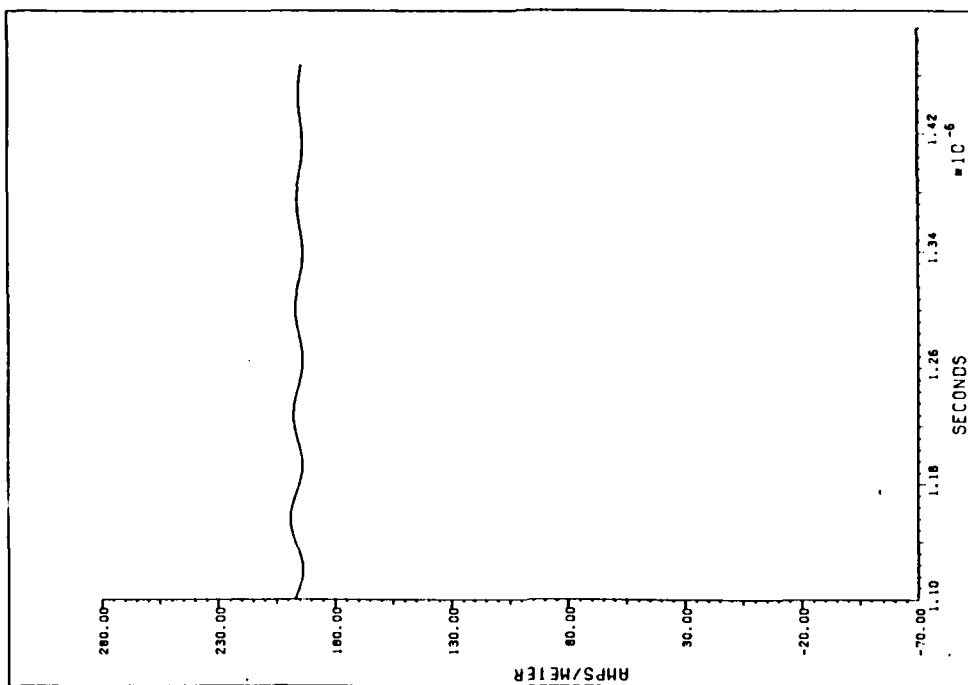


(b) RBC

Figure 49. Sensor Six, H-field, Vertical Stabilizer, $H_x(22,18,14)$



(a) ABC



(b) RBC

Figure 50. Sensor Six, H-field, Vertical Stabilizer, $H_x(22,18,14)$

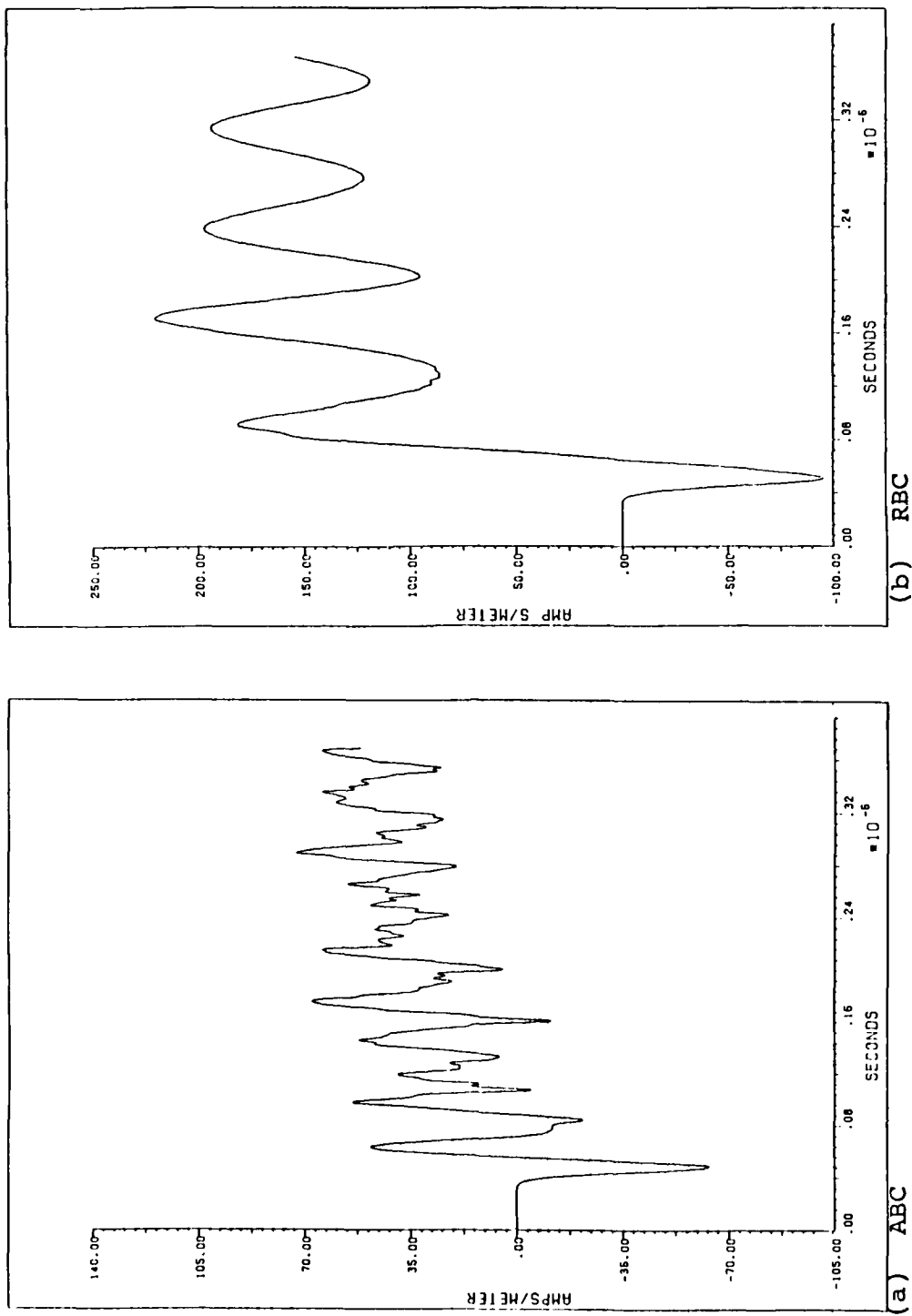
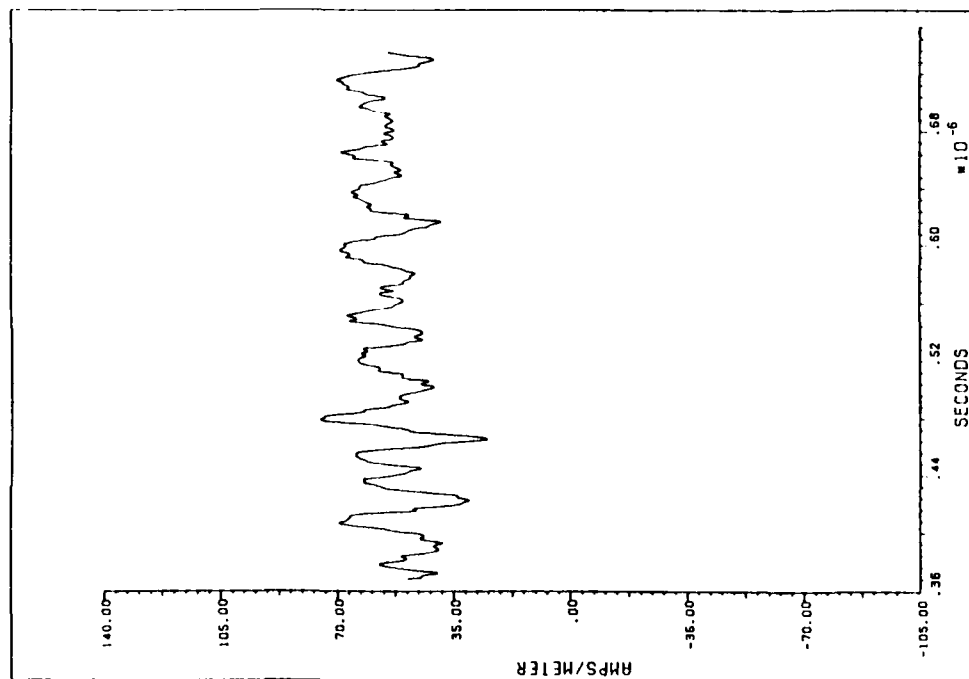
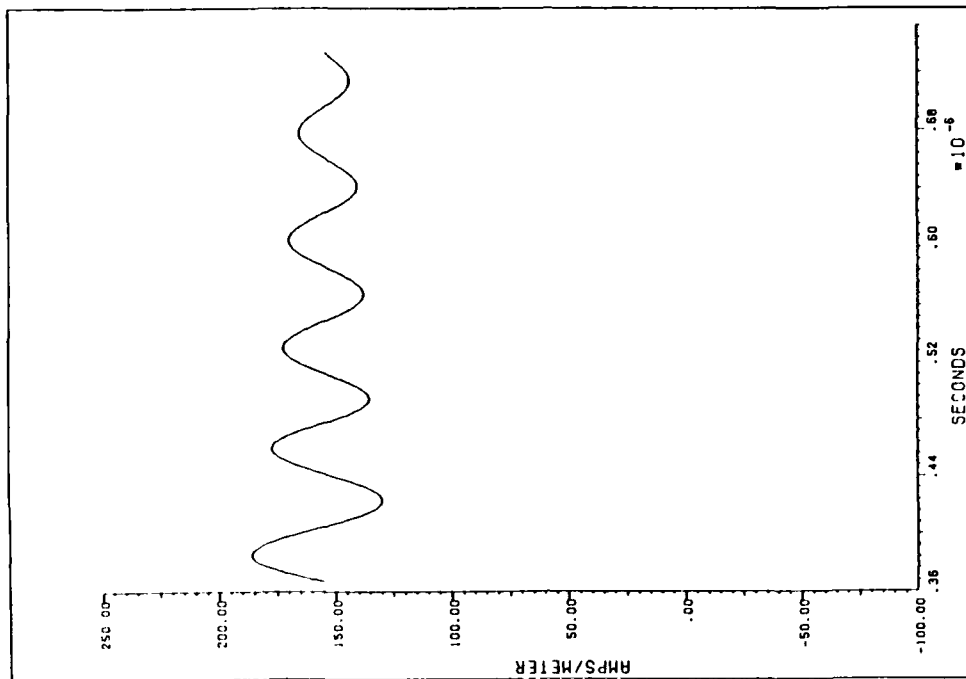


Figure 51. Sensor Seven, H-field, Left Wing, $H_x(18,10,23)$

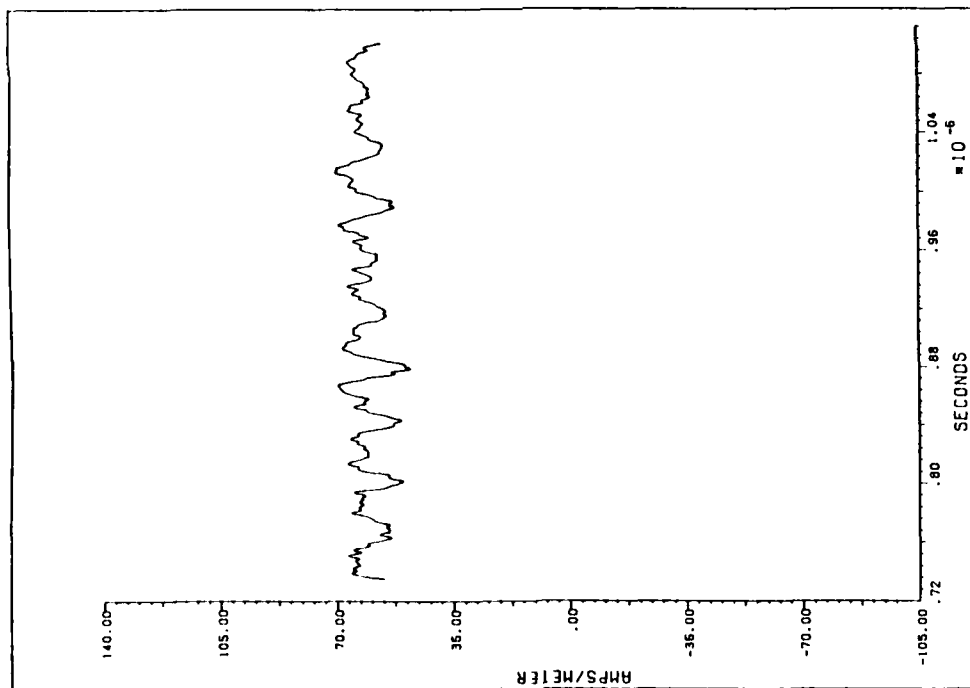


(a) ABC

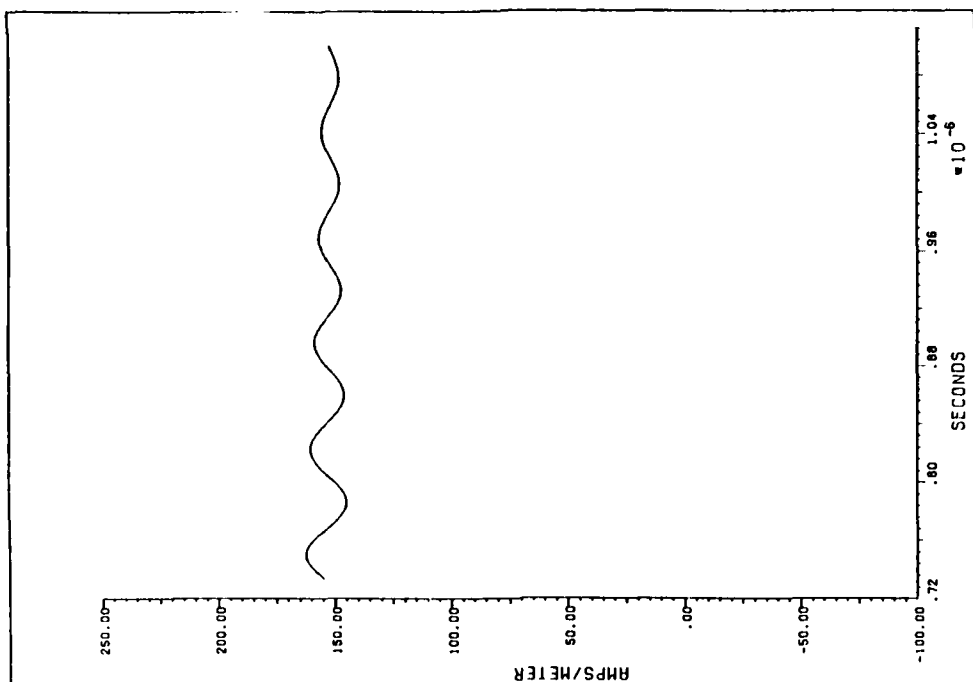


(b) RBC

Figure 52. Sensor Seven, H-field, Left Wing, $H_x(18,10,23)$

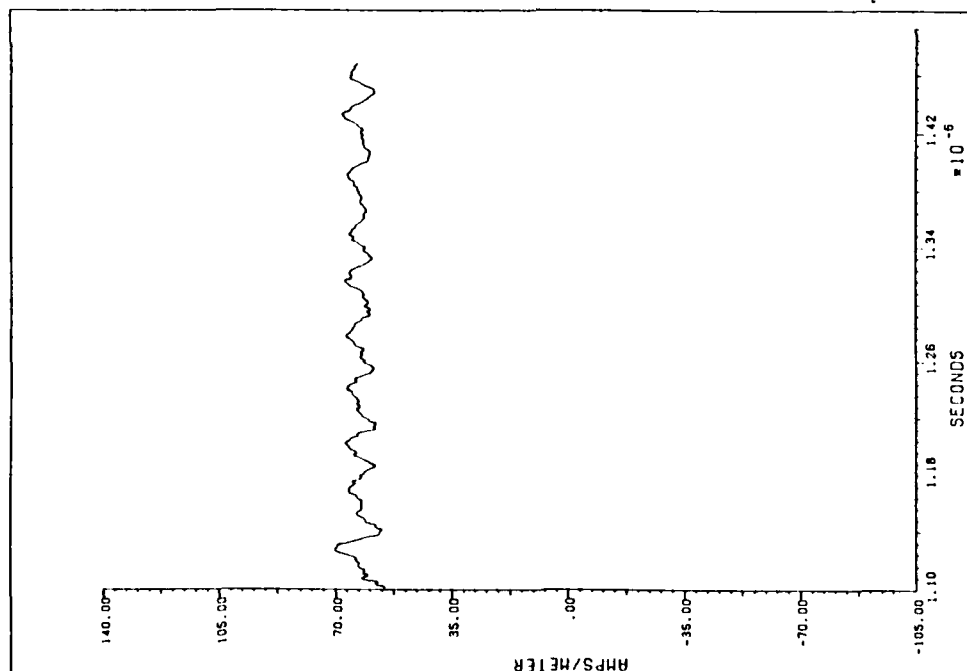


(a) ABC

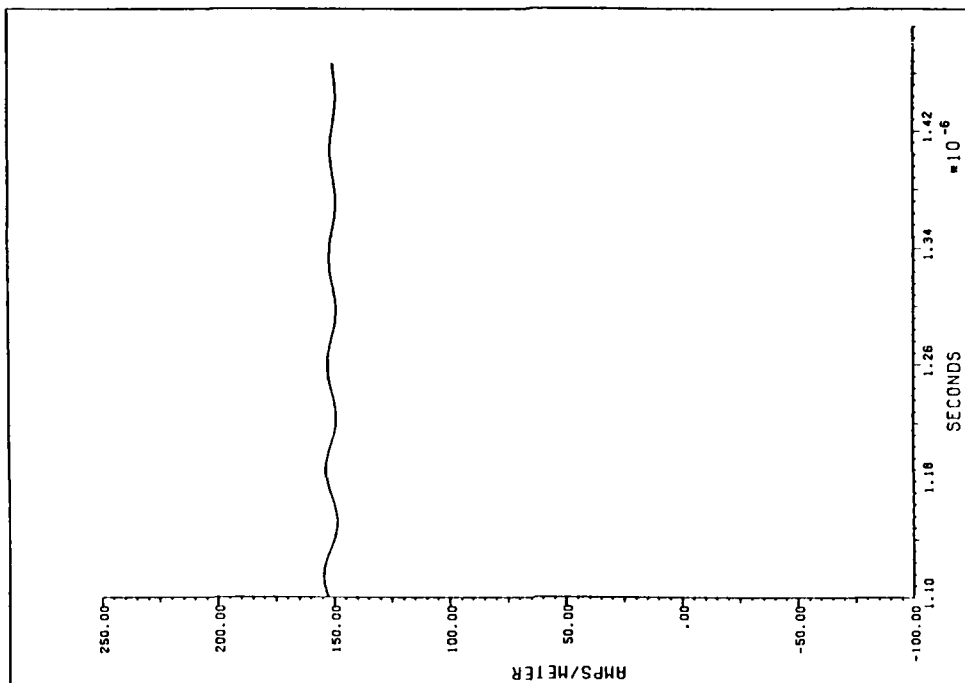


(b) RBC

Figure 53. Sensor Seven, H-field, Left Wing, $H_x(18,10,23)$

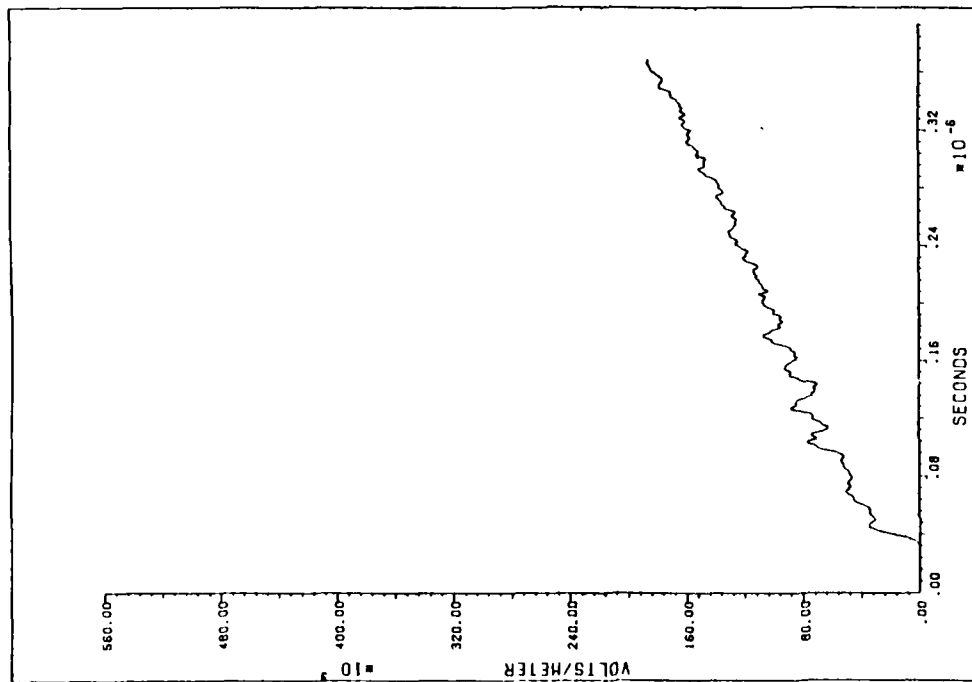


(a) ABC

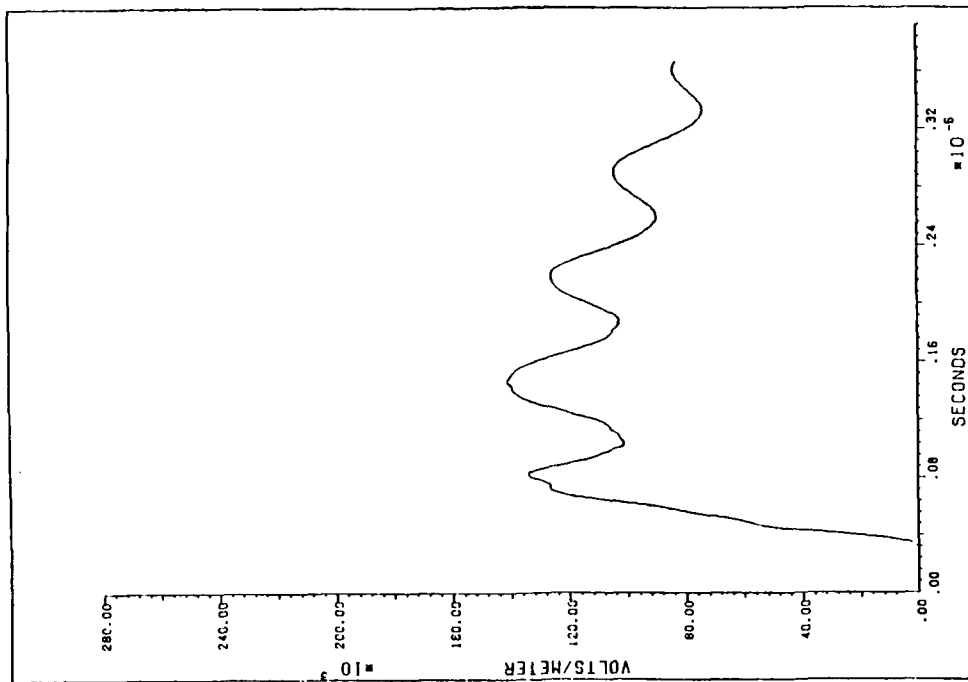


(b) RBC

Figure 54. Sensor Seven, H-field, Left Wing, $H_x(18,10,23)$



(a) ABC



(b) RBC

Figure 55. Sensor Eight, E-field, Right Wing, $E_y(17,11,10)$

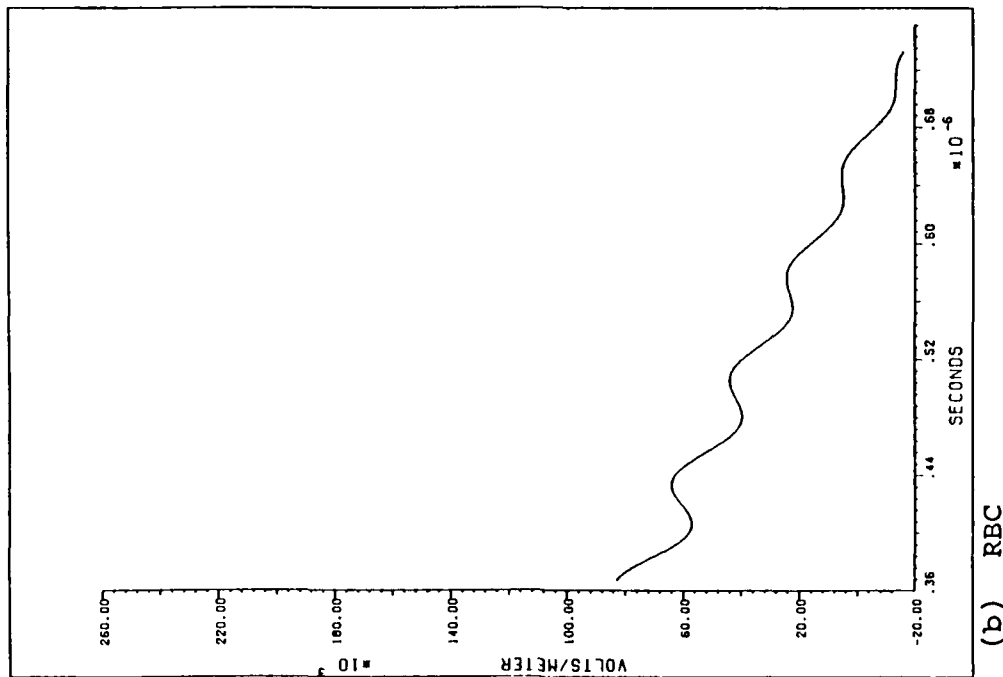
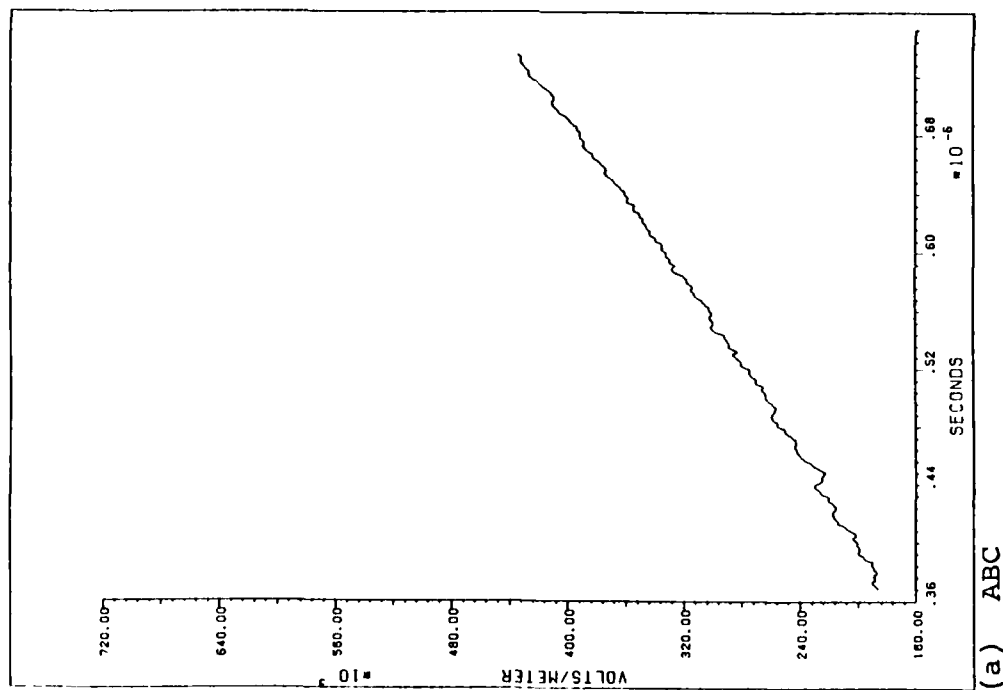
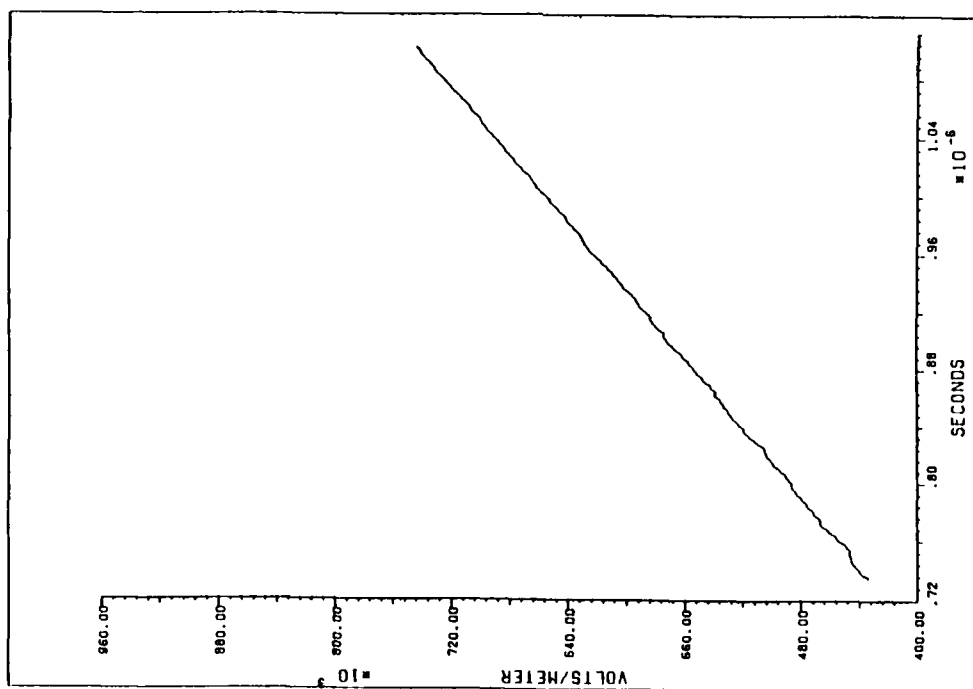
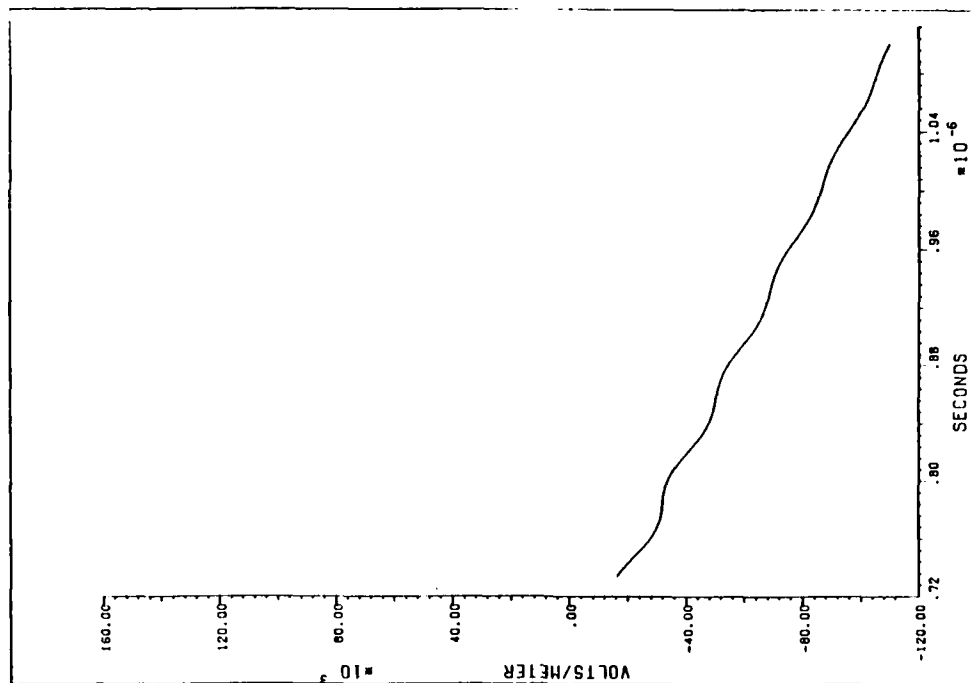


Figure 56. Sensor Eight, E-field, Right Wing, $E_y(17,11,10)$

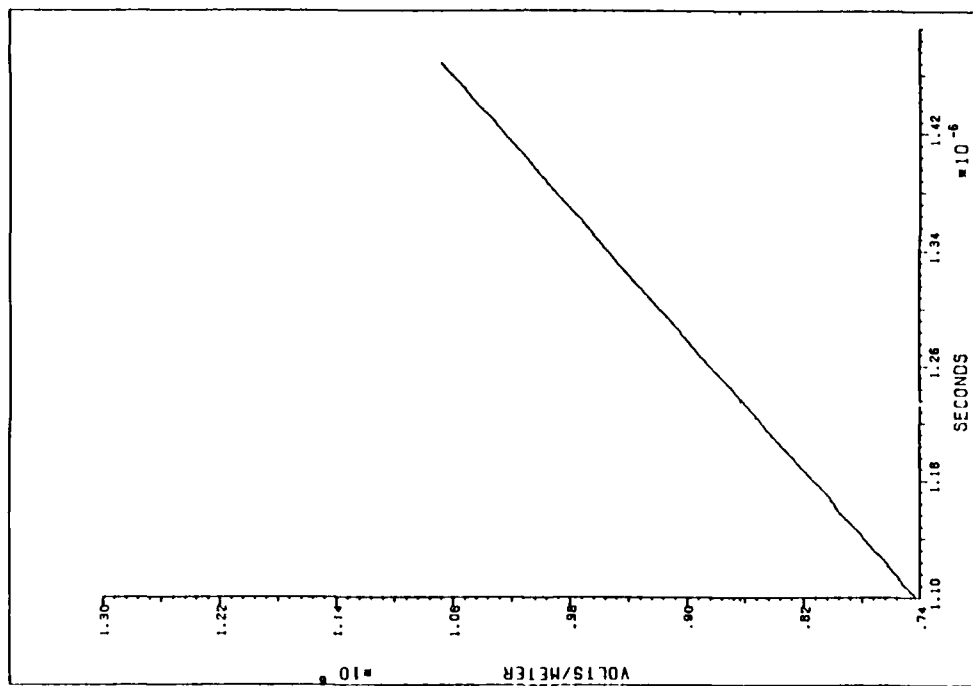


(a) ABC

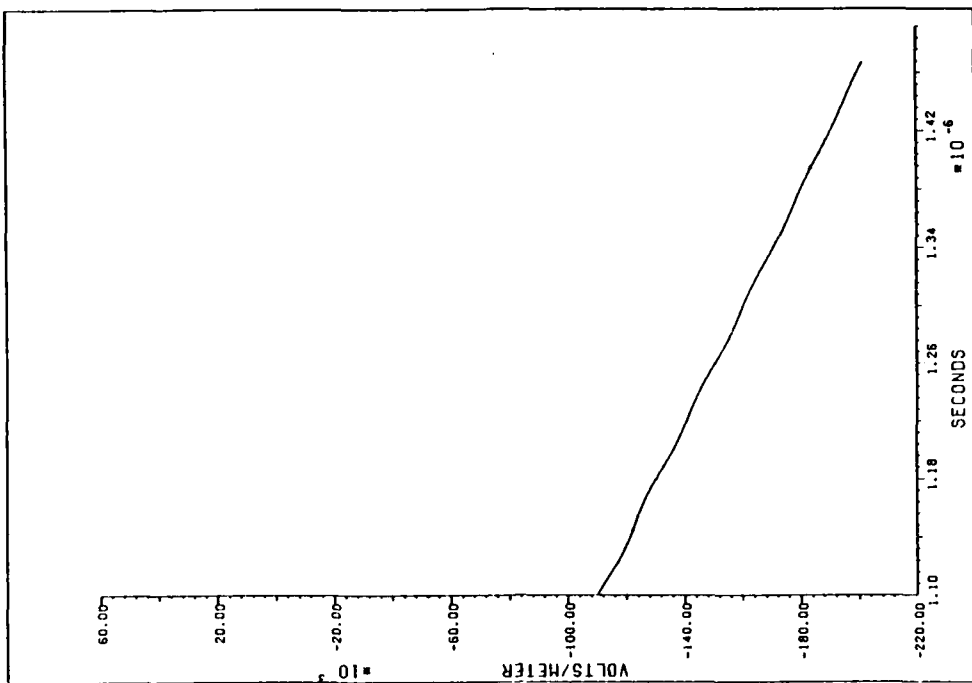


(b) RBC

Figure 57. Sensor Eight, E-field, Right Wing, $E_y(17,11,10)$

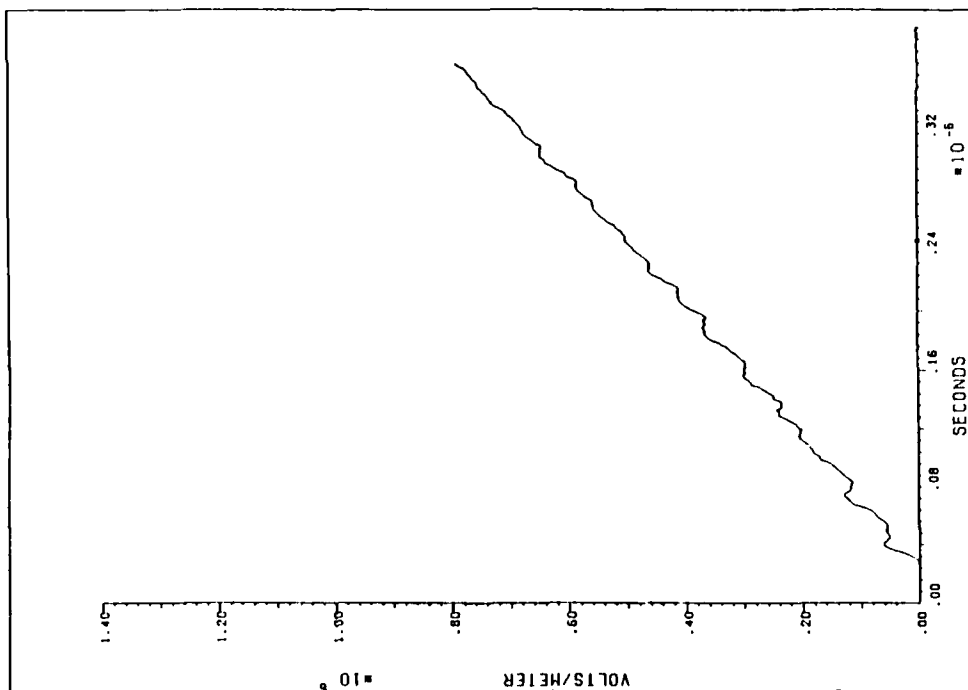


(a) ABC

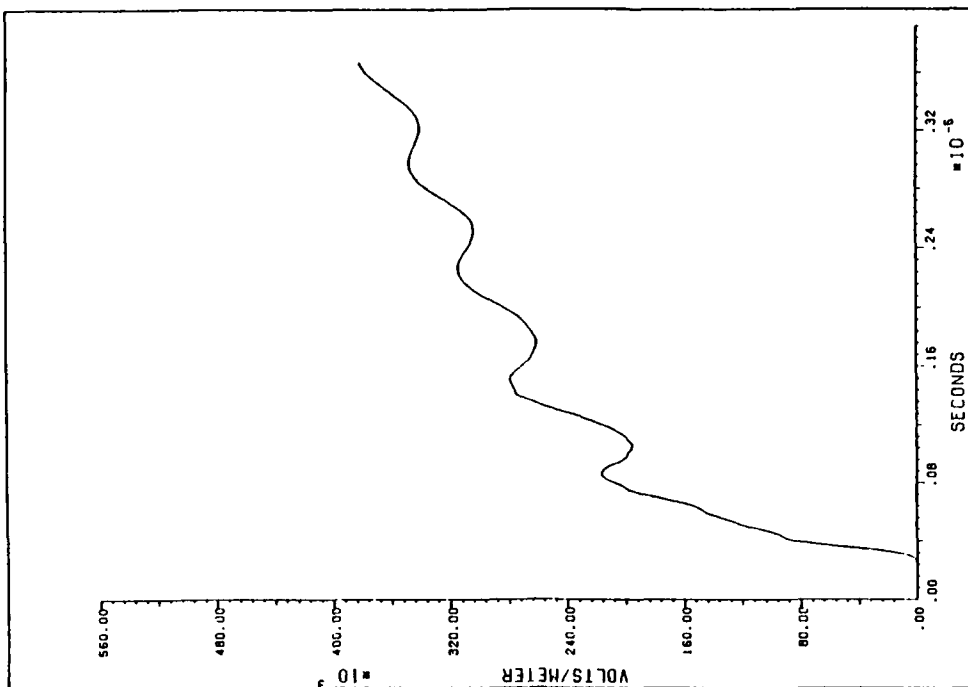


(b) RBC

Figure 58. Sensor Eight, E-field, Right Wing, $E_y(17,11,10)$

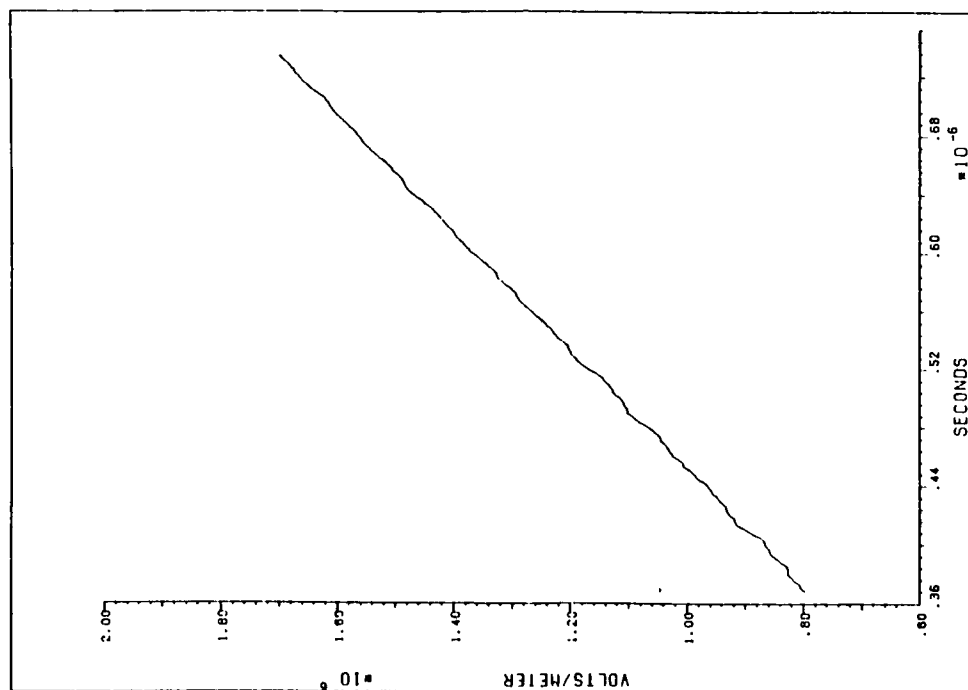


(a) ABC

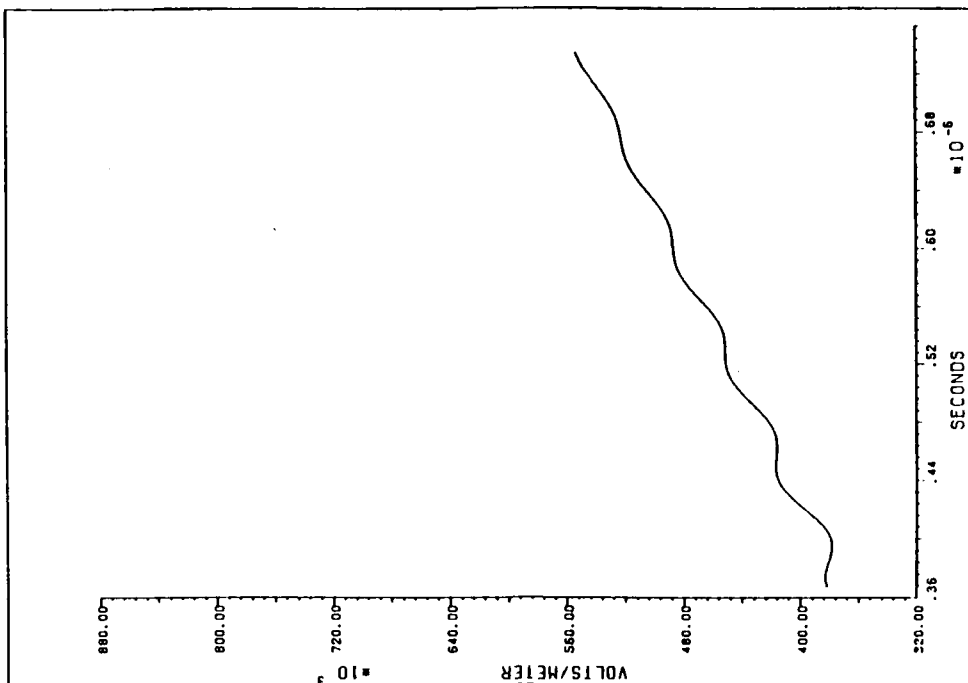


(b) RBC

Figure 59. Sensor Nine, E-field, Middle Fuselage Top, $E_y(15,13,14)$

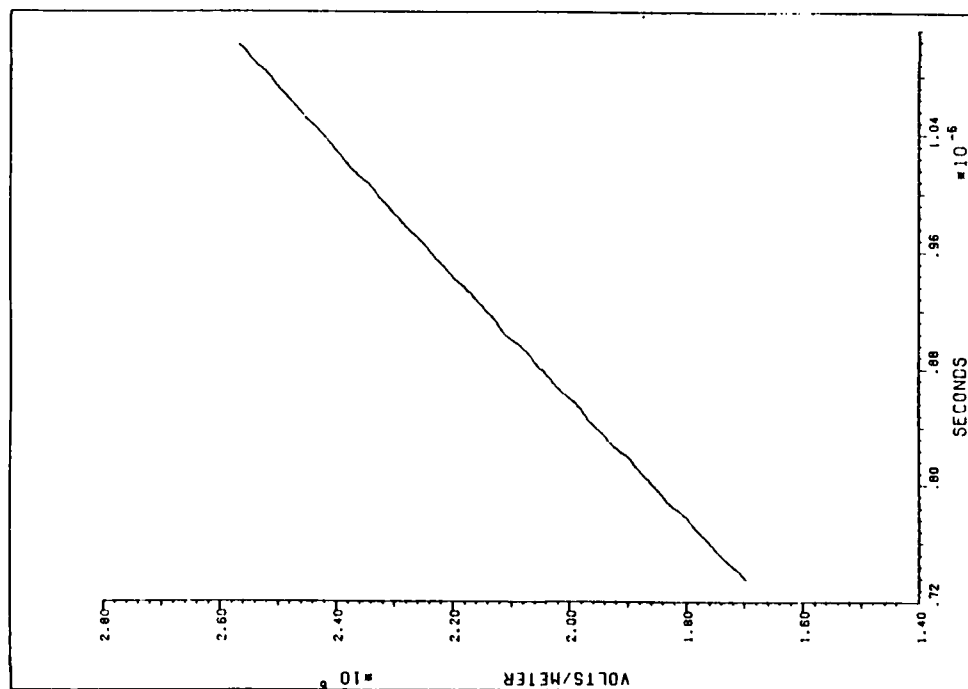


(a) ABC

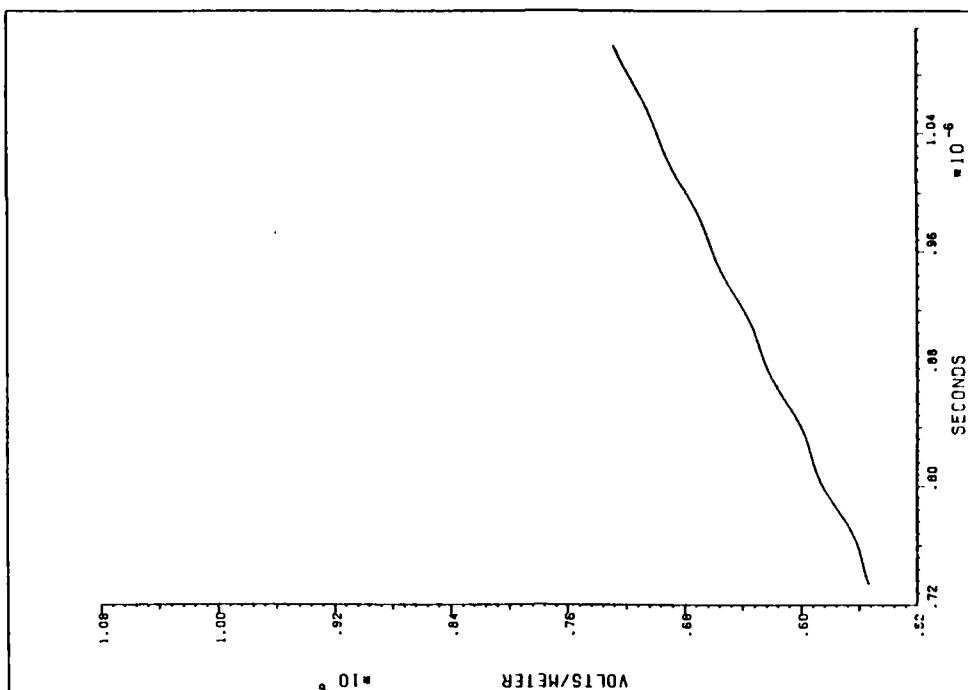


(b) RBC

Figure 60. Sensor Nine, E-field, Middle Fuselage Top, $E_y(15,13,14)$

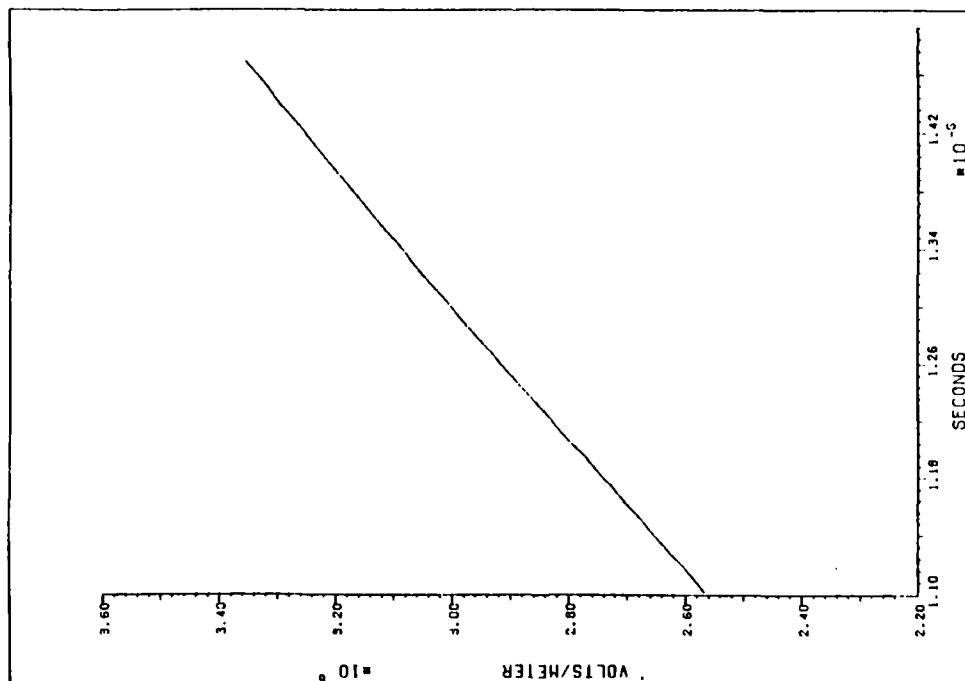


(a) ABC

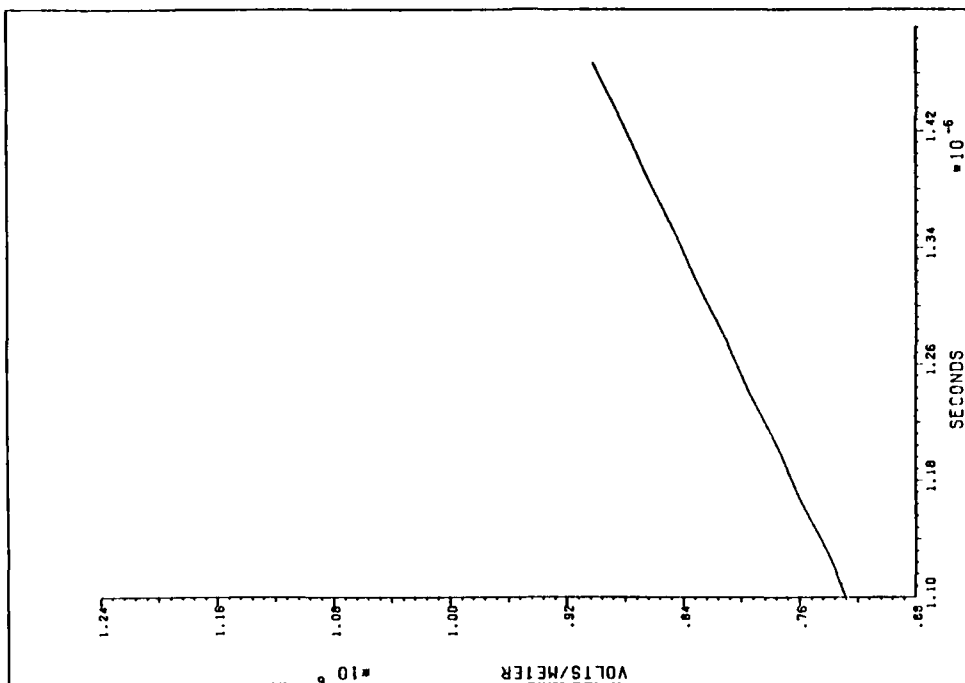


(b) RBC

Figure 61. Sensor Nine, E-field, Middle Fuselage Top, $E_y(15,13,14)$

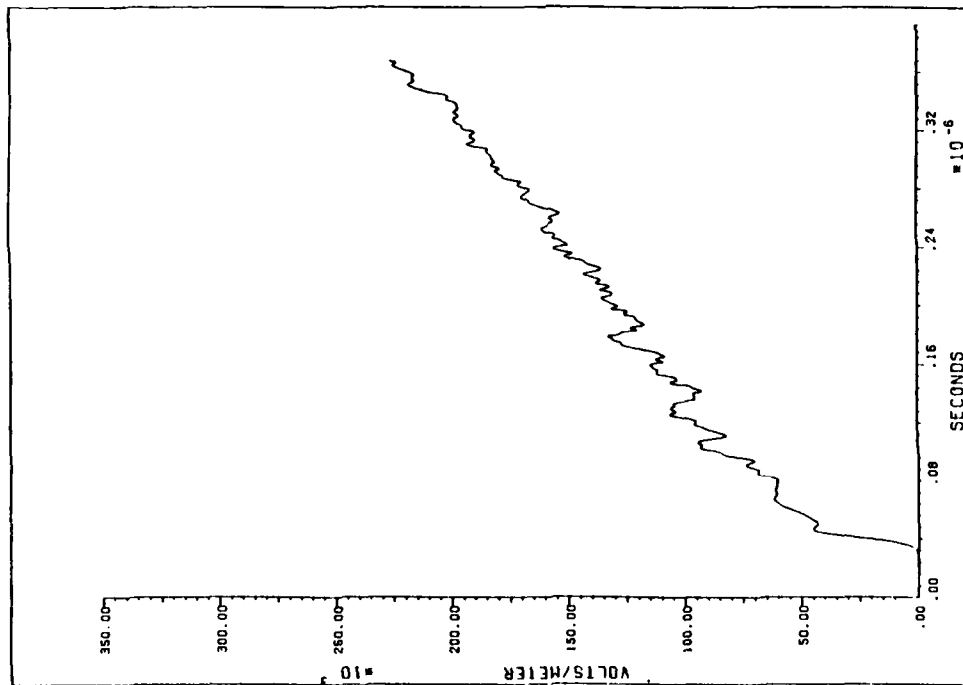


(a) ABC

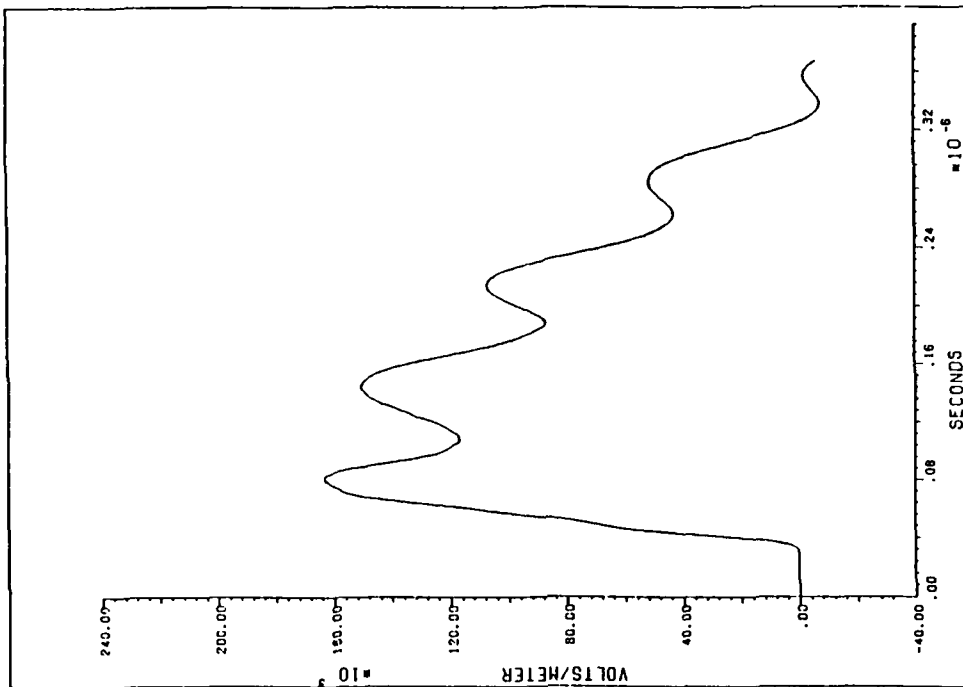


(b) RBC

Figure 62. Sensor Nine, E-field, Middle Fuselage Top, $E_y(15,13,14)$

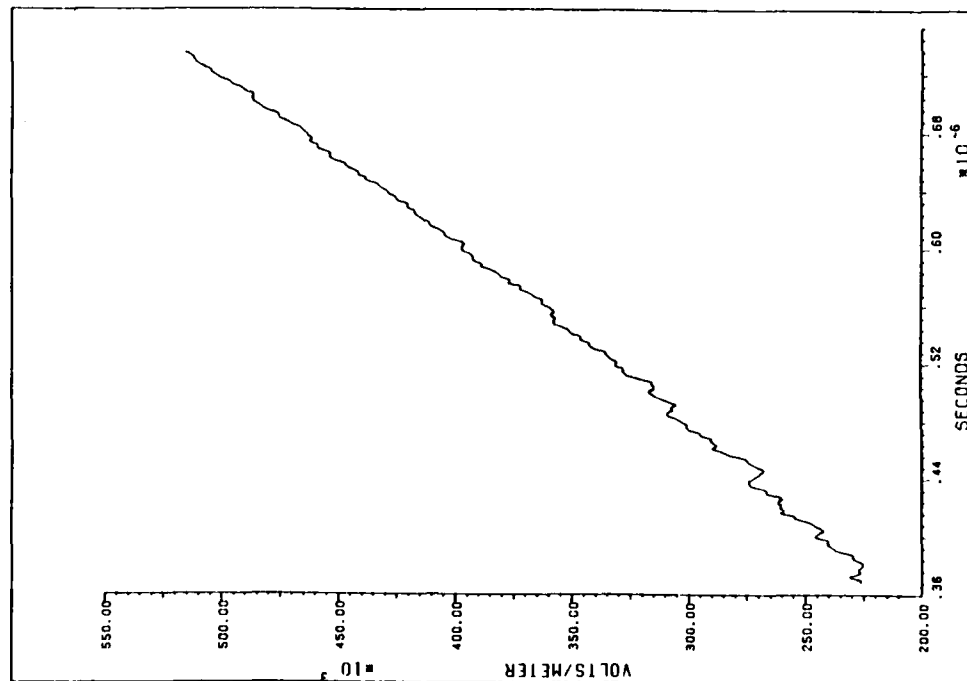


(a) ABC

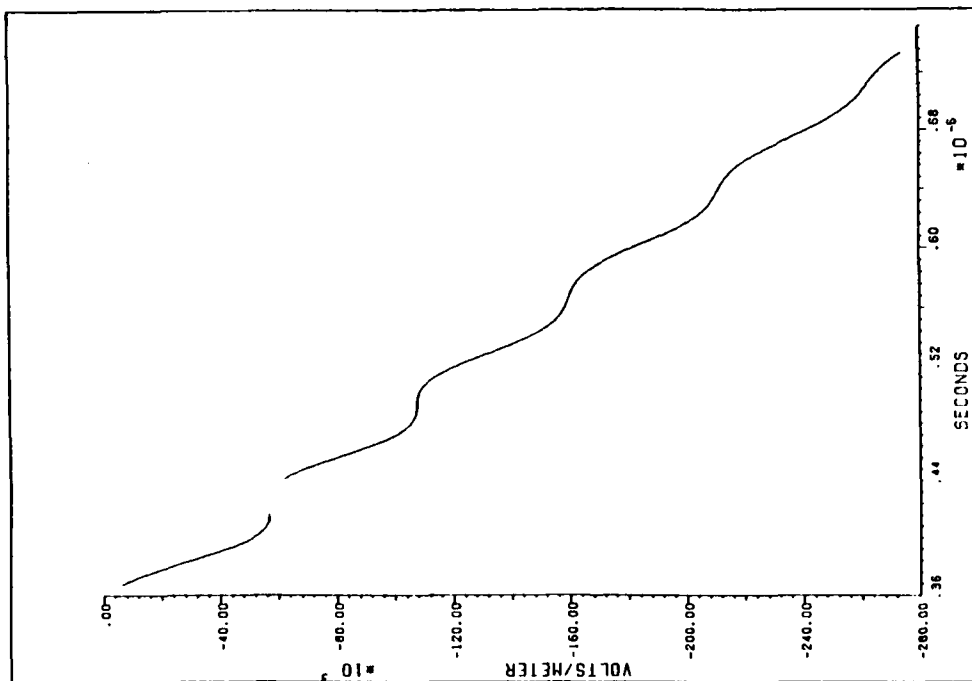


(b) RBC

Figure 63. Sensor Ten, E-field, Left Wing, $E_y(17,11,18)$

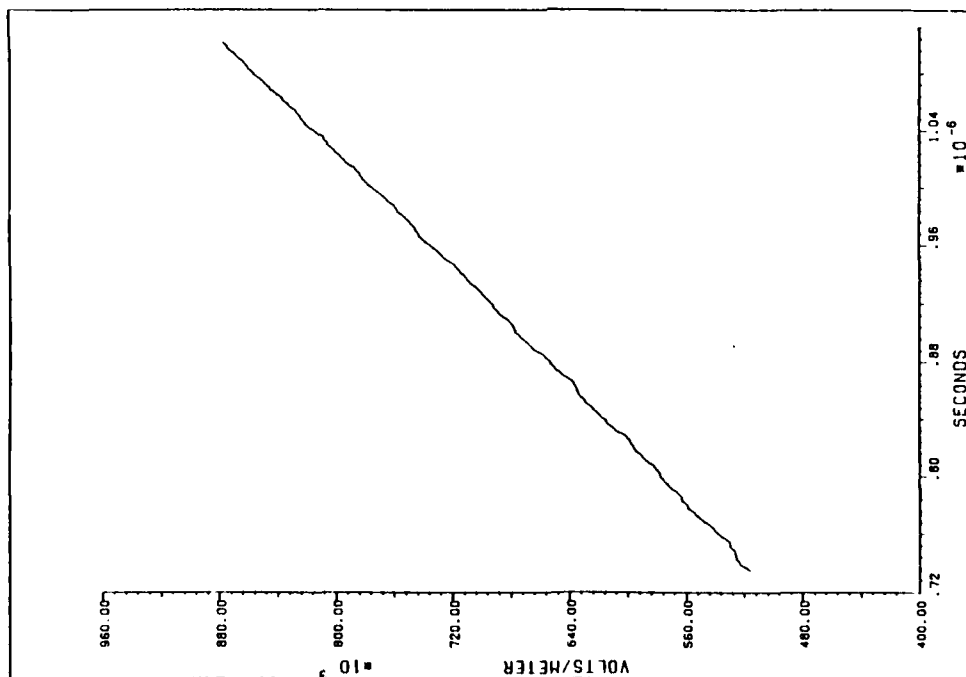


(a) ABC

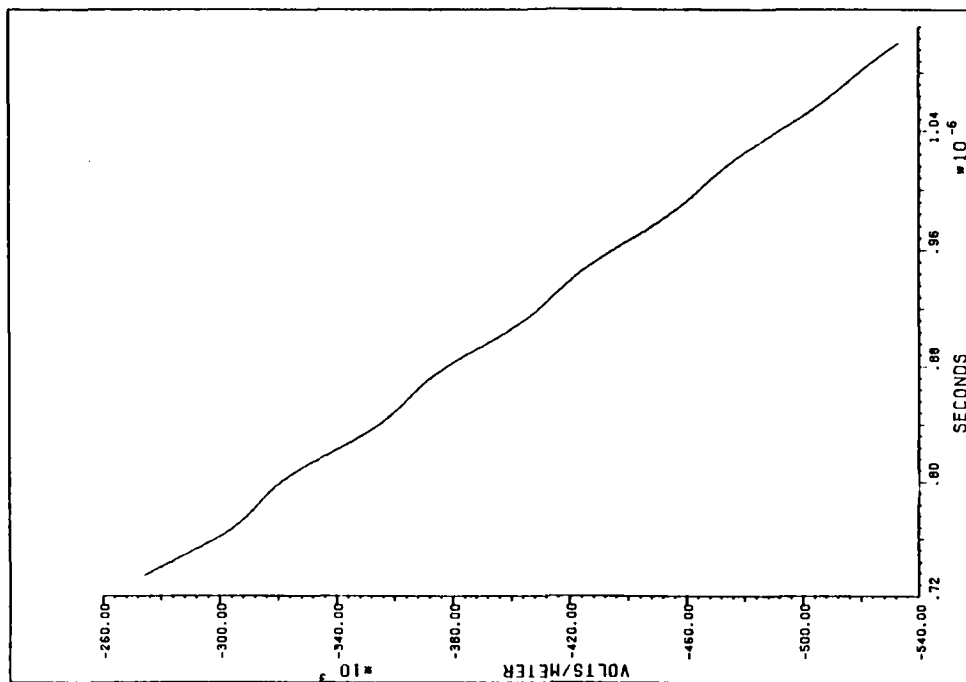


(b) RBC

Figure 64. Sensor Ten, E-field, Left Wing, E_y (17,11,18)

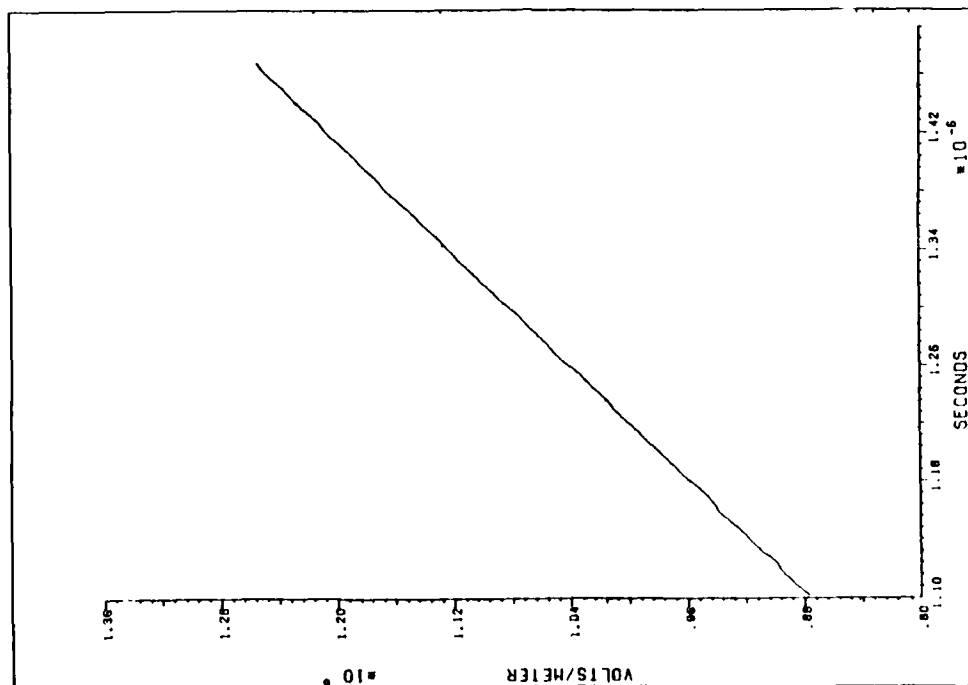


(a) ABC

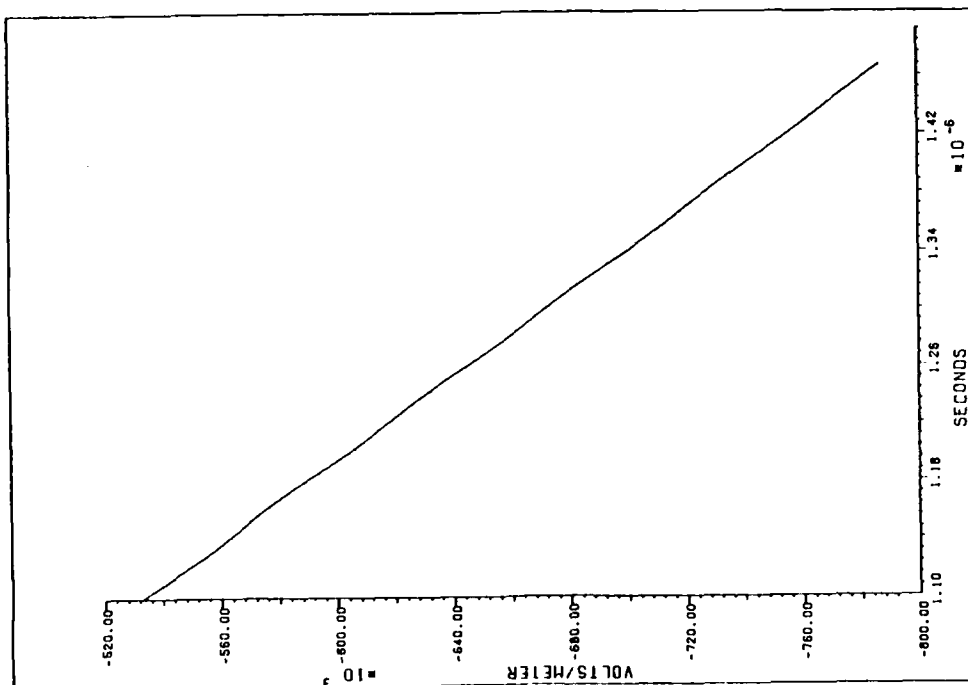


(b) RBC

Figure 65. Sensor Ten, E-field, Left Wing, $E_y(17,11,18)$



(a) ABC



(b) RBC

Figure 66. Sensor Ten, E-field, Left Wing, $E_y(17,11,18)$

Bibliography

1. Abrams, C.R. EMP (Electro-Magnetic Pulse) Protection of Advanced Flight Control Systems: Final Report. Project Number F41423. Naval Air Development Center, Aircraft and Crew Systems Technology Directorate, Warminster, Pa, November 1984 (AD-B088966L).
2. Auckland, D. and R. Wallenberg. Electromagnetic System Trade-Offs and Data Base Management for Advanced Composite Aircraft Study--Composite Coupling Analysis: Final Report, 1 August 1978--31 December 1980. Contract N00014-78-C-0673. Syracuse Research Corporation, Syracuse, New York, February 1981 (AD-A097741).
3. Auckland, D.T. and J.A. Birken. Electromagnetic Coupling Calculations on an Advance Composite and Metal F-14A Fighter Aircraft: Final Report, 30 October 1980--30 June 1981. Contract Number N00019-80-C-0172. Syracuse Research Corporation, New York, January 1982 (AD-B064566L).
4. Bayliss, Alvin and Eli Turkel. "Radiation Boundary Conditions for Wave-Like Equations," Communications on Pure and Applied Mathematics, Volume XXXIII: pages 707 to 725 (1980)
5. Burkley, R.A. Lightning Protection of Plastic and Isolated Aircraft Surfaces: Engineering Report. Goodyear Aerospace Corporation, Akron OH, August 1952 (AD-883378).
6. Butters, W.G., D.W. Clifford, K.P. Murphy and K.S. Zeisel. Assessment of Lightning Simulation Test Techniques, Part I: Final Report, July 1980--October 1981. McDonnell Aircraft Company, St Louis MO, October 1981 (AD-A112626).
7. Conte, Samuel D. and Carl de Boor. Elementary Numerical Analysis an Algorithmic Approach (Third Edition). New York: McGraw-Hill Book Company, 1980.
8. Cukr, Jeffrey M. An Analysis and Comparison of Lightning Return Stroke Models at Altitude. Master's Thesis. Air Force Institute of Technology, Wright-Patterson AFB, Ohio, December 1981 (AD-A151841).
9. Department of the Air Force. F-16 A/B Flight Manual. Technical Order 1F-16A-1, General Dynamics Forth Worth Division, 9 October 1981.

10. DuBro, Gary A. Atmospheric Electricity-Aircraft Interaction. Lecture series. Advisory group for Aerospace Research and Development Neuilly-Sur-Seine, France, May 1980 (AD-A087976).
11. Edwards, V.E., C.F. Williams, A. Husain, S. Ghash, and D.P. Pledger. Distributed and Embedded, Pulse-Tolerant, Hierarchical Flight Control System (DEPTH-FCS): Final Report, October 1982--August 1983. Contract Number N62269-82-C-0274. Honeywell Systems and Research Center, Minneapolis, Mn, August 1983 (AD-B089827L).
12. Engquist, Bjorn and Andrew Majda "Absorbing Boundary Conditions for the Numerical Simulation of Waves," Mathematics of Computation, Volume 31, Number 139: Pages 629 to 651 (July 1977).
13. Eriksen, F.J., T.H. Rudolph, and Rodney Perala. Atmospheric Electricity Hazards Analytical Model Development and Application. Volume III. Electromagnetic Coupling Modeling of the Lightning/Aircraft Interaction Event: Final Report, August 1979--June 1981. Electro Magnetic Applications Inc, Denver, Colorado, June 1981 (AD-A114017).
14. Fisher, Frank A. Analysis and Calculations of Lightning Interactions with Aircraft Electrical Circuits: Final Technical Report, 16 May 1976--21 February 1978. Contract F33615-76-C-3122. General Electric Company Corporate Research and Development, Schenectady, New York, August 1978 (AD-A062606).
15. Harrington, Roger F. Field Computation by Moment Methods. Malabar, Florida: Robert E. Krieger Publishing Company, 1983.
16. Hebert, James L. and Carlos Sannchez-Castro Implementation of a Three-Dimensional Finite Difference Electromagnetic Code for Analysis of Lightning Interaction with a FAA CV-580 Aircraft. Final Technical Report, April 1984--January 1985. Wright-Patterson AFB, Ohio: Flight Dynamics Laboratory, Air Force Wright Aeronautical Laboratories (AFWL/FIESL), in publication.

17. Hebert, James L. F-16/LANTIRN Lightning Susceptibility Tests. Final Technical Report. Wright-Patterson AFB, Ohio: Flight Dynamics Laboratory, Air Force Wright Aeronautical Laboratories (AFWAL/FIESL), in publication.
18. Hebert, James L., Lawrence C. Walko, and John G. Schneider "Design of a Fast Risettime Lightning Generator," Proceedings of the 10th International Aerospace and Ground Conference on Lightning and Static Electricity: pages (July 1985).
19. Hebert, James L. Lightning Analysis and Characterization Engineer. Personal interviews. AFWAL/FIESL, Wright-Patterson AFB, Ohio; 24 June 1985 - 15 November 1985.
20. Holland, Richard "THREDE: A Free-Field EMP Coupling and Scattering Code," IEEE Transactions on Nuclear Science, Volume NS-24, Number 6: pages 2416 to 2421 (December 1977).
21. Holland, Richard, Larry Simpson and R.H. St.John "Code Optimization for Solving Large 3D EMP Problems," IEEE Transactions on Nuclear Science, Volume NS-26, Number 6: pages 4964 to 4969 (December 1979).
22. Holland, Richard, Larry Simpson, and Karl S. Kunz "Finite-Difference Analysis of EMP Coupling to Lossy Dielectric Structures," IEEE Transactions on Electromagnetic Compatibility, Volume EMC-22, Number 3: pages 203 to 209 (August 1980).
23. Jaeger, D. Increasing Significance of Electromagnetic Effects in Modern Aircraft Development. Messerschmitt-Boelkow-Blohm GMBH Military Aircraft Division, Munich, Germany F R, October 1983 (AD-P002844/AD-A135100).
24. Kraus, John D. and Keith R. Carver Electromagnetics (Second Edition). New York: McGraw-Hill, 1973.
25. Kreyszig, Erwin. Advanced Engineering Mathematics (Third Edition). New York: John Wiley and Sons, Inc., 1972.
26. Kunz, Karl S. and Larry Simpson "A Technique for Increasing the Resolution of Finite-Difference Solutions of the Maxwell Equation," IEEE Transactions on Electromagnetic Compatibility, Volume EMC-23, Number 4: pages 419 to 422 (November 1981).

27. Kunz, Karl S. and Kuan-Min Lee "A Three-Dimensional Finite-Difference Solution of the External Response of an Aircraft to a Complex Transient EM Environment: Part I--The Method and Its Implementation," IEEE Transactions on Electromagnetic Compatibility, Volume EMC-20, No.2: pages 328 to 333 (May 1978).
28. Kunz, Karl S. and Kuan-Min Lee "A Three-Dimensional Finite-Difference Solution of the External Response of an Aircraft to a Complex Transient EM Environment: Part II-- Comparison of Predictions and Measurements," IEEE Transactions on Electromagnetic Compatibility, Volume EMC-20, No.2: pages 333 to 341 (May 1978).
29. Kunz, K.S. and B.W. Torres. THREDE User's Manual. Contract Number N60921-77-C-0117. Prepared for Naval Surface Weapons Center, White Oaks, Silver Spring, Maryland. Mission Research Corporation (MRC/AMRC-R-113), Albuquerque, NM, December 1977.
30. Kunz, Karl S., B.W. Torres, R.A. Peralá, J.M. Hamm, M.L. Van Blaricum, and J.F. Prewitt "Surface Current Injection Techniques: A Theoretical Investigation," IEEE Transactions on Nuclear Science, Volume NS-25, Number 6: pages 1422 to 1427 (December 1978).
31. Kurzthals, P.R. and R. Onken. Integrity in Electronic Flight Control Systems: Advisory Report. Advisory Group for Aerospace Research and Development Neuilly-Sur-Seine (France), July 1979 (AD-A074614).
32. Lax, P.D. "Differential Equations, Difference Equations and Matrix Theory," Communications on Pure and Applied Mathematics, Volume XI: pages 175 to 194 (1958).
33. Longmire, Conrad L. "State of the Art in IEMP and SGEMP Calculations," IEEE Transactions on Nuclear Science, Volume 22, Number 6: pages 2340 to 2344 (December 1975).
34. Maxwell, K. J., F.A. Fisher, J.A. Plummer, and P.R. Rogers. Computer Programs for Prediction of Lightning Induced Voltages in Aircraft Electrical Circuits: Final Report, 1 February 1974--30 November 1974. Contract F33615-74-C-3068. General Electric Corporate Research and Development, Schenectady, New York, April 1975 (AD-A015174).

35. Mazur, V., B.D. Fisher, J.C. Gerlach. Conditions Conductive to Lightning Striking an Aircraft in a Thunderstorm. Cooperative Institute for Mesoscale Meteorological Studies, Norman, Ok., 1983 (AD-P002235/AD-A135100)
36. McGlasson, Allan J. Forecasting the Lightning Strike Hazard to Aircraft, Student Research Report, ACSC-1665-81. Air Command and Staff College, Maxwell AFB, Alabama, May 1981 (AD-B057560L).
37. Mei, Kenneth K., Andreas Cangellaris, and Diogenes J. Angelakos "Conformal Time Domain Finite Difference Method," Radio Science, Volume 19, Number 5: pages 1145 to 1147 (September-October 1984).
38. Merewether, David E. "Transient Currents Induced on a Metallic Body of Revolution by an Electromagnetic Pulse," IEEE Transactions on Electromagnetic Compatibility, Volume EMC-13, Number 2: pages 41 to 44 (May 1971)
39. Merewether, David E. and Robert Fisher. Finite Difference Solution of Maxwell's Equation for EMP Applications: Final Report. Contract number DNA001-78-C-0231. Prepared for Defense Nuclear Agency (DNA 5301F). Electro Magnetic Applications, INC. (EMC-79-R-4), Albuquerque NM, 22 April 1980.
40. Muhleisen, R. and H.J. Fischer. Lightening Danger to Jet Aircraft, Part I. Report Number FTD-ID(RS)T-1382-77. Foreign Technology Division, Wright-Patterson AFB, Ohio, September 1977 (AD-B025455L).
41. Mur, Gerrit "Absorbing Boundary Conditions for the Finite-difference Approximation of the Time-Domain Electromagnetic-Field Equations," IEEE Transactions on Electromagnetic Compatibility, Volume EMC-23, Number 4: pages 377 to 382 (November 1981).
42. Pierce, Edward T. Triggered Lightning and Some Un-suspected Lightning Hazards: Scientific note number 15. Stanford Research Institute, Menlo Park CA, January 1972 (AD-735917).
43. Rasch, Nickolus O. A Compendium of Lightning Effects on Future Aircraft Electronic Systems: Final Report. Federal Aviation Administration Technical Center, Atlantic City, New Jersey, February 1982 (AD-A114117)

44. Robb, John D. Atmospheric Electricity Hazards Analytical Model Development and Application, Volume II: Simulation of the Lightning/Aircraft Interaction Event: Final Report, August 1979--June 1981. Contract F-33615-79-C-3412. Electro Magnetic Applications, Inc., Denver, Colorado, June 1981 (AD-A114016).
45. Robb, John D. and J.R. Stahmann. Aircraft Protection from Thunderstorm Electromagnetic Effects. Lightning and Transients Research Institute, Minneapolis MINN, May 1963 (AD-414903).
46. Rustan, Peter L. and James L. Hebert "Lightning Measurements on an Aircraft Flying at Low Altitude," Second International Conference on the Aviation Weather System: pages 220-225 (June 1985).
47. Rustan, Peter L., B. Kuhlman, and John Showalter. Electromagnetic Measurements of Lightning Attachment to Aircraft. Air Force Wright Aeronautical Labs, Wright-Patterson AFB, Ohio, 1983 (AD-P002198/AD-A135100).
48. Rymes, M.D. T3DFD User's Manual: Final Technical Report, August 1979--June 1981. Prepared for Air Force Flight Dynamics Laboratory (FES), Wright-Patterson AFB, Ohio. Contract number F 33615-79-C-3412. Electro Magnetic Applications, INC. (EMA-81-r-24), Denver CO, April 1981.
49. Schowalter, Jeffrey S. Direct Lightning Strikes to Aircraft. Master's Thesis. Air Force Institute of Technology, Wright-Patterson AFB, Ohio, June 1982 (AD-A118075).
50. Shaeffer, John F. and Gustave L. Weinstock. Aircraft Related Lightning Mechanisms: Technical Report. Contract F33615-71-C-1581. McDonnell Aircraft Company, St. Louis, Missouri, October 1972 (AD906805).
51. Sommer, David L. Protection of Advanced Electrical Power Systems from Atmospheric Electromagnetic Hazards: Final Report, June 1979--October 1981. Contract F3345-79-C-2006. Boeing Military Airplane Company, Seattle, Washington, December 1981 (AD-A112612).
52. Sommer, David L. Protection of Electrical Systems from EM Hazards-Design Guide: Interim Report, June 1979--October 1981. Contract F3345-79-C-2006. Boeing Military Airplane Company, Seattle, Washington, September 1981 (AD-A112707).

53. Stutzman, Warren L. and Gary A. Thiele Antenna Theory and Design. New York: John Wiley & Sons, 1981.
54. Taflove, Allen "Application of the Finite-Difference Time-Domain Method to Sinusoidal Steady-State Electromagnetic-Penetration Problems," IEEE Transactions on Electromagnetic Compatibility, Volume EMC-22, Number 3: pages 191 to 202 (August 1980).
55. Taflove, Allen and Morris E. Brodwin "Numerical Solution of Steady-State Electromagnetic Scattering Problems Using the Time-Dependent Maxwell's Equations," IEEE Transactions on Microwave Theory and Techniques, Volume MTT-23, Number 8: pages 623 to 630 (August 1975).
56. Taflove, Allen and Korada Umashankar "A Hybrid Moment Method/Finite-Difference Time-Domain Approach to Electromagnetic Coupling and Aperture Penetration into Complex Geometries," IEEE Transactions on Antennas and Propagation, Volume AP-30, Number 4: pages 617 to 627 (July 1982).
57. Taflove, Allen and Korada Umashankar " Radar Cross Section of General Three-Dimensional Scatterers," IEEE Transactions on Electromagnetic Compatibility, Volume EMC-25, Number 4: pages 433 to 440 (November 1983).
58. Taillet, Joseph. Conference on Certification of Aircraft for Lightning and Atmospheric Electricity Hazards (Conference sur la Certification des Aeronefs Contre les Dangers du Foudroiement et de L'Electricite Atmospherique) held ONERA-Chatillon (France) 14-21 September 1978: Final Report, 1 July 1978--30 June 1979. Office National D'Etudes et de Recherches Aerospatiales Chatillon-Sous-Bagneux (France), July 1979 (AD-A078536).
59. Taylor, Clayborne D., Dong-Hoa Lam, and Thomas H. Shumpert Electromagnetic Pulse Scattering in Time-Varying Inhomogeneous Media, " IEEE Transactions on Antennas and Propagation, Volume AP-17, No.5: pages 585 to 589 (September 1969).
60. Tellier, H. LE. GORF: A VAX-11/FORTRAN 77 Improved version of the THREDE Code for the Finite Difference Solution of Maxwell's Equations in Time-Varying EMP Scattering Problems. Supported by the French Ministry of Defense and currently in residence at Naval Surface Weapons Center-White Oak, December 1983.

61. Uman, Martin A. Lightning. New York: McGraw-Hill Book Company, 1969.
62. Umashankar, Korada and Allen Taflove "A Novel Method to Analyze Electromagnetic Scattering of Complex Objects," IEEE Transactions on Electromagnetic Compatibility, Volume EMC-24, Number 4: pages 397 to 324 (November 1982).
63. Weinstock, G.L. A Realistic Approach to Aircraft Lightning Protection. McDonnell Aircraft Co., St Louis, Mo, 1983 (AD-P002189/AD-A135100).
64. Yee, Kane S. "Numerical Solution of Initial Boundary Value Problems Involving Maxwell's Equations in Isotropic Media," IEEE Transactions on Antennas and Propagation, Volume AP-14, Number 3: pages 302 to 307 (May 1966).

VITA

Captain Clifford F. Williford was born on 12 July 1950 in Norfolk, Virginia. He graduated from high school (Frederick Military Academy, Portsmouth, Virginia) in 1968. He attended Virginia Polytechnic Institute for one year, then transferred to Old Dominion University. On 13 February 1970, Capt Williford enlisted in the Air Force. In December of 1973, he was selected for the Airman Education and Commissioning Program (AECF). He attended Virginia Polytechnic Institute and State University from January 1974 till March 1976, where he received his Bachelor of Science in Electrical Engineering. Upon graduation, he attended the Flight Screening Program in Hondo, Texas, and then attended Officer Training School, Medina Annex, Lackland AFB, Texas. After commissioning, he attended Undergraduate Pilot Training at Williams AFB, and earned his Pilots' wings in July 1977. His first assignment after UPT was RAF Lakenheath, where Capt. Williford flew the F-111F. He was a Pilot Weapons Systems Officer in the 492nd TFS, and later an Aircraft Commander in the 495rd TFS. Following his return to the States, Capt. Williford served as an Aircraft Commander, Flight Instructor and Flight Examiner in the 522 TFS until entering the School of Engineering, Air Force Institute of Technology, in June 1984.

Permanent address: 1926 E. Ocean View Ave.
Norfolk, Virginia 23503

UNCLASSIFIED

SECURITY CLASSIFICATION OF THIS PAGE

AD A163 828

REPORT DOCUMENTATION PAGE

1a. REPORT SECURITY CLASSIFICATION UNCLASSIFIED			1b. RESTRICTIVE MARKINGS		
2a. SECURITY CLASSIFICATION AUTHORITY			3. DISTRIBUTION/AVAILABILITY OF REPORT Approved for Public release; distribution unlimited		
2b. DECLASSIFICATION/DOWNGRADING SCHEDULE					
4. PERFORMING ORGANIZATION REPORT NUMBER(S) AFIT/GE/ENG/85D-53			5. MONITORING ORGANIZATION REPORT NUMBER(S)		
6a. NAME OF PERFORMING ORGANIZATION School of Engineering		6b. OFFICE SYMBOL (If applicable) AFIT/ENG		7a. NAME OF MONITORING ORGANIZATION	
6c. ADDRESS (City, State and ZIP Code) Air Force Institute of Technology Wright-Patterson AFB, Ohio 45433			7b. ADDRESS (City, State and ZIP Code)		
8a. NAME OF FUNDING/SPONSORING ORGANIZATION Atmospheric Electricity Hazards Group		8b. OFFICE SYMBOL (If applicable) AFWAL/FIESL		9. PROCUREMENT INSTRUMENT IDENTIFICATION NUMBER	
8c. ADDRESS (City, State and ZIP Code) Wright-Patterson AFB, Ohio 45433			10. SOURCE OF FUNDING NOS.		
11. TITLE (Include Security Classification) See Box 19			PROGRAM ELEMENT NO. 62201F		PROJECT NO. 2402
			TASK NO. 02		WORK UNIT NO. 23
12. PERSONAL AUTHOR(S) Clifford F. Williford, B.S., Capt., USAF					
13a. TYPE OF REPORT MS Thesis		13b. TIME COVERED FROM _____ TO _____		14. DATE OF REPORT (Yr., Mo., Day) 1985 December	
				15. PAGE COUNT 184	
16. SUPPLEMENTARY NOTATION					
17. COSATI CODES			18. SUBJECT TERMS (Continue on reverse if necessary and identify by block number)		
FIELD	GROUP	SUB. GR.	Lightning Lightning Model		
04	01		Lightning & Aircraft Boundary Conditions		
09	02		Electromagnetic Computer Codes		
19. ABSTRACT (Continue on reverse if necessary and identify by block number)					
20 03					
Approved for public release: IAW AFR 190-1/ LYNN E. WOLVER 16 JAN 86 Dean for Research and Professional Development Air Force Institute of Technology (AFIT) Wright-Patterson AFB OH 45433					
Title: COMPARISON OF ABSORPTION AND RADIATION BOUNDARY CONDITIONS USING A TIME DOMAIN THREE-DIMENSIONAL FINITE-DIFFERENCE ELECTROMAGNETIC COMPUTER CODE					
Thesis Chairman: Randy J. Jost, 1Lt, USAF Instructor of Electrical Engineering					
20. DISTRIBUTION/AVAILABILITY OF ABSTRACT UNCLASSIFIED/UNLIMITED <input checked="" type="checkbox"/> SAME AS RPT. <input type="checkbox"/> DTIC USERS <input type="checkbox"/>			21. ABSTRACT SECURITY CLASSIFICATION UNCLASSIFIED		
22a. NAME OF RESPONSIBLE INDIVIDUAL Randy J. Jost, 1Lt, USAF			22b. TELEPHONE NUMBER (Include Area Code) (513) 255-3576		22c. OFFICE SYMBOL AFIT/ENG

Abstract

The Three-Dimensional Finite Difference (3DFD) computer code is compared using Absorption Boundary Conditions (ABS) versus Radiation Boundary Conditions (RBC). This comparison is made when the 3DFD code is used to study the interaction of lightning with an aircraft. The 3DFD computer code is a modified version of Rymes' 3DFD. The aircraft modeled for the paper is an F-16 'Fighting Falcon'. The ABC used simulates an infinite free-space by setting the conductivity of the boundary space to that of distilled water, to "absorb" the outgoing electromagnetic waves. The RBC simulates free-space by assigning the boundary fields to a previously calculated value. The value is calculated with a parabolic interpolation of three previous field values, which are offset in space. Therefore, the calculated value is also extrapolated to account for the time delay and position change. The results of incorporating RBC were dramatic. The ten locations sampled for the test showed marked improvement in the waveforms when using RBC's. Depending on the purpose of the analysis, this improved waveform output may be overshadowed by the 25% increase in CPU time that is needed for the more sophisticated RBC.

END

FILMED

3-86

DTIC